

# **Public Comments**

## **Item 6 – Revised LCLUP (Continued)**

Written Comments Received After 12pm on 04/22/2024



*April 22, 2024*  
*City Council Meeting*

---

**From:** DeJarnatt, Anne [REDACTED]  
**Sent:** Monday, April 22, 2024 3:11 PM  
**To:** \_City Council; Public Comment; Coffey, Sarah  
**Subject:** NO PUBLIC INPUT ?

**[CAUTION: External Email]**

I think Jeff has a valid point.

I urge you to direct staff to remove the SRA concept and treat all residents, homes, and businesses the same under the fCoastal Act. Do not concede our rights or require restrictions that force us to give them up to the Coastal Commission.

CITY COUNCIL REPRESENTS PACIFICA RESIDENTS, NOT THE COASTAL COMMISSION.

Respectfully

Anne DeJarnatt

**CAUTION: This email originated from outside of the City of Pacifica. Unless you recognize the sender's email address and know the content is safe, do not click links, open attachments or reply.**

---

**From:** Richard Harris [REDACTED]  
**Sent:** Monday, April 22, 2024 3:39 PM  
**To:** \_City Council; Public Comment; Coffey, Sarah; Pacifica Permit Tech; City Manager; CoastalPlan  
**Cc:** Vaterlaus, Sue; Bigstyck, Tygarjas; Beckmeyer, Sue; Bier, Mary; Boles, Christine; Murdock, Christian; 'Phil Ginsburg'; 'Potter, Spencer (REC)'; Cervantes, Stefanie; Woodhouse, Kevin  
**Subject:** Pacifica City Council Mtg Apr. 22, 2024, LCLUP Study #4 / CORRECTED Further comment of SF Pub. Golf Alliance  
**Attachments:** Ltr.SFPGA.to Pac.Ci.Cil.re.Pacifica.LCLUP.4.22.24.pdf

**[CAUTION: External Email]**

Pacifica City Council Mtg Apr. 22, 2024, LCLUP Study #4 / CORRECTED Further comment of SF Pub. Golf Alliance

Pacifica City Clerk Sarah Coffey – Sarah – I had a typographical error in the Apr. 22 letter of SF Public Golf Alliance submitted at 2:54 p.m. – at page 3, in the citation of the Public Resources Code. I have corrected that mis-citation in the above-attached letter. Please replace in the record the copy mailed at 2:54 with the above-attached, and in distribution to Council and Staff. And please acknowledge receipt. I will come early to tonight’s meeting and deliver hard copies to help correct this mistake. Apologies for making your job harder. Please acknowledge receipt, include in Council’s Correspondence file in the Study Session #4 file, continued, include in Council’s Agenda Packet (if possible at this late hour), and forward to City Council, Planning Commissioners, Planning Department, and Staff.

Mayor Sue Vaterlaus, Pacifica City Council and Pacifica Planning Department

Dear Mayor Vaterlaus, Councilmembers, and Planning Department Staff  
Enclosed please find CORRECTED VERSION of SF Public Golf Alliance’s further comment letter, dated April 22, for Council’s April 22 Local Coastal LUP Study Session #4, continued. Please include in the public record and in Councilmembers’ and Staff’s meeting packets. We look forward to seeing you again.  
Very Best Regards

**Richard Harris**  
**San Francisco Public Golf Alliance**  
826 Stanyan Street  
San Francisco, CA 94117-2726  
Phone: (415) 290-5718

**CAUTION: This email originated from outside of the City of Pacifica. Unless you recognize the sender's email address and know the content is safe, do not click links, open attachments or reply.**



April 22, 2024

Pacifica City Council and Mayor Sue Vaterlaus  
540 Crespi Dr.  
Pacifica, CA. 94044

**Pacifica City Council Meeting / April 22, 2024 / Local Coastal LUP Study #4, cont.**

**SF Public Golf Alliance Further Comments.2: Pacifica's LCLUP Draft is Problematic: (1) Environmental Justice Problems; (2) Uncertain legal effects of: (i) the new California Resources Code Section 30985 (Jan. 1, 2024); and (ii) Takings issues raised by the recent U.S. Supreme Court Decision in Sheetz vs. County of El Dorado.**

Dear Mayor Vaterlaus and Council Members,

We submit this additional letter on behalf of the non-profit San Francisco Public Golf Alliance and its highly diverse 7,000-plus men and women members, a substantial number of which are Pacifica residents and Sharp Park golfers. This supplements our previously submitted letters to Council, dated February 27, 2024<sup>1</sup>, March 25, 2024,<sup>2</sup> April 8, 2024<sup>3</sup>, April 14, 2024,<sup>4</sup> and April 20, 2024,<sup>5</sup> which prior letters are incorporated herein by this reference.

---

<sup>1</sup> Letter, SF Public Golf Alliance to Pacifica City Council, re Consultation Draft LCLUP.2.27.24  
[https://drive.google.com/file/d/12cwdlvP5KlwHlw46TGtNkEA63\\_pRFg1/view?usp=drive\\_link](https://drive.google.com/file/d/12cwdlvP5KlwHlw46TGtNkEA63_pRFg1/view?usp=drive_link)

<sup>2</sup> Letter, SF Public Golf Alliance to Pacifica City Council, re Consultation Draft LCLUP.3.25.24  
[https://drive.google.com/file/d/1vHuMe1pqU1zxoQUy4fP9A9KB6MNGSXem/view?usp=drive\\_link](https://drive.google.com/file/d/1vHuMe1pqU1zxoQUy4fP9A9KB6MNGSXem/view?usp=drive_link)

<sup>3</sup> Letter, SF Public Golf Alliance to Pacifica City Council, re April 2024 Draft LCLUP.4.8.24  
[https://drive.google.com/file/d/1KuFZfa5um7qMXNpesOaJ72IW5SP7oR0I/view?usp=drive\\_link](https://drive.google.com/file/d/1KuFZfa5um7qMXNpesOaJ72IW5SP7oR0I/view?usp=drive_link)

<sup>4</sup> Letter, SF Public Golf Alliance to Pacifica City Council, re April 2024 Draft LCLUP.4.14.24  
[https://drive.google.com/file/d/19n109KQLQXkMM6w3quLTY752JMHeW0Yn/view?usp=drive\\_link](https://drive.google.com/file/d/19n109KQLQXkMM6w3quLTY752JMHeW0Yn/view?usp=drive_link)

<sup>5</sup> Letter, SF Public Golf Alliance to Pacifica City Council, re April 2024 Draft LCLUP.4.20.24  
[https://drive.google.com/file/d/1\\_-03aFI4RPoKI7ZuyrWztWv23\\_CxqR1G/view?usp=drive\\_link](https://drive.google.com/file/d/1_-03aFI4RPoKI7ZuyrWztWv23_CxqR1G/view?usp=drive_link)

## 1. Environmental Justice

Our prior letters, incorporated at footnotes 1-5, above, set forth facts and issues of lower-cost public recreation, wetland, species, ESHA, public coastal access, scenic, and reasonably-priced and lower cost housing that are recognized and protected as significant protected coastal assets by both the Coastal Act (California Public Resources Code Section 30000 et seq<sup>6</sup>) and by the California Coastal Commission's Environmental Justice Policy.<sup>7</sup>

Staff's April 15, 2024 Report to City Council at its April 15, 2024 council meeting on the matter of the Pacifica Local Coastal Land Use Plan Update, reports at page 6, efforts by "CCC Staff" to pressure Pacifica to not protect the Sharp Park-West Fairway Park-Mori Point sub areas with a "Special Resiliency Area" designation in Pacifica's Local Coastal Land Use Plan.<sup>8</sup> If true, such efforts to deny protection to coastal assets specifically recognized as areas to be protected under the Coastal Commission's own Environmental Justice Policy would be contrary to the Commission's commitments – "as an agency" in that same Environmental Justice Policy to:

**"(4) Strongly encourage local governments to amend their local coastal programs to address environmental justice issues.. ."<sup>9</sup> and . . . (7) "Staff will continue to work collaboratively with partner agencies, the public, and commissioners to ensure that coastal management decisions at all levels appropriately consider environmental justice concepts and values."<sup>10</sup>**

## 2. Issues raised by the new Coastal Act / California Resources Code Section 30985

Pacifica Staff's April 15, 2024 Council Agenda Summary Report includes, at page 2, this cryptic note: "Lastly, an update to Pacifica's LCLUP to account for SLR is inevitable. State law, as enacted in late 2023 with Senate Bill (SB) 272, now requires LCLUPs throughout California

---

<sup>6</sup> California Public Resources Code Section 30000, et seq.:

[https://leginfo.legislature.ca.gov/faces/codes\\_displayexpandedbranch.xhtml?tocCode=PRC&division=20.&title=&part=&chapter=&article=&nodetreepath=43](https://leginfo.legislature.ca.gov/faces/codes_displayexpandedbranch.xhtml?tocCode=PRC&division=20.&title=&part=&chapter=&article=&nodetreepath=43)

<sup>7</sup> California Coastal Commission Environmental Justice Policy, Adopted March 8, 2019,

[https://documents.coastal.ca.gov/assets/env-justice/CCC\\_EJ\\_Policy\\_FINAL.pdf](https://documents.coastal.ca.gov/assets/env-justice/CCC_EJ_Policy_FINAL.pdf)

<sup>8</sup> City of Pacifica Council Agenda Summary Report, 4/15/24, at Page 6 : "CCC staff indicated that if the City [of Pacifica] were to include a southward boundary extension, then they would likely need to prepare a suggested modification to remove it from the LCLUP prior to certification. They {CCC Staff} were concerned that this would undermine the overall approach of coordination and compromise between the two agencies and would suggest ongoing disagreements heading into the CCC certification hearing."

[https://drive.google.com/file/d/1uaZYj6luDf6wODwd7qFS32DzFFv9E3K2/view?usp=drive\\_link](https://drive.google.com/file/d/1uaZYj6luDf6wODwd7qFS32DzFFv9E3K2/view?usp=drive_link)

<sup>9</sup> California Coastal Commission, Environmental Justice Policy, *supra*, "Implementation" at P. 16 (20/25)

[https://documents.coastal.ca.gov/assets/env-justice/CCC\\_EJ\\_Policy\\_FINAL.pdf](https://documents.coastal.ca.gov/assets/env-justice/CCC_EJ_Policy_FINAL.pdf)

<sup>10</sup> California Coastal Commission, Environmental Justice Policy, *supra*, "Implementation" at P. 16 (20/25)

[https://documents.coastal.ca.gov/assets/env-justice/CCC\\_EJ\\_Policy\\_FINAL.pdf](https://documents.coastal.ca.gov/assets/env-justice/CCC_EJ_Policy_FINAL.pdf)

to be updated to include a plan to address SLR.”<sup>11</sup> The Agenda Summary Report contained no further discussion or description of the new law.

Senate Bill 272 was enacted as California Resources Code Section 30985, effective January 1, 2024.<sup>12</sup> Its provisions, and the provisions of its subsections include, inter alia:

**30985**

- (a) “A local government lying within the coastal zone . . shall develop a sea level rise plan . .
- (b) [The plan] . . . shall include . . . best available science . . . .
- (d) All local governments . . shall comply with this section by **January 1, 2034**

**30985.2**

- (a) On or before December 31, 2024, the California Coastal Commission, in close coordination with the Ocean Protection Council and the California Sea Level Rise State and Regional Support Collaborative, shall establish guidelines for the preparation of the sea level rise plan required pursuant to subdivision (a) of Section 30985. The guidelines shall recognize and build upon the baseline policies as described in the “Sea Level Rise Working Group: 2021 Work Products” as published by the California Coastal Commission on December 3, 2021. . . .

**30985.5**

Local governments that receive approval by the California Coastal Commission or the San Francisco Bay Conservation and Development Commission, as applicable, pursuant to subdivision (a) of Section 30985 shall be prioritized for funding, upon appropriation by the Legislature, for the implementation of sea level rise adaptation strategies and recommended projects in the local government’s approved sea level rise plan.

**30985.6**

The operation of this division is contingent upon an appropriation for its purposes by the Legislature in the annual Budget Act or another statute.

Before Pacifica submits a revised Local Coastal Land Use Plan to the Coastal Commission for final approval, we suggest Pacifica closely analyze and consider – including public consideration – the implications of this new law.

---

<sup>11</sup> City of Pacifica Council Agenda Summary Report, 4/15/24, at Page 2:  
[https://drive.google.com/file/d/1uaZYj6luDf6wODwd7qFS32DzFFv9E3K2/view?usp=drive\\_link](https://drive.google.com/file/d/1uaZYj6luDf6wODwd7qFS32DzFFv9E3K2/view?usp=drive_link)

<sup>12</sup> California Public Resources Code Section 30985, Sea Level Rise Planning and Adaptation,  
[https://leginfo.legislature.ca.gov/faces/codes\\_displayText.xhtml?lawCode=PRC&division=20.6.9.&title=&part=&chapter=&article=](https://leginfo.legislature.ca.gov/faces/codes_displayText.xhtml?lawCode=PRC&division=20.6.9.&title=&part=&chapter=&article=)

**3. Issues raised by the U.S. Supreme Court's April 12, 2024 decision in Sheetz v. County of El Dorado.**

At page 4 of our April 20, 2024 letter to Council<sup>13</sup> we called Council's attention to the Supreme Court's recent Sheetz<sup>14</sup> decision. We suggest that the interplay of the recently-enacted Public Resources Code Section 30985 (discussed on the previous page) and Sheetz is worthy of serious legal analysis and consideration – including public input -- before Pacifica proceeds further. This is not a time to rush. Or be rushed.

Respectfully submitted,

*Richard Harris*

President, San Francisco Public Golf Alliance

cc: City Manager Kevin Woodhouse, Planning Director Christian Murdock, Deputy Planning Director Stefanie Cervantes, Planning Commission and Commissioners, City Clerk Sarah Coffey, Phil Ginsburg, Gen. Mgr., San Francisco Recreation and Parks Dept., Spencer Potter, Esq., San Francisco Recreation and Parks Dept.

---

<sup>13</sup> Letter, SF Public Golf Alliance to Pacifica City Council, re April 2024 Draft LCLUP.4.20.24  
[https://drive.google.com/file/d/1\\_03aFI4RPoKI7ZuyrWztWv23\\_CxqR1G/view?usp=drive\\_link](https://drive.google.com/file/d/1_03aFI4RPoKI7ZuyrWztWv23_CxqR1G/view?usp=drive_link)

<sup>14</sup> Sheetz vs. County of El Dorado, California, U.S. Supreme Court October Term, 2023, No. 22-1074  
[https://www.supremecourt.gov/opinions/23pdf/22-1074\\_bqmd.pdf](https://www.supremecourt.gov/opinions/23pdf/22-1074_bqmd.pdf)

provided @ mtg 4/22/24  
Richard Harris

# SAN FRANCISCO PUBLIC GOLF ALLIANCE



826 Stanyan St., San Francisco, CA 94117 • 415-290-5718 • [info@sfpublicgolf.org](mailto:info@sfpublicgolf.org)



April 22, 2024

Pacifica City Council and Mayor Sue Vaterlaus  
540 Crespi Dr.  
Pacifica, CA. 94044

## **Pacifica City Council Meeting / April 22, 2024 / Local Coastal LUP Study #4, cont.**

**SF Public Golf Alliance Further Comments.2: Pacifica's LCLUP Draft is Problematic: (1) Environmental Justice Problems; (2) Uncertain legal effects of: (i) the new California Resources Code Section 30985 (Jan. 1, 2024); and (ii) Takings issues raised by the recent U.S. Supreme Court Decision in Sheetz vs. County of El Dorado.**

Dear Mayor Vaterlaus and Council Members,

We submit this additional letter on behalf of the non-profit San Francisco Public Golf Alliance and its highly diverse 7,000-plus men and women members, a substantial number of which are Pacifica residents and Sharp Park golfers. This supplements our previously submitted letters to Council, dated February 27, 2024<sup>1</sup>, March 25, 2024,<sup>2</sup> April 8, 2024<sup>3</sup>, April 14, 2024,<sup>4</sup> and April 20, 2024,<sup>5</sup> which prior letters are incorporated herein by this reference.

<sup>1</sup> Letter, SF Public Golf Alliance to Pacifica City Council, re Consultation Draft LCLUP.2.27.24  
[https://drive.google.com/file/d/12cwdlvP5KlwHlw46TGtNkEA63\\_pRFg1/view?usp=drive\\_link](https://drive.google.com/file/d/12cwdlvP5KlwHlw46TGtNkEA63_pRFg1/view?usp=drive_link)

<sup>2</sup> Letter, SF Public Golf Alliance to Pacifica City Council, re Consultation Draft LCLUP.3.25.24  
[https://drive.google.com/file/d/1vHuMe1pqU1zxoQUy4fP9A9KB6MNGSXem/view?usp=drive\\_link](https://drive.google.com/file/d/1vHuMe1pqU1zxoQUy4fP9A9KB6MNGSXem/view?usp=drive_link)

<sup>3</sup> Letter, SF Public Golf Alliance to Pacifica City Council, re April 2024 Draft LCLUP.4.8.24  
[https://drive.google.com/file/d/1KuFZfa5um7qMXNpesOaJ72IW5SP7oR0l/view?usp=drive\\_link](https://drive.google.com/file/d/1KuFZfa5um7qMXNpesOaJ72IW5SP7oR0l/view?usp=drive_link)

<sup>4</sup> Letter, SF Public Golf Alliance to Pacifica City Council, re April 2024 Draft LCLUP.4.14.24  
[https://drive.google.com/file/d/19n109KQLQXkMM6w3quLTY752JMHew0Yn/view?usp=drive\\_link](https://drive.google.com/file/d/19n109KQLQXkMM6w3quLTY752JMHew0Yn/view?usp=drive_link)

<sup>5</sup> Letter, SF Public Golf Alliance to Pacifica City Council, re April 2024 Draft LCLUP.4.20.24  
[https://drive.google.com/file/d/1\\_03aFI4RPoKI7ZuyrWztWv23\\_CxqR1G/view?usp=drive\\_link](https://drive.google.com/file/d/1_03aFI4RPoKI7ZuyrWztWv23_CxqR1G/view?usp=drive_link)



## 1. Environmental Justice

Our prior letters, incorporated at footnotes 1-5, above, set forth facts and issues of lower-cost public recreation, wetland, species, ESHA, public coastal access, scenic, and reasonably-priced and lower cost housing that are recognized and protected as significant protected coastal assets by both the Coastal Act (California Public Resources Code Section 30000 et seq<sup>6</sup>) and by the California Coastal Commission's Environmental Justice Policy.<sup>7</sup>

Staff's April 15, 2024 Report to City Council at its April 15, 2024 council meeting on the matter of the Pacifica Local Coastal Land Use Plan Update, reports at page 6, efforts by "CCC Staff" to pressure Pacifica to not protect the Sharp Park-West Fairway Park-Mori Point sub areas with a "Special Resiliency Area" designation in Pacifica's Local Coastal Land Use Plan.<sup>8</sup> If true, such efforts to deny protection to coastal assets specifically recognized as areas to be protected under the Coastal Commission's own Environmental Justice Policy would be contrary to the Commission's commitments – "as an agency" in that same Environmental Justice Policy to:

**"(4) Strongly encourage local governments to amend their local coastal programs to address environmental justice issues.. ."<sup>9</sup> and . . . (7) "Staff will continue to work collaboratively with partner agencies, the public, and commissioners to ensure that coastal management decisions at all levels appropriately consider environmental justice concepts and values."<sup>10</sup>**

## 2. Issues raised by the new Coastal Act / California Resources Code Section 30985

Pacifica Staff's April 15, 2024 Council Agenda Summary Report includes, at page 2, this cryptic note: "Lastly, an update to Pacifica's LCLUP to account for SLR is inevitable. State law, as enacted in late 2023 with Senate Bill (SB) 272, now requires LCLUPs throughout California

---

<sup>6</sup> California Public Resources Code Section 30000, et seq.:

[https://leginfo.ca.gov/faces/codes\\_displayexpandedbranch.xhtml?tocCode=PRC&division=20.&title=&part=&chapter=&article=&nodetreepath=43](https://leginfo.ca.gov/faces/codes_displayexpandedbranch.xhtml?tocCode=PRC&division=20.&title=&part=&chapter=&article=&nodetreepath=43)

<sup>7</sup> California Coastal Commission Environmental Justice Policy, Adopted March 8, 2019,

[https://documents.coastal.ca.gov/assets/env-justice/CCC\\_EJ\\_Policy\\_FINAL.pdf](https://documents.coastal.ca.gov/assets/env-justice/CCC_EJ_Policy_FINAL.pdf)

<sup>8</sup> City of Pacifica Council Agenda Summary Report, 4/15/24, at Page 6 : "CCC staff indicated that if the City [of Pacifica] were to include a southward boundary extension, then they would likely need to prepare a suggested modification to remove it from the LCLUP prior to certification. They [CCC Staff] were concerned that this would undermine the overall approach of coordination and compromise between the two agencies and would suggest ongoing disagreements heading into the CCC certification hearing."

[https://drive.google.com/file/d/1uaZYj6luDf6wODwd7qFS32DzFFv9E3K2/view?usp=drive\\_link](https://drive.google.com/file/d/1uaZYj6luDf6wODwd7qFS32DzFFv9E3K2/view?usp=drive_link)

<sup>9</sup> California Coastal Commission, Environmental Justice Policy, *supra*, "Implementation" at P. 16 (20/25)

[https://documents.coastal.ca.gov/assets/env-justice/CCC\\_EJ\\_Policy\\_FINAL.pdf](https://documents.coastal.ca.gov/assets/env-justice/CCC_EJ_Policy_FINAL.pdf)

<sup>10</sup> California Coastal Commission, Environmental Justice Policy, *supra*, "Implementation" at P. 16 (20/25)

[https://documents.coastal.ca.gov/assets/env-justice/CCC\\_EJ\\_Policy\\_FINAL.pdf](https://documents.coastal.ca.gov/assets/env-justice/CCC_EJ_Policy_FINAL.pdf)

to be updated to include a plan to address SLR.”<sup>11</sup> The Agenda Summary Report contained no further discussion or description of the new law.

Senate Bill 272 was enacted as California Resources Code Section 30985, effective January 1, 2024.<sup>12</sup> Its provisions, and the provisions of its subsections include, inter alia:

**30985**

- (a) “A local government lying within the coastal zone . . shall develop a sea level rise plan . .
- (b) [The plan] . . . shall include . . . best available science . . . .
- (d) All local governments . . shall comply with this section by **January 1, 2034**

**30985.2**

- (a) On or before December 31, 2024, the California Coastal Commission, in close coordination with the Ocean Protection Council and the California Sea Level Rise State and Regional Support Collaborative, shall establish guidelines for the preparation of the sea level rise plan required pursuant to subdivision (a) of Section 30985. The guidelines shall recognize and build upon the baseline policies as described in the “Sea Level Rise Working Group: 2021 Work Products” as published by the California Coastal Commission on December 3, 2021. . . .

**30985.5**

Local governments that receive approval by the California Coastal Commission or the San Francisco Bay Conservation and Development Commission, as applicable, pursuant to subdivision (a) of Section 30985 shall be prioritized for funding, upon appropriation by the Legislature, for the implementation of sea level rise adaptation strategies and recommended projects in the local government’s approved sea level rise plan.

**30985.6**

The operation of this division is contingent upon an appropriation for its purposes by the Legislature in the annual Budget Act or another statute.

Before Pacifica submits a revised Local Coastal Land Use Plan to the Coastal Commission for final approval, we suggest Pacifica closely analyze and consider – including public consideration – the implications of this new law.

---

<sup>11</sup> City of Pacifica Council Agenda Summary Report, 4/15/24, at Page 2:  
[https://drive.google.com/file/d/1uaZYj6luDf6wODwd7qFS32DzFFv9E3K2/view?usp=drive\\_link](https://drive.google.com/file/d/1uaZYj6luDf6wODwd7qFS32DzFFv9E3K2/view?usp=drive_link)

<sup>12</sup> California Public Resources Code Section 30985, Sea Level Rise Planning and Adaptation,  
[https://leginfo.legislature.ca.gov/faces/codes\\_displayText.xhtml?lawCode=PRC&division=20.6.9.&title=&part=&chapter=&article=](https://leginfo.legislature.ca.gov/faces/codes_displayText.xhtml?lawCode=PRC&division=20.6.9.&title=&part=&chapter=&article=)

**3. Issues raised by the U.S. Supreme Court's April 12, 2024 decision in Sheetz v. County of El Dorado.**

At page 4 of our April 20, 2024 letter to Council<sup>13</sup> we called Council's attention to the Supreme Court's recent Sheetz<sup>14</sup> decision. We suggest that the interplay of the recently-enacted Public Resources Code Section 30985 (discussed on the previous page) and Sheetz is worthy of serious legal analysis and consideration – including public input -- before Pacifica proceeds further. This is not a time to rush. Or be rushed.

Respectfully submitted,

*Richard Harris*

President, San Francisco Public Golf Alliance

cc: City Manager Kevin Woodhouse, Planning Director Christian Murdock, Deputy Planning Director Stefanie Cervantes, Planning Commission and Commissioners, City Clerk Sarah Coffey, Phil Ginsburg, Gen. Mgr., San Francisco Recreation and Parks Dept., Spencer Potter, Esq., San Francisco Recreation and Parks Dept.

---

<sup>13</sup> Letter, SF Public Golf Alliance to Pacifica City Council, re April 2024 Draft LCLUP.4.20.24  
[https://drive.google.com/file/d/1\\_03aFI4RPoKI7ZuyrWztWv23\\_CxqR1G/view?usp=drive\\_link](https://drive.google.com/file/d/1_03aFI4RPoKI7ZuyrWztWv23_CxqR1G/view?usp=drive_link)

<sup>14</sup> Sheetz vs. County of El Dorado, California, U.S. Supreme Court October Term, 2023, No. 22-1074  
[https://www.supremecourt.gov/opinions/23pdf/22-1074\\_bqmd.pdf](https://www.supremecourt.gov/opinions/23pdf/22-1074_bqmd.pdf)

---

**From:** Beckmeyer, Sue  
**Sent:** Monday, April 22, 2024 3:58 PM  
**To:** Public Comment  
**Cc:** Woodhouse, Kevin  
**Subject:** Fwd: Continuation of LCLUP Review Meeting

Please include Frank's comments in the public record for the LCLUP.  
Thank you,  
— Sue B.

---

**From:** Frank Vella [REDACTED]  
**Sent:** Sunday, April 21, 2024 9:55:33 PM  
**To:** \_City Council <citycouncil@ci.pacifica.ca.us>  
**Subject:** Continuation of LCLUP Review Meeting

**[CAUTION: External Email]**

Can anyone tell me about the coastal commission having jurisdiction over linda mar up to Peralta? None of the residents have been notified of this. Is this city council going to allow this? No one bought a property in that area realizing something like this could happen. This is a taking of our personal property that should not happen. What else is our council giving away to the coastal commission that does not care about our city's economic well being, our homes, or our business? Is our council standing up for our citizens or going along with the coastal commission for some reason? From what council member Boles stated, protecting private property is not what we are required to do. Questions come to every residents mind as to what we are doing as we pay tax's and fees for our property, our permits, and for services. If this is the case, then why must a deed restriction be placed upon a resident applying for a permit for their property removing liability to the city. What a deal for all of pacifica. Thanks for the great negotiating on our behalf!

We continually hear that staff is so busy with everything, yet our city manager and council took this task upon themselves and did not seek the assistance or cooperation of other cities who are dealing with the same types of issues or groups like Smart Coast California.

Our city is ripe for litigation with this type of legislation.

And tomorrow's council meeting regarding the Local Coastal plan offers no public comments? Unbelievable. We deserve so much better than this.

Frank Vella  
[REDACTED]  
[REDACTED]  
[REDACTED]

**CAUTION: This email originated from outside of the City of Pacifica. Unless you recognize the sender's email address and know the content is safe, do not click links, open attachments or reply.**

---

**From:** Ed Ochi [REDACTED]  
**Sent:** Monday, April 22, 2024 4:20 PM  
**To:** \_City Council; Public Comment; Coffey, Sarah  
**Subject:** Proposed Local Coastal Land Use Plan (LCLUP)  
**Attachments:** 2024-0422 City Council re LCLUP.pdf

[CAUTION: External Email]

Please find attached a letter outlining my concerns, as a Pacifica resident and property owner regarding the proposed Local Coastal Land Use Plan (LCLUP). In summary, I strongly recommend that you vote against the approval of the Draft LCLUP and its submission in its current form to the California Coastal Commission.

Thank you very much for the time you've invested to date on this and other drafts of the LCLUP and in your continued efforts in creating an appropriate update to the LCLUP on behalf of the residents and property owners of Pacifica.

- Ed

CAUTION: This email originated from outside of the City of Pacifica. Unless you recognize the sender's email address and know the content is safe, do not click links, open attachments or reply.

## Transmitted by Email

April 22, 2024

Pacifica City Council  
540 Crespi Drive  
Pacifica, CA 94044

RE: Proposed Local Coastal Land Use Plan (LCLUP)

Dear Mayor Vaterlaus, Mayor pro Tem Beckmeyer, and Council Members Bier, Bigstyck, and Boles,

After extended consideration and deliberation, as a resident and property owner in Pacifica I am writing you to urge you to vote NO on the approval of the Revised Certification Draft Local Coastal Land Use Plan (LCLUP, referred to hereafter as The Plan) currently under consideration by the Pacifica City Council for transmittal to the California Coastal Commission (CCC). I am basing my recommendation on three factors. As written:

1. The Plan is premature and insufficiently developed,
2. The Plan is divisive to residents and property owners in Pacifica, and
3. The Plan contains unnecessary detail and minutia.

Please note that the this recommendation should not be considered to reflect poorly on Pacifica City Staff, who have in fact done a remarkable job creating and modifying The Plan, particularly considering the limited number of staff available as well as the short time frame, nor of the City Council members who have spent numerous hours in meetings and reviewing The Plan. Unfortunately it is this intense effort that has caused a loss of focus on the “Big Picture” and countless hours refining a flawed plan leading participants to believe they’re creating a workable document.

To expand on the basis for my recommendation:

### **1. The Plan is premature and insufficiently developed:**

The Plan has been repeatedly described as the culmination of many years of efforts to update Pacifica’s LCLUP. This is incorrect, in the present form and particularly with regards to the Special Resiliency Areas (SRAs) and the details needed to address both the SRAs and other areas in Pacifica, The Plan is less than 6 months old and continues to change in response to comments made. This is not a “mature” nor well-vetted plan which is the product of many years of deliberation.

- 1.1. As illustrated by “unofficial” comments made by an employee of the San Francisco Recreation and Parks Department (SFRP) at the April 15<sup>th</sup>, 2024 Special Council Meeting, discussions have not been held with potential partners to create a cohesive plan for all of Pacifica. Instead areas are excluded as not being within Pacifica jurisdictional boundaries, but will in fact greatly impact Pacifica residents and property owners.

- 1.2. The Plan is completely different from other LCLUPs either approved, in draft form, or rejected by the CCC. As there are currently many LCLUPs being updated within the State of California Pacifica, with its extremely limited staffing and budget has little to gain by being “the first”, and much to lose if the City is to become the test bed for implementation, developing new permitting processes, furthering claims real and perceived that the City is slow in the permitting review and issuance process, and defending against lawsuits by residents and property owners who’s rights have changed or whose property values or insurability have been adversely impacted.
- 1.3. The State of California’s Ocean Protection Council is on the brink of releasing new Sea Level Rise Guidance. It is a mistake to be finalizing long-term long-lasting policies such as The Plan when there are strong indications that keystone guidance may change.

**2. The Plan is divisive to residents and property owners in Pacifica:**

In establishing the SRAs The Plan is arbitrarily creating two groups of residents and property owners, those who are within an SRA and those who are not, with different requirements and processes for the two groups. Complicated because some residents and property should be placed into an SRA but are not because The Plan does not address all the oceanfront which makes up Pacifica, The Plan is setting up future division between residents on the locations of significant housing developments, constructing a replacement for the improperly designed and/or aging Sharp Park seawall, and infrastructure creation, upgrading, or replacement projects Citywide all of which will be detrimental to the long-term functionality and well-being of the City. It also creates the potential for every future project such as stormwater system improvements, fire protection, school improvements, access and egress routing, and street repairs and optimizing to be split into camps of those directly impacted or benefiting the most from a project versus those in other parts of town who in a less divided environment understand that such projects help the town as a whole and should be funded out of the City budget. Instead, like earlier versions of the revised LCLUP, The Plan should establish a single standard and set of requirements for all parts of the City.

**3. The Plan contains unnecessary detail and minutia.**

As illustrated in the “comparison table” (*Exhibit A, Revised Certification Draft Local Coastal Land Use Plan (LCLUP) With Alternative Modifications As Approved By City Council On April 15, 2024*) being used to summarize changes to Plan language between the City’s Certification Draft, CCC Suggested Modifications, and Draft Alternative Modifications, significant amounts of time have been invested by City and CCC staff and Council Members to develop grammatically correct language that the City and CCC can agree upon for Plan elements. What has been lost, however, is the “bigger picture” intent of the plan elements as well as whether specific elements are needed in the first place. As a few examples of a widespread problem:

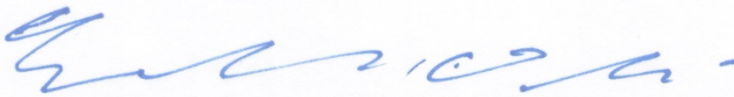
- Modification 7.10, the Glossary Definition of a Substantial (Exterior) Structural Modification (SSM). Edits proposed by the CCC and further

modified by City staff have become increasingly explicit, while failing to define what the actual goal is. Specific roofing system components such as plywood roof sheathing are identified, while other types of roof sheathing (planks, oriented strand board) may not be excluded from being a SSM depending on the interpretation of "other roof materials". Similarly (a) installation of a non-covered appliance like solar panels may require structural upgrades to older buildings and (b) seismic retrofits may be performed not because of specific State or Federal laws and regulations but rather because of other work being performed in the vicinity, because rate reductions to insurance policies can be obtained (or insurance can be continued with the insurance company dropping coverage if the work is not performed), or with eye to future sales of home where the retrofit work will be required. Instead of adding such clarifications and refinements elements should identify the purpose of the element and define prohibited activities.

- Modification 6.9, Critical Transportation Infrastructure. City transportation goals should be part of general planning documents, not part of The Plan. CCC proposed language gives undue focus or weight to transportation with regards to coast resource public access and recreation. As legal obligations are already defined in the California Coastal Act this discussion and special language is unnecessary.
- Modification 4.10, Coastal Environment and Special Species Status Communities; 4.12, Protection of Biological Resources with New Development; and 5.3, Reduce Risk (*examples only*). The Certification Draft of the Plan makes relatively simple statements, which are being expanded with each iteration. The question is whether these expansions are actually necessary and whether the expanded definitions give undue focus and emphasis to coastal areas, particularly those under CCC jurisdiction compared to other locations within the City which may actually have greater needs.

With the above in mind I strongly encourage you to vote NO on the approval of the Revised Certification Draft Local Coastal Land Use Plan.

Respectfully,



Edward Ochi  
Pacifica Resident



---

**From:** Beckmeyer, Sue  
**Sent:** Monday, April 22, 2024 4:22 PM  
**To:** Public Comment  
**Subject:** Fwd: Please reject current SRA plan

Please add this comment to the public record for the LCLUP.  
Thank you,

- Sue B.

---

**From:** [REDACTED]  
**Sent:** Monday, April 22, 2024 10:53:09 AM  
**To:** \_City Council <citycouncil@ci.pacifica.ca.us>  
**Subject:** Please reject current SRA plan

**[CAUTION: External Email]**

Hello Council Members and fellow Pacificans,

I am writing to express my concern with the current SRA plan, the one council is considering returning to the Coastal Commission on behalf of our city.

As a resident and voter I feel it is the Council's duty to protect the City of Pacifica from unreasonable restrictions that will diminish the value and happiness of its' residents and businesses along the coast.

I would like the Council to look at and use the most recent sea-level projections. We know every part of this coast is unique and needs to be considered individually in any SRA.

Please don't let the Coastal Commission bully our city into any uninformed and broad-brushed coastal plan. I'd like you all to continue fighting for our right to keep and protect the residents and businesses that add color and prosperity to our coastal town.

Thanks you for reading this.

Paolo Vescia  
West Fairview

**CAUTION: This email originated from outside of the City of Pacifica. Unless you recognize the sender's email address and know the content is safe, do not click links, open attachments or reply.**

---

**From:** Beckmeyer, Sue  
**Sent:** Monday, April 22, 2024 4:34 PM  
**To:** Public Comment  
**Subject:** Fwd: Approval of LCLUP 4/22/24

Please include Dan's comments in the public record for the draft LCLUP.

— Sue B.

---

**From:** Dan Yonts [REDACTED]  
**Sent:** Monday, April 22, 2024 2:07:41 PM  
**To:** Vaterlaus, Sue <svaterlaus@pacificacounty.gov>; Beckmeyer, Sue <sbeckmeyer@pacificacounty.gov>; Bier, Mary <mbier@pacificacounty.gov>; Bigstyk, Tygarjas <tbigstyk@pacificacounty.gov>; Boles, Christine <CBoles@pacificacounty.gov>  
**Subject:** Approval of LCLUP 4/22/24

[CAUTION: External Email]

Mayor Sue Vaterlaus  
Mayor Pro Tem Sue Beckmeyer  
Council Member Mary Bier  
Council Member Tygarjas Bigstyk  
Council Member Christine Boles

There is so much in this LCLUP draft that can be interpreted as a 'Taking' of property through the adoption of a 'Managed Retreat' policy.

Regarding the portion being addressed tonight;

From Sec. 6.1 where there's the removal of 'Rights' from the phrase 'Protection of Property Rights' to the Glossary where there's the deletion of the entire definition of 'Existing Structures' in 7.7 and the deletion of Coastal Act 30212 (b)(2) from the definition of SSM's in Sec. 7.10, this draft of the LCLUP is ripe with language and policies that will lead to future litigations against the City of Pacifica.

There's a pending case at the appellate court level regarding the definition of Existing Structures in HMB. A SM County Superior Court judge found in favor of the property owners in the Casa Mira v. CCC, upholding the long standing interpretation that Existing means at the time of the Permit request.

If this case goes to the US SC it is likely the current Justices will find in favor of property owner's rights. It is a Court that is interpreting Constitutional rights from a conservative view. On 4/12/24 they found in favor of the property owner in Sheetz v. El Dorado. They determined that the Takings Clause does not distinguish between legislative and administrative permit conditions.

I'm sure you're all familiar with how the Beachwood property case, Yamagiwa v. HMB, was judged to be a Taking and almost bankrupt HMB.

Regarding the removal of the language from Coastal Act 30212 in this LCLUP. It defines what is allowed to be done to Existing Structures.

(b)(2) states:

“The demolition and reconstruction of a single-family residence; provided, that the reconstructed residence shall not exceed either the floor area, height or bulk of the former structure by more than 10 percent, and that the reconstructed residence shall be sited in the same location on the affected property as the former structure.”

If my grandchildren are not allowed to rebuild our home it would be a slow managed retreat and eventually a Taking. A deed restriction would make my house uninsurable and therefore unsellable since no bank would issue a loan. The devaluing of my property based on a (not scientifically agreed upon) future hazard, so that the State can buy it on the cheap and rent it back to me is a Taking.

There is language in this LCLUP that mentions the waiving of actual existing property rights. The phrases ‘Anticipated life’ and ‘Life expectancy’ absolutely imply the adoption of a Managed Retreat policy.

I want Beach Blvd and Rockaway to have the protections the original Coastal Act allows. But this current LCLUP would be incredibly detrimental to the Beautiful City of Pacifica and would be devastating to it’s wonderful people. The adoption of this current version of the LCLUP would result in many lawsuits against the City, not against the CCC; And the CCC would have no legal responsibility to assist us. Pacifica would not be able to survive one lawsuit as costly as the Beachwood Property case in HMB, let alone 100’s.

Please protect Pacifica and it's Residents. Do not approve this version of the LCLUP.

With much respect,  
Dan Yonts

[REDACTED]

CAUTION: This email originated from outside of the City of Pacifica. Unless you recognize the sender's email address and know the content is safe, do not click links, open attachments or reply.

---

**From:** Ruth Reynolds [REDACTED]  
**Sent:** Monday, April 22, 2024 7:58 PM  
**To:** Public Comment  
**Subject:** Public meet tonight, put last on agenda. No public in put. Hope my husband is wrong

[CAUTION: External Email]

Sent from my iPhone. He said no point in saying anything, they will do what ever they want! Don't believe that will stand.

CAUTION: This email originated from outside of the City of Pacifica. Unless you recognize the sender's email address and know the content is safe, do not click links, open attachments or reply.

---

**From:** Cherie Chan [REDACTED]  
**Sent:** Monday, April 22, 2024 11:55 PM  
**To:** Public Comment; Beckmeyer, Sue; Christine Boles; Vaterlaus, Sue; Murdock, Christian; Bier, Mary; Bigstycck, Tygarjas  
**Subject:** Subject Line: Item X: 05/XX/2024: Continuation of Adjourned Special Meeting from April 12, 2024 - Modifications to the City of Pacifica's Revised Certification Draft Local Coastal Land Use Plan (LCLUP), including the Special Resiliency Area policies, a...  
**Attachments:** 2024-05-XX\_Chan-LCLUP\_Comments.docx

**[CAUTION: External Email]**

Attached are my questions following tonight's meeting.  
Thank you for your continued diligence.

**CAUTION: This email originated from outside of the City of Pacifica. Unless you recognize the sender's email address and know the content is safe, do not click links, open attachments or reply.**

To: [publiccomment@pacifica.gov](mailto:publiccomment@pacifica.gov)  
CC: via [NorthCentralCoast@coastal.ca.gov](mailto:NorthCentralCoast@coastal.ca.gov)

Subject Line: Item X: 4/21/2024: Continuation of Adjourned Special Meeting from April 12, 2024 - Modifications to the City of Pacifica's Revised Certification Draft Local Coastal Land Use Plan (LCLUP), including the Special Resiliency Area policies, and direction to staff regarding transmittal of alternative modifications to the California Coastal Commission

Dear City of Pacifica Decision-Makers,

Since questions from my councilmember in district five centered around personal property values and legal risk, I'd like to submit this question: What risk is the City under, if it makes a ministerial change without regard to the conditions on the ground to change a Land Use Designation from Commercial Recreation, which allows for low-intensity coastal-oriented visitor-serving uses to a substantially higher-intensity residential mixed-use, and removes my right to walk to the California Coast?

## Background

My husband and I purchased our home in 2008, a full eighteen months after being prequalified for our loans and following extensive research in Pacifica. We did our research, checked with relevant agencies, and insurance and eliminated several homes with high potential for fire, landslide, and sea level rise risk, which we took very seriously in Pacifica.

We thoroughly researched the vacant five-acre parcel in the wetlands across the street from our house, as we recognized that any significant change would drastically affect our quality of life, and took several walks through the field, and met many potential neighbors. We learned that it had been a golf driving range which had been purchased from the Catholic Church in the late 1990s. We determined from US Fish and Wildlife that it was a Federally mapped wetlands as shown below.

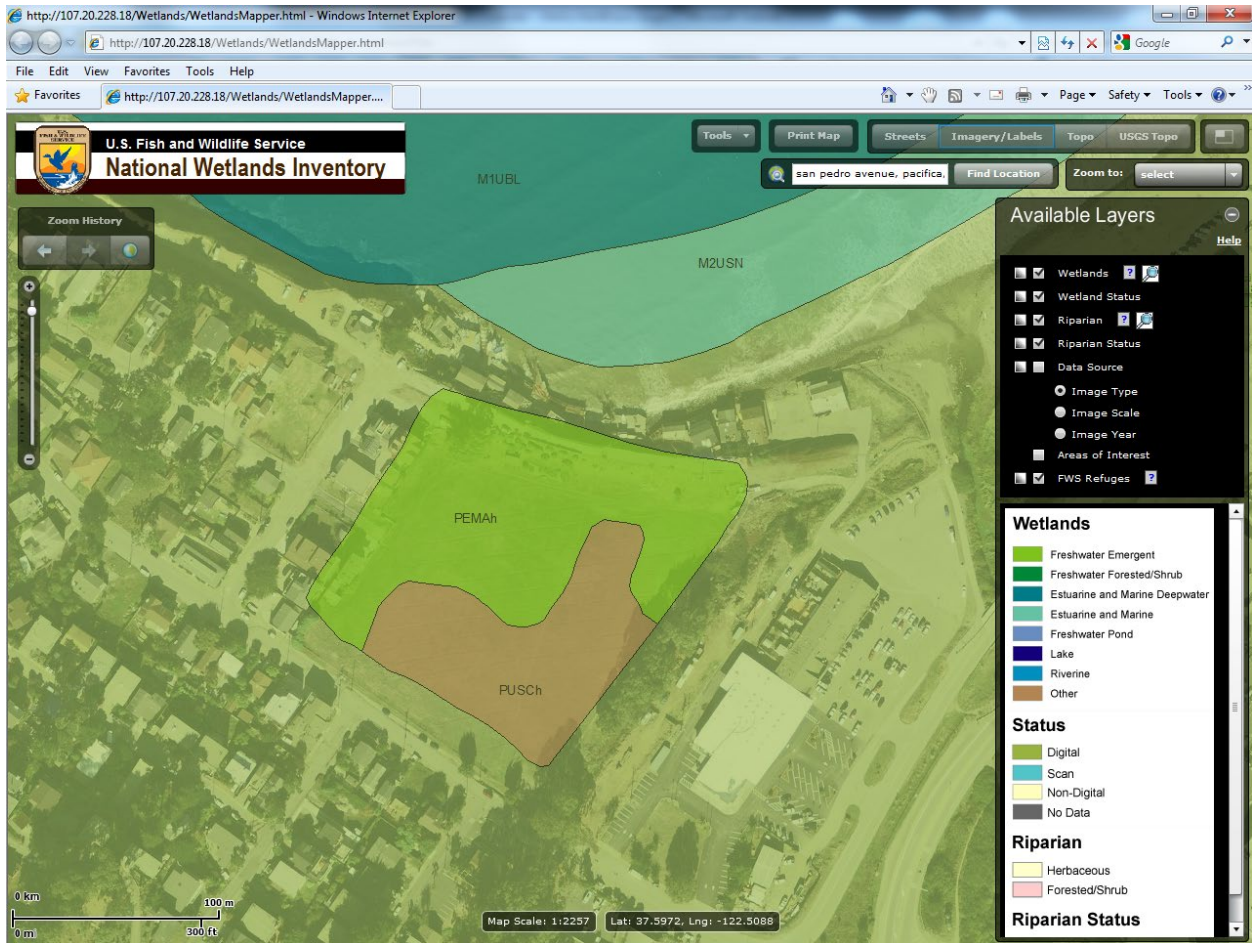
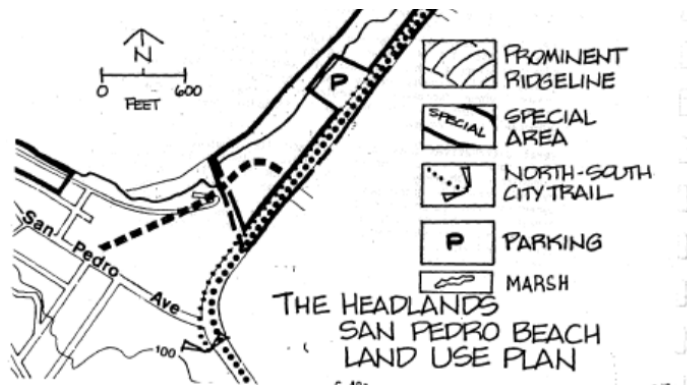


Figure 1 US Fish and Wildlife Service map from 2012

We learned that the wetlands would be a vital part of the planned California Coastal Trail.<sup>1</sup>

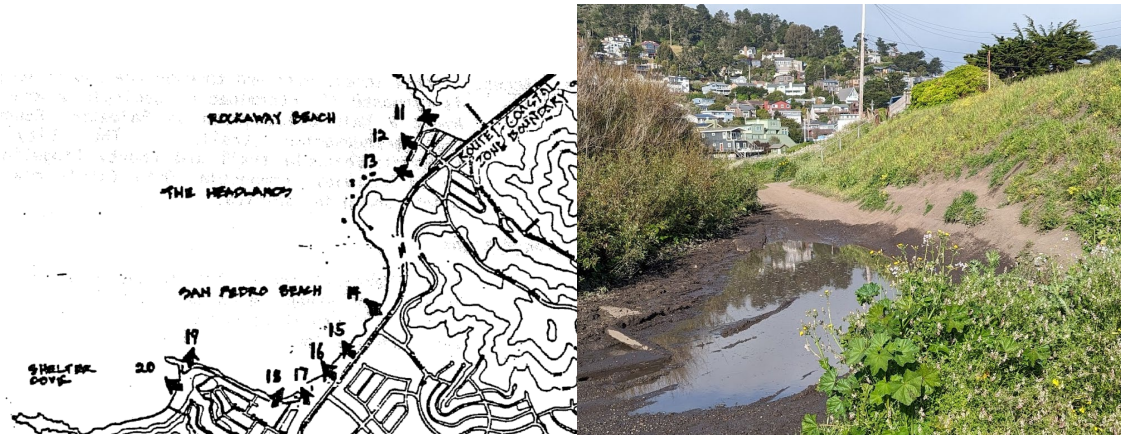


(Excerpt from current LCP)

We learned that the Coastal Act and the City of Pacifica through their Certified Land Use plan promised this access, and that this access would be retained, acknowledging the known hydrological challenges of being in a seasonal wetlands. For example, access to point 17 in the

<sup>1</sup> "Completing the California Coastal Trail. California Coastal Conservancy, January 2003. Report is prepared pursuant to Senate Bill 908, Chapter 446, Statutes of 2001.

current LCP, below, on the map, is currently blocked as shown below (picture taken yesterday) due to seasonal flooding.



The City, in proposing a change in the Land Use Designation to Coastal Residential Mixed Uses, rather than what is in the current LCP, seeks to deprive my family, and an entire community, of the right to enjoy the Coast.

Residents and visitors have been crossing the Field for years to access the California Coast, our primary reason for moving to Pedro Point. Will there be compensation for these property owners when their property rights are taken away through Force Majeure or climate change, but purely through a capricious administrative determination to take away theirs and the public's right to enjoy coastal access?

The Pedro Point Community Association has already spent thousands of dollars hiring former Pacifica planning directors to mediate public meetings, lawyers, biologists, and CEQA experts to fight this unsupported, ill-conceived change. Please provide any justification for why this change should be made.

Thank you.

Cherie Chan

San Pedro Avenue



---

**From:** Linda Acosta [REDACTED]  
**Sent:** Tuesday, April 23, 2024 8:55 PM  
**To:** Bigstycck, Tygarjas; Public Comment; Vaterlaus, Sue; Boles, Christine; \_City Council; Bier, Mary; Beckmeyer, Sue; Coffey, Sarah  
**Subject:** Re: Reject SRA concept in response to Coastal Commission

**[CAUTION: External Email]**

I own a home in West Fairway. When I had to sign off last night (at around 10:30 pm) the council seemed to be moving toward not voting in the LCLUP.

What was the final decision and next steps?

It is unbelievable to me that while I live in an area that has a very little chance of flood or erosion, I am paying the highest price, while those who are near the cliff's edge are being protected by you.

When you were elected into your positions you were to represent all of Pacifica. You talked a lot about not having updated the LCLUP for the last 40 years. The fact that you have spent the last few years spending our precious tax dollars on building a new office for yourselves and buying pretty street lamps for Palmetto, while buildings had already fallen into the ocean and we knew sea level rise was happening, is absurd.

My house on Pinehaven is not in any flood or erosion zone. You must protect us homeowners and our hard earned assets, especially against a threat that doesn't even exist for us. We will not be used as an offering up to the Coastal Commission in order to protect your favored areas. We will fight back.

Linda Acosta

On Mon, Apr 22, 2024 at 10:19 AM Linda Acosta [REDACTED] wrote:

Dear Mayor Vaterlaus and Council Members,

Once again, I urge City Council to reject the SRA concept in the response to Coastal Commission staff's proposed changes, especially as you review Chapter 6 of this proposal.

As you have heard, no one in Pacifica likes these LCLUP changes. You may hear staff say that this is a sign of good negotiations because no one gets everything they want. But this is not a negotiation between Pacifica's residents (that was done with the 2020 LCLUP Draft), this is a negotiation between Coastal Commission's staff and city staff. With this proposal CCC staff is getting everything they want.

SRAs are not about giving two areas, West Sharp Park and Rockaway Beach, special treatment. It's really about removing rights from all the other coastal areas in Pacifica they are entitled to by the Coastal Act. This is arbitrary, not fair, and not legal.

Ask yourself and staff why changing floor structures, such as adding earthquake bracing, constitutes an SSM? What does this have to do with addressing climate change? This is punishing people for doing the right thing. The Coastal Commission should not be in the remodeling business.

Consider the following examples about the proposed LCLUP:

- A pre-Coastal Act home in a non-SRA location with a second story added in 1980 is **instantly** considered an SSM when they get a permit.
- That same home will have to “correct any legal nonconformities”, but there is no definition of what that means.
- Homes in non-SRA areas such as West Fairway Park (1/2 mile from the shoreline) would have more restrictions than homes on Beach Blvd at ground zero for sea level rise hazards.
- Insurance rates will skyrocket and/or policies cancelled due to new restrictions.
- Property values and tax assessments will plummet.
- As mentioned earlier, the Coastal Vulnerability Maps are error-ridden and not accurate. The Coastal Commission and the City are using them for policies, even though the disclaimer below each CVZ map says they are not intended for this purpose.
- OPC will be approving their new 2024 Sea Level Guidance on June 4. That's only 44 days away. This is the best available science which predicts 3.1ft of sea level rise by 2100 instead of the 5.7ft prediction in the old 2017 guidance. There is **no reason** to push this through now and hope that Coastal Commission will accept an amendment. This is foolish, irresponsible, and contrary to the LCLUP's statement that it uses the “best available science”.
- Coastal Commission's amendment and public comment review process will take months/years for an amendment to happen. As an example, Dana Point proposed an amendment to their LCP-5-DPT-21-0079-2 on April 17, 2023. On June 22, 2023, Coastal Commission staff requested and received a one-year extension for Coastal Commission action. Public comment has been reopened again. It is still ongoing with no decision in sight. Please don't be fooled when city staff says they think an amendment will take a few months.

It must be clear to Council, as it is to us residents, that the Coastal Commission's goal is to remove all development (homes, businesses, and shoreline protections) from Pacifica's coast.

This LCLUP proposal shifts Coastal Commission's legal responsibilities to the City, exposing the City to multiple single- and class-action lawsuits. This disastrous outcome will bankrupt Pacifica.

I urge you to direct staff to remove the SRA concept and treat all residents, homes, and businesses the same under the Coastal Act. Do not concede our rights or require restrictions that force us to give them up to the Coastal Commission. City Council represent Pacifica residents, not the Coastal Commission.

Respectfully,

Linda and Emiliano Acosta

**CAUTION:** This email originated from outside of the City of Pacifica. Unless you recognize the sender's email address and know the content is safe, do not click links, open attachments or reply.

---

**From:** Lawrence Bothen [REDACTED]  
**Sent:** Thursday, April 25, 2024 5:07 PM  
**To:** \_City Council; \_City Council  
**Cc:** Public Comment; Public Comment; Coffey, Sarah; Woodhouse, Kevin; Murdock, Christian; Cervantes, Stefanie; Cervantes, Stefanie  
**Subject:** Comments on LCLUP Meeting 4.5, 22 Apr 24

[CAUTION: External Email]

Monday night I watched Pacifica's City Council grapple again with the complexities of the LCLUP when the reason you've been stuck for so long dawned on me. It just doesn't make sense. It doesn't seem possible. Try to explain to a rational person not familiar with the subject that an omnipotent, imperial state agency is trying to destroy your coastal city and they look at you like little green men are poking out through your tinfoil hat. Try explaining that to friends at a dinner party. They ask, "why would anyone want to do that? Are you feeling ok? What's next? Alien abductions?"

NO! They're telling us you either get managed retreat in all the coastal zones, or you can carve out SRA's for 2 small areas and everyone else still gets the shaft. Pretend shoreline protections aren't there. Unless you're in an SRA. But once they're gone so are you. You can replace your roof but if the joists are rotted it's an SSM, and you have to sign a deed restriction.

Or you can't be in an SRA because you will only get flooding, not erosion. And no matter how arbitrary or contradictory, it's explained to you in a calm, rational voice, not with wild-eyed arm waving. But on paper the words look like the ravings of a lunatic.

Yet last night I could see the light bulbs turning on. You asked probing questions about these topics again and still the answer makes no sense. It's because it doesn't. For every response that seems to have a basis in fact there are tangents that take it down the nearest rabbit hole. Suddenly you're Alice in Wonderland and the White Knight is talking backwards.

Mary Bier noted that folks on both sides of the issue oppose the LCLUP even if for different reasons. There's something in it for everyone to hate and nothing to love. "We have to help the people," she said. Tygar compared it to a choice of "having your arms and legs cut off or just two arms and a foot." It's like choosing poison or a bullet. Both will kill you, in different ways.

Sue Beckmeyer brought it into focus. "We are NOT on the same page," she said, noting that the CCC struck "protection of private property" from the city's 2020 Draft LCLUP. "How can we ever get agreement?" she asked. She suggested it be set aside to wait for the Ocean Protection Council's new data predicting almost 50% LESS sea level rise than the 2017 model. Let other cities take the point. We should also wait out the tidal wave of lawsuits that are starting to wash over the Coastal Commission. Courts do not look kindly on takings. Precedents set in other cases are likely favorable to us as well.

Woodhouse responded with a condescending explanation of the purpose of an LCLUP, skirting its effect. Murdock talked about the time CCC staff has devoted to his staff and the great working relationship they've developed. Great for them. Pacifica does all the compromise. If we set this one aside we would have to start over and wait several more years for approval. Considering what they've turned this one into that sounds like a damn good idea.

Beckmeyer countered that the perception of CCC overreach is everywhere in the coastal zones, where homeowners are being told to make sacrifices others don't have to. It's an issue of equal protection under the law. She has real concerns about the legal liabilities the LCLUP could bring down on Pacifica. They are more than justified. They will happen.

Four councilmembers voted to continue to study the LCLUP at a date to be determined. But Beckmeyer's NO vote is the only rational choice. You've all displayed misgivings about the plan. But you've pulled back because you don't want to lose momentum, or the relationship Planning has with CCC is too special to let go. Those are hollow excuses for terrible policy.

Would you play along just to spare their feelings? Secretly you must be wondering "how will I ever sell this hot mess to my constituents?" You can't, because the current LCLUP offers only two choices - disastrous or apocalyptic. So do the right thing. Set this hot mess aside, line up behind Sue Beckmeyer and follow the leader.

Sincerely,

Larry Bothen  
Rockaway

CAUTION: This email originated from outside of the City of Pacifica. Unless you recognize the sender's email address and know the content is safe, do not click links, open attachments or reply.

---

**From:** Beckmeyer, Sue  
**Sent:** Monday, April 29, 2024 9:39 PM  
**To:** Public Comment  
**Subject:** Fwd: The LCLUP

Please add this comment to the public record for the LCLUP.

Thank you,  
— Sue B.

---

**From:** ANDY PATTERSON [REDACTED]  
**Sent:** Monday, April 29, 2024 4:51:09 PM  
**To:** \_City Council <citycouncil@ci.pacifica.ca.us>  
**Subject:** The LCLUP

**[CAUTION: External Email]**

Good Evening to you all,

Please know that we understand the complexity of the plan changes and we don't think that you need to be first to complete it. Advising you to put it on the back burner and wait till others complete theirs'. There will be more environmental information within the next few months, that just might assist you in answering the California Coastal Commission. Don't feel pressured to be the first to respond.

Respectfully,  
Andy and Kerry Patterson

**CAUTION: This email originated from outside of the City of Pacifica. Unless you recognize the sender's email address and know the content is safe, do not click links, open attachments or reply.**

---

**From:** Coffey, Sarah  
**Sent:** Wednesday, May 1, 2024 9:56 AM  
**To:** Public Comment  
**Cc:** Murdock, Christian; Cervantes, Stefanie  
**Subject:** FW: Huge Misunderstanding on SRA's - Pacifica LCLUP April 22, 2024 Mtg

---

**From:** Therese Swan [REDACTED]  
**Sent:** Wednesday, May 1, 2024 9:53 AM  
**To:** \_City Council <citycouncil@ci.pacifica.ca.us>; Coffey, Sarah <scoffey@pacifica.gov>; Woodhouse, Kevin <kwoodhouse@pacifica.gov>; Vaterlaus, Sue <svaterlaus@pacifica.gov>; Beckmeyer, Sue <sbeckmeyer@pacifica.gov>; Bier, Mary <mbier@pacifica.gov>; Bigstyck, Tygarjas <tbigstyck@pacifica.gov>; Boles, Christine <CBoles@pacifica.gov>  
**Subject:** Huge Misunderstanding on SRA's - Pacifica LCLUP April 22, 2024 Mtg

**[CAUTION: External Email]**

To: Pacifica City Council

I have a home on Beach Blvd in Pacifica and have been attending as many of the LCLUP meetings as I have been able to do, considering my work schedule.

First, I wanted to thank City Council for all their work on this. It was apparent to me from the April 22<sup>nd</sup> meeting that each and every one of you are trying to do what is best for the community. The problem is, that nobody, including myself, really knows what “best” means. It must be very stressful for all of you to go through this process.

Second, I also wanted to apologize. While I consider myself a reasonably intelligent person, it became clear to me during the April 22 meeting that I have been terribly confused on the concept of SRA's. There may be other members of the community who have this same confusion.

Prior to April 22 meeting, I considered SRA's to be bad and that they would harm those of us who live in West Sharp Park and I made public comments related to this. But, I was comparing SRA's to “Today As We Know It”. I was not considering that “Today As We Know It” will likely not exist in the future if we are stuck living with California Coastal Commission's grips on us. If Pacifica does move forward with the new LCLUP that has been being discussed, then we ABSOLUTELY MUST HAVE SRA's to minimize the damage to those of us owning properties built after the Coastal Commission was established. While there may be other neighborhoods who don't like this, as was pointed out during the meeting, adding those neighborhoods could be considered disingenuous. However, maybe there is something else the City could do to help those neighborhoods with their specific issues. Harming Sharp Park does not help them in any way.

So, my first choice would be to immediately rebuild the seawall but otherwise leave things as they are “Today As We Know It”. But, if that is not possible, then SRA's have to be put in place in a new LCLUP. It would make no sense for people living along the beach in homes built pre-1972 to have protections but their neighbors' homes built after that not to have protections.

Also, I think there may be others in the community who have been as confused about SRA's as I have been. It sure would be nice if there was a handbook available "LCLUP for Dummies". 😊

Thank you,

Marie Swan  
[REDACTED]  
[REDACTED]

**CAUTION:** This email originated from outside of the City of Pacifica. Unless you recognize the sender's email address and know the content is safe, do not click links, open attachments or reply.



---

**From:** Beckmeyer, Sue  
**Sent:** Saturday, May 4, 2024 7:48 AM  
**To:** Public Comment  
**Subject:** Fwd: Please include the latest Probabilistic tsunami hazard analysis (PTHA) data for California (2023 release)" in LCLUP draft!  
**Attachments:** AECOM-ProbabilisticTsunamiHazardMapsForCalifornia-Phase2-2.pdf; Dear City council and city planning.pdf

Please include Jiaheng Qiu's comment and attachments in the permanent public record for the LCLUP.

Thank you,

— Sue B.

Get [Outlook for iOS](#)

---

**From:** J Qiu [REDACTED]  
**Sent:** Saturday, May 4, 2024 12:54 AM  
**To:** Vaterlaus, Sue <svaterlaus@pacific.gov>; Bigstycck, Tygarjas <tbigstycck@pacific.gov>; Beckmeyer, Sue <sbeckmeyer@pacific.gov>; Boles, Christine <CBoles@pacific.gov>; Bier, Mary <mbier@pacific.gov>; Woodhouse, Kevin <kwoodhouse@pacific.gov>; Coffey, Sarah <scoffey@pacific.gov>; Pacifica Permit Tech <permittech@pacific.gov>  
**Subject:** Please include the latest Probabilistic tsunami hazard analysis (PTHA) data for California (2023 release)" in LCLUP draft!

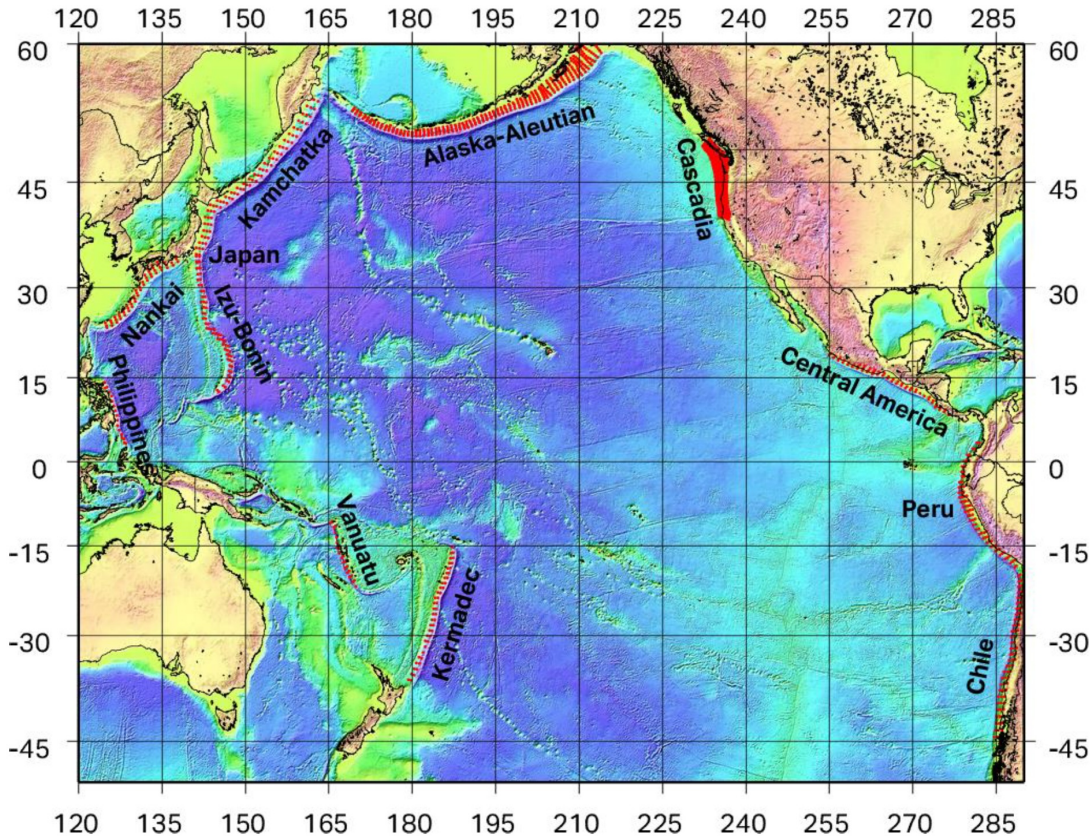
**[CAUTION: External Email]**

Dear City council and city planning team (please kindly forward to Mr Murdock),

My name is Jiaheng Qiu. I'm a statistician and data scientist who has received rigorous training of statistics (I hold a PhD of biostatistics from UCLA), and have over 10 years industry experience of analyzing and modeling data. As a Pacifica resident and home owner since 2016, I really appreciate the city planning team, and city council's diligent work in the recent development of LCLUP draft and difficult negotiation with CCC. However, I'm deeply concerned about the mention of the tsunami inundation zone in the current LCLUP draft ( and thanks again for pushing back the wording of tsunami evacuation zone!) I strongly recommend that the city planning team clearly define the tsunami inundation zone in the LCLUP as "Tsunami hazard map of ARP 475 years based on Probabilistic tsunami hazard analysis (PTHA) data for California (2023 release)". The reasons are as follows.

As many of the public comments have rightly pointed out: The California inundation map, published in 2009, "are intended for local jurisdictional, coastal evacuation planning uses only. They are not legal documents and do not meet disclosure requirements for real estate transactions nor for any other regulatory purpose. " (source <https://www.conservation.ca.gov/cgs/tsunami/maps>). Why is that? Per their disclosed methodology, the tsunami sources selected for inclusion in development of the new maps represent large, realistic events primarily from the Alaska and Cascadia subduction zones, equivalent to a baseline of the 975-year average return period (ARP)! (source <https://www.conservation.ca.gov/cgs/Documents/Tsunami/Tsunami-inundation-map-methodology-2019.pdf>). The 2009 maps (15 years old!) were developed for emergency response use

only, and because of the nature of their purpose they are purposely conservative based on knowledge of tsunami sources at the time.



Last year 2023, CGS published the latest study of Probabilistic Tsunami Hazard Maps for the State of California (Phase 2) (<https://www.conservation.ca.gov/cgs/tsunami/reports>). The report “**provides probabilistic maps that have been developed according to common standards in engineering practice and cover a range of probability (risk) levels. Their potential use therefore goes beyond the emergency response application of the previous mapping projects, into areas of land-use and construction planning (California PTHA Work Group, 2015).**” All the maps are available for download in <https://doc.app.box.com/v/capthadata1?sortColumn=name&sortDirection=ASC>. The study provided tsunami hazard maps based on ARP of 100 year, 475 year, and 975 year etc. For our discussion of LCLUP, I strongly recommend to use the 475 year hazard map (i.e. the hazard map for Tsunami occurs on average every 475 years). The reason is that the major cause of Tsunami is an earthquake underneath the ocean, and the tsunami that would threaten California is primarily from the Alaska and Cascadia subduction zones. As pointed out in the above report (pg 21), “for the shorter return periods (475 yr), the Alaska source region has a larger contribution to the hazard than Cascadia”, whereas “at the longer return period, the Cascadia subduction zone becomes rapidly more important and dominates the hazard at 2475 year ARP. ”

Exceedance waveheights: 975 yr

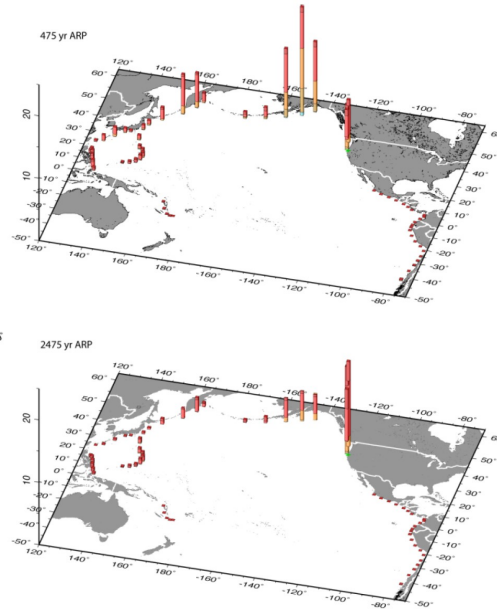
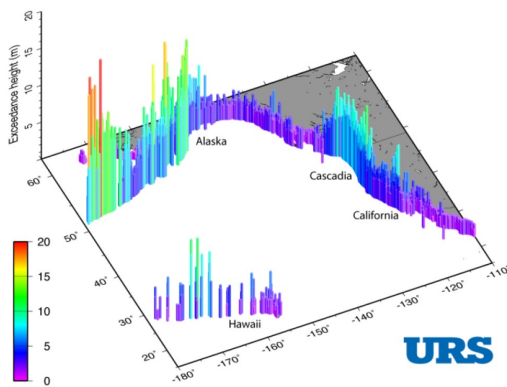


Figure 9. Probabilistic offshore hazard. a (top) shows the offshore hazard, with bar height and colors indicating the exceedance amplitude in meters. b (right) – Source disaggregation showing the relative contribution for different return periods. The colors indicate magnitude ranges.

Note that the Alaska-Aleutian Trench hosted the second largest earthquake (M9.2) recorded by modern seismic instrumentation, which happened in March 27, 1964 earthquake. And according to geologic records, the last major earthquake in Cascadia subduction zone happened in 1700. In other words, the “imminent” tsunami risk has been significantly reduced since 60 years ago, and therefore even if we use the tsunami hazard map based on an ARP of 475 years, we are talking about the next major tsunami that may arrive in Pacifica in 400 years later! I would request the city council to put it into perspective of 100 years expected life span of a residual house, and a general time horizon of 20 years for city development plan! The tsunami hazard map of ARP of 475 strikes a really good balance between the consideration of sea level rise, appropriate risk level of tsunami in the next 100 years and the LCLUP's immediate significant impact, once passed, to ALL the Pacifica homeowners! (Worth-noting that Flood Insurance Rate Maps (FIRMs) generally identify areas of greater flood risk (100 and 500 year events)).

Lastly, I would like to include the **Probabilistic** Tsunami Hazard Maps for the State of California (Phase 2) of ARP 475 years for your reference. I'm more than happy to provide help to obtain the map from the CGS website <https://doc.app.box.com/v/capthadata1?sortColumn=name&sortDirection=ASC>. Also in attachment is the report of Probabilistic Tsunami Hazard Maps for the State of California (Phase 2) as well as the pdf copy of this email. Again, I strongly recommend the city planning team to clearly define the tsunami inundation zone as “**Tsunami hazard map of ARP 475 years based on Probabilistic tsunami hazard analysis (PTHA) data for California (2023 release)**”.

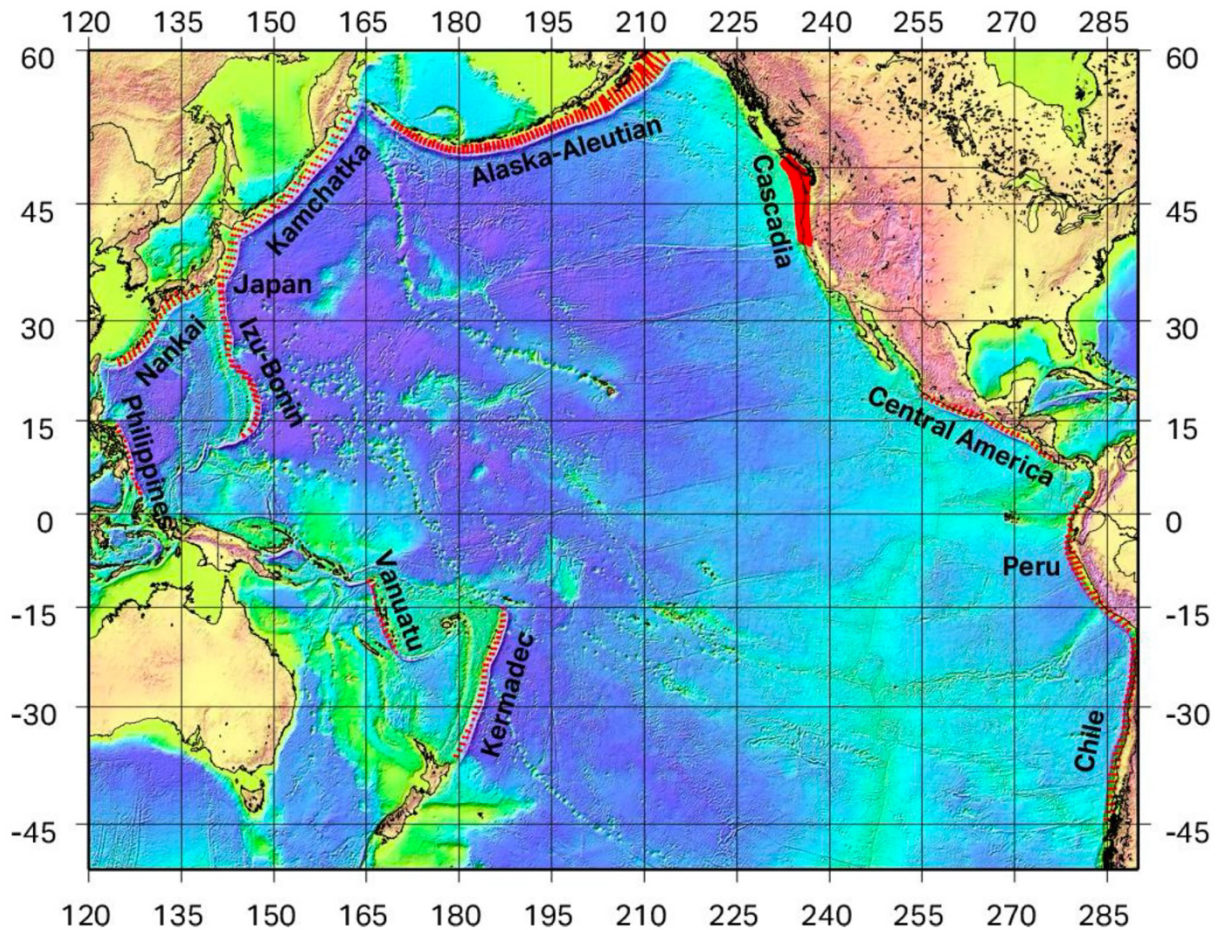
Best regards,  
 Jiaheng  
 Phone # [REDACTED]

Dear City council and city planning team (please kindly forward to Mr Murdock),

My name is Jiaheng Qiu. I'm a statistician and data scientist who has received rigorous training of statistics (I hold a PhD of biostatistics from UCLA), and have over 10 years industry experience of analyzing and modeling data. As a Pacifica resident and home owner since 2016, I really appreciate the city planning team, and city council's diligent work in the recent development of LCLUP draft and difficult negotiation with CCC. However, I'm deeply concerned about the mention of the tsunami inundation zone in the current LCLUP draft ( and thanks again for pushing back the wording of tsunami evacuation zone!) I strongly recommend that the city planning team clearly define the tsunami inundation zone in the LCLUP as **“Tsunami hazard map of ARP 475 years based on Probabilistic tsunami hazard analysis (PTHA) data for California (2023 release)”**. The reasons are as follows.

As many of the public comments have rightly pointed out: The California inundation map, published in 2009, "are intended for local jurisdictional, coastal evacuation planning uses only. They are not legal documents and do not meet disclosure requirements for real estate transactions nor for any other regulatory purpose.

“ (source <https://www.conservation.ca.gov/cgs/tsunami/maps>). Why is that? Per their disclosed methodology, the tsunami sources selected for inclusion in development of the new maps represent large, realistic events primarily from the Alaska and Cascadia subduction zones, equivalent to a baseline of the 975-year average return period (ARP)!(source <https://www.conservation.ca.gov/cgs/Documents/Tsunami/Tsunami-inundation-map-methodology-2019.pdf>). The 2009 maps (15 years old!) were developed for emergency response use only, and because of the **nature of their purpose they are purposely conservative based on knowledge of tsunami sources at the time.**



Last year 2023, CGS published the latest study of Probabilistic Tsunami Hazard Maps for the State of California (Phase 2) (<https://www.conservation.ca.gov/cgs/tsunami/reports>). The report “**provides probabilistic maps that have been developed according to common standards in engineering practice and cover a range of probability (risk) levels. Their potential use therefore goes beyond the emergency response application of the previous mapping projects, into areas of land-use and construction planning (California PTHA Work Group, 2015).**” All the maps are available for download in <https://doc.app.box.com/v/caphadatav1?sortColumn=name&sortDirection=ASC>. The study provided tsunami hazard maps based on ARP of 100 year, 475 year, and 975 year etc. For our discussion of LCLUP, I strongly recommend to use the 475 year hazard map (i.e. the hazard map for Tsunami occurs on average every 475 years). The reason is that the major cause of Tsunami is an earthquake underneath the ocean, and the tsunami that would threaten California is primarily from the Alaska and Cascadia subduction zones. As pointed out in the above report (pg 21), “for the shorter return periods (475 yr), the Alaska source region has a larger contribution to the hazard than Cascadia”, whereas “at the longer return period, the Cascadia subduction zone becomes rapidly more important and dominates the hazard at 2475 year ARP. ”

Exceedance waveheights:975 yr

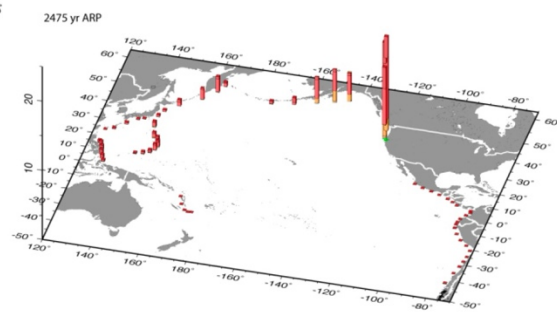
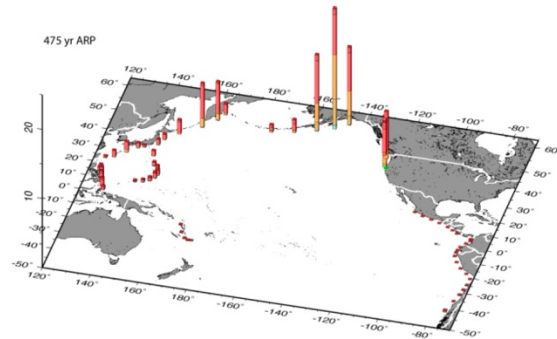
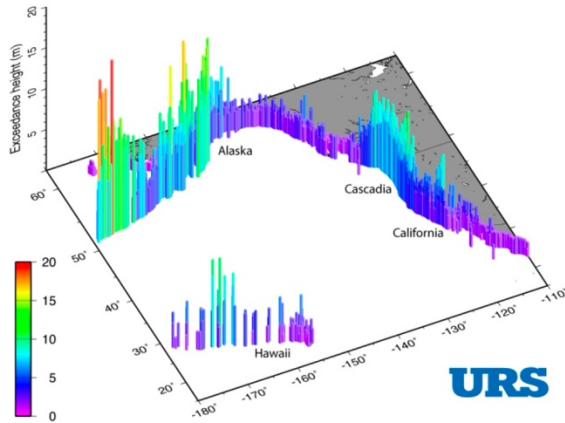
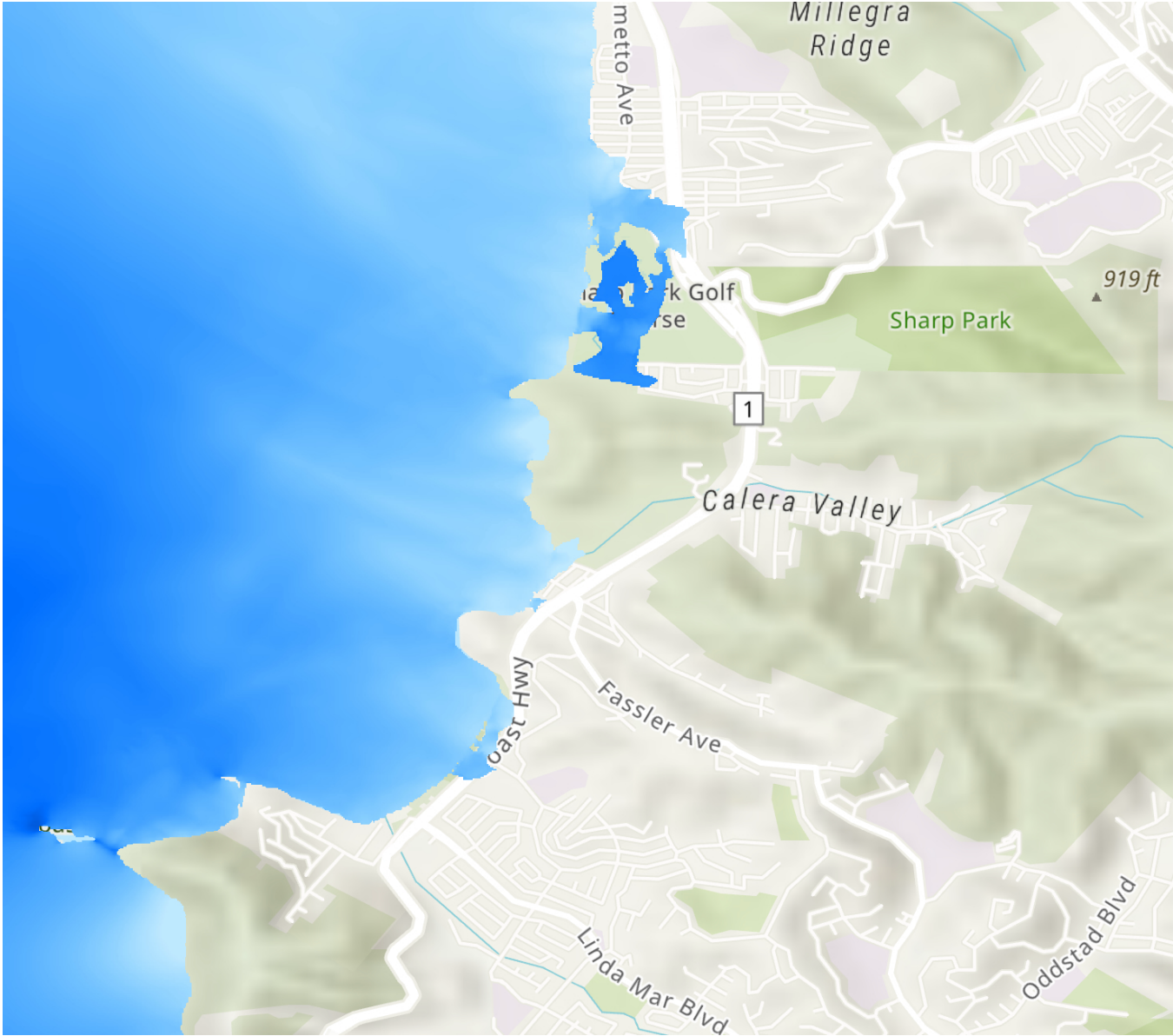


Figure 9. Probabilistic offshore hazard. a (top) shows the offshore hazard, with bar height and colors indicating the exceedance amplitude in meters. b (right) – Source disaggregation showing the relative contribution for different return periods. The colors indicate magnitude ranges.

Note that the Alaska-Aleutian Trench hosted the second largest earthquake (M9.2) recorded by modern seismic instrumentation, which happened in March 27, 1964 earthquake. And according to geologic records, the last major earthquake in Cascadia subduction zone happened in 1700. In other words, the “imminent” tsunami risk has been significantly reduced since 60 years ago, and therefore even if we use the tsunami hazard map based on an ARP of 475 years, we are talking about the next major tsunami that may arrive in Pacifica in 400 years later! I would request the city council to put it into perspective of 100 years expected life span of a residual house, and a general time horizon of 20 years for city development plan! The tsunami hazard map of ARP of 475 strikes a good balance between the consideration of sea level rise, appropriate risk level of tsunami in the next 100 years and the LCLUP's immediate significant impact, once passed, to ALL the Pacifica homeowners! (Worth-noting that Flood Insurance Rate Maps (FIRMs) generally identify areas of greater flood risk (100 and 500 year events)).

Lastly, I would like to include the **Probabilistic** Tsunami Hazard Maps for the State of California (Phase 2) of ARP 475 years below. I’m more than happy to provide help to obtain the map from the CGS website <https://doc.app.box.com/v/capthadatav1?sortColumn=name&sortDirection=A>

SC. Also attached is the report of Probabilistic Tsunami Hazard Maps for the State of California (Phase 2) for your reference. Again, I strongly recommend the city planning team to clearly define the tsunami inundation zone as **“Tsunami hazard map of ARP 475 years based on Probabilistic tsunami hazard analysis (PTHA) data for California (2023 release)”**.



Best regards,  
Jiaheng  
Phone # [REDACTED]

# Probabilistic Tsunami Hazard Maps for the State of California (Phase 2)

---

*Hong Kie Thio*

*AECOM Technical Services*

*One California Plaza*

*300 S. Grand Ave*

*Los Angeles, CA 90071*

December 2019 Technical Report to accompany probabilistic tsunami hazard analysis products provided by AECOM to the State of California, Department of Conservation, California Geological Survey.





Glossary..... 4

1. Introduction ..... 6

    1.1 Background ..... 6

    1.2 Related efforts ..... 7

    1.3 Previous tsunami hazard mapping efforts in California ..... 7

2. Methodology..... 8

    2.1 Probabilistic Tsunami Hazard Analysis (PTHA) ..... 8

    2.2 Epistemic uncertainty ..... 10

    2.3 Aleatory variability ..... 11

    2.4 Overview of the PTHA methodology ..... 11

3. Source characterization ..... 11

    3.1 Geometrical representation of the fault surface..... 11

    3.2 Earthquake recurrence model ..... 12

    3.3 Generation of slip models..... 13

    3.4 Surface deformation ..... 13

4. Source zones ..... 14

    4.1 Cascadia subduction zone..... 14

    4.2 Alaska subduction zone ..... 16

    4.3 Other sources..... 17

5. Tsunami propagation modeling..... 17

    5.1 Algorithms..... 18

        5.1.1 Linear long-wave finite difference method ..... 18

        5.1.2 Non-linear finite volume method ..... 18

    5.2 Elevation models..... 18

    5.3 Modeling error ..... 19

    5.4 Green’s function summation ..... 19

6. Offshore tsunami hazard ..... 20

    6.1 Source integration ..... 20

    6.2 Application of modeling variability and tides ..... 20

        6.2.1 Tidal variability ..... 20

        6.2.2 Modeling error ..... 21

    6.3 Results - Offshore exceedance amplitudes ..... 21

7. Inundation..... 22

    7.1 Computational model ..... 22

    7.2 Probabilistic inundation ..... 22

        7.2.1 Scenario probabilities ..... 23

        7.2.2 On-land hazard curves ..... 24

    7.3 Aleatory variability ..... 25

    7.4 Results – Inundation maps..... 26

    7.5 Compliance with ASCE 7-16 ..... 27

    7.6 Limitations..... 28

8. Comparisons ..... 30

    8.1 Previous tsunami hazard studies ..... 30

    8.2 In relation to other hazards ..... 31

9. Acknowledgments.....	31
10. References .....	32
Appendix A. Offshore tsunami modeling .....	36
Appendix B. Subduction zone earthquakes .....	42
Appendix C. The Cascadia megathrust.....	54
Appendix D. Probabilistic Analysis.....	61
Appendix E. Source parameters for inundation events.....	69
Appendix F. Tsunami code validation .....	77
Appendix G. Tsunami velocity validation .....	151
Appendix H. Offshore amplitude match (ASCE 7-16).....	168

## Glossary

Term	Abbreviations	Definitions
Aleatory variability	sigma, $\sigma$	The natural variability in the outcome of physical processes due to inherent randomness
Aseismic displacement		Displacement on a fault that occurs at very low rate of movement, so that no seismic or tsunami waves are generated
Asperity		Area on a fault where the two side of the fault are tightly locked and where the slip during an earthquake is higher than the average slip
Average return period	ARP	Average time period (in years) between events. The inverse of the Recurrence Rate
Bottom friction		A mechanism by which a tsunami loses energy due to the viscous friction with the seafloor. Can be expressed in numerical models in various ways, such as through the Manning's coefficient
Epistemic uncertainty		Uncertainty in our models due to an imperfect understanding and limited knowledge of natural processes (e.g. alternative source characteristics)?
Green's function		Response of a natural system, e.g. a body of water, to an impulse force (e.g. a unit uplift of the seafloor)
Inundation		Flooding due to the tsunami
Performance Based Engineering	PBE	Design approach in engineering where buildings and other structures are expected to perform to a certain level (operational, life-safety) for certain probabilities of exceedance of a hazard
Poissonian distribution		A temporal distribution where the occurrence of an event is independent of the last occurrence
Probabilistic Seismic Hazard Analysis	PSHA	Standard hazard analysis technique where one determines the ground motion levels that will be exceeded for a particular probability level
Probabilistic Tsunami Hazard Analysis	PTHA	The tsunami equivalent of PSHA.

Recurrence rate		Frequency (per year) at which an event occurs on average. The inverse is called Average Return Period (ARP)
Runup line		The line delineating the furthest extent of the tsunami inundation on dry land
Seismic efficiency		Fraction of the convergence rate at subduction zones that is accommodated by earthquakes. Efficiency of 1 means all the convergence is seismic, 0 means aseismic (Creep)
Subfault		Subdivision of a seismogenic fault. The concept is used to facilitate the modeling of Green's functions

## 1. Introduction

In this report, we present the probabilistic tsunami hazard analysis (PTHA) and related products for the State of California. This effort has been commissioned by the California Geological Survey (CGS) and builds on previous work supported by the Pacific Earthquake Engineering Research Center (PEER) and the California Department of Transportation (Caltrans). There is also considerable overlap between this project and the latest edition of the American Society of Civil Engineers' "Minimum Design Loads for Buildings and Other Structures" (ASCE 7-16) which includes a new chapter on "Tsunami Loads and Effects". For CGS, these products provide the advanced hazard analysis for implementation of potential "Tsunami Zones of Required Investigation" required for the Seismic Hazard Mapping Act as well as other land-use and construction regulations.

### 1.1 Background

The methodology and results presented in this report are the culmination of several successive and parallel projects originating with the initial development of the offshore probabilistic tsunami hazard analysis supported by the U.S. Geological Survey (USGS) under the National Earthquake Hazards Reduction Program (NEHRP) program (Thio et al., 2007). In this work, we developed the method of using tsunami Green's function summation to efficiently compute tsunami waves from sources around the Pacific Ocean (Figure 1) used for the development of models of probabilistic offshore amplitude exceedance. This methodology was further developed and applied to California probabilistic inundation hazard by Thio et al. (2010), funded by Caltrans through PEER. A major improvement in that study included the inclusion of aleatory variability in the tsunami calculations and the computation of probabilistic inundation anchored on the offshore exceedance amplitudes. The current project, commissioned by the CGS and the California Office of Emergency Services (CalOES) builds on these previous studies with improvements in source characterization, on-shore model resolution (10m for inundation), characterization of aleatory variability and epistemic uncertainty and updated methodologies and algorithms for inundation modeling. All these features will be described in more detail in the following sections.

In Phase 1 of this study (California PTHA Work Group, 2015), an approach developed by URS (now AECOM) was evaluated in conjunction with a similar effort by the University of Washington (Gonzalez et al., 2013) and recommendations were presented regarding the final procedures for creating the PTHA products for the state. The main improvements to the maps, addressed in this report relative to the Phase 1 report are:

- The complete USGS-CGS recurrence model for the Cascadia Subduction Zone has been adopted;
- Two types of long-term slip models are used for the Cascadia Subduction Zone (uniform and increasing to the north);
- Smaller subfaults are included, and every subfault is curved to a resolution of 1x1 km; and,
- Adoption of a Clawpack-based inundation code instead of the URS (now AECOM) code

These improvements will be described in greater detail in the next sections as well as in the Appendices.

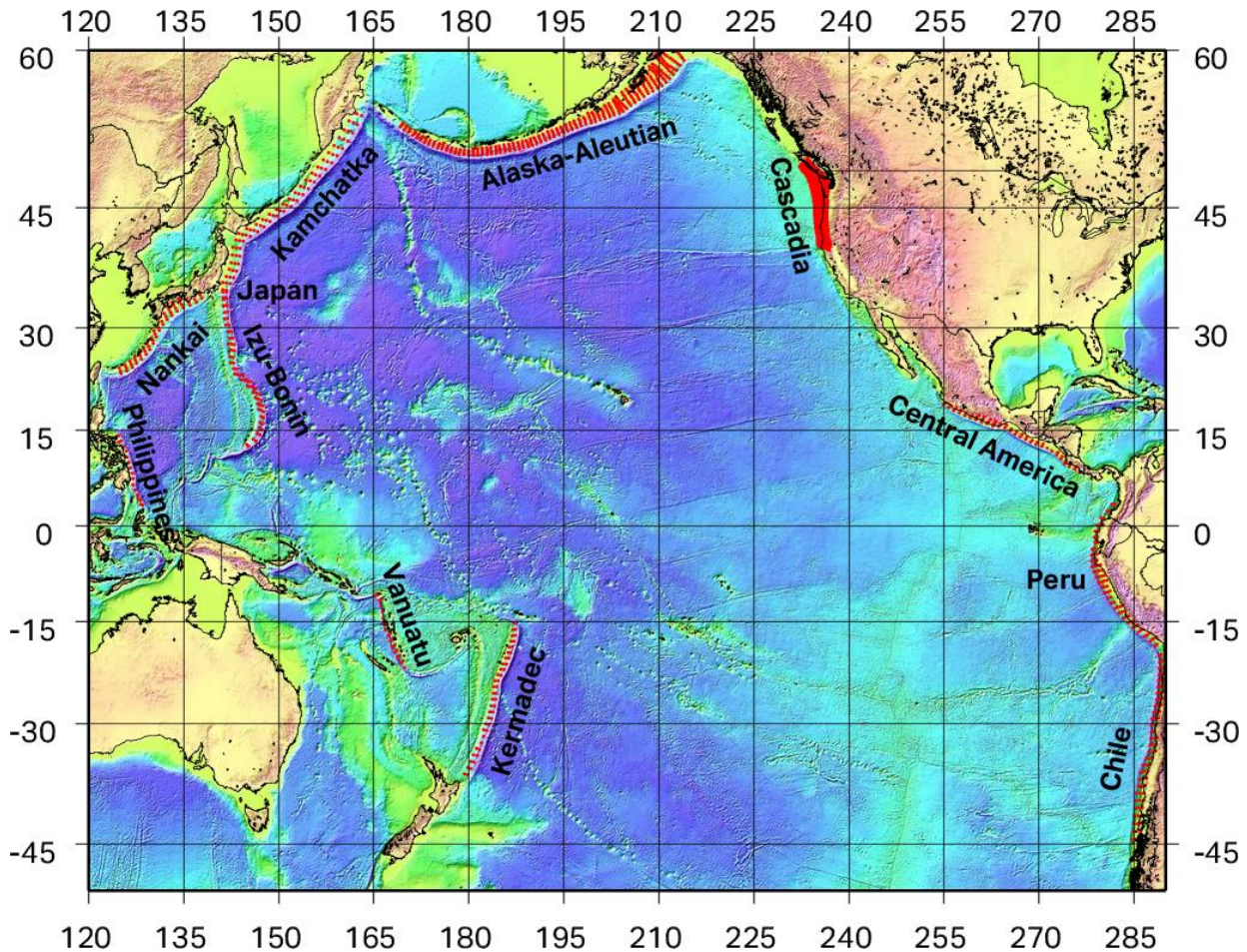


Figure 1. Source zones around the Pacific Ocean that are included in this work.

**1.2 Related efforts**

The development of the California probabilistic inundation maps is closely related to the development of the “Tsunami Design Zones” that will be included in the upcoming revision of the ASCE 7 “Design Guidelines for Buildings and Other Structures” (ASCE 2017). In particular, the offshore exceedance amplitudes for the California section of ASCE 7-16 (Thio et al., 2017) are identical to the 2,475-year offshore exceedance amplitudes discussed in this report.

**1.3 Previous tsunami hazard mapping efforts in California**

The first systematic mapping of tsunami hazard in California was published in 2001 by Eisner et al. (2001), which was based on multiple, deterministic worst-case scenarios (earthquakes and landslides) for local offshore sources. In 2009, the State of California produced second-generation tsunami inundation maps of the low-lying populated areas for the State’s coastline for emergency response purposes (Barberopoulou et al., 2009; Barberopoulou et al., 2011). In addition to higher resolution modeling (30-to-90m vs 125m), these maps also included additional local and distant sources, both landslide and earthquake. Both the first and second generation maps were developed for emergency response use only, and because of the nature of their purpose they are

purposely conservative based on knowledge of tsunami sources at the time. The current study provides probabilistic maps that have been developed according to common standards in engineering practice and cover a range of probability (risk) levels. Their potential use therefore goes beyond the emergency response application of the previous mapping projects, into areas of land-use and construction planning (California PTHA Work Group, 2015).

## 2. Methodology

### 2.1 Probabilistic Tsunami Hazard Analysis (PTHA)

In an earlier project, URS (Thio et al., 2010) created a map of probabilistic offshore tsunami wave-heights by using a Green’s function summation approach. This approach enabled the integration over a wide range of source zones and magnitudes and the inclusion of epistemic uncertainties that describe our incomplete knowledge and understanding of natural processes, and aleatory

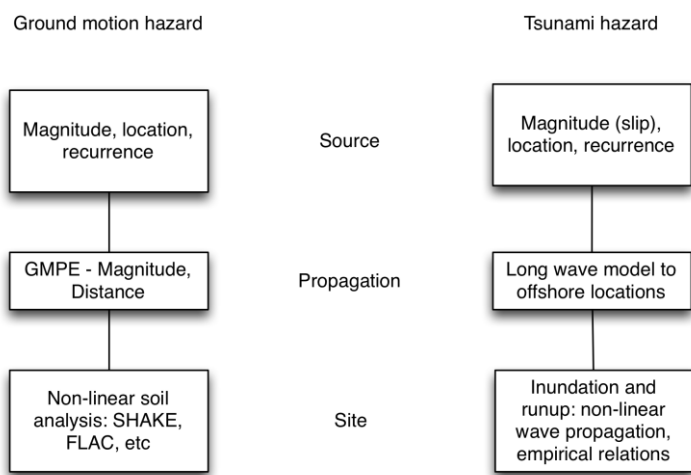


Figure 2. Schematic comparison between PSHA and PTHA.

variability, which expresses the randomness in natural processes. The methodology is similar to the common approach in Probabilistic Seismic Hazard Analysis (PSHA) and the similarities are shown in Figure 2. Both methods use an integration over a range of earthquake magnitudes and locations. While PSHA uses Ground Motion Prediction Equations (GMPEs) to compute the ground motion amplitude at a site, in our approach of PTHA we use numerical models to predict the wave-heights and inundation areas.

PSHA has been a primary tool in the development of design criteria for buildings and infrastructure in engineering for the last few decades. Its use is intricately linked to the use of Performance Based Engineering (PBE) principles, where building design is based on several levels of performance (safe-use, collapse prevention, etc.), which are linked to a particular probability of exceedance of a ground motion level. Risk-based analyses also inherently depend on a probabilistic expression of the hazard, and it is thus desirable to follow a similar framework for tsunami hazard analysis (McGuire, 2004).

For PTHA, the most obvious metric is the exceedance of a water level, wave amplitude or flow depth, as these are the most visible and recorded aspects of tsunami waves. There are, however, other metrics that may be more suited for certain purposes, such as flow velocities in ports and harbors or momentum for impact on structures. The current methodology has been developed to compute probabilities of wave-height exceedance but can be adapted to analyze other metrics as well.

The probabilities are computed in terms of the annual rate of exceedance, which, if we assume that the event occurrence follows a Poissonian (i.e. time-independent) distribution, can be translated into probability of exceedance in a certain amount of time through:

$$P = 1 - e^{(-\gamma t)}$$

where  $P$  is the probability of exceedance in a time period  $t$  (also called exposure time), and  $\gamma$  the annual rate of exceedance. In engineering applications, we are usually interested in certain probability levels that are expressed in terms of  $P$ , such as a 2% (0.02) probability of exceedance in 50 years, where 50 years is the exposure time  $t$ . Inverting the above equation as:

$$\gamma = \frac{-\ln(1 - P)}{t}$$

we can then calculate the corresponding annual rate of exceedance as 0.00040405 year<sup>-1</sup>, or a recurrence time, often referred to as Average Return Period (ARP), of 2475 years. Other periods of engineering interest are 50%, 10% and 5% in 50 years, which correspond to 72, 475 and 975 years ARP respectively. In comparison, in flooding hazard the 100, 200 and 500 year ARP's are common. In this report, we have produced maps for all these probability levels and the 3000 year ARP as well.

The annual frequency of exceedance is calculated as follows:

$$\phi(s) = \sum_{i=1}^{Faults} \left( \iint_{m,r} f(m)(P(A > s|m, r)P(r|m)dmdr) \right)_i$$

where:

$f(m)$  = probability density function for earthquake events of magnitude  $m$

$P(A>s|m,r)$  = probability that tsunami amplitude  $A$  exceeds  $s$  given magnitude  $m$  and source at  $r$

$P(r|m)$  = probability for a source at location  $r$ , given a source of magnitude  $m$ .

The earthquake recurrence rate is of course an important and directly relatable parameter with regards to the tsunami exceedance rates, but it is only one of several parameters which contribute to the ultimate tsunami probabilities. A probabilistic analysis is an integration over a potentially large number of tsunamigenic events on different faults, but also includes the effect of natural variability (or aleatory uncertainty) of physical processes. Extreme outcomes have a low, but finite probability, and since we are determining the exceedance of a certain hazard



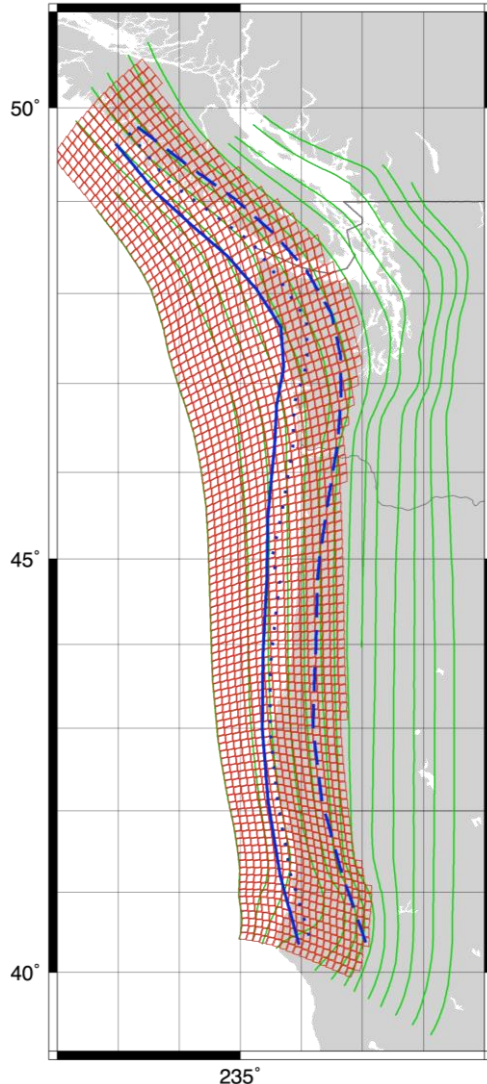


Figure 3. Fault geometry of the Cascadia subduction zone. Green lines are the contours from Hayes et al. (2012). Grid shows the subdivision of the fault. Blue solid, dotted and dashed lines show the alternative rupture terminations at depth (epistemic).

parameter (such as maximum wave amplitude), the hazard will continue to increase with decreasing probability as we are sampling further into the tail ends of the aleatory variability distributions.

In performance-based engineering, these probability levels may be tied to a specific performance level. For example, a building may be designed to remain operable for 475 year ARP level ground motions, be temporarily inoperable but repairable within a reasonable amount of time for the 975 year ground motion levels, and not collapse but be permanently inoperable for 2475 year events (“life-safety”).

### 2.2 Epistemic uncertainty

Probabilistic tsunami hazard analysis, like its seismic counterpart, follows a dualistic approach to probability. Whereas some aspects are defined in the familiar terms of frequency of occurrence (such as intermediate earthquake recurrence, magnitude distribution), others are more based on judgment, which is a subjective approach (Vick, 2002). For instance, we may characterize the recurrence of intermediate earthquakes in terms of a Gutenberg-Richter distribution, constrained by a catalog of historical earthquakes. The assumption is that the occurrence of earthquakes is a stationary process, and that the catalog represents a homogenous sample of the long-term seismic behavior of a source. For large earthquakes however, the return times are often so long relative to our historic record, even when paleo-seismic data is included, that the recurrence properties of these events cannot be described with a stationary model based on a regression of observed earthquake occurrence. We therefore need to introduce the concept of judgment,

where we use our current understanding of earthquake processes, including analyses of similar structures elsewhere, such as local geological conditions, strain rates etc., to make assumptions on the recurrence of large earthquakes. This is a subjective or epistemic approach to probability, centered on the observer rather than the observations, and will inevitably be different from one practitioner to another. A rigorous PTHA model therefore includes the use of logic trees to express alternative understandings of the same process, e.g. large earthquake recurrence models, weighted by the subjective likelihood of that alternative model (“degree of belief”), where the weights of the alternatives sum to unity. We shall explain in a later section how this distinction is manifested in the handling of uncertainties throughout the analysis.

## 2.3 Aleatory variability

All aspects of earthquake occurrence and effects contain a measure of natural randomness, even if certain average behavior and measures are clearly identified. This variability is usually expressed in terms of distribution functions around the mean and are included in a PTHA by sampling or integrating over this distribution function. More details on the aleatory variability are discussed in the sections on the various components that contribute to the PTHA.

## 2.4 Overview of the PTHA methodology

In order to ensure consistency with seismic practice, the URS (now AECOM) approach closely follows, where possible, the PSHA practice. For instance, the overall framework and inputs remain quite similar to facilitate model exchange between the PSHA and PTHA. There are however some important differences between PSHA and PTHA. The most important difference between the two is the impracticality of using something similar to GMPEs in tsunami hazard due to the very strong dependence of tsunami wave-heights on bathymetry, which precludes the use of simple magnitude distance relations. Fortunately, since the global bathymetry is relatively well constrained and computational algorithms are sufficiently accurate and efficient, it is possible to replace the GMPE-type relations with actual computed tsunami waveforms. We can summarize the methodology with the following list of steps, with details discussed in later sections:

1. Identification and setup (subfault partitioning) of earthquake sources;
2. Computation of fundamental Green's functions for every subfault to near-shore locations;
3. Definition of earthquake recurrence model;
4. Generation of a large set of scenario events that represents the full integration over earthquake magnitudes, locations and sources, for every logic-tree branch;
5. Computation of near-shore probabilistic wave-height exceedance rates;
6. Identification of dominant sources through source dis-aggregation;
7. Computation of probabilistic inundation hazard using a non-linear runup model anchored by offshore wave-heights.

In practice, the main process can conveniently be divided into generation, propagation, and inundation models. In the next sections, we will discuss these various steps in more detail.

## 3. Source characterization

The source characterization for the tsunami models consists of a geometrical characterization of the source, recurrence models for earthquakes that define magnitudes and their recurrence rate, and a generation mechanism for slip distribution on the fault.

### 3.1 Geometrical representation of the fault surface

The subduction zone source representations used in this study are based on the Slab1.0 model of Hayes et al. (2012). Based on recommendation from the Phase 1 report (California PTHA Work Group, 2015), we fit the depth contours for every subduction zone with a set of quasi-rectangular subfaults that are small enough to represent the slip variability of large tsunamigenic earthquakes (Figure 3). The nominal dimension for these elementary subfaults is 30 km along

strike by 10 km in the dip direction, but varies according to the curvature of the fault. In order to capture the curvature of the subduction interface, these subfaults are further divided into small patches of 1x1 km. This fine subdivision is strictly meant to accommodate the geometrical complexity; for the actual analysis, the slip on every 30x10 km subfault is uniform.

### 3.2 Earthquake recurrence model

The earthquake recurrence model defines the magnitude of earthquake with their rate of occurrence. In seismic hazard practice the most common magnitude distributions that are used are the (truncated) Gutenberg-Richter (G-R) relation, the Maximum Magnitude (MM) model and the Characteristic Model (CM) (Appendix D). Whereas the G-R model is most often used to describe the background seismicity, it is often assumed that the MM and CM models are more appropriate for large faults. In any case, it is important to define the upper limit for the magnitude that can occur on a fault and for this purpose we make use of earthquake scaling relations. For example, for any rupture configuration we can determine the area ( $A - km^2$ ), which through the published scaling relations (Figure 4, Strasser et al., 2010):

$$M = 4.441 + 0.841 * \log (A), \sigma = 0.286$$

gives us magnitude ( $M$ ), and thus earthquake moment ( $M_0$ – in Nm):

$$M = \frac{\log(M_0) - 9.1}{1.5}$$

The average slip ( $D$ ) is then obtained through:

$$D = \frac{M}{\mu A}$$

where  $\mu$  is the elastic shear modulus, we have used a typical crustal value of 30 GPa. In the first equation, the sigma term represents the aleatory variability as the standard deviation of the distribution around the mean. We approximate this distribution using a discrete set of alternative values ( $-2\sigma$ ,  $-\sigma$ , median,  $+\sigma$ ,  $+2\sigma$ ) with weights derived from the normal distribution (.4, .24 and .06 for median,  $\pm\sigma$  and  $\pm2\sigma$  respectively).

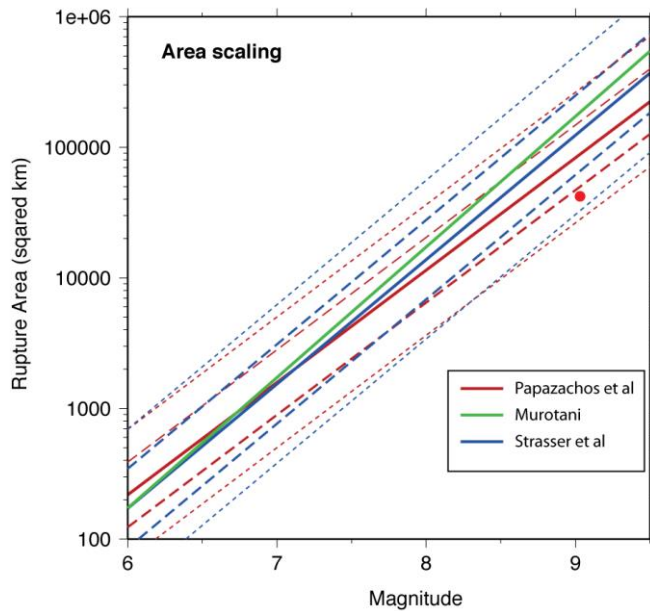


Figure 4. Area magnitude scaling relations. Different colors represent different scaling relations (epistemic). Dashed lines are 1 sigma, dotted lines are 2 sigma levels (aleatory). The red dot represents the 2011 Tohoku earthquake.

Various authors have developed scaling relationship for subduction zone earthquakes, which vary significantly due to different assumptions and regression models used. In order to take these different views of the earthquake scaling relations into account, we have applied several logic tree branches that represent these different models. The model we considered are from Strasser et al., 2010, Papazachos et al. (2004) and Murotani (2008, 2013) (Figure 4).

### 3.3 Generation of slip models

In previous analyses (e.g. Thio et al., 2010), we have used uniform slip models to produce tsunami waves. At local distances however, the slip variability becomes an important factor and asperities with large amounts of slip can cause significantly

higher tsunami waves, especially locally, as is illustrated by the recent Tohoku earthquake where the maximum slip exceeded the average slip by at least a factor of 2.

Murotani et al. (2008) studied the slip distributions of several subduction zone earthquakes and found a ratio of maximum slip over average slip of 2.2. To include this aleatory slip variability, we used variable slip rupture models with one third of the rupture as an asperity with twice the average slip and the other two-thirds of the rupture at half the average slip. In order to achieve uniform long-term slip, we computed a total of three scenarios (Figure 5) for each event where the asperity occupies every part of the rupture once. This way, we avoid the risk that in some areas the hazard is over- or under-estimated due to incomplete or overlapping asperity coverage offshore.

### 3.4 Surface deformation

In order to generate tsunamis from earthquake slip distributed on a fault, we need to compute the surface deformation from the slip. There are several methods available to accomplish this. The most commonly used is the analytical method of Okada (1992), which gives the surface deformation due to uniform slip on a rectangular fault in an elastically homogeneous half-space. However, Savage (1987, 1998) demonstrated that using a half-space approximation gives relative large bias compared to a layered (1-D) model. The difference between 1-D and even more realistic 3-D models (Wald and Graves, 2001) is much smaller, and we therefore used a 1-D frequency-wavenumber integration (FK) technique (Wang et al., 2003) to compute the static deformation at the surface.

The elastic deformation due to slip on a fault is linear, and we can use this principle to efficiently compute the vertical deformation at the surface by pre-computing the surface deformation from

the elementary subfaults, after which we can reproduce surface deformation from arbitrary slip distributions by a weighted sum (weighted according to slip) of the individual contributions of each subfault. The linear approximation is extended further to the tsunami propagation as described in section 5.

## **4. Source zones**

We have included megathrust sources from around the Pacific (Figure 1) and they are described in Appendix B. The recurrence model for most of these sources is quite generic, except for Cascadia (Appendix C) and Alaska (Appendix B) where we used a more extensive logic tree, since they are the most important sources for tsunami hazard in California.

### **4.1 Cascadia subduction zone**

The Cascadia subduction zone is used in a slightly different manner than the distant sources, since for Northern California this source is local and causes significant co-seismic uplift or subsidence, which needs to be considered when computing the inundation. Also, since it is a local source, details in the source geometry and slip distribution are more important than in the distant sources.

Following the Phase 1 report (California PTHA Work Group, 2015), we adopted the recurrence model and geometry from the 2014 revision of the National Seismic Hazard Maps (Petersen et al., 2014, updated by Chen et al., 2014) for the Cascadia subduction zone. This model has gone through a thorough review process with input from experts in the field over several years. The

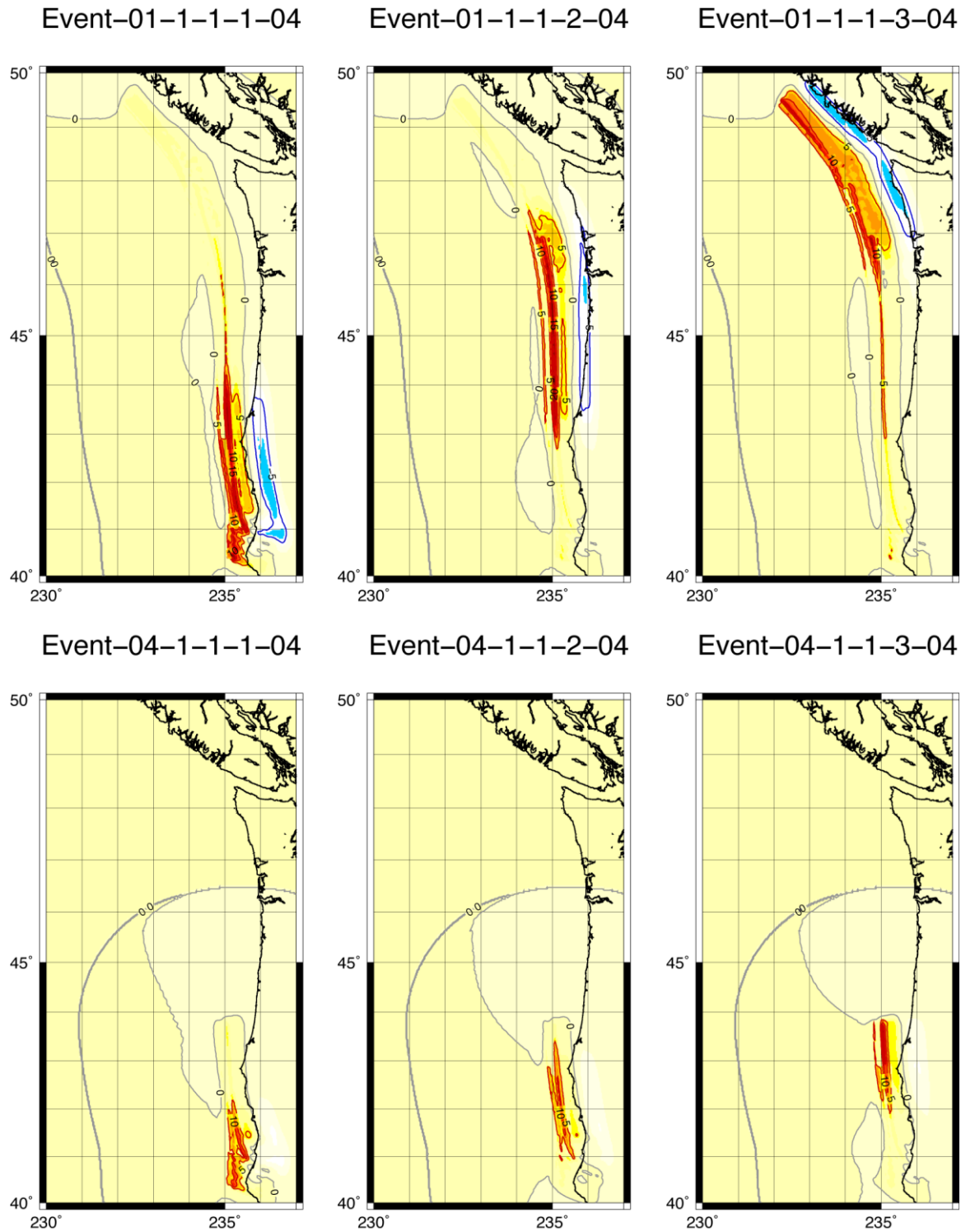


Figure 5. Vertical displacement field (res=uplift) for two scenarios. Top is a full rupture earthquake, bottom is a partial rupture, each shown three times with different asperity locations.

logic tree we developed for the Cascadia subduction zone is shown in Figure 6, and in Appendix C we give a more general description of this subduction zone. Our model differs in a few places from the USGS model. Since current PSHA studies do not take slip distributions into account, we

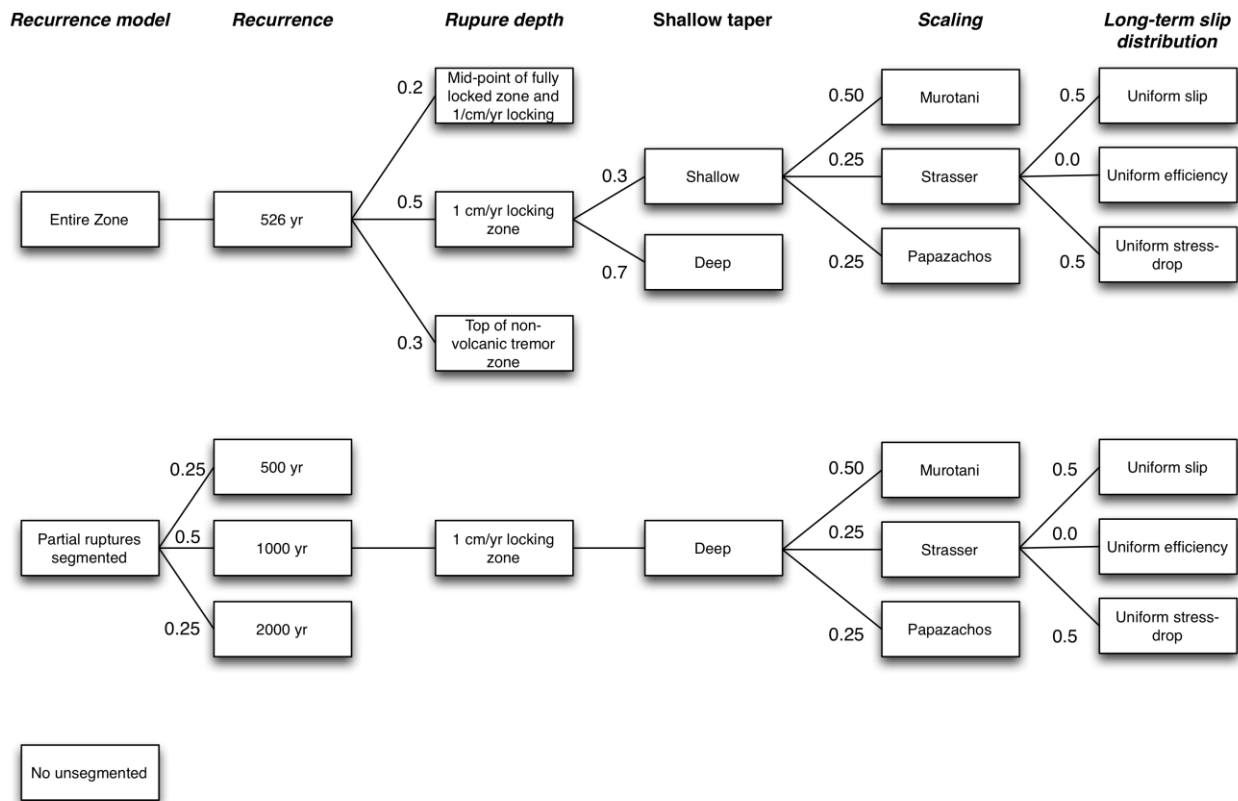


Figure 6. Logic tree for the Cascadia subduction zone. (adapted from the 2014 USGS National Seismic Hazard Map, Petersen et al., 2014)

added a set of branches concerning the long-term (multi-cycle) slip distribution over the Cascadia Subduction Zone. In the Uniform Slip branch, the long-term slip is evenly distributed along strike across the megathrust, whereas for the Uniform Stress Drop branch, the long-term slip is higher where the fault is wider, which effectively means that the long-term slip is higher to the north. The long-term behavior is achieved by adjusting the amount of slip along strike of the individual scenarios. We have also assigned a larger weight than the USGS did to the updated Murotani (2013) magnitude scaling relations as these are the most up-to-date, and are consistent with the asperity model.

#### 4.2 Alaska subduction zone

The USGS Seismic Hazard map for Alaska was developed more than a decade ago (Wesson et al., 2007), and since that time considerable paleo-seismic work in the Aleutians has yielded significant amounts of data that have shed new light on the occurrence of large earthquake in the region (Witter et al., 2016). Also, the 2007 USGS maps only considered segmented ruptures whereas for the tsunami we have to take into account the occurrence of multi-segment ruptures (Shannon et al., 2009). The segmentation model that we developed in-house for the Alaska subduction zone is shown in Figure 7, and the source zone is described in more detail in Appendix B.

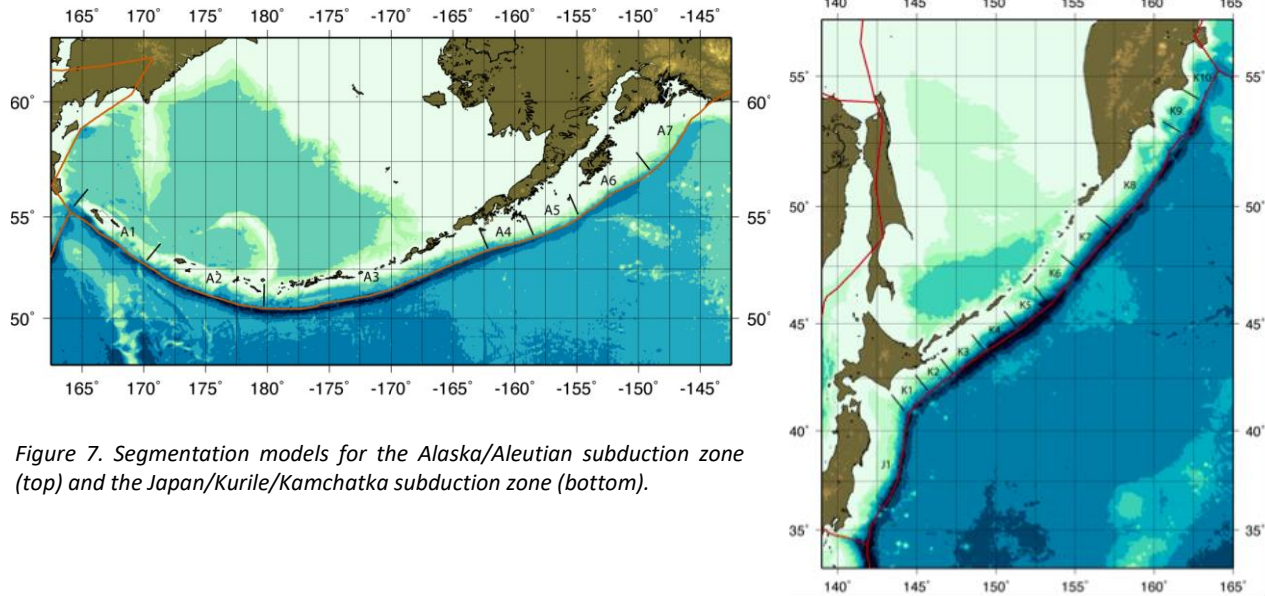


Figure 7. Segmentation models for the Alaska/Aleutian subduction zone (top) and the Japan/Kurile/Kamchatka subduction zone (bottom).

### 4.3 Other sources

In Figure 7 we also show the source model for the Kuriles. This map shows the segmented model that is used in seismic hazard studies (Earthquake Research Committee, 2005), and which are one principal branch on our logic tree. The other principal branch contains multi-segment ruptures. These are typically events that have not been observed (in historical times) but for which no good reason exists to preclude them from our model. For tsunami generation, these models are very significant since tsunamis scale directly with slip, whereas such models would only have limited impact on seismic hazard analysis due to the saturation of ground motions with magnitude. The recurrence models for the remaining circum-Pacific sources (Figure 1) have the following general characteristics:

- Epistemic branches include a full rupture across the entire fault zone, with weights determined from the literature
- Recurrence rates are based on plate convergence rates, with several branches for seismic coupling.
- Source geometry is taken from Hayes et al. (2012)

While the general recurrence models used for the remaining subduction zones have similar logic tree branches, they differ markedly in how the weights are applied to the different branches. Several authors have studied the correlation between the age of the subduction plates, dip of the interface, and convergence velocity with the maximum magnitude and seismic efficiency. We have used these results to set the weights for the seismic efficiency and the maximum magnitude as shown in Appendix B.

## 5. Tsunami propagation modeling

Contrary to traditional seismic practice, the actual propagation term in the hazard equation for tsunamis is solved using numerical models rather than empirical relationships. This is due to: 1)



the very strong lateral heterogeneity in the propagating medium (the oceans) which limits the usefulness for simple empirical relationships; and 2) the greater accuracy in tsunami modeling compared to high-frequency seismic modeling.

All tsunami simulation algorithms use the same initial condition, namely the vertical deformation, whether instantaneous or distributed over time, of the sea surface. This deformation is set equal to the deformation of the underlying seafloor.

## **5.1 Algorithms**

In this project, we have used two approaches to computing tsunami waves, reflecting the trade-off between accuracy of near- and on-shore modeling and computational efficiency that allows for large ensemble computation. Both methods feature a two-dimensional (depth averaged) approximation, which is standard for tsunami modeling.

### **5.1.1 Linear long-wave finite difference method**

This method is very efficient and accurate for ocean-wide propagation but does not model inundation or non-linear effects such as bottom friction. We have used this algorithm to compute the fundamental Green's functions along the offshore 100 meter depth contour where we computed the probabilistic offshore exceedance amplitudes. For this part of the project, we used the code Comcot by Liu et al. (1995). Since we are using this code for offshore wave-heights, we have not activated the non-linear and inundation components of the code.

### **5.1.2 Non-linear finite volume method**

The assumption of linearity is not valid for tsunamis where the amplitudes are comparable to the water depth. Also, the detailed bathymetry near the shoreline is important to estimate the final run-up heights. For these cases, a nonlinear method is necessary to compute the run-up heights correctly. At the recommendation of the Phase 1 review panel (California PTHA Work Group, 2015) we have developed an in-house code that uses the Clawpack library (Mandli et al., 2016) to solve the tsunami inundation problem. Compared to the finite difference method, the finite volume method is more accurate, especially in the presence of shockwaves, a condition that exists in the near-source regime, but much slower than the linear long-wave approximation. It includes several nonlinear (e.g. bottom friction, advection) effects and a moving boundary, which allows for inundation. This code allows for nested gridding, which means that we use coarse grids for deep ocean modeling and increasingly finer grids towards the coastline so that we can capture fine detail without overdue computational burden. Details on these propagation models are given in Appendix A and a report on the validation of the Clawpack-based AECOM code is included as Appendices G and H.

## **5.2 Elevation models**

For the deep ocean modeling (both with the linear and non-linear codes) we have used the SRTM30+ model (Becker et al., 2009) which is a combination of satellite derived bathymetry and sounding data. For the United States coastal areas, this model is primarily based on the National Oceanic and Atmospheric Administration (NOAA) near-shore grids and thus provides an accurate, convenient and seamless model of the entire Pacific Ocean. We have used this digital elevation model (DEM) at a resolution of 30 arc-seconds (1/120 degree latitude, which is about 1 km).

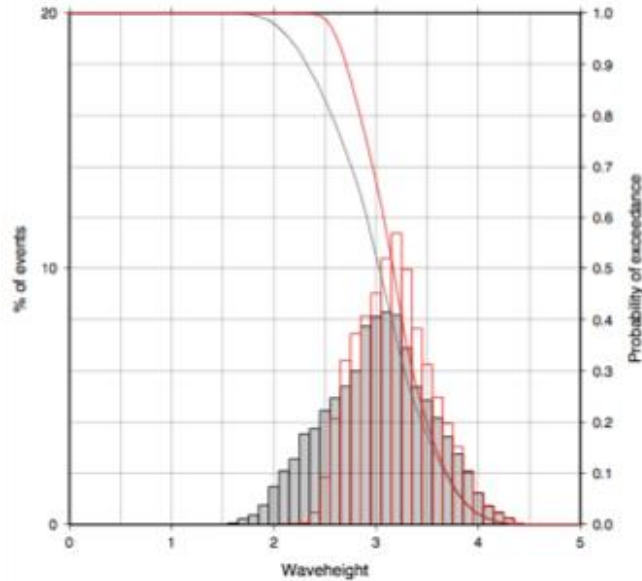


Figure 8. Tidal distribution functions. Original (grey) and convolved with a tsunami timeseries with a simple structure (one dominant peak) (red),

For the nearshore and inundation modeling, we used higher resolution models that are based on the NOAA Tsunami Gridding Program (Eakins and Taylor, 2010) at decreasing grid sizes down to 10 m at the shoreline and in-land. At these resolutions, many details in the bathymetry and topography are well-resolved and the nested gridding thus provides a good trade-off between accuracy and computational feasibility.

### 5.3 Modeling error

Although the numerical models are quite accurate in predicting tsunami waveforms, especially for ocean propagation, we still need to consider the misfit between observed amplitudes and model amplitudes. This misfit is similar to the

sigma term in GMPEs. Whereas the latter is an inherent product of the regression process as the standard deviation of the misfit distribution, for our sigma we need to explicitly estimate them from the misfit between model and data. We will refer to this as the modeling sigma, although it's not strictly the result of modeling errors only. Rather, the sigma is made up of several different contributions since, when deriving this term, we do not have full control over the input parameters used to compute the model wave-heights and therefore the sigma also includes the effect from incomplete or inaccurate information regarding the input source. We have constrained the sigma by modeling the observed tsunami data from several well-constrained earthquakes, such as the 2010 Maule (Chile) and 2011 Tohoku (Japan) earthquakes.

### 5.4 Green's function summation

The underlying principle for this approach is the validity of the linear behavior of tsunami waves. This enables us to deconstruct a tsunami that is generated by an earthquake into a sum of individual tsunami waveforms (Green's functions) from a set of subfaults that adequately describe the earthquake rupture. By pre-computing and storing the tsunami waveforms at points along the coast generated by each subfault for a unit slip, we can efficiently synthesize tsunami waveforms for any slip distribution by summing the individual subfault tsunami waveforms (weighted by their slip). The same principle is used in the inversion of tsunami waves for earthquake rupture (e.g., Satake 1996). This efficiency makes it feasible to use Green's function summation in lieu of attenuation relations to provide very accurate estimates of tsunami height for probabilistic calculations, where one typically needs to compute thousands of earthquake scenarios. For instance, in the example in section 6.3, the probabilistic tsunami heights results are based on more than 10,000 scenarios that were computed (using the Green's functions summation) on a 30-node cluster computer.

## **6. Offshore tsunami hazard**

### **6.1 Source integration**

In order to compute the probabilistic offshore exceedance amplitudes, we integrate over earthquakes in all the source regions described in section 4. The Green's function summation allows a full integration over more than 10,000 events that span the magnitude range of significance, the various epistemic branches and aleatory source variability.

### **6.2 Application of modeling variability and tides**

#### **6.2.1 Tidal variability**

The tidal variability is included in the offshore wave-heights for the tele-tsunami sources by convolving the time-series with a local tidal record (Figure 8) (Houston and Garcia, 1978; Mofjeld et al., 2007). This ensures that if the tsunami consists of a succession of high wave arrivals rather than a single dominant peak arrival, the probability of coinciding with a high tide is properly taken into account. For the Cascadia source, our original intent was to compute scenarios at a number of tide levels, and weigh them according to a similar distribution function (Gonzalez et al., 2013). However, as that would increase the number of runs dramatically, it was decided instead to include the tidal component for the local runs in the same way as the aleatory uncertainty for the inundation, i.e. applying a distribution function to the amplitudes after the inundation has been computed. Since this is still a quasi-static tidal correction, it does not address the potentially substantial effect of the tides on currents, especially in inlets and other constricted water bodies.

Exceedance waveheights: 975 yr

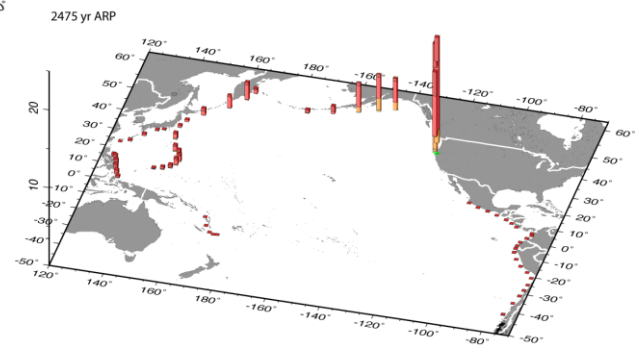
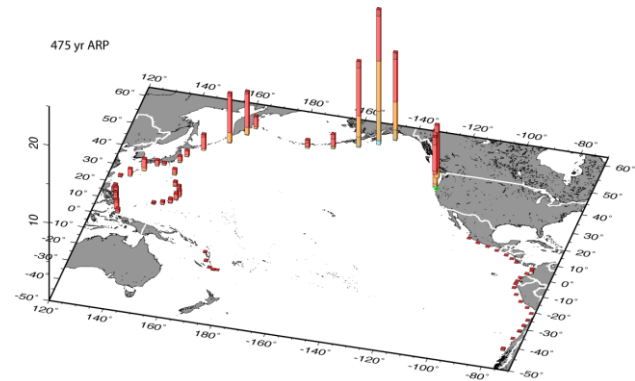
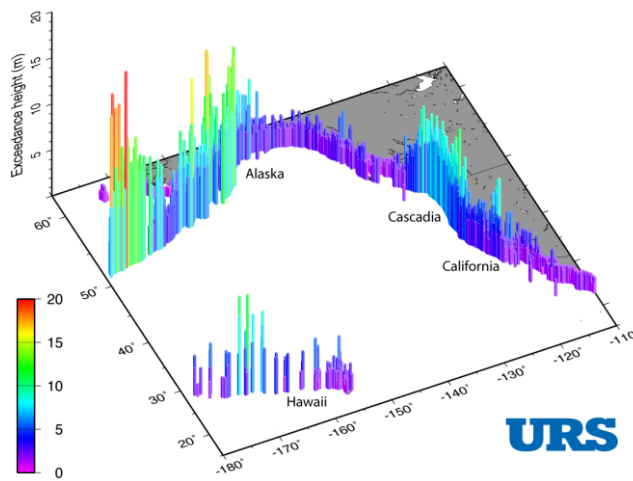


Figure 9. Probabilistic offshore hazard. a (top) shows the offshore hazard, with bar height and colors indicating the exceedance amplitude in meters. b (right) – Source disaggregation showing the relative contribution for different return periods. The colors indicate magnitude ranges.

### 6.2.2 Modeling error

The modeling error component of the aleatory variability (section 5.2) is applied at the offshore points. In analogy to the seismic GMPE’s, we regard the model tsunami amplitudes as a distribution centered on a mean value, which in the numerical case is assumed to be the computed amplitudes. Since we are computing probabilities of exceeding a target amplitude, we can simply obtain this from the cumulative probability of the amplitude distribution centered around the computed “mean”.

### 6.3 Results - Offshore exceedance amplitudes

The offshore probabilistic wave-heights (Figure 9a) contain both the epistemic (alternative source characterizations) and aleatory variability (modeling error, tides, etc.) and as such are fully probabilistic. The regional pattern of exceedance amplitudes shows the expected large values for Alaska and Cascadia, and the rapid decrease in amplitude toward southern California. Disaggregation of the hazard (Figure 9b) enables us to identify the most significant sources that contribute to the hazard at a particular location for a particular return period. In the case of Crescent city, the dominant sources are the eastern Aleutian subduction zone, the Kuriles and of course the locally important Cascadia subduction zone. Note that for the shorter return periods (475 yr), the Alaska source region has a larger contribution to the hazard than Cascadia, whereas at the longer return period Cascadia is dominant.

To achieve the combined hazard from local and distant sources, we start with the hazard curve and source disaggregation for offshore Crescent City. From the disaggregation, we can deduce which of the source zones contribute significantly to the hazard at Crescent City, and their relative

importance. For Crescent City, at short return periods the contributions are primarily from Alaska, the Kuriles and to a lesser extent Chile. As we go to lower probabilities and thus longer return periods, the Cascadia subduction zone becomes rapidly more important and dominates the hazard at 2475 year ARP. The hazard curve gives us the probabilistic hazard levels for different probabilities, and thus gives us as target offshore amplitudes for the inundation studies.

## 7. Inundation

### 7.1 Computational model

Using these offshore wave-heights, we compute the actual probabilistic inundation in the second stage of this project by performing fully non-linear tsunami inundation simulations for a suite of scenarios that provide offshore amplitudes that are consistent with the maps computed in the first stage. For these computations, we used the Clawpack-based code that was developed in-house. The final maps were computed for high-resolution grids (10 m horizontal) from NOAA (Eakins and Taylor, 2010) that were specifically developed for tsunami inundation modeling. These are so-called “bare-Earth” models that are stripped of any building structures and use a single Manning’s friction coefficient (0.025) for all areas.

The selection of these scenarios is based on a disaggregation analysis of the hazard, which is essentially a bookkeeping tool that shows us the relative contribution to the hazard for every source. This procedure is somewhat similar to the process of spectral matching used in seismic hazard analysis, where a seismogram is scaled up so that its spectral envelope matches the amplitudes from the probabilistic seismic hazard analysis. In both cases, the actual scenario or time series used to compute the final hazard is usually well above the mean that would be expected for the particular dominant magnitude and source location because of the contribution of the aleatory variability, which, for decreasing probabilities gives rise to an increase of the hazard. When we compute the final probabilistic inundation by computing tsunamis all the way from the source, the scaling is applied to the initial condition, which is the same as scaling the slip on the fault and thus increasing the nominal magnitude of the earthquake. The latter can thus be much larger than the magnitude one would use for a deterministic tsunami scenario. The same happens in seismic hazard, but there the effect is implicit since one scales the individual time series rather than the input earthquake.

### 7.2 Probabilistic inundation

There are several ways in which we can obtain the probabilistic inundation from the offshore exceedance amplitudes:

- Onshore projection using empirical relationships or analytical runup laws – These functions typically yield the amplification from the offshore point to the final runup point as function of local parameters such as slope of the topography/bathymetry, period of the wave, offshore amplitude, etc. This method is the least accurate of the three but can handle large areas efficiently and is therefore very useful for large scale loss estimates (Løvholt et al., 2012).
- Offshore amplitude matching – Scenarios are selected, using the source disaggregation, with their magnitude adjusted so that their offshore amplitudes match the probabilistic

exceedance amplitudes. The inundation is then a direct reflection of the offshore exceedance amplitudes. This is the method used in Thio et al. (2010) and also by Wei et al. (2017) to obtain the inundation design zones for ASCE 7-16.

- Sampling of the offshore hazard curve – Instead of directly matching the offshore exceedance amplitudes, we define a reduced suite of scenarios represent the probabilistic hazard

The last method is used for this project and discussed in this report and has the advantage of allowing us to apply an aleatory variability of the inundation to the runup result. We have computed 30 distant scenarios from Alaska, Chile and the Kuriles, the dominant distant sources in California, that span a range of sizes and cover the entire range of offshore exceedance amplitudes (Figure 10a). For areas along the Cascadia subduction zone, we expanded this set with another 30 Cascadia scenarios. Our assumption is that this event set is representative for the tsunami hazard in California.

### 7.2.1 Scenario probabilities

To compute the probabilistic inundation from this set, we need to determine the rate of occurrence for each scenario, i.e. the probability distribution of the reduced event set.

The metrics that we use are the offshore amplitudes of these scenarios at the same locations for which we derived the offshore hazard curves. Since we are considering a discrete number of events, the probability distribution of the offshore amplitudes of the reduced set ( $p$ ) is a Probability Mass Function (PMF), which can be determined from the offshore hazard curve ( $P$ ), a Cumulative Density Function (CDF), since the probabilities of the reduced event set need to satisfy the offshore hazard curves.

In summary:

The probabilities are anchored to the probabilistic offshore amplitudes, so we define the probability for event  $i$ ,  $p_i$ , as the probability of its offshore amplitude  $a_i$ :  $p_i = p(a_i)$ .

The events are sorted according to their offshore amplitudes:  $a_i < a_{i+1}$ , with the number of events in our reduced set  $n$ .

The offshore hazard curve (CDF), expresses the probability of exceeding an amplitude  $A$ :  $P(a \geq A)$ .

Then:

$$p_i = p(a_i) = P(a \geq a_i) - \sum_{k=i+1}^n p(a_k)$$

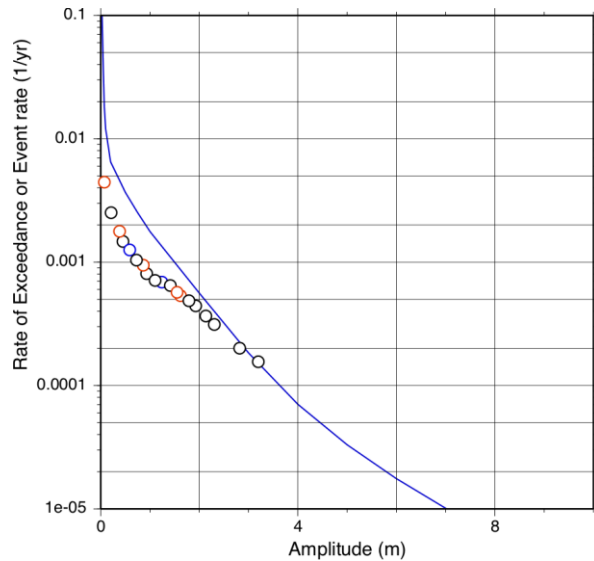


Figure 10. Schematic example of the relationship between the offshore hazard curve (blue line) and the probabilities of the reduce event set (circles, color coded according to source zone). Note that the event probability of the largest amplitude is equal to the exceedance probability of the offshore hazard curve.

Note that this is essentially the inverse of the process by which the offshore hazard curves were obtained from the original, comprehensive, set of events (section 6), which was several orders of magnitude larger. As an alternative to the numerical approach, we can also obtain the rates from the slope of the hazard curve, which yields similar results, which indicates that our sampling of the hazard curve is sufficiently dense.

Once the event probabilities, or rates, have been determined, it is possible to compute the inundation hazard curves at every cell in the same way as the offshore hazard curves were computed. We note that at each cell the hazard curve is computed independently, so that in theory the inundation at the same probability level in different cells can be affected by different scenarios from the reduced event set, which is preferable over

the other approaches where one or two scenarios determine the inundation in the entire model. Such a situation might arise if different source regions yield very different inundation patterns. In our experience in California, this source dependence does not seem to play a large role for the distant events but may be an issue in some near-source environments in Cascadia. A comparison between two inundation maps, one produced with the full event set and one with only distant events (Figure 11) suggest that the sensitivity to the sources is small with this method.

The event rates are also used to compute the probabilistic maps for flow velocity and momentum flux. Since these parameters show a much stronger complexity and variability between scenarios compared to wave amplitudes, we believe the current method is much better suited for resolving these details than the single- or dual-scenario approaches. A more systematic analysis of these parameters is recommended for future work.

### 7.2.2 On-land hazard curves

The only complication when computing the hazard curves is that the on-land amplitudes are truncated by the topography (for some or all scenarios a grid point remains dry) whereas the offshore amplitudes have finite values everywhere for every event. We normally interpolate the inundation hazard curve to obtain exceedance amplitudes for specific return periods. In the case

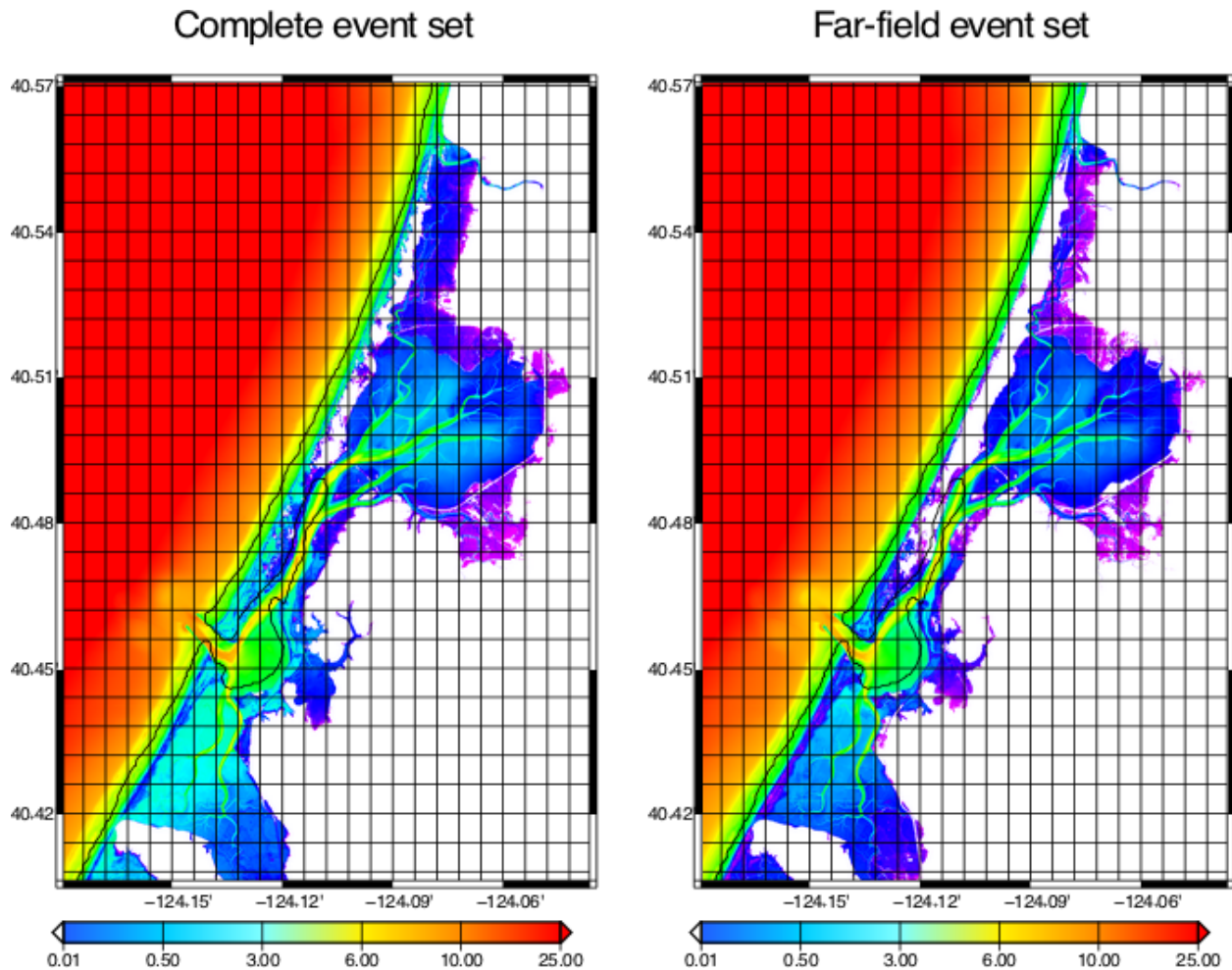


Figure 11. Comparison for the 2475 year Humboldt Bay probabilistic flowdepth maps for a model using the full event set (Left) and only the far-field event set (right). The overall inundation pattern appears quite stable.

where a specific probability level falls below the lowest scenario amplitude in a cell, we can use an extrapolation of the two lowest scenario amplitudes to estimate amplitude for the target probability. Likewise, when we apply an additional aleatory variability, a scenario amplitude may be increased to the extent that it would flood cells that had remained dry. In order to solve this issue we also apply an extrapolation from a larger “wet” scenario amplitude using the amplitude ratio between the two scenarios for the nearest cell where both scenarios had non-zero amplitudes.

### 7.3 Aleatory variability

For the aleatory variability in the inundation and runup phase of the tsunami, we need to develop separate sigma contributions. The recent Tohoku earthquake provides a wealth of data for this purpose, since there is data from both the shoreline as well as the final runup. This allows us to separate the runup portion from the propagation sigma that is described in section 5. The Okushiri benchmarking exercise (Appendix F) does provide data that can be used for this purpose as well, and in Figure 12 we show the comparison of our model and the data. If we simply



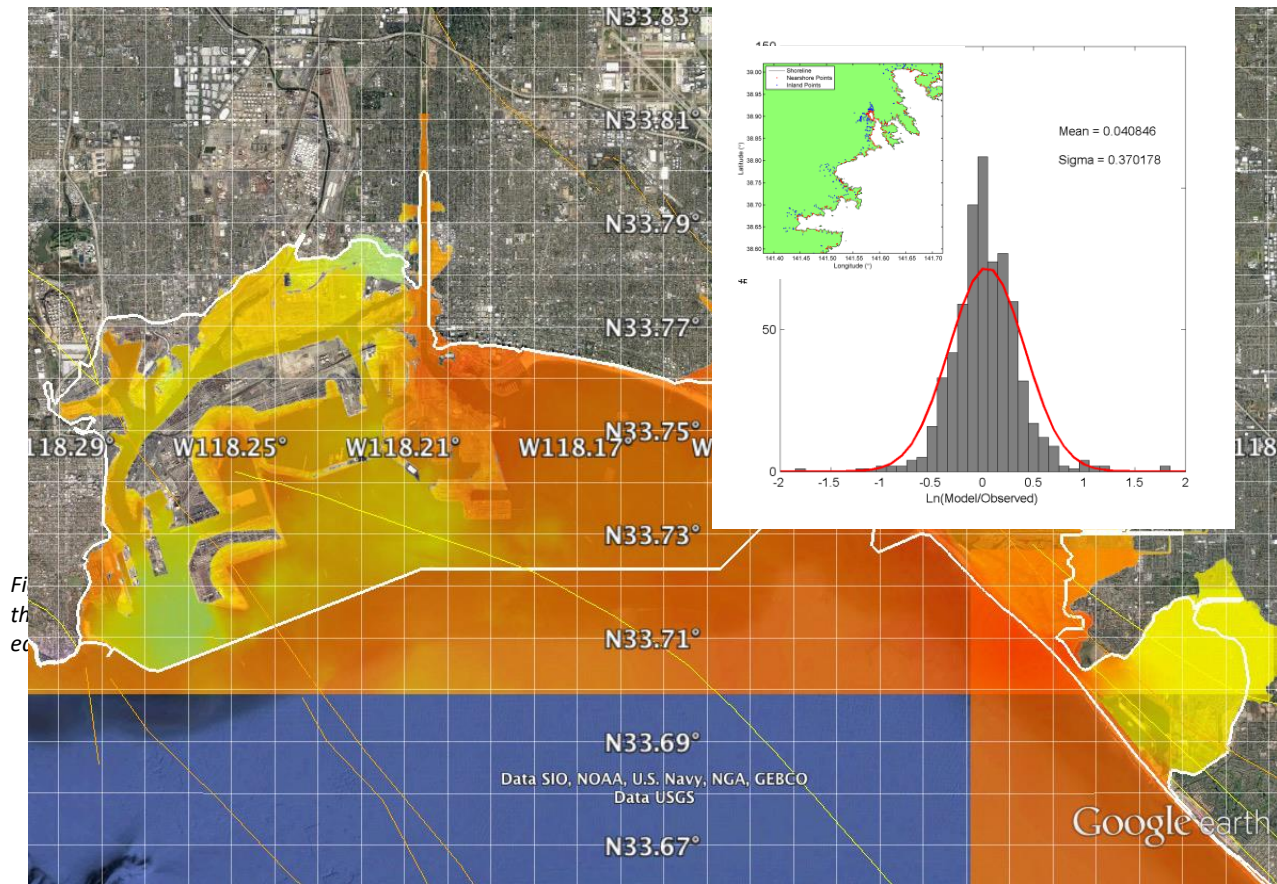


Figure 13. Examples of 2,475 year ARP (2% in 50 years) inundation maps, color coded for exceedance amplitude, for the Ports of Los Angeles and Long Beach as well as northern Orange County. Outlined in white are the inundation zones from the second-generation maps <reference needed>..

compare the average values and perform a regression over the ratio  $\ln(\text{data})/\ln(\text{model})$  we obtain a standard deviation (for a lognormal distribution) of 0.37 (Figure 12) and only a small bias (0.04).

#### 7.4 Results – Inundation maps

The results we present here are based on a combination of tele-tsunami sources (primarily Alaska and the Kuriles) and the Cascadia subduction zone (Appendix E). We present results as maps of exceedance amplitudes (Figures 13), and flow velocity exceedance (Figure 14). The wave-height maps are relative to Mean High Water (MHW), but, in the case of Cascadia, not necessarily to the same ground surface since different earthquakes cause different uplift or subsidence. The flow-depth maps are therefore more consistent and useful in practice. The flow velocity maps show very strong concentrations of high velocities near sharp contrasts in bathymetry, such as Ports as well as at the shorelines.

The maps that we have produced cover a range of ARP's between 72 and 3,000 years. These are typical ranges for engineering practice as well as other types of hazard and risk analysis. We have created maps for exceedance amplitude, flow-depth, flow velocity and momentum flux. Figure 15 shows the complete set of 10m high-resolution inundation maps that are available.

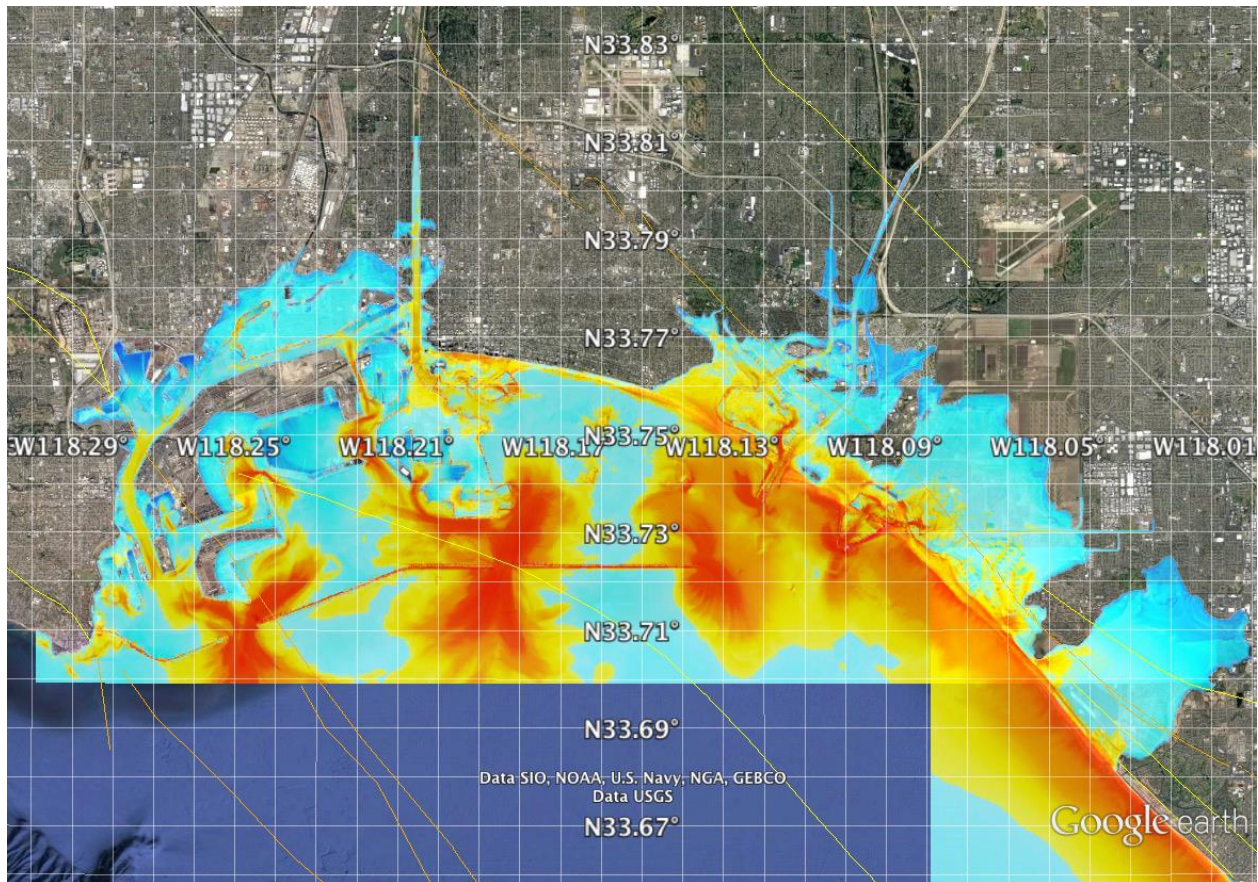


Figure 14. Exceedance flow velocities (2475 yr ARP) in the Ports of Los Angeles and Long Beach and northern Orange Count.

## 7.5 Compliance with ASCE 7-16

The procedure to obtain the probabilistic inundation maps does not involve a direct mapping of one scenario that a-priori matches the offshore exceedance amplitudes, but instead uses the integration over a set of scenarios that sample the offshore hazard curve. It is therefore necessary to check whether the final runup line, which in ASCE 7-16 anchors the Grade Line Energy method, still matches the offshore hazard criteria, which state that the average of offshore exceedance amplitudes exceeds average ASCE amplitudes and no offshore amplitude is below 80%, over a 60-80 km range. We performed a back calculation from the runup line to the offshore hazard points. For every runup location, we determined the bracketing (or extrapolating) scenarios and the ratio of our gridded flow depth to that of the bracketing events. Using the same ratios, we then computed the corresponding offshore amplitude for every grid point at every offshore hazard point. In Figure 16, we show examples of the ratio of the back-calculated offshore amplitudes and the ASCE offshore amplitudes. A complete set of comparisons is shown in Appendix H.

## 7.6 Limitations

Although these model results show well-defined demarcations of inundation and other parameters, we need to recall some of the limitations that are present:

- Finite grid resolution - Certain features, such as dunes, breakwaters, and levees, with dimensions below 25-20m are not resolved completely through modeling. In the case of breakwaters, which are often permeable, this problem may not be as serious. However, in the case of levees, which are meant to prevent flooding, an insufficient resolution may lead to spurious inundation.
- Bare Earth – The models are devoid of any buildings, which can significantly alter the course of inundation, and we have assumed single bottom friction throughout.
- Flow velocity and momentum flux – Whereas the wave amplitudes and inundation are quite stable in terms of details of the input source and numerical model, flow velocities, and even more momentum flux, behave highly chaotically and therefore are very sensitive to details of both the physical environment as well as the details of the algorithms used to compute the tsunami (e.g. Lynett et al., 2017). Therefore, care should be taken when interpreting or using these data, especially in areas with pronounced topographic features and built-up areas.

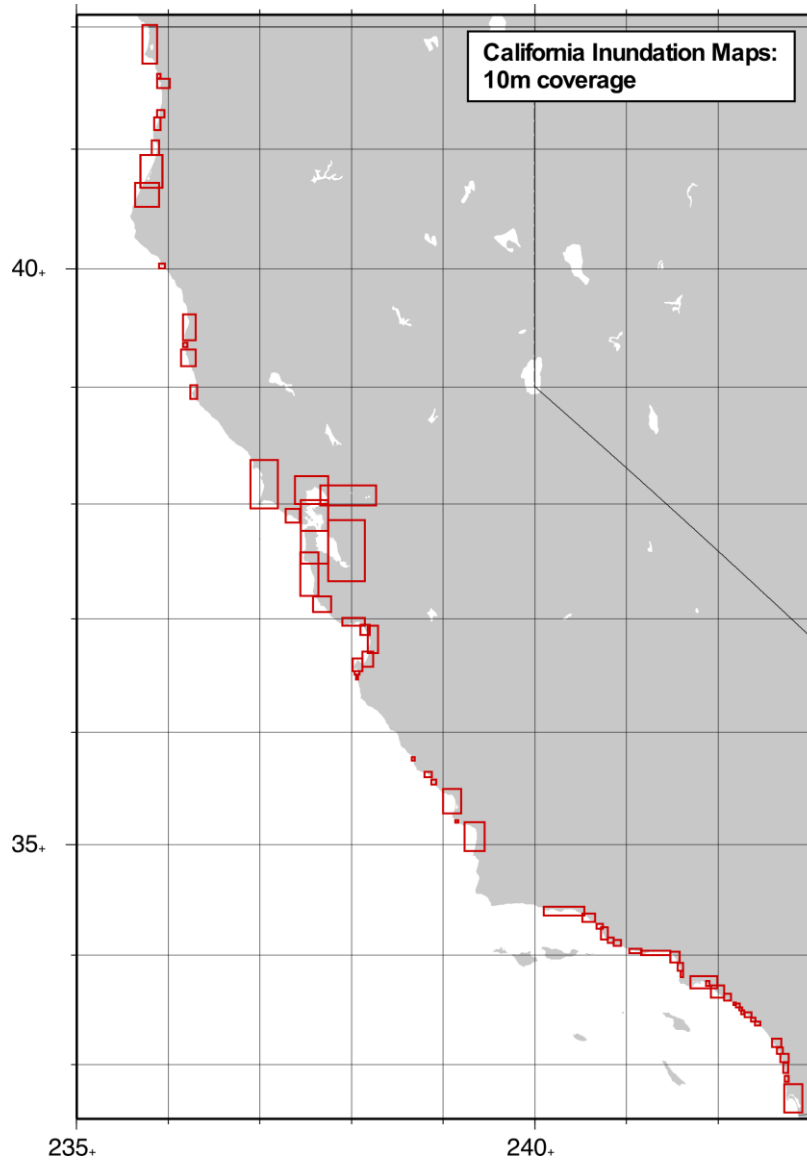


Figure 15. Coverage of the detailed 10m inundation maps for the State of California.

To reduce the impact of topographic issues on inundation, the model results were analyzed by referencing higher resolution digital elevation models (1-m coastal Lidar, circa 2009-11; source: NOAA Digital Coast website, 2016-17), and evaluating the products in the field along the ocean-beach interface and levees and breakwaters. Changes were made to the final PTHA maps where there were clear errors in the model results.

**31\_Cambria**

**07\_Humboldt\_Bay**

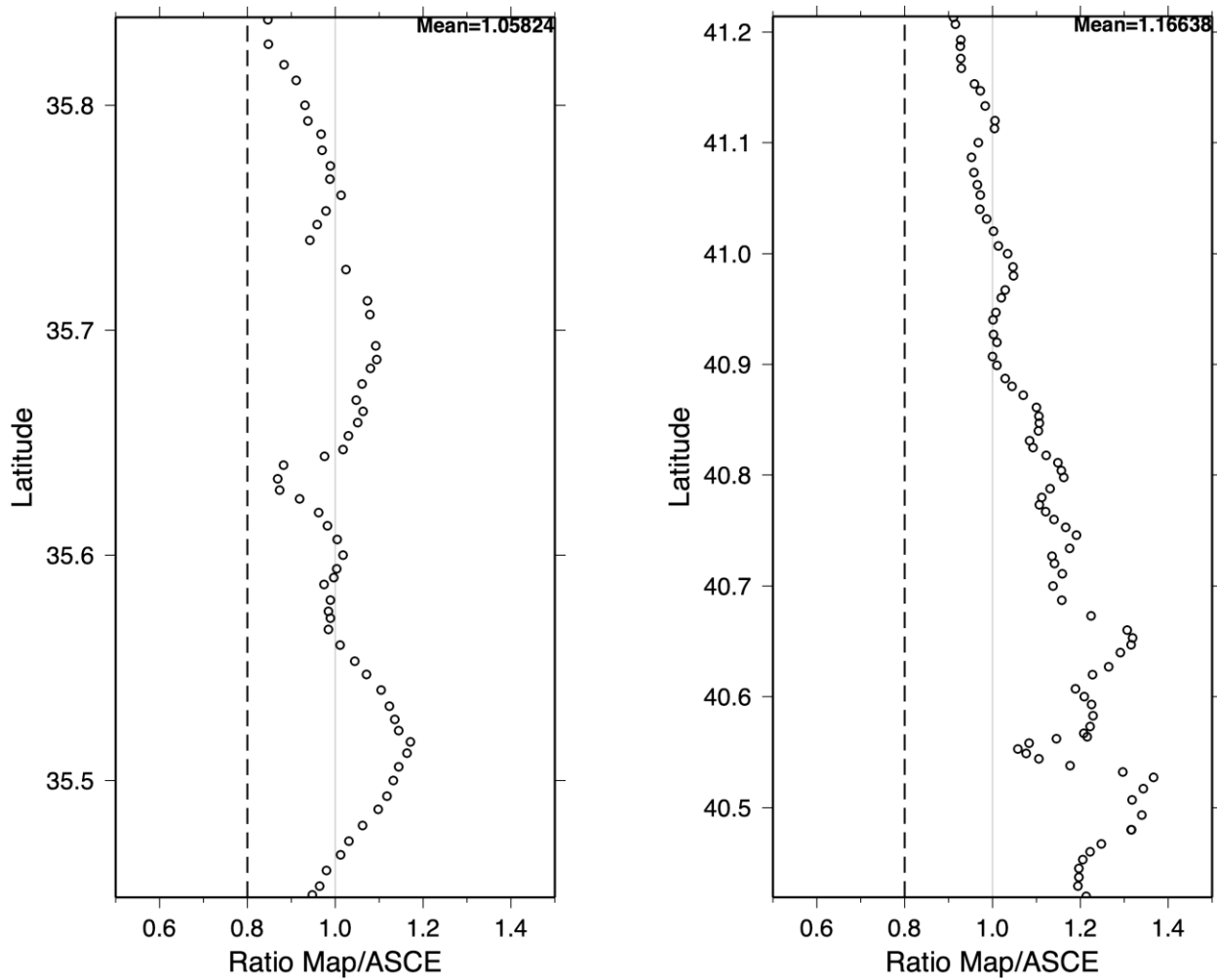


Figure 16. Examples of offshore ratios between gridded inundation and ASCE values. Cambria (left) and Humboldt Bay (right). Vertical axis – latitude, horizontal axis – ratio of gridded/ASCE offshore values.

## 8. Comparisons

### 8.1 Previous tsunami hazard studies

The previous generation hazard maps for California were based on worst-case models from local and distant earthquake and landslide sources. There are therefore substantial differences between those source models and the current set. Yet, in many cases our 2,475 and 3,000 year ARP maps appear to be close to the previous generation worst-case maps. This similarity is somewhat fortuitous, as the worst-case scenarios tended to be local earthquake and landslide scenarios that can generate large tsunamis, but which tend to have very long recurrence intervals, which is why they were not considered in this study. Although in some cases, this may be due to a pronounced topography such as a cliff, the fact that our maps approach these worst case maps is due to the inclusion of the aleatory variability in our analysis.

## 8.2 In relation to other hazards

Tsunami hazard is characterized by its low-probability/high-impact character and it is important to point out some significant differences with other types of natural hazards. In terms of sources, earthquake hazard is the closest related hazard and shares many of the input models and parameters (see the comparison between PSHA and PTHA in Figure 2). Our choice of return periods also follows the earthquake hazard, which compared to other hazards also falls in the range of low-probability/large-impact category. Tsunami affect much larger areas than earthquakes, the largest causing damage and casualties over the entire Pacific Ocean, thousands of kilometers from the earthquake source. On the flip-side, these events do allow for significant warning times, which influences how the current hazard models are to be used as compared to, say, earthquake hazard maps where significant early warning is not as practical. In terms of losses, tsunamis are characterized by very steep fragility relations, which can make loss estimation very sensitive to the hazard results.

Flooding hazard due to storms or other weather-related phenomena are of course directly comparable to tsunami hazard, but here, there are also very important distinctions. Wavelengths in storm waves are several orders of magnitudes shorter than tsunami waves and thus similar wave amplitudes between storms and tsunamis stand for very different scales of energy, force and amounts of flooding. Furthermore, current storm flooding hazard models, which are based on a frequentist approach, tend to saturate at relatively short return periods on the order of several hundred years, whereas, tsunami hazard tends to increase with decreasing probability levels.

## 9. Acknowledgments

We appreciate the reviews of draft versions of this report by:

Rui Chen (CGS), Art Frankel (USGS), Eric Geist (USGS), Yvette LaDuke (CalOES), Patrick Lynett (USC), Kevin Miller (CalOES), Stephanie Ross (USGS), Rick Wilson (CGS).

## 10. References

- ASCE (American Society of Civil Engineers), 2017. ASCE 7-16 Minimum Design Loads For Buildings and Other Structures, Reston, VA.
- Atwater, B.F., Stuiver, M., and Yamaguchi, D.K. 1991. Radiocarbon test of earthquake magnitude at the Cascadia subduction zone, *Nature*, **353**(6340), 156–158, doi:10.1038/353156a0.
- Barberopoulou, A., Borrero, J.C., Uslu, B., Kalligeris, N., Goltz, J.D., Wilson, R.I., and Synolakis, C.E., 2009. New Maps of California to Improve Tsunami Preparedness, *Eos, Transactions American Geophysical Union*, **90**(16), 137–138, doi:10.1029/2009EO160001.
- Barberopoulou, A., Borrero, J.C., Uslu, B., Legg, M.R. & Synolakis, C.E., 2011. A Second Generation of Tsunami Inundation Maps for the State of California. *Pure and Applied Geophysics* **168**(11), 2133–2146.
- Becker, J.J., Sandwell, D.T., Smith, W.H.F., Braud, J., Binder, B., Depner, J., Fabre, D., Factor, J., Ingalls, S., Kim, S.-H., Ladner, R., Marks, K., Nelson, S., Pharaoh, A., Trimmer, R., Rosenberg, Von, J., Wallace, G., and Weatherall, P., 2009. Global Bathymetry and Elevation Data at 30 Arc Seconds Resolution: SRTM30\_PLUS. *Marine Geodesy* **32**(4), 355–371.
- California PTHA Work Group, 2015. Evaluation and Application of Probabilistic Tsunami Hazard Analysis in California, 33 p. California Geological Survey Special Report 237, pp. 1–33.
- Chen, R., Frankel, A. & Petersen, M., 2014. Implementation of the Cascadia Subduction Zone Source Models for the 2014 Update of the National Seismic Hazard Maps, 12pp.
- Eakins B.W., and Taylor L.A., 2010. Seamlessly integrating bathymetric and topographic data to support tsunami modeling and forecasting efforts, in *Ocean Globe*, ed. by J. Breman, ESRI Press, Redlands, 37-56.
- Earthquake Research Committee, 2005. National seismic hazard maps for Japan, Headquarters of Earthquake Research Promotion, Japan.
- Eisner, R.K., Borrero, J.C., and Synolakis, C.E., 2001. Inundation maps for the State of California. In Proceedings of the International Tsunami Symposium 2001.
- Gonzalez, F.I., LeVeque, R.J., and Adams, L.M., 2013. Probabilistic Tsunami Hazard Assessment (PTHA) for Crescent City, CA, Final Report on Phase I, January 31, 2013: University of Washington Report, 70 p.
- Hayes, G.P., Wald, D.J. and Johnson, R.L., 2012. Slab1.0: A three-dimensional model of global subduction zone geometries. *Journal of Geophysical Research: Solid Earth* **117**(B1), B01302.
- Heaton, T. H., and Kanamori, H., 1984. Seismic potential associated with subduction in the northwestern United States, *Bull. Seismol. Soc. Am*, **74**(3), 933–941.
- Houston, J.R., and Garcia, A.W., 1978. Type 16 Flood Insurance Study: Tsunami Predictions for the West Coast of the Continental United States. Technical Report H 78-26, USACE Waterways Experimental Station, Vicksburg.

- Liu, P.L.F., Cho, Y.S., Briggs, M.J., Kânoğlu, U., and Synolakis, C.E., 1995. Runup of solitary waves on a circular island. *Journal of Fluid Mechanics* **302**, 259–286.
- Løvholt, F., Glimsdal, S., Harbitz, C.B., Zamora, N., Nadim, F., Peduzzi, P., Dao, H., and Smebye, H., 2012. Tsunami hazard and exposure on the global scale. *Earth Science Reviews* **110**(1-4), 58–73.
- Ludwin, R.S., Dennis, R., Carver, D., McMillan, A.D., Losey, R., Clague, J., Jonientz-Trisler, C., Bowe chop, J., Wray, J., and James, K., 2005. Dating the 1700 Cascadia earthquake: great coastal earthquakes in Native stories, *Seismol. Res. Lett.*, **76**(2), 140–148.
- Lynett, P.J., Gately, K., Wilson, R., Montoya, L., Arcas, D., Aytore, B., Bai, Y., Bricker, J.D., Castro, M.J., Cheung, K.F., David, C.G., Dogan, G.G., Escalante, C., González-Vida, J.M., Grilli, S.T., Heitmann, T.W., Horrillo, J., Kânoğlu, U., Kian, R., Kirby, J.T., Li, W., Macías, J., Nicolosky, D.J., Ortega, S., Pampell-Manis, A., Park, Y.S., Roeber, V., Sharghivand, N., Shelby, M., Shi, F., Tehranirad, B., Tolkova, E., Thio, H.K., Velioğlu, D., Yalçiner, A.C., Yamazaki, Y., Zaytsev, A., and Zhang, Y.J., 2017. Inter-model analysis of tsunami-induced coastal currents. *Ocean Modelling* **114**, 14–32.
- Mandli, K.T., Ahmadi, A.J., Berger, M.J., Calhoun, D.A., George, D.L., Hadjimichael, Y., Ketcheson, D.I., Lemoine, G.I., and LeVeque, R.J., 2016. Clawpack: building an open source ecosystem for solving hyperbolic PDEs. *PeerJ Computer Science*. doi:10.7717/peerj-cs.68
- McGuire, R.K., 2004. Seismic hazard and risk analysis, Earthquake Engineering Research Institute, MNO-10, 240 pp.
- Mofjeld, H.O., González, F.I., Titov, V.V., Venturato, A.J., and Newman, J.C., 2007. Effects of Tides on Maximum Tsunami Wave Heights: Probability Distributions\*, *J. Atmos. Oceanic Technol.*, **24**(1), 117–123, doi:10.1175/JTECH1955.1.
- Murotani, S., Miyake, H., and Koketsu, K., 2008. Scaling of characterized slip models for plate-boundary earthquakes. *Earth, Planets and Space* **60**(9), 987.
- Murotani, S., Satake, K. & Fujii, Y. 2013. Scaling relations of seismic moment, rupture area, average slip, and asperity size for M~9 subduction-zone earthquakes. *Geophysical Research Letters* **40**(19), 5070–5074.
- Okada, Y., 1992. Internal deformation due to shear and tensile faults in a half-space. *Bulletin of the Seismological Society of America* **82**(2), 1018–1040.
- Papazachos, B., Scordilis, E., Panagiotopoulos, D., Papazachos, C.B., and Karakaisis, G.F., 2004. Global relations between seismic fault parameters and moment magnitude of earthquakes. *Bulletin of the Geological Society of Greece* **36**(3), 1482–1489.
- Petersen, M.D., Moschetti, M.P., Powers, P.M., Mueller, C.S., Haller, K.M., Frankel, A.D., Zeng, Y., Rezaeian, S., Harmsen, S.C., Boyd, O.S., Field, N., Chen, R., Rukstales, K.S., Luco, N., Wheeler, R.L., Williams, R.A., and Olsen, A.H., 2014. *Documentation for the 2014 Update of the United States National Seismic Hazard Maps*, USGS Open File Report 2014-1091.



- Satake, K., Shimazaki, K., Tsuji, Y., and Ueda, K., 1996. Time and size of a giant earthquake in Cascadia inferred from Japanese tsunami records of January 1700. *Nature* **379**(6562), 246–249.
- Savage, J.C., 1987. Effect of crustal layering upon dislocation modeling. *Journal of Geophysical Research: Solid Earth* **92**(B10), 10595–10600.
- Savage, J.C., 1998. Displacement field for an edge dislocation in a layered half-space. *Journal of Geophysical Research: Solid Earth* **103**(B2), 2439–2446.
- Shennan, I., Bruhn, R., and Plafker, G., 2009. Multi-segment earthquakes and tsunami potential of the Aleutian megathrust. *Quaternary Science Reviews* **28**(1-2), 7–13.
- Strasser, F.O., Arango, M.C., and Bommer, J.J., 2010. Scaling of the Source Dimensions of Interface and Intraslab Subduction-zone Earthquakes with Moment Magnitude, *Seismol. Res. Lett.*, **81**(6), 941–950, doi:10.1785/gssrl.81.6.941.
- Thio, H.K., Somerville, P.G., Ichinose, G.A., 2007. Probabilistic analysis of strong ground motion and tsunami hazards in Southeast Asia. *Journal of Earthquake and Tsunami* **1**(02), 119–137.
- Thio, H.K., Somerville, P.G., and Polet, J., 2010. Probabilistic tsunami hazard in California: *Pacific Earthquake Engineering Research Center Report*, v. **108**, p. 331.
- Thio, H.K., Wei, Y., Chock, G., and Li, W., 2017. Development of Offshore Probabilistic Tsunami Exceedance Amplitudes for ASCE 7-16. In Proceedings of the Sixteenth World Conference on Earthquake Engineering, Santiago.
- Vick, Steven G., 2002. *Degrees of belief: subjective probability and engineering judgment*. Reston, Va: ASCE Press
- Wald, D.J., and Graves, R.W., 2001. Resolution analysis of finite fault source inversion using one- and three-dimensional Green's functions: 2. Combining seismic and geodetic data. *Journal of Geophysical Research: Solid Earth* **106**(B5), 8767–8788.
- Wang, R., Martin, F.L., and Roth, F., 2003. Computation of deformation induced by earthquakes in a multi-layered elastic crust--FORTRAN programs EDGRN/EDCMP, *Computers & Geosciences*, **29**(2), 195–207.
- Wesson, R.L., Boyd, O.S., Mueller, C.S., Bufe, C.G., Frankel, A.D., and Petersen, M.D., 2007. *Revision of time-independent probabilistic seismic hazard maps for Alaska*, US Department of the Interior, US Geological Survey Open File Report 2007-1043.
- Wei, Y., Thio, H.K., Titov, V., Chock, G., Zhou, H., Tang, L., and Moore, C., 2017. Inundation Modeling to Create 2,500-Year Return Period Tsunami Design Zone Maps for the Asce 7-16 Standard. In Proceedings of the Sixteenth World Conference on Earthquake Engineering, Santiago.
- Witter, R.C., Carver, G.A., Briggs, R.W., Gelfenbaum, G., Koehler, R.D., La Selle, S., Bender, A.M., Engelhart, S.E., Hemphill-Haley, E., and Hill, T.D., 2016. Unusually large tsunamis frequent a currently creeping part of the Aleutian megathrust. *Geophysical Research Letters* **43**(1), 76–84.



## **Appendix A. Offshore tsunami modeling**

In this section we describe the theory and algorithm that we used for the tsunami excitation, propagation and offshore amplitudes. The algorithm used for the inundation models is described in Appendix G.

### **A.1. Source excitation model**

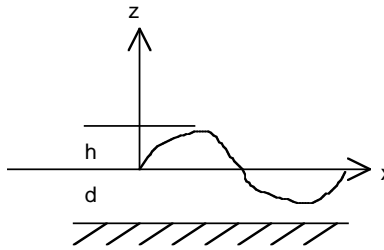
The tsunami excitation by earthquake sources is modeled by translating the vertical deformation field of the earthquake source (surface faulting) into a vertical displacement of the water column. This method is commonly used in tsunami studies (e.g. Titov and Synolakis, 1996; Satake, 1995). The static displacement fields were computed using a frequency-wave-number integration technique (FK) using a simple layered crustal model (Wang et al., 2003; 2006).

### **A.2. Tsunami computation**

We take an Eulerian approach to describe the particle motion of the fluid. Only the velocity changes of the fluid are described at some point and at some instant of time rather than describing its absolute displacement. We consider a wave that is a propagating disturbance from an equilibrium state. Gravity waves occur when the only restoring force is gravity. When the horizontal scale of motion is much larger than the water depth, then the vertical acceleration of water is much smaller than the gravity acceleration and thus negligible. This means that the whole water mass from the bottom to the surface is assumed to move uniformly in a horizontal direction. This kind of gravity wave is also known as a “long-wave.” Long wave approximations are appropriate when the water depth of lakes and oceans (< 5 km) is much smaller than the length of the disturbance (fault lengths ~ 10-1000 km). This approximation gives an accurate description of tsunami wave propagation in the open ocean. In order to also model the propagation of tsunami waves in coastal areas, we use an approximation to the wave equation where the low-amplitude linear long-wave requirements are relaxed, as shown in the following sections.

#### *General Linear Gravity Wave*

The following is a derivation of the general case of gravity waves for two dimensions where  $x$  is the horizontal direction and  $z$  is vertical direction. We start from the Euler’s equation of motion that considers the conservation of momentum on a volume of water. The Newton equations can be simplified as:

$$\frac{d}{dt}V = g - \frac{1}{\rho} \nabla p$$


where  $d/dt$  is the total and  $\partial/\partial t$  is the partial derivative with respect to time,  $g$  is the gravitational acceleration,  $V = (u, w)$  are the depth averaged velocities in the  $x$  and  $z$  directions,  $\rho$  is the density, and  $p$  is the fluid pressure. The figure shows that  $h$  is the tsunami wave height and  $d$  is the water depth. We next consider the conservation of mass to derive the equation of continuity,

$$\frac{\partial r}{\partial t} + \nabla \cdot (rV) = 0$$

and for incompressible fluid becomes,

$$\nabla \cdot V = 0.$$

From the Euler's equation of motion the horizontal and vertical acceleration components are,

$$\frac{du}{dt} = -\frac{1}{\rho} \frac{\partial p}{\partial x}$$

$$\frac{dw}{dt} = -g - \frac{1}{\rho} \frac{\partial p}{\partial z}$$

The relationship between  $h$  and  $p$  is related through the hydrostatic pressure equation,

$$p = -\rho g(h - z) + p_0$$

where  $h$  is the wave height,  $z$  is the water depth, and  $p_0$  is the pressure of one atmosphere at  $z = 0$  and  $h = 0$ . The horizontal and vertical pressure gradients given from the slope of the water surface,

$$\frac{\partial p}{\partial z} = \rho g$$

$$\frac{\partial p}{\partial x} = -\rho g \frac{\partial h}{\partial x}$$

are combined with the Euler's equation to give the horizontal and vertical components,

$$\frac{du}{dt} = -g \frac{\partial h}{\partial x}$$

$$\frac{dw}{dt} = 0$$

For ocean tsunamis, the non-linear advective term is small and can be ignored, therefore the equation of motion is,

$$\frac{du}{dt} = \frac{\partial u}{\partial t} + u \frac{\partial u}{\partial x} \gg \frac{\partial u}{\partial t}$$

$$\frac{\partial u}{\partial t} = -g \frac{\partial h}{\partial x}$$

We next consider the conservation of mass for a region with a small length  $dx$ . Since the volume change per unit time must be equal to the flow rate of water going out of this region, we can therefore write

$$\frac{\partial}{\partial t} \{ (h + d) dx \} = - \frac{\partial}{\partial x} \{ u(h + d) \} dx$$

$$\frac{\partial h}{\partial t} = - \frac{\partial}{\partial x} \{ u(h + d) \}$$

$$\frac{\partial h}{\partial t} = - \frac{\partial}{\partial x} (du)$$

which is the simplified equation of continuity when the amplitude of the wave is small compared to the water depth. The so-called small-amplitude, linear, long wave assumption is valid for most of tsunami propagation paths except near coasts.

### *Nonlinear Gravity Waves and Shallow Water Waves*

Without a viscous force to dissipate wave energy, the water motion will continue forever. In order to include the viscous effect, we can add a term for viscous stress to the equation of motion. We only consider a shear stress at the water bottom ( $\tau_x^b$ ) and the normal stress is already included and equal to the pressure. The shear stress is experimentally estimated as

$$\tau_x^b \gg C_f v_x \sqrt{v_x^2 + v_y^2}$$

and the frictional force is

$$F_x^b = C_f \frac{v_x \sqrt{v_x^2 + v_y^2}}{d + h}.$$

Satake [1995] adopted two types of frictional coefficients from engineering hydrodynamics for including bottom friction for tsunamis. These are the De Chezy ( $C_c$ ) and Mannings's roughness ( $n$ ) coefficients. These have different dimensions therefore a non-dimensional frictional coefficient  $C_f$  is related to these two coefficients by

$$C_f^2 = \frac{g}{C_c^2}$$

and

$$C_f = \frac{gn^2}{(d+h)^{1/3}}$$

The Manning's roughness coefficient  $n$  is used for a uniform turbulent flow on a rough surface. It indicates that the bottom friction varies with water depth. We use an  $n$  of  $0.03 \text{ m}^{-1/3} \text{ s}$ , typical for coastal waters. If  $n$  is translated to  $C_f$ , then  $n$  becomes  $2.3 \times 10^{-3}$  for a total depth of 50 m and  $1 \times 10^{-2}$  for a total depth of 0.6 m, which agree well with observational values of tidal flow and run-up of solitary waves (see Satake, 1995).

Since the earth is rotating, there is a force apparently acting on a body of water. In an inertial reference frame (fixed on the rotating Earth), this force is called the Coriolis force. The derivation of this term is beyond the scope of this report and we refer the reader to textbooks on analytical mechanics. The vertical acceleration due to the Coriolis force is much smaller than gravity ( $3 \text{ cm/s}^2$  compared to  $980 \text{ cm/s}^2$  at 4000 m depth). In a local Cartesian coordinate system, the horizontal components are given by

$$F_x^{cor} = -fv_y$$

$$F_y^{cor} = fv_x$$

where  $f$  is the Coriolis parameter, and this force always acts to the right hand side of the motion in the northern hemisphere. The Coriolis force is only significant for long propagation times and distances along lines of latitude near the equator.

We derive the equations for general gravity waves without making the small amplitude, linear long-wave approximation appropriate when the wave height is much smaller than the water depth ( $h \ll d$ ). If we expand the hyperbolic tangent function using the Taylor series expansion and include the first and second order terms then the corresponding equation of motion becomes

$$\frac{\partial u}{\partial t} = -g \frac{\partial h}{\partial x} + \frac{1}{3} d^2 \frac{\partial^3 u}{\partial x^2 \partial t}$$

which is also known as the Boussinesq equation. After relaxing the small amplitude assumption, the equation of motion and continuity are given as

$$\begin{aligned} \frac{du}{dt} + u \frac{\partial u}{\partial x} &= -g \frac{\partial h}{\partial x} \\ \frac{\partial h}{\partial t} &= -\frac{\partial}{\partial x} \{u(h+d)\} \end{aligned}$$

These equations are for the finite-amplitude shallow water waves. For the linear case, the phase velocity is given by the following Taylor series expansion of the hyperbolic tangent function,

$$c = \sqrt{gd} \left[ 1 - \frac{2p^2}{3} \frac{d}{\lambda} \right]$$

where  $\lambda$  is the wavelength. In the nonlinear case the  $d$ -term in the phase velocity is replaced by the total height of the water column ( $d+h$ ), which gives us a phase velocity of the form

$$c \sim \sqrt{g(d+h)}$$

Note that in the nonlinear case a phenomena of amplitude dispersion, the larger the amplitude, the faster the wave speed. As a consequence, peaks of a wave catch up with troughs in front of them, and the forward facing portion of the wave continues to get steeper. This wave will eventually break.

Including the bottom friction and Coriolis force, the equation of motion for shallow water waves can be written for a two-dimensional case as follows:

$$\frac{\partial U}{\partial t} + U \frac{\partial U}{\partial x} + V \frac{\partial U}{\partial y} = -fV - g \frac{\partial h}{\partial x} - C_f \frac{U \sqrt{U^2 + V^2}}{d+h}$$

$$\frac{\partial V}{\partial t} + U \frac{\partial V}{\partial x} + V \frac{\partial V}{\partial y} = -fU - g \frac{\partial h}{\partial y} - C_f \frac{V \sqrt{U^2 + V^2}}{d+h}$$

and the equation of continuity is

$$\frac{\partial h}{\partial t} + \frac{\partial}{\partial x} \{U(h+d)\} + \frac{\partial}{\partial y} \{V(h+d)\} = 0$$

where the coordinate system is  $x$ =East  $y$ =South,  $f$  is the Coriolis parameter,  $C_f$  is a non-dimensional frictional coefficient, and  $U$  and  $V$  are the average velocities in the  $x$  and  $y$  directions, respectively. The first term on the left hand side (lhs) is the local acceleration term, the second and third terms on the lhs are the advection terms, the first term on the right hand side (rhs) is the Coriolis force, the second term on the rhs is the restoring force from gravitation acceleration, and the third term on the rhs is the bottom friction force.

### Numerical Computation

The equations of motion and equation of continuity are converted from Cartesian to a spherical coordinate system  $(x,y,z) \rightarrow (r, \theta, \phi)$  with the origin at the Earth's center, but  $r$  is constant and equal to the earth's radius  $R$ . Note that  $\theta$  is the colatitude and measured southward from the North Pole and  $\phi$  corresponds to longitude measured eastward from the Greenwich meridian. These equations are solved by finite-difference method using the staggered leapfrog method (e.g., Satake, 1995). For the advection terms, an upwind difference scheme is used (e.g., Press et al. 2007). The land-sea boundary condition in the linear computation is total reflection and in the nonlinear case there is a moving boundary condition and run-up is considered. The time step of

computation is determined to satisfy the stability condition (Courant condition) of the linear and by trial and error for the nonlinear finite-difference computations.

### *Variable grid finite difference*

The variable grid setup consists of a master grid with coarse grid spacing and a number of nested finer grids with decreasing grid sizes around areas of interest. Our code allows for more than one area with decreased grid size. Currently, our code uses a fixed time-step, which generally is controlled by the finest grid-size.

### **A.3. Highly non-linear flow and inundation**

The URS code, like many other tsunami simulators (e.g. Method of Splitting Tsunamis, MOST), is based on a solution of the wave equations in terms of velocities. This is a highly efficient approach, which allows us to compute waveforms for a large ensemble of sources in a relatively short amount of time. This approach is not as accurate in the case of breaking waves and thus for inundation because momentum is not conserved across hydraulic jumps. We therefore used a different code for inundation modeling, based on the Clawpack libraries of LeVeque et al. (2014). This code is described and validated in Appendices F and G.

### **A.4. References**

- LeVeque, R.J., Berger, M.J., et. al., Clawpack Software 4.6.3, [www.clawpack.org](http://www.clawpack.org), accessed 02/2014
- Press, H., Teukolsky, S. A., Vetterling, W. T., and Flannery, B. P., 2007. *Numerical Recipes: The Art of Scientific Computing* (3rd ed.). New York: Cambridge University Press. p. xi. ISBN 978-0-521-88068-8.
- Satake, K., 1995. Linear and nonlinear computations of the 1992 Nicaragua earthquake tsunami. *Pure and Applied Geophysics* **144**(3), 455–470.
- Titov, V.V., and Synolakis, C.E., 1996. Numerical modeling of long wave runup using VTCS-3, in *Long Wave Runup Models*, Yeh H., et al (ed), 242-248, World Scientific, Singapore
- Wang, R., Martin, F.L., and Roth, F., 2003. Computation of deformation induced by earthquakes in a multi-layered elastic crust--FORTRAN programs EDGRN/EDCMP. *Computers & Geosciences* **29**(2), 195–207.
- Wang, R., Lorenzo-Martín, F., and Roth, F., 2006. Erratum to: 'Computation of deformation induced by earthquakes in a multi-layered elastic crust—FORTRAN programs EDGRN/EDCMP'. *Computers & Geosciences* **32**(10), 1817.



## Appendix B. Subduction zone earthquakes

### B.1. Introduction

Subduction zones are the main cause of the world's most devastating tsunamis and, since subduction zone dynamics are quite different than those of continental earthquakes, we will briefly discuss the most important aspects of these earthquakes. Our source model for tsunami hazard in California consists entirely of subduction zone earthquakes, and we will therefore focus on several characteristics that are of particular interest to earthquake and tsunami hazard analysis.

### B.2. The subduction cycle

Like any other earthquake, the overall temporal behavior of subduction zone seismicity is best described as stick-slip, i.e. the locking of the fault while stresses due to differential plate movements across the interface are built up, and the occasional catastrophic un-locking of the interface during an earthquake when these stresses are relieved.

While the interiors of the tectonic plates are thought to move continuously with respect to each other while their interfaces remain locked, it follows that, at the interfaces, stress and strain build up. In the case of a subduction zone, this process leads to inter-seismic uplift and subsidence, which normally are in the opposite sense as the co-seismic ground deformation, though not necessarily in the same amounts (i.e. zero-sum).

### B.3. Earthquake magnitudes

Earthquake ruptures tend to follow systematic relationships between their fault dimensions and slip. The most commonly used relationship have been derived by Wells and Coppersmith (1994), but more recently other relations have been published such as Hanks and Bakun (2002). These relations were derived exclusively for continental earthquakes and may not be applicable to megathrust events. Recently, several regression models have become available that were derived specifically for subduction zone (megathrust) earthquakes (Papazachos et al., 2004; Blaser et al., 2010; Strasser et al., 2010; Murotani et al., 2008, 2013).

#### *Multi-mode rupturing*

One of the most vexing problems in probabilistic hazard analysis is the correct identification of the event recurrence. In this report we used two main types of recurrence relations, truncated Gutenberg-Richter (G-R) and Maximum Magnitude. The distribution function for the Gutenberg-Richter relations shows an exponential decay of number of events with magnitude, whereas the Maximum Magnitude model is represented by a normal distribution around the Maximum Magnitude and is used by the USGS for the National Seismic Hazard maps (e.g. Petersen et al., 2014). For large fault systems, especially at subduction zone interfaces, the Maximum Magnitude is often used, e.g., Annaka et al. (2007). Even if globally the distribution of earthquakes for very large magnitudes follows a G-R relation, this does not imply that a G-R relation would be appropriate for recurrence relations on a single interface. The global G-R relation could be a

manifestation of a size distribution of subduction zone interfaces, which at a local level would be consistent with a Maximum Magnitude distribution.

$M_{Max}$ , and thus the maximum slip that can occur, affects the probabilistic tsunami hazard in two opposite ways; larger slip will result in longer recurrence since it will take more time to accumulate the amount of slip, and tsunami wave-height is proportional to the vertical deformation and thus the slip of an event. The latter is not true in seismic hazard where the ground motions tend to saturate with large magnitudes, so that the probabilistic shaking hazard actually declines with increasing  $M_{Max}$ .

Geologic evidence points to subduction zone earthquakes occurring on quite different scales, sometimes rupturing single segments, sometimes multiple segments. Along the Kuriles, Nanayama et al. (2003) inferred historic ruptures along the Kurile subduction zone that spanned multiple segments (in this case, at least the Tokachi-Oki and Nemuro-Oki segments). Similarly, along the Alaska subduction zone, Shennan et al. (2009) found that the previous ruptures along the 1964 segment also included rupture of the neighboring Yakutat segment. Schwarz (1999) argued on the basis of seismological analysis of several large subduction zone earthquakes that their repeated ruptures are complex and not characteristic, with subsequent earthquakes re-rupturing sections of previous large events. Other observations of multiple segment ruptures are presented below with the individual source descriptions.

#### *Downdip extent*

The down-dip rupture extent is relevant for tsunami hazard estimates because it governs where the hinge line is located between uplift and subsidence, and because it limits the overall width and area of the rupture and thus the size of the earthquake. Oleskevich et al. (1999) carried out a systematic study of the depths of the rupture limits, and found a good correlation with the 350° temperature limit for younger subduction zones, and a limit of 40 km for older (steeper) subduction zones. Brown et al. (2013) found a good correlation between the zone of seismic tremor and the bottom of the seismogenic zone, similar to what was found in Japan (Ide et al., 2007).

### **B.4. Earthquake recurrence**

Although there is general agreement on the convergence rates on most of the major subduction zones, this information only provides an upper bound on recurrence models of earthquakes since subduction zones often show ample evidence of a-seismic movement. In this section we discuss various studies that have tried to determine a value of the seismic to non-seismic deformation as well as the evidence from field observations of non-seismic deformation.

#### *Seismic efficiency and earthquake recurrence*

To estimate the recurrence rates of subduction zone earthquakes, we typically rely on two lines of evidence. The most direct evidence would be the actual historical record of tsunamis, or at least subduction zone earthquakes. The problem here, as in seismic hazard, is that the historical record is very short compared to the recurrence time of large earthquakes, especially the giant subduction zone events. Geological studies of tsunami deposits can extend this record extensively (e.g. Atwater and Moore 1992; Satake et al., 1996; Sieh, et al., 2008; Nanayama et

al., 2003; Pinegina, et al., 2003; Cisternas et al., 2005), but currently the geographical extent of these studies is rather limited. The 2004 Sumatra earthquake and tsunami have given a fresh impetus to studies of the geological record of tsunamis and some interesting results have already been found regarding previous events along the same structure (Monecke et al., 2008; Jankaew et al., 2008). Another issue is that in order to estimate the size of the earthquake, it is necessary to find coincident observations along the rupture plane, which, even if such data is available, is not unambiguous since the standard deviation of age determinations leaves the possibility of two or more clustered, yet separate events.

Alternatively, we can estimate recurrence rates by using convergence rates from plate models and assume that convergence is primarily accommodated by seismic release. This is regular practice for crustal faults in seismic hazard analysis but it appears that in subduction zones sometimes only a fraction of the total convergence rate is released in earthquakes (Pacheco et al., 1993).

### *Seismic Coupling*

Uyeda and Kanamori (1979) recognized that the seismic behavior of subduction zones differed considerably around the world, with some subduction zones (“Chilean-type”) capable of generating very large earthquakes whereas in others (“Marianas-type”) the deformation is primarily aseismic. This difference is likely caused by differences in the overall normal stresses on the subduction zone interface (Scholz and Campos, 2012). The term coupling describes the frictional nature of the contact between the overriding and subducting plate. Here, we define full coupling as the state where the interface is locked, and stress is only released by distinct earthquakes. For un-coupled systems, the assumption is that the movement along the interface between the two plates is quasi-continuous without the stress build-up that would result in earthquakes. The seismic coupling coefficient, which is the ratio between the seismic slip rate and the total slip rate, has been the subject of several studies. Pacheco et al. (1993) computed coupling coefficients for all subduction zones and found that the coupling coefficient, based on 90 years of observations, is very low for most subduction zones. A low coupling coefficient could simply be the result of the return time being much longer than 90 years, but from a statistical analysis they argued that the observed earthquake recurrences can be explained, on a worldwide basis, with a single coupling coefficient of 0.3. McCaffrey (1997) has demonstrated that on the basis of seismic observations alone it is not possible to demonstrate variation in the seismic coupling, and that all the data can be represented with a coupling coefficient of 0.3.

### *Observations of aseismic slip*

Aseismic slip, or creep, is observed along sections of many subduction zones. In some cases, it occurs as “after-slip” following a great earthquake (Perfettini et al., 2010), in other cases the creep seems related to tremor activity (Kao et al., 2005), or simply the characteristic behavior of a particular section of the subduction zone (Fournier and Feymueller, 2007). Since the occurrence of creep is primarily demonstrated by geodetic data, the observations are generally limited to relatively short timespans, which makes it impossible to tell whether creep is a stationary phenomenon in time. But in some cases, such as the creeping Shumagin section of the Aleutian chain, which is well-documented (Fournier and Feymueller, 2007) from geodetic data, it appears

that aseismic behavior has persisted, at least locally, on a longer time-scale of a few thousand years (Witter et al., 2014).

### **B.5. Variation of convergence rate along subduction zones**

Due to the large extent of subduction zones, it is likely that local convergence rates change along strike, due to changes in local geometry, plate boundaries and also simply because of the sphericity of the Earth's surface.

### **B.6. Splay faulting**

Splay faults are faults that branch off main fault systems. Although secondary in terms of the overall tectonic environment, splay faults sometimes accommodate a very substantial fraction of the total slip on a fault, and in some cases all the slip. There are numerous observations of splay faults off the main subduction interface (e.g. Cummins et al., 2001), which appear to have accommodated a significant amount of slip during giant earthquakes. In many cases, the evidence is ambiguous because the surface trace of those faults is below water. However, the earliest and best-documented example is that of the 1964 Alaska earthquake (Plafker, 1965) where up to 10 meters of slip occurred on the Patton Bay fault. The effect of splay faulting on distant tsunami is very limited (Johnsen et al., 1996).

### **B.7. A generic recurrence model for (non-Alaska/Cascadia) subduction zones**

Given the relatively short history of direct observations on large subduction zone earthquakes and the need to include a large set of different subduction zones into our model, we think it is appropriate to define a "generic" source model that is to be used as an epistemic branch of the logic tree that also includes more fault-specific branches.

To compute the recurrence intervals on the general subduction zone, we used trench-perpendicular plate rates (Bird, 2003) and coupling coefficients from Scholz and Campos (2012). Because the coupling coefficients may be biased due to the short seismic history for most of the subduction zones, we used a coupling coefficient of 0.3 (Pacheco et al., 1993) as a lower bound so that every subduction zone is assumed to be capable of producing megathrust earthquakes. For the down-dip limit of the rupture, we used a depth of 40 km, whereas all the models are allowed to rupture to the sea floor. The overall recurrence parameters for the subduction sources are shown in Table B-1.

### **B.8. Alaska recurrence model**

The most recent source model from the national seismic hazard maps dates back almost a decade (Wesson et al., 2007) and a significant amount of paleo-seismic and paleo-tsunami data has been acquired since then. Whereas the Wesson et al. (2007) model consisted of individual and independent rupture segments, more recent observations suggest that multi-segment ruptures do occur more frequently. It should be noted that the concept of segmentation is often guided by the most recent events that occurred on a subduction zone, not necessarily a consistent re-rupturing of a particular segment.

Nevertheless, we will use the segmentation models of the Alaska-Aleutian subduction zone as the smallest building block of major earthquakes. Several segmentation models are available,

and we chose the model from Nishenko and Jacob (1990) since it provides the smallest segments, and therefore the most flexible in terms of possible rupture scenarios. From east to west, they are named:

- Yakataga
- Prince-William Sound
- Kodiak
- Semidi
- Shumagin
- Unimak
- Fox Island
- Andreanof
- Delarof
- Rat Island
- Near Island
- Komandorsky

These segments are shown in Table B - 2 with the historic earthquake occurrences as well as Table B - 3, which shows slip rates and coupling coefficients and in Table B - 4, which shows the different rupture alternatives with the epistemic weights. For this model, we used the maximum magnitude model with the central magnitude determined from the dimensions of the rupture and scaling relations. We have defined four epistemic branches in terms of size of the ruptures. The first branch consists of only single-segment ruptures, whereas the second and third branch consists of two- and three –segment ruptures respectively, where feasible. Since it appears that the Shumagin Gap has not been active for at least the last 2,000-3,000 years (Witter et al., 2014), we have not made it active in these first three branches. Only in the case of the fourth branch, with ruptures of four segments or more is this section allowed to break. The weights and segmentations were chosen such that the return times for the individual segments is consistent with recent paleoseismic and paleotsunami data (Nelson et al., 2015; Witter et al., 2014; Shennan et al., 2014; von Huene et al., 2016). It should be noted that for California, the segments from Yakataga through Unimak are the main sources. Further to the west, the main tsunami energy is directed away from California.

## B.9. References

- Annaka, T., Satake, K., Sakakiyama, T., Yanagisawa, K., and Shuto, N., 2007. Logic-tree Approach for Probabilistic Tsunami Hazard Analysis and its Applications to the Japanese Coasts. *Pure and Applied Geophysics* **164**(2-3), 577–592.
- Atwater, B.F., and Moore, A.L., 1992. A tsunami about 1000 years ago in Puget Sound, Washington, *Science*, **258**, 1614-1617.
- Bird, P., 2003. An updated digital model of plate boundaries, *Geochem. Geophys. Geosyst.*, **4**(3), 1–52, doi:10.1029/2001GC000252.

- Blaser, L., Kruger, F., Ohrnberger, M., and Scherbaum, F., 2010. Scaling Relations of Earthquake Source Parameter Estimates with Special Focus on Subduction Environment. *Bulletin of the Seismological Society of America*, 100, no. 6, p. 2914–2926, doi: 10.1785/0120100111.
- Brown, J.R., Prejean, S.G., Beroza, G.C., Gomberg, J.S., and Haeussler, 2013. Deep low-frequency earthquakes in tectonic tremor along the Alaska-Aleutian subduction zone, *J. Geophys. Res. Solid Earth*, 118(3), 1079–1090, doi:10.1029/2012JB009459.
- Cisternas, M., Atwater, B.F., Torrejon, F., Sawai, Y., Machuca, G., Lagos, M., Eipert, A., Youlton, C., Salgado, I., Kamataki, T., Shishikura, M., Rajendran, C.P., Malik, J.K., Rizal, Y., and Husni, M., 2005. Predecessors of the giant 1960 Chile earthquake. *Nature* 437(7057), 404–407.
- Cummins, P. R., Hori, T., and Kaneda, Y., 2001. Splay fault and megathrust earthquake slip in the Nankai Trough, *Earth Planets Space*, 53(4), 243–248.
- Fournier, T.J., and Freymueller, J.T., 2007. Transition from locked to creeping subduction in the Shumagin region, Alaska. *Geophysical Research Letters* 34(6), L06303.
- Ide, S., Shelly, D.R., and Beroza, G.C., 2007. Mechanism of deep low frequency earthquakes: Further evidence that deep non-volcanic tremor is generated by shear slip on the plate interface. *Geophysical Research Letters* 34(3), 2191–5.
- Jankaew, K., Atwater, B.F., Sawai, Y., Choowong, M., Charoentitirat, T., Martin, M.E., and Prendergast, A., 2008. Medieval forewarning of the 2004 Indian Ocean tsunami in Thailand. *Nature* 455(7217), 1228–1231.
- Johnson, J.M., Satake, K., Holdahl, S.R., and Sauber, J., 1996. The 1964 Prince William Sound earthquake: Joint inversion of tsunami and geodetic data. *Journal of Geophysical Research: Solid Earth* 101, 523–532.
- Kao, H., Shan, S., Dragert, H., Rogers, G., Cassidy, J.F., and Ramachandran, K., 2005. A wide depth distribution of seismic tremors along the northern Cascadia margin. *Nature* 7052, 841.
- McCaffrey, R., 1997. Statistical significance of the seismic coupling coefficient. *Bulletin of the Seismological Society of America* 87(4), 1069–1073.
- Monecke, K., Finger, W., Klarer, D., Kongko, W., Mcadoo, B.G., Moore, A.L., and Sudrajat, S.U., 2008. A 1,000-year sediment record of tsunami recurrence in northern Sumatra. *Nature* 455(7217), 1232–1234.
- Murotani, S., Miyake, H., and Koketsu, K., 2008. Scaling of characterized slip models for plate-boundary earthquakes. *Earth, Planets and Space* 60(9), 987.
- Murotani, S., Satake, K., and Fujii, Y., 2013. Scaling relations of seismic moment, rupture area, average slip, and asperity size for  $M \sim 9$  subduction-zone earthquakes. *Geophysical Research Letters* 40(19), 5070–5074.
- Nanayama, F., Satake, K., Furukawa, R., and Shimokawa, K., 2003, Unusually large earthquakes inferred from tsunami deposits along the Kuril trench, *Nature*, 424(6949), 660–663, doi:10.1038/nature01864.

- Nelson, A.R., Briggs, R.W., Dura, T., Engelhart, S.E., Gelfenbaum, G., Bradley, L.-A., Forman, S.L., Vane, C.H., and Kelley, K.A., 2015. Tsunami recurrence in the eastern Alaska-Aleutian arc: A Holocene stratigraphic record from Chirikof Island, Alaska. *Geosphere* **11**(4), 1172–1203.
- Nishenko, S.P., and Jacob, K.H., 1990. Seismic potential of the Queen Charlotte-Alaska-Aleutian Seismic Zone. *Journal of Geophysical Research: Oceans* **95**(B3), 2511–2532.
- Oleskevich, D.A., Hyndman, R.D., and Wang, K., 1999. The updip and downdip limits to great subduction earthquakes: Thermal and structural models of Cascadia, south Alaska, SW Japan, and Chile. *Journal of Geophysical Research: Solid Earth* **104**(B7), 14965–14991.
- Pacheco, J., Sykes, L., and Scholz, C., 1993. Nature of seismic coupling along simple plate boundaries of the subduction type, *Journal of Geophysical Research, Solid Earth*, **98**(B8).
- Papazachos, B., Scordilis, E., Panagiotopoulos, D., Papazachos, C.B., and Karakaisis, G.F., 2004. Global relations between seismic fault parameters and moment magnitude of earthquakes, *Bulletin of the Geological Society of Greece*, **36**(3), 1482–1489.
- Perfettini, H., Avouac, J.-P., Tavera, H., Kositsky, A., Nocquet, J.-M., Bondoux, F., Chlieh, M., Sladen, A., Audin, L., Farber, D.L., and Soler, P., 2010. Seismic and aseismic slip on the Central Peru megathrust. *Nature* **465**(7294), 78–81.
- Petersen, M.D., Moschetti, M.P., Powers, P.M., Mueller, C.S., Haller, K.M., Frankel, A.D., Zeng, Yuehua, Rezaeian, Sanaz, Harmsen, S.C., Boyd, O.S., Field, Ned, Chen, Rui, Rukstales, K.S., Luco, Nico, Wheeler, R.L., Williams, R.A., and Olsen, A.H., 2014, Documentation for the 2014 update of the United States national seismic hazard maps: U.S. Geological Survey Open-File Report 2014–1091, 243 p., <https://dx.doi.org/10.3133/ofr20141091>.
- Pinegina, T.K., Bourgeois, J., Bazanova, L.I., Melekestsev, I.V., and Braitseva, O.A., 2003. A millennial-scale record of Holocene tsunamis on the Kronotskiy Bay coast, Kamchatka, Russia. *Quaternary Research* **59**(1), 36–47.
- Plafker, G., 1965. Tectonic Deformation Associated with the 1964 Alaska Earthquake. *Science* **148**(3678), 1675–1687.
- Ruff, L.J., and Kanamori, H., 1980. Seismicity and the subduction process. *Physics of the Earth and Planetary Interiors* **23**(3), 240–252.
- Satake, K., Shimazaki, K., Tsuji, Y., and Ueda, K., 1996. Time and size of a giant earthquake in Cascadia inferred from Japanese tsunami records of January 1700, *Nature*, **379**, 246–249.
- Scholz, C.H., and Campos, J., 2012. The seismic coupling of subduction zones revisited. *Journal of Geophysical Research: Solid Earth* **117**(B5).
- Shennan, I., Bruhn, R., and Plafker, G., 2009. Multi-segment earthquakes and tsunami potential of the Aleutian megathrust. *Quaternary Science Reviews* **28**(1-2), 7–13.

- Sieh, K., Natawidjaja, D.H., Meltzner, A.J., Shen, C.-C., Cheng, H., Li, K.-S., Suwargadi, B.W., Galetzka, J., Philibosian, B., and Edwards, R.L., 2008. Earthquake Supercycles Inferred from Sea-Level Changes Recorded in the Corals of West Sumatra. *Science* **322**(5908), 1674–1678.
- Schwartz, S.Y., 1999. Noncharacteristic behavior and complex recurrence of large subduction zone earthquakes. *Journal of Geophysical Research: Solid Earth* **104**(B10), 23111–23125.
- Shennan, I., Barlow, N., Carver, G., Davies, F., Garrett, E., and Hocking, E., 2014. Great tsunamigenic earthquakes during the past 1000 yr on the Alaska megathrust. *Geology* **42**(8), 687–690.
- Strasser, F.O., Arango, M.C., and Bommer, J.J., 2010. Scaling of the Source Dimensions of Interface and Intraslab Subduction-zone Earthquakes with Moment Magnitude. *Seismological Research Letters* **81**(6), 941–950.
- Uyeda, S., and Kanamori, H., 1979. Back-arc opening and the mode of subduction. *Journal of Geophysical Research: Solid Earth* **84**(B3), 1049–1061.
- von Huene, von, R., Miller, J.J., and Dartnell, P., 2016. A possible transoceanic tsunami directed toward the U.S. west coast from the Semidi segment, Alaska convergent margin. *Geochemistry Geophysics Geosystems* **17**(3), 645–659.
- Wells, D.L., and Coppersmith, K.J., 1994. New empirical relationships among magnitude, rupture length, rupture width, rupture area, and surface displacement. *Bulletin of the Seismological Society of America* **84**(4), 974–1002.
- Wesson, R.L., Boyd, O.S., Mueller, C.S., Bufe, C.G., Frankel, A.D., and Petersen, M.D., 2007. *Revision of time-independent probabilistic seismic hazard maps for Alaska*, US Geological Survey, Open File Report 2007-1043.
- Witter, R.C., Briggs, R.W., and Engelhart, S.E., 2014. Little late Holocene strain accumulation and release on the Aleutian megathrust below the Shumagin Islands, Alaska. *Geophysical Research Letters*.



## B.10. Tables

Table B-1. Overall recurrence parameters of the subduction zone sources. The recurrence models are either Maximum magnitude (M) or truncated Gutenberg-Richter ( $\beta=1.0$ ,  $M_{\min}=7.5$ ). The event rates are either constrained by the slip rates (S) or observed Recurrence times (R).

Name	Slip rate (mm/yr)	Coupling coefficient	$M_{\max}$	Recurrence Model	Rate constraint
Alaska/Aleutian	5-65	0.6-0.96	9.3	M	R
Cascadia	29-45	0.6	9.3	M	R
Central America	70-90	0.9	8.9	M	S
Chile	70-80	1.0	9.5	M	S
Izu-Bonin	22-32	0.3	8.3	G-R	S
Kurile/Kamchatka	26-30	0.6	9.1	M	R/S
Marianas	22-34	0.3	8.5	G-R	S
Nankai	10-15	1.0	9.1	M	R/S
Peru	60-65	0.8	9.1	M	S
Philippines	33-45	0.8	9.0	M	S
Ryukyu	18-21	0.3	8.5	M	S

Table B - 2. Segmentation models of the Alaska-Aleutian subduction zone and the extent of recent large earthquakes. + means the entire segment ruptures, - means partial rupture

Segmentation model			Year of Historical Events									
			1849	1899	1917	1938	1946	1957	1964	1965	1985	
Nishenko & Jacobs (1990)	Wesson et al. (2007)	McCaffrey (1997)										
Yakataga	Yakataga	Alaska		+								
Prince-William Sound	Prince-William Sound								+			
Kodiak	Kodiak								+			
Semidi	Semidi					+						
Shumagin	Shumagin				-							
Unimak	Western Aleutian	Eastern Aleutians					+					
Fox Island							-					
Andreanof												+
Delarof									+			
Rat Island		Western Aleutians									+	
Near Island											+	
Komandorsky	Komandorsky		+									

Table B-3. Trench perpendicular convergence rates and coupling coefficients for the Alaska-Aleutian subduction zone.

Segment	Rate (mm/yr)	Coupling
Yakataga	54	0.6
Prince-William Sound	55	0.62
Kodiak	64	0.8
Semidi	68	0.8-0.9
Shumagin	69	0.0-0.3
Unimak	70	.6-.9
Fox Island	65	0.9
Andreanof	61	.96
Delarof	50	.9
Rat Island	35	.6
Near Island	10	.6
Komandorsky	5	.6

Table B - 4. Epistemic model for large earthquakes on the Alaska-Aleutian subduction zone. The four rightmost columns show the rupture combinations, with identically colored adjacent rows forming a multi-segment rupture. The 50% weight column consists of individual segments rupturing. The white areas indicate that no rupture occurs for that particular segment.

Segmentation model			Epistemic weights			
Nishenko & Jacobs (1990)	Wesson et al. (2007)	McCaffrey (1997)	50%	30%	20%	10%
Yakataga	Yakataga	Alaska	Dark Gray	White	White	Dark Gray
Prince-William Sound	Prince-William Sound		Light Gray	Dark Gray	Light Gray	Dark Gray
Kodiak	Kodiak		Dark Gray	Dark Gray	Light Gray	Dark Gray
Semidi	Semidi 59		Light Gray	Light Gray	Light Gray	Dark Gray
Shumagin	Shumagin		White	White	White	Dark Gray
Unimak	Western Aleutian		Eastern Aleutians	Light Gray	Dark Gray	Dark Gray
Fox Island		Dark Gray		Dark Gray	Dark Gray	Light Gray
Andreanof		Light Gray		Light Gray	Dark Gray	Light Gray
Delarof		Dark Gray		Light Gray	Dark Gray	Light Gray
Rat Island		Light Gray		Dark Gray	Light Gray	Dark Gray
Near Island		Dark Gray	Light Gray	Light Gray	Dark Gray	
Komandorsky		Komandorsky	Western Aleutians	Light Gray	White	Light Gray

## Appendix C. The Cascadia megathrust

In the quarter century since the first realization that the Cascadia subduction zone might be capable of large, Chile-type subduction interface earthquakes (Heaton and Kanamori, 1984), many studies have been carried out to characterize this source in terms of seismic potential and recurrence. The only large subduction zone event to have occurred in historical times is the 1700 earthquake (Atwater et al., 1991; Satake et al., 1996) although there are no direct reports from this event as the source area was sparsely populated and no written records exist from that time in the source area.

Our rupture model for the Cascadia Subduction Zone is based on paleoseismic and paleotsunami observations (e.g. Goldfinger et al., 2011; Leonard et al., 2010). Most pertinent observations constrain the occurrence of large earthquakes and their extent, but there are few observations that enable us to constrain the actual size of any earthquake. For this, we have to resort to earthquake scaling relations (e.g. Strasser et al., 2010).

### C.1. Earthquakes

#### *The 1700 Cascadia earthquake*

Satake et al. (1996) inferred from tsunami records in Japan dating back to 1700 that a large earthquake had occurred along the Cascadia subduction zone. As far as we are aware, these are the only direct tsunami observations of this event but there are many observations in the Cascadia region, which support this conclusion from tree records (Atwater et al., 1991; Jacoby, 1997) and even native oral tradition (Ludwin et al., 2005). From a combined study of the tsunami observations in Japan and local subsidence data, Satake et al (2003) concluded that the most likely scenario for the 1700 earthquake involved rupture along the entire Cascadia subduction zone with a relatively narrow width (~50 km).

#### *Concurrence of observed paleo-tsunami deposits and other paleo-seismological evidence*

Since direct observations of slip on the subduction zone interface are not feasible, we can only deduce the size of earthquakes through indirect means, most notably by the observation, such as tsunami deposits and tree records, of concurrent events in different locations along the rupture that can constrain the extent of the rupture. The width can be deduced by studying the uplift and subsidence patterns found in marshes and other environments.

Some of the uncertainties are in the actual identification of the tsunamigenic event, the accuracy of the dating, and the assumption that two spatially separated observations with similar dates are actually the results of a single event. It is not uncommon for adjacent large ruptures to occur within a few years from each other, presumably one triggered by the changes of the stress field from the preceding event. A recent example is the occurrence of the  $M_w=8.6$  Nias earthquake which occurred just three months after the  $M_w=9.1$  Aceh-Andaman earthquake. Paleotsunami data from these events would yield similar dates and might be interpreted as resulting from a single event.

Goldfinger et al. (2011) determined from the turbidite observations a record of large earthquakes (assuming a direct correlation between earthquakes and turbidites) spanning 10,000 years with 40 events identified. Using spatial correlations they also determined rupture lengths for these events. Leonard et al. (2010) and Witter et al. (2012) correlated many of these events with coastal subsidence events deduced from marsh records.

## **C.2. Source model**

The relatively large amounts of geologic observations of past events provide important constraints to the recurrence model.

The convergence rate across the Cascadia subduction zone provides a constraint on the recurrence relations, since the total slip rate is an upper bound to the event recurrence rate times the slip per event. Most models of the Cascadia subduction zone predict an increase of convergence rate from the south to the north. McCrory et al. (2012) show the convergence rate increasing from 29 mm/yr in northern California to 45 mm/yr at Vancouver Island.

Since little is known about the seismic efficiency along the Cascadia subduction zone compared to the amount of data on recurrence times of events, we are using the event recurrence times as our primary input to the probabilistic models, and will only use the plate rates as a check afterwards.

Our current implementation of the recurrence model yields a maximum displacement rate of 20 mm/yr, which is well below the plate convergence rate in the north, and implies a seismic efficiency of 0.5, i.e. half of the convergence rate is accommodated by mechanisms other than earthquakes in the north. To the south, the convergence rate is actually more similar to our slip rate.

### *Source geometry and parameterization*

The geometry of the Cascadia subduction has been analyzed in several papers (e.g. Fluck et al., 1997; Wang et al., 2003; McCrory et al., 2006) and we have adapted the latter in this study (Figure 6, in main text). Our model consists of quasi-rectangular subfaults, with target length and width of 20 km, which follow the contours of the McCrory et al. (2012) model. For the main slab interface we have defined 480 subfaults, but it should be noted that in the current analysis many of these subfaults are not used because they are more than 50% in area outside the limit of the seismogenic zone. It is however conceivable that they will be used in future models for alternative logic tree branches.

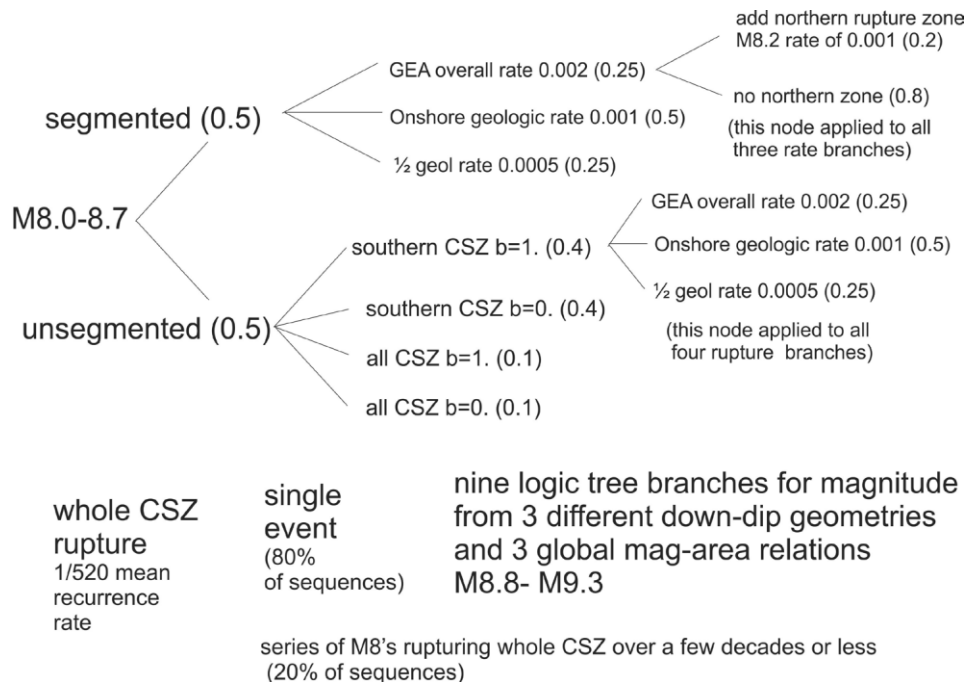


Figure C-1. Logic tree for Cascadia recurrence, from Frankel and Petersen (2012).

### C.3. The USGS recurrence model

Frankel and Petersen (2012) presented an earlier version of the Cascadia earthquake recurrence model as a source element to the National Seismic Hazard Maps (Petersen et al., 2014). Based on discussion with the review panel (California PTHA Work Group, 2015), it was decided to adopt the USGS model, which is the result of an extensive peer-review process and includes all the recent science on Cascadia earthquake source recurrence. Details and background of the model can be found in Frankel and Petersen (2012). Initially, Frankel (pers. comm., 2012) developed a set of six different rupture extents along the Cascadia subduction zone with associated average return periods based on the aforementioned work of Goldfinger et al. (2011) and other studies. Most of these were used in the 2014 NSHM and the final model scenarios were provided to us by Chen (pers. comm, 10/1/2013). These scenarios are shown in Figure C-1. These ruptures, which are only defined in terms of length segments along the Cascadia zone form the basis of our source model, are further defined in a logic tree framework that addresses the epistemic uncertainties in fault width, splay faulting, and aleatory uncertainties such as slip variability.

### C.4. Additional epistemic uncertainties

#### *Up dip rupture termination and splay faulting*

It is often assumed that the shallow part of a subduction zone cannot support large differential stresses and that earthquakes cannot nucleate here (e.g. Scholz, 1998), but can penetrate at least partially into it. Lay et al. (2012) concluded, on the basis of observed tsunamigenic earthquakes that this zone can deform aseismically but can also sustain large earthquakes but with slower

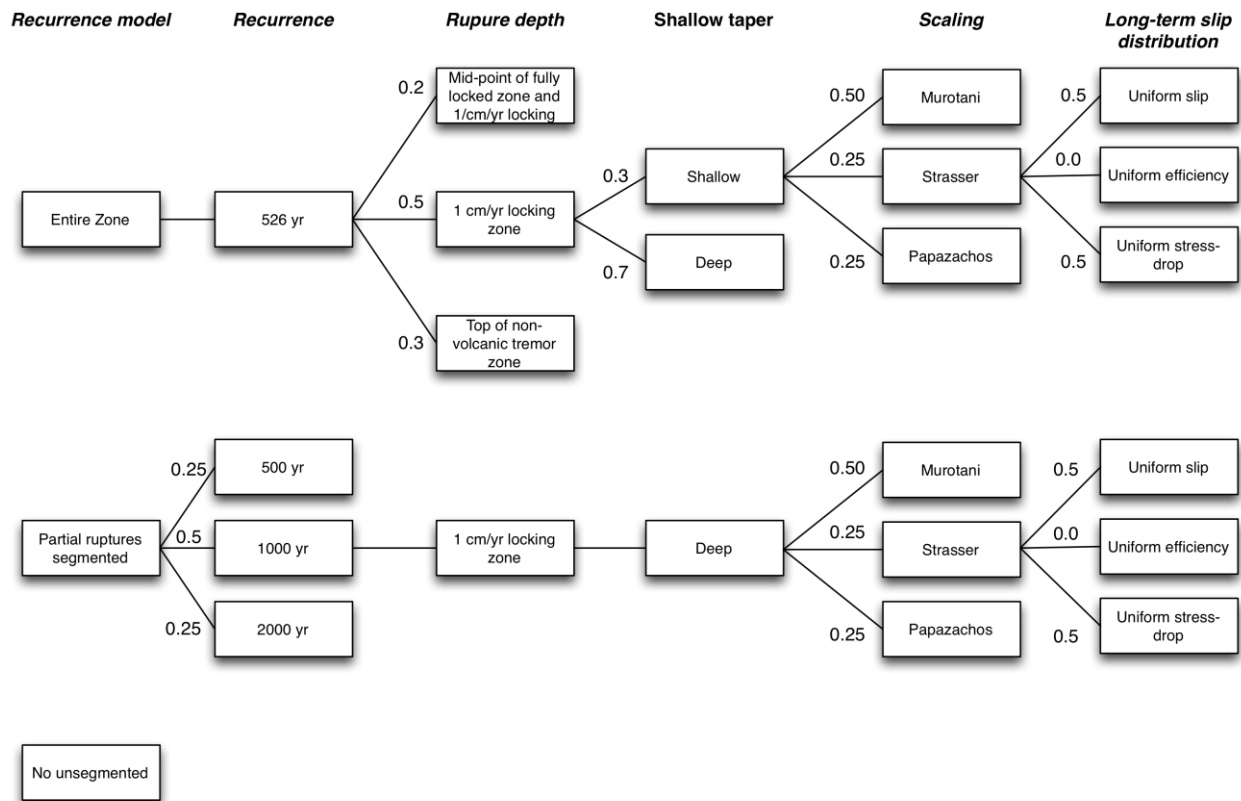


Figure C-2. Final logic tree for the Cascadia subduction zone.

rupture velocities and thus longer durations compared to deeper events. In our model we therefore include two alternative branches that allow slip that is tapered at a very shallow depth (< 1 km) and slip that is tapered over the top 5 km of the megathrust. (Figure C-2).

Movement along splay faults has been observed or inferred in several large subduction zones, the most unambiguous and prominent case being the movement along the Patton Bay Fault during the 1964 Alaska earthquake (Plafker 1967). The Cascadia subduction zone features a zone of splay faulting, especially further north along the Oregon and Washington coasts. Understanding the complexity of that zone and mode of deformation (e.g. discrete faulting style vs. distributed deformation) however exceeds well beyond the current scope but may be an important factor to consider in future updates to the model.

*Down dip rupture termination*

Although slip at the deepest part of the rupture may not contribute directly to the tsunami generation, it is still very important for the following reasons:

- The uplift and subsidence of the coast line are strongly dependent on the location of the rupture termination
- Since the magnitude and slip are tied to the rupture area through scaling relations, a larger width of the fault will increase the average slip on the fault.



The down dip termination has been studied extensively (e.g. Wang et al., 2003) and there is general agreement on the fact that the Cascadia rupture is quite narrow (< 50 km) compared to other major subduction zone systems.

In our final model, we adopted the geometry from the USGS model (Frankel and Petersen, 2012, updated by Chen et al., 2014), which recognizes three alternative depths for the deep rupture termination:

1. the 1 cm/yr locking depth. The locking depth is the depth at which the current geodetic data suggests that the movement across the interface falls below 1 cm/yr. Given a roughly 4 cm/yr relative motion between the plates, this implies that below this depth the seismic coupling drops below .25.
2. the top of the zone of seismic tremor. Seismic tremor are events with an extended duration and often coincide with slow slip that has been observed with GPS intermittently. The tremors are thought to be associated with fluid flow at depth.
3. the base of the locked zone from thermal modeling and uplift data.

### *Maximum magnitude*

The maximum magnitude for earthquakes along the Cascadia subduction zone is primarily constrained by the dimension of the rupture and global scaling relations. For Cascadia, the USGS model consists of three alternative models, all based on regressions of subduction zone earthquake data.

### *Length of Cascadia ruptures*

The lengths of paleo-ruptures are usually determined by correlating tsunami related deposits (marsh deposits) or events (e.g. tree deaths), onshore as well as offshore (e.g. turbidites), in different locations along the Cascadia subduction zone that occurred simultaneously along the coast. This kind of analysis has given us a record of large tsunamigenic earthquakes for the last 10,000 years (Goldfinger et al., 2011).

## **C.5. References**

- Atwater, B.F., Stuiver, M., and Yamaguchi, D.K., 1991. Radiocarbon test of earthquake magnitude at the Cascadia subduction zone. *Nature* 353 (Sept. 12),. 156-8.
- California PTHA Work Group, 2015. Evaluation and Application of Probabilistic Tsunami Hazard Analysis in California, 33 p. California Geological Survey Special Report 237, pp. 1–33.
- Fluck, P., Hyndman, R.D., and Wang, K., 1997. Three-dimensional dislocation model for great earthquakes of the Cascadia subduction zone. *Journal of Geophysical Research: Solid Earth* **102**(B9), 20539–20–550.
- Frankel, A.D., and Petersen, M.D., 2012. *Appendix P—Models of Earthquake Recurrence and Down-Dip Edge of Rupture for the Cascadia Subduction Zone*, 13 p. USGS Open File Report pp. 1–13. USGS Open File Report.
- Goldfinger, C., Nelson, C.H., Morey, A., Johnson, J.E., Gutierrez-Pastor, J., Eriksson, A.T., Karabanov, E., Patton, J., Gracia, E., and Enkin, R., 2011. *Turbidite Event History: Methods*

- and Implications for Holocene Paleoseismicity of the Cascadia Subduction Zone*, USGS Professional Paper 1661-F, Reston, VA. US Geological Survey, 332.
- Heaton, T.H., and Kanamori, H., 1984. Seismic potential associated with subduction in the northwestern United States. *Bulletin of the Seismological Society of America* **74**(3), 933–941.
- Jacoby, G.C., Bunker, D.E., and Benson, B.E., 1997. Tree-ring evidence for an AD 1700 Cascadia earthquake in Washington and northern Oregon. *Geology* **25**(11), 999–1002.
- Lay, T., Kanamori, H., Ammon, C.J., Koper, K.D., Hutko, A.R., Ye, L., Yue, H., and Rushing, T.M., 2012. Depth-varying rupture properties of subduction zone megathrust faults. *Journal of Geophysical Research: Solid Earth* **117**(B4), B04311.
- Leonard, L.J., Currie, C.A., Mazzotti, S., and Hyndman, R.D., 2010. Rupture area and displacement of past Cascadia great earthquakes from coastal coseismic subsidence. *Geological Society of America Bulletin* **122**(11-12), 2079–2096.
- Ludwin, R.S., Dennis, R., Carver, D., McMillan, A.D., Losey, R., Clague, J., Jonientz-Trisler, C., Bowe chop, J., Wray, J., and James, K., 2005. Dating the 1700 Cascadia earthquake: great coastal earthquakes in Native stories. *Seismological Research Letters* **76**(2), 140–148.
- McCrorry, P.A., Blair, J.L., Waldhauser, F., and Oppenheimer, D.H., 2012. Juan de Fuca slab geometry and its relation to Wadati-Benioff zone seismicity. *Journal of Geophysical Research: Solid Earth* **117**(B9), B09306.
- Petersen, M.D., Moschetti, M.P., Powers, P.M., Mueller, C.S., Haller, K.M., Frankel, A.D., Zeng, Y., Rezaeian, S., Harmsen, S.C., Boyd, O.S., and others, 2014. *Documentation for the 2014 update of the United States national seismic hazard maps*, 255 p. USGS Open File Report pp. 1–255.
- Plafker, G., 1967. *Surface faults on Montague Island associated with the 1964 Alaska earthquake*: US Geol. United States Geological Survey Professional Paper, 543.
- Satake, K., Shimazaki, K., Tsuji, Y., and Ueda, K., 1996. Time and size of a giant earthquake in Cascadia inferred from Japanese tsunami records of January 1700. *Nature* **379**(6562), 246–249.
- Satake, K., Wang, K., and Atwater, B.F., 2003. Fault slip and seismic moment of the 1700 Cascadia earthquake inferred from Japanese tsunami descriptions. *Journal of Geophysical Research: Solid Earth* **108**(B11), 2535.
- Scholz, C.H., 1998. Earthquakes and friction laws. *Nature* **391**(6662), 37–42.
- Strasser, F.O., Arango, M.C., and Bommer, J.J., 2010. Scaling of the Source Dimensions of Interface and Intraslab Subduction-zone Earthquakes with Moment Magnitude. *Seismological Research Letters* **81**(6), 941–950.

Wang, K., Wells, R., Mazzotti, S., Hyndman, R.D., and Sagiya, T., 2003. A revised dislocation model of interseismic deformation of the Cascadia subduction zone. *Journal of Geophysical Research: Solid Earth* **108**(B1), 2026.

Witter, R.C., Zhang, Y., Wang, K., Goldfinger, C., Priest, G.R., and Allan, J.C., 2012. Coseismic slip on the southern Cascadia megathrust implied by tsunami deposits in an Oregon lake and earthquake-triggered marine turbidites. *Journal of Geophysical Research: Solid Earth* **117**(B10), B10303.

## Appendix D. Probabilistic Analysis

Probabilistic seismic hazard analysis (PSHA) has become standard practice in the evaluation and mitigation of seismic hazard to populations, in particular with respect to structures, infrastructure, and lifelines. Its ability to condense the complexities and variability of seismic activity into a manageable set of parameters greatly facilitates the design of effective seismic resistant buildings and also the planning of infrastructure projects. Probabilistic tsunami hazard analysis (PTHA) achieves the same goal for hazards posed by tsunami. Although this field is not very developed yet, this method offers great advantages for evaluating the total risk (seismic and tsunami) to coastal communities, facilities, and infrastructure.

Previous work on PTHA includes Downes and Stirling (2001), who proposed to use an empirical attenuation relation similar to ground motion attenuation relations. Although they recognize that such attenuation relations would have to be source and site specific, it is doubtful whether enough data would ever be available for such attenuation relations to be derived consistently. On the other hand, Geist and Parsons (2006) developed a method that uses the full linear calculations for a limited number of scenarios for earthquakes near the site. The main difference with their work is that through the Green's function summation, many more fault scenarios can be generated and at arbitrary distances including teleseismic, which allows us to run full probabilistic analyses over a much wider area. Also, our method is very efficient for the analysis of many sites simultaneously, which allows us to quickly identify areas at elevated risk. Such information is indispensable for the effective allocation of funds for tsunami hazard mitigation work.

The method that we have developed is based on the traditional PSHA and is therefore completely consistent with standard seismic hazard practice. It provides an overview of the tsunami hazard along entire coastlines, and helps identify the specific tsunami source regions that a particular site on the coastline is sensitive to.

### D.1. Probabilistic offshore wave-height hazard

#### *Overview*

The methodology behind PSHA is well known (e.g., McGuire, 2004) and here we will only briefly describe the adaptations that are made for PTHA. Whereas in PSHA we are usually interested in the exceedance of some ground motion measure such as peak ground acceleration (PGA) or spectral accelerations (SA), in PTHA a parameter of interest (not necessarily the only one) is the maximum tsunami height that is expected to be exceeded at sites along the coast. The statistical earthquake model behind the two methods is the same, the only difference being that in PTHA we are not concerned with earthquakes that are completely inland and that PTHA's need to consider sources at very great distances across oceans. The difference between the two methods lies in the part that in PSHA is referred to as attenuation relations. These relate a certain moment release on a fault (or an area) to the ground motion parameters as a function of distance. Because of the strong laterally varying nature of tsunami propagation, we have adopted a waveform excitation and propagation approach instead of trying to develop analogous tsunami attenuation relations. In fact, current developments in traditional PSHA include the replacement of the

attenuation relations with ensembles of numerically generated ground motions, which is entirely analogous to the approach proposed here.

The excitation and propagation of tsunamis in deeper water can be modeled using the shallow water wave approximation, which for amplitudes that are significantly smaller than the water depth are linear (Satake, 1995). We can solve the equation of motion numerically using a finite-difference method, which has been validated to produce accurate tsunami heights for propagation through the oceans, although for very shallow water the amplitudes may become too large, and more sophisticated nonlinear methods are required to model the details of the run-up accurately. Nevertheless, the linear approach provides a very good first approximation of tsunami propagation, taking into account the effects of lateral variations in seafloor depth.

#### *Earthquake recurrence behavior*

Currently, the recurrence model for earthquakes is Poissonian, which is a time-independent model, i.e. the probability of occurrence is independent of time, and therefore independent of the occurrence of a previous earthquake.

#### *Magnitude distributions*

There are several models in use to define the distribution of earthquake magnitudes with which the strain on an earthquake source is released. The models included in the code are the Gutenberg-Richter (G-R) relation (Gutenberg and Richter, 1944), Characteristic Earthquake model (Schwartz et al., 1981; Schwartz and Coppersmith, 1984) and the Maximum Magnitude model. Below we will briefly describe their characteristics. For distant tsunami, it is usually sufficient to truncate the magnitude distribution at  $M=7.5$ , which usually means that the G-R part of any seismicity catalog is not of great importance (unless only the G-R relation is used). The tsunami hazard will generally be dominated by events at the larger magnitude end. For local tsunamis however, ignoring the smaller earthquakes (as happens in the maximum magnitude model) may not be appropriate since events as small as  $M=6.5$  are capable of generating significant near-field tsunamis. In a probabilistic analysis, these events might dominate the local hazard at the shorter return periods, depending of course on the details of the recurrence model.

#### *Gutenberg-Richter model*

In the Gutenberg-Richter model, the number of earthquakes on a fault decreases exponentially with increasing magnitude. The original relationship is:

### Truncated exponential distribution

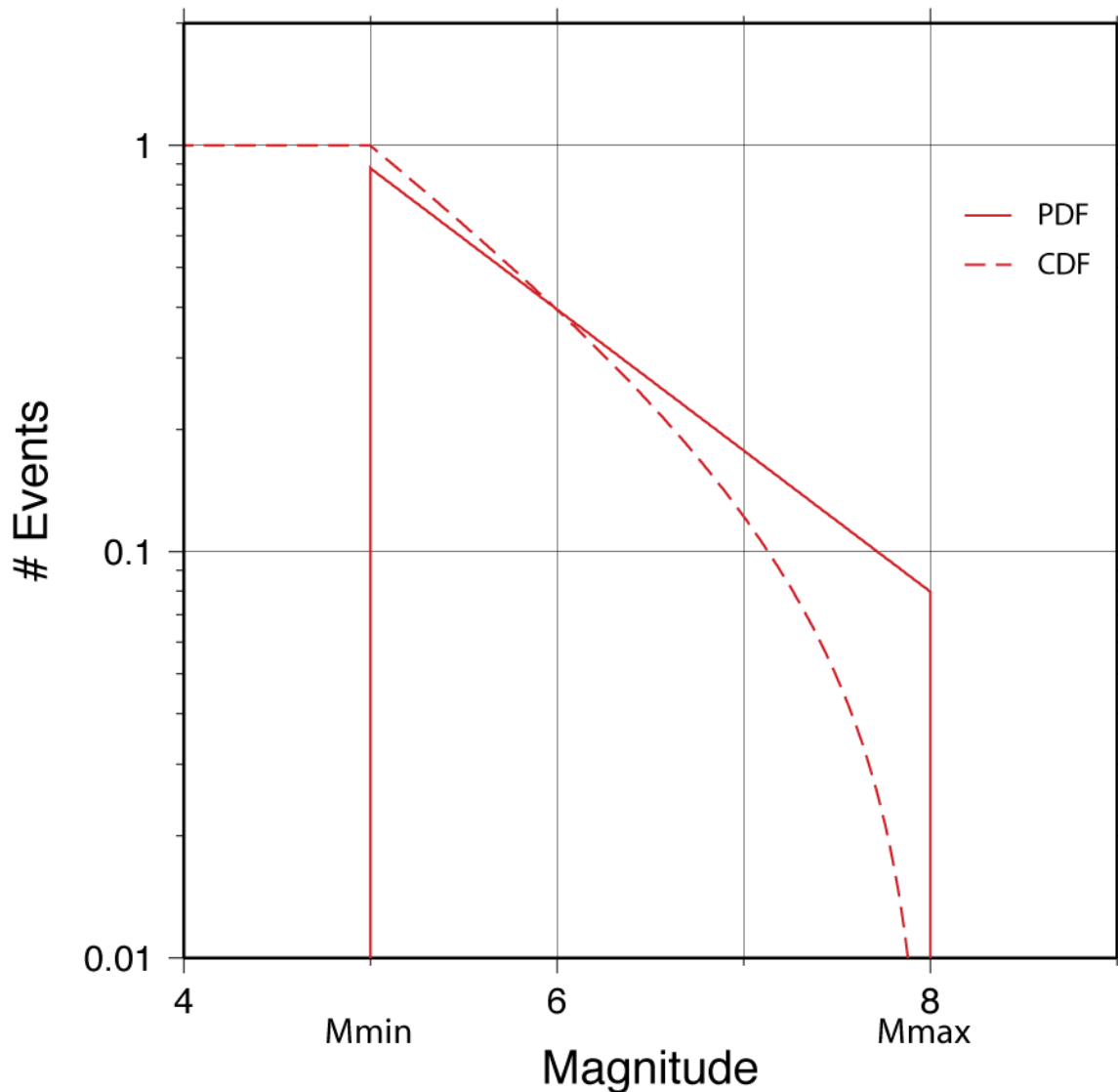


Figure D - 1 Probability and Cumulative Density Functions for the truncated exponential distribution.

$$N(M) = 10^{a-bM}$$

where  $N(M)$ , the cumulative distribution function (CDF), is the number of earthquakes with magnitude larger than  $M$ . A more convenient notation is to express the G-R relations in exponential form:

$$N(M) = e^{\alpha-\beta M}$$

where

$$\alpha = a \ln(10) \text{ and } \beta = b \ln(10).$$

The (normalized) probability density function (PDF) is:

$$n(M) = \beta e^{-\beta M}$$

The G-R is often referred to as the exponential distribution. Whereas the original formulation was defined for events with  $M > 0$ , the distribution is often used in truncated form. The main reason for an upper magnitude bound is that for any finite source there is presumably an associated maximum magnitude, often defined using the maximum dimensions of the source and source scaling relations (e.g. Wells and Coppersmith, 1994; Papazachos et al., 2004). The lower bound is often chosen as a cut-off below which events are not of interest for the particular hazard being analyzed. In earthquake hazard, this is often chosen at  $M=5$ , but for tsunami hazard, this bound should probably be at  $M=6.5$  for sources that are very close to the site, to  $M=7.5-8$  for very distant sources.

The PDF for the (doubly) truncated exponential distribution (Figure D - 2) can be derived by substituting  $M$  with  $(M-Mmin)$  and re-normalizing the original:

$$n(M) = \beta \frac{e^{-\beta(M-Mmin)}}{1 - e^{-\beta(Mmax-Mmin)}}$$

The CDF for the truncated exponential distribution can then be obtained by integrating the PDF between  $Mmin$  and  $M$  and multiplying with the total number of events with  $M > Mmin$  ( $N(Mmin)$ ):

$$\begin{aligned} N(M) &= N(Mmin) \cdot \int_{m=Mmin}^M n(m)dm \cdot \int_{m=Mmin}^M n(m)dm \\ &= N(Mmin) \cdot \left[ 1 - \frac{1 - e^{-\beta(M-Mmin)}}{1 - e^{-\beta(Mmax-Mmin)}} \right] \end{aligned}$$

*Maximum Magnitude model*

This is a simple normal distribution around a maximum magnitude (Wells and Coppersmith, 1994), which is usually constrained by the dimensions of the fault, but may also be defined by the size of historic earthquakes. Note that in this case the maximum magnitude is not the upper truncation of the distribution, but the center of the peak of the distribution.

The PDF (Figure D - 3) is a normal distribution:

$$n(M) = \frac{1}{\sqrt{2\pi}\sigma} e^{-\frac{(M-Mmax)^2}{2\sigma^2}}$$

The normal distribution is unbounded, so for practical purposes we apply bounds as with the truncated exponential distribution. Since the width of this distribution is defined by a

### Maximum magnitude distribution

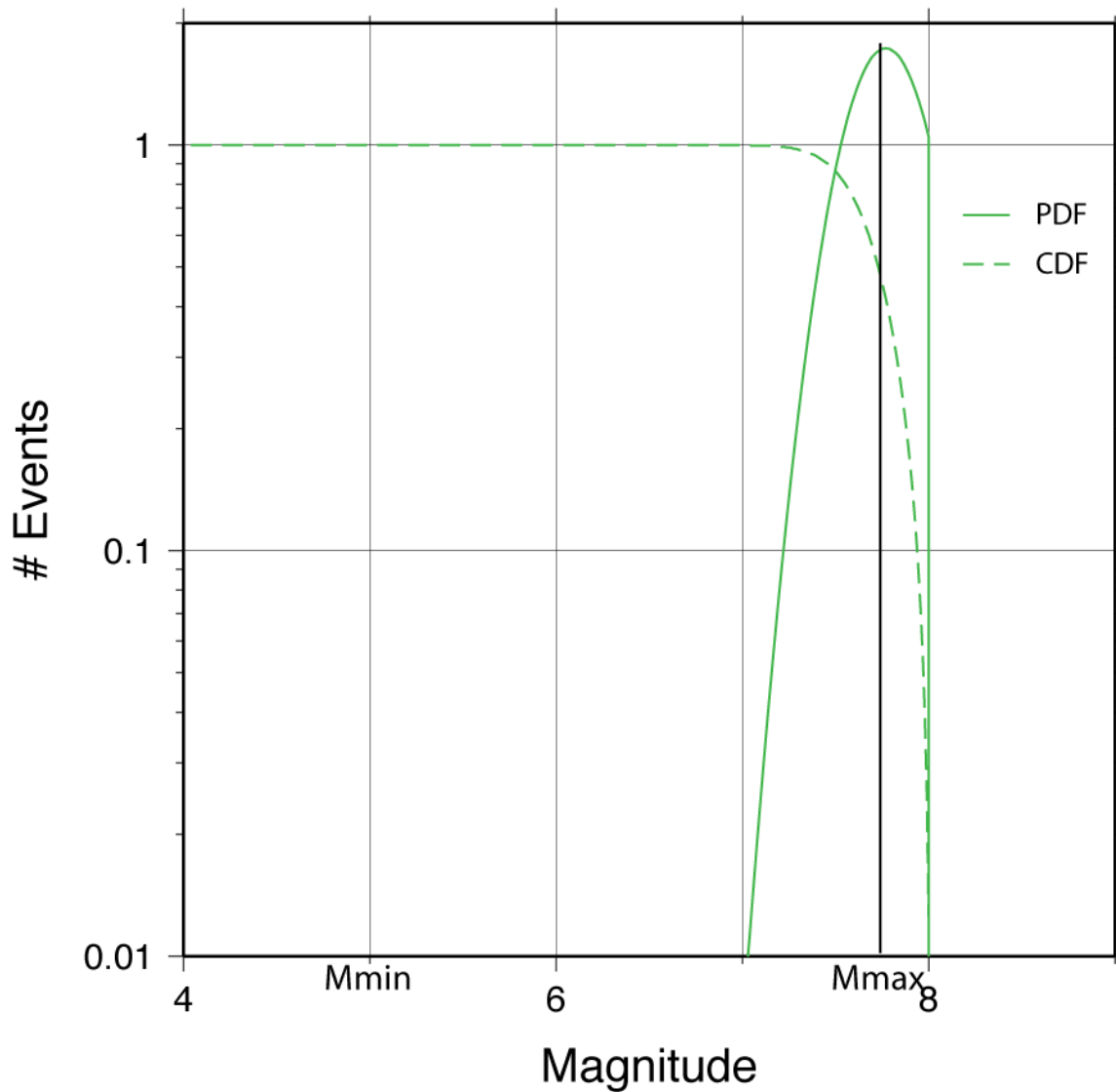


Figure D - 3 PDF and CDF for the maximum magnitude distribution.

standard deviation, which typically comes from a scaling relation, it is more convenient to choose the upper bound in terms of the number of standard deviations away from the mean ( $M_{max}$ ). For a lower bound, it is often sufficient to choose the magnitude below which we expect no contributions to the hazard.

Since there is no closed form solution for CDF, we use the following polynomial approximation (Hastings, 1955):



### Characteristic distribution

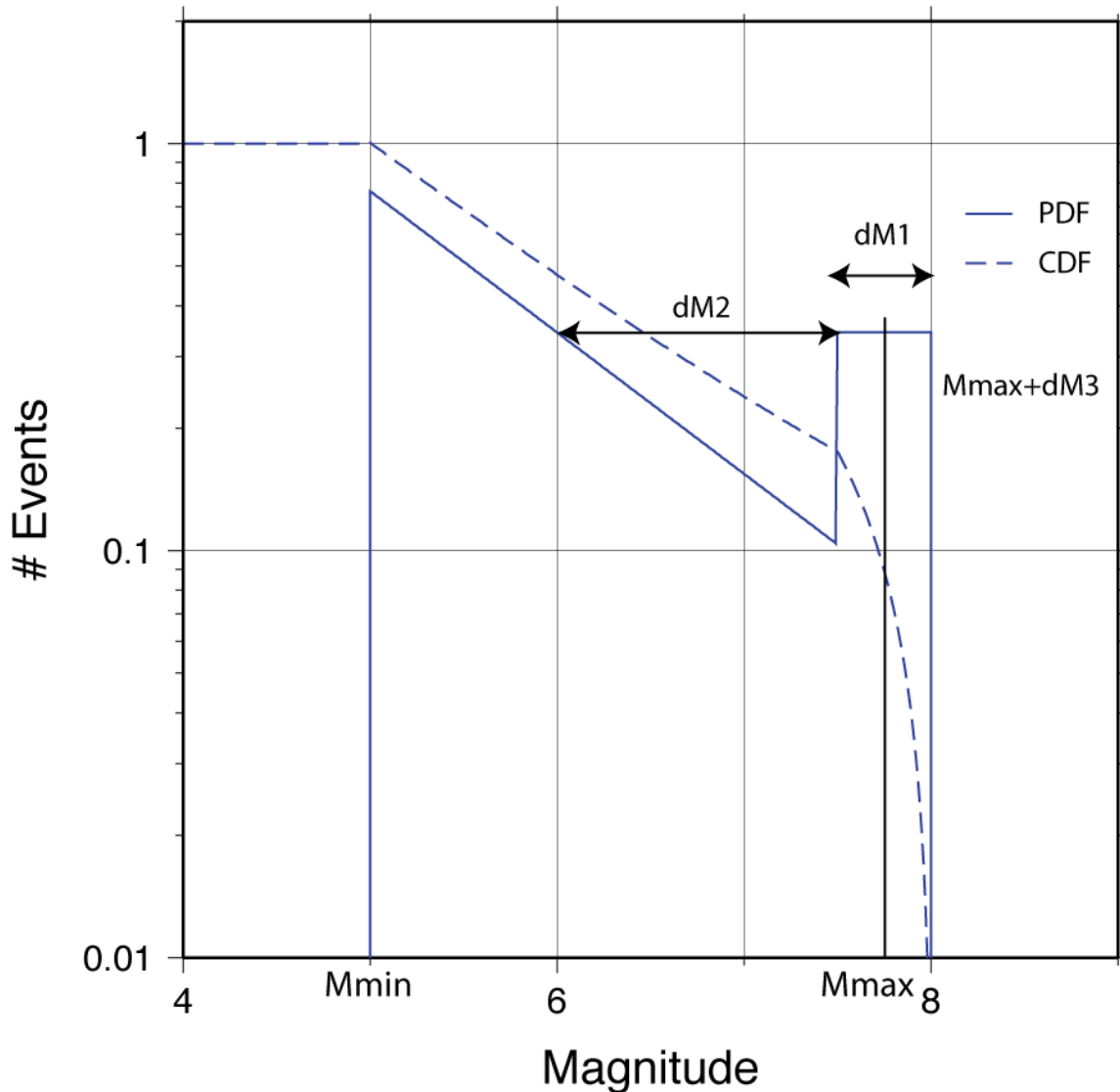


Figure D - 5 PDF and CDF for the characteristic distribution.

$$N(M) = N(Min) \cdot \left( 1 - \frac{1}{2(1 + \sum_{i=1}^6 c_i s)^{16}} \right)$$

with  $s = \frac{M - Mmax}{\sigma}$ ,  $c1 = 0.049867347$ ,  $c2 = 0.0211410061$ ,  $c3 = 0.0032776263$ ,  $c4 = 0.0000380036$ ,  $c5 = 0.0000488906$ , and  $c6 = 0.0000053830$ .

#### Characteristic Magnitude model

This relationship was developed in the 1980's (Schwartz and Coppersmith, 1984) based on paleoseismic observation on several large faults where it appears that the rate of large earthquakes is much larger than is predicted by a G-R relation. The current model form of this distribution

consists of two parts: a truncated exponential distribution below a certain magnitude threshold, and a flat (platform) distribution above this threshold (Figure D - 3).

It appears that the characteristic model is more appropriate when describing the seismicity on individual faults whereas the Gutenberg-Richter relation is more applicable to areal source regions, or ensembles of multiple source zones. The PDF of the characteristic model can be expressed as:

$$n(M) = \beta \frac{e^{(M-M_{min})}}{1 - e^{-\beta(M_{max}-M_{min})}}, \text{ if } M_{min} < M < M_1$$

$$n(M) = \text{constant}, \quad \text{if } M_1 < M < M_{max}$$

The CDF is shown in Figure D - 3.

## D.2. References

- Downes, G.L. and Stirling, M.W., 2001. Groundwork for development of a probabilistic tsunami hazard model for New Zealand, International Tsunami Symposium 2001, Seattle, Washington, pp. 293–301.
- Geist, E.L. & Parsons, T. 2006. Probabilistic Analysis of Tsunami Hazards. *Natural Hazards* **37**(3), 277–314.
- Gutenberg, R., and Richter, C.F., 1944. Frequency of earthquakes in California, Bulletin of the Seismological Society of America, 34, pp. 185-188.
- Hastings Jr. C., 1955. *Approximations for digital computers*, Princeton University Press, Princeton, N. J.
- McGuire, R.K., 2004. Seismic hazard and risk analysis, Earthquake Engineering Research Institute, MNO-10, 240 pp.
- Papazachos, B., Scordilis, E., Panagiotopoulos, D., Papazachos, C.B., and Karakaisis, G.F., 2004. Global relations between seismic fault parameters and moment magnitude of earthquakes. *Bulletin of the Geological Society of Greece* **36**(3), 1482–1489.
- Satake, K., 1995. Linear and nonlinear computations of the 1992 Nicaragua earthquake tsunami. *Pure and Applied Geophysics* **144**(3), 455–470.
- Schwartz, D. P., K. J. Coppersmith, F. H. Swan III, P. Somerville, and W. U. Savage, Characteristic earthquakes on intraplate normal faults (abstract), *Earthquake Notes*, 52, 71, 1981.
- Schwartz, D.P. & Coppersmith, K.J. 1984. Fault behavior and characteristic earthquakes: Examples from the Wasatch and San Andreas Fault Zones. *Journal of Geophysical Research: Solid Earth* **89**(B7), 5681–5698.

Wells, D.L., and Coppersmith, K.J., 1994. New empirical relationships among magnitude, rupture length, rupture width, rupture area, and surface displacement: Bulletin of the Seismological Society of America, **84**, pp. 974-1002.

## **Appendix E. Source parameters for inundation events**

For the inundation part of this study, we selected a range of scenarios, both local and distant, which were used to sample the offshore hazard curves and determine the resultant probabilistic inundation maps. In the following tables, we present the main parameters of all the scenarios used.

Some of the distant scenarios in particular have implausibly large magnitudes. This is due to the fact that we need to account for the aleatory variability in the offshore hazard results, which requires us to scale up our inundation scenarios. Since these scenarios are computed from the source, it is easiest to apply these scaling factors at the source by scaling the slip. This does not mean that we consider that these large magnitudes can occur, it is just a mechanism to allow for the effect of the aleatory variability on the inundation.

**Table E-1 Distant scenarios**

ID	M <sub>w</sub>	D <sub>AVE</sub> (m)	L (km)	W (km)
Kurile_1	9.10	18.74	800	125
Kurile_2	9.20	26.48	800	125
Kurile_3	9.30	37.40	800	125
Kurile_4	9.40	52.83	800	125
Kurile_5	9.50	74.62	800	125
Chile_1	9.10	15.00	1000	125
Chile_2	9.20	21.18	1000	125
Chile_3	9.30	29.92	1000	125
Chile_4	9.50	59.70	1000	125
Chile_5	9.70	119.12	1000	125
Alaska_w_1	8.90	8.95	700	150
Alaska_w_2	9.00	12.64	700	150
Alaska_w_3	9.10	17.85	700	150
Alaska_w_4	9.20	25.22	700	150
Alaska_w_5	9.30	35.62	700	150
Alaska_w_6	9.40	50.31	700	150
Alaska_w_7	9.50	71.07	700	150
Alaska_w_8	9.60	100.39	700	150
Alaska_e_1	8.40	1.91	500	175
Alaska_e_2	8.70	5.38	500	175
Alaska_e_3	8.80	7.60	500	175
Alaska_e_4	8.90	10.74	500	175

Alaska_e_5	9.00	15.17	500	175
Alaska_e_6	9.10	21.42	500	175
Alaska_e_7	9.30	42.74	500	175
Alaska_e_8	9.40	60.38	500	175
Alaska_e_9	9.50	85.28	500	175
Alaska_a_1	9.50	35.54	1200	175
Alaska_a_2	9.60	50.19	1200	175
Alaska_a_3	9.70	70.90	1200	175

**Table E-2 Cascadia events**

ID	M <sub>w</sub>	M <sub>0</sub> (dyne.cm)	D <sub>ave</sub> (m)	Area (km <sup>2</sup> )
Event-1-01-1-1-1-01	8.44	5.84E+28	2.49	117560
Event-1-01-1-1-1-02	8.73	1.57E+29	6.67	117560
Event-1-01-1-1-1-03	9.02	4.21E+29	17.92	117560
Event-1-01-1-1-2-01	8.44	5.84E+28	2.49	117560
Event-1-01-1-1-2-02	8.73	1.57E+29	6.67	117560
Event-1-01-1-1-2-03	9.02	4.21E+29	17.92	117560
Event-1-01-1-1-3-01	8.44	5.84E+28	2.49	117560
Event-1-01-1-1-3-02	8.73	1.57E+29	6.67	117560
Event-1-01-1-1-3-03	9.02	4.21E+29	17.92	117560
Event-1-01-1-2-1-01	8.46	6.11E+28	2.51	121732
Event-1-01-1-2-1-02	8.74	1.64E+29	6.74	121732
Event-1-01-1-2-1-03	9.03	4.40E+29	18.09	121732

ID	M <sub>w</sub>	M <sub>0</sub> (dyne.cm)	D <sub>ave</sub> (m)	Area (km <sup>2</sup> )
Event-1-01-1-2-2-01	8.46	6.11E+28	2.51	121732
Event-1-01-1-2-2-02	8.74	1.64E+29	6.74	121732
Event-1-01-1-2-2-03	9.03	4.40E+29	18.09	121732
Event-1-01-1-2-3-01	8.46	6.11E+28	2.51	121732
Event-1-01-1-2-3-02	8.74	1.64E+29	6.74	121732
Event-1-01-1-2-3-03	9.03	4.40E+29	18.09	121732
Event-1-01-2-1-1-01	8.44	5.84E+28	2.49	117560
Event-1-01-2-1-1-02	8.73	1.57E+29	6.67	117560
Event-1-01-2-1-1-03	9.02	4.21E+29	17.92	117560
Event-1-01-2-1-2-01	8.44	5.84E+28	2.49	117560
Event-1-01-2-1-2-02	8.73	1.57E+29	6.67	117560
Event-1-01-2-1-2-03	9.02	4.21E+29	17.92	117560
Event-1-01-2-1-3-01	8.44	5.84E+28	2.49	117560
Event-1-01-2-1-3-02	8.73	1.57E+29	6.67	117560
Event-1-01-2-1-3-03	9.02	4.21E+29	17.92	117560
Event-1-01-2-2-1-01	8.46	6.11E+28	2.51	121732
Event-1-01-2-2-1-02	8.74	1.64E+29	6.74	121732
Event-1-01-2-2-1-03	9.03	4.40E+29	18.09	121732
Event-1-01-2-2-2-01	8.46	6.11E+28	2.51	121732
Event-1-01-2-2-2-02	8.74	1.64E+29	6.74	121732
Event-1-01-2-2-2-03	9.03	4.40E+29	18.09	121732
Event-1-01-2-2-3-01	8.46	6.11E+28	2.51	121732
Event-1-01-2-2-3-02	8.74	1.64E+29	6.74	121732

ID	M <sub>w</sub>	M <sub>0</sub> (dyne.cm)	D <sub>ave</sub> (m)	Area (km <sup>2</sup> )
Event-1-01-2-2-3-03	9.03	4.40E+29	18.09	121732
Event-1-01-3-1-1-01	8.33	3.96E+28	2.29	86478
Event-1-01-3-1-1-02	8.62	1.06E+29	6.14	86478
Event-1-01-3-1-1-03	8.90	2.85E+29	16.5	86478
Event-1-01-3-1-2-01	8.33	3.96E+28	2.29	86478
Event-1-01-3-1-2-02	8.62	1.06E+29	6.14	86478
Event-1-01-3-1-2-03	8.90	2.85E+29	16.5	86478
Event-1-01-3-1-3-01	8.33	3.96E+28	2.29	86478
Event-1-01-3-1-3-02	8.62	1.06E+29	6.14	86478
Event-1-01-3-1-3-03	8.90	2.85E+29	16.5	86478
Event-1-01-3-2-1-01	8.35	4.20E+28	2.32	90650
Event-1-01-3-2-1-02	8.64	1.13E+29	6.22	90650
Event-1-01-3-2-1-03	8.92	3.03E+29	16.71	90650
Event-1-01-3-2-2-01	8.35	4.20E+28	2.32	90650
Event-1-01-3-2-2-02	8.64	1.13E+29	6.22	90650
Event-1-01-3-2-2-03	8.92	3.03E+29	16.71	90650
Event-1-01-3-2-3-01	8.35	4.20E+28	2.32	90650
Event-1-01-3-2-3-02	8.64	1.13E+29	6.22	90650
Event-1-01-3-2-3-03	8.92	3.03E+29	16.71	90650
Event-2-01-1-1-1-01	8.93	3.08E+29	13.1	117560
Event-2-01-1-1-1-02	9.18	7.30E+29	31.07	117560
Event-2-01-1-1-1-03	9.43	1.73E+30	73.67	117560
Event-2-01-1-1-2-01	8.93	3.08E+29	13.1	117560



ID	M <sub>w</sub>	M <sub>0</sub> (dyne.cm)	D <sub>ave</sub> (m)	Area (km <sup>2</sup> )
Event-2-01-1-1-2-02	9.18	7.30E+29	31.07	117560
Event-2-01-1-1-2-03	9.43	1.73E+30	73.67	117560
Event-2-01-1-1-3-01	8.93	3.08E+29	13.1	117560
Event-2-01-1-1-3-02	9.18	7.30E+29	31.07	117560
Event-2-01-1-1-3-03	9.43	1.73E+30	73.67	117560
Event-2-01-1-2-1-01	8.94	3.27E+29	13.44	121732
Event-2-01-1-2-1-02	9.19	7.76E+29	31.88	121732
Event-2-01-1-2-1-03	9.44	1.84E+30	75.61	121732
Event-2-01-1-2-2-01	8.94	3.27E+29	13.44	121732
Event-2-01-1-2-2-02	9.19	7.76E+29	31.88	121732
Event-2-01-1-2-2-03	9.44	1.84E+30	75.61	121732
Event-2-01-1-2-3-01	8.94	3.27E+29	13.44	121732
Event-2-01-1-2-3-02	9.19	7.76E+29	31.88	121732
Event-2-01-1-2-3-03	9.44	1.84E+30	75.61	121732
Event-2-01-2-1-1-01	8.93	3.08E+29	13.1	117560
Event-2-01-2-1-1-02	9.18	7.30E+29	31.07	117560
Event-2-01-2-1-1-03	9.43	1.73E+30	73.67	117560
Event-2-01-2-1-2-01	8.93	3.08E+29	13.1	117560
Event-2-01-2-1-2-02	9.18	7.30E+29	31.07	117560
Event-2-01-2-1-2-03	9.43	1.73E+30	73.67	117560
Event-2-01-2-1-3-01	8.93	3.08E+29	13.1	117560
Event-2-01-2-1-3-02	9.18	7.30E+29	31.07	117560
Event-2-01-2-1-3-03	9.43	1.73E+30	73.67	117560

ID	M <sub>w</sub>	M <sub>0</sub> (dyne.cm)	D <sub>ave</sub> (m)	Area (km <sup>2</sup> )
Event-2-01-2-2-1-01	8.94	3.27E+29	13.44	121732
Event-2-01-2-2-1-02	9.19	7.76E+29	31.88	121732
Event-2-01-2-2-1-03	9.44	1.84E+30	75.61	121732
Event-2-01-2-2-2-01	8.94	3.27E+29	13.44	121732
Event-2-01-2-2-2-02	9.19	7.76E+29	31.88	121732
Event-2-01-2-2-2-03	9.44	1.84E+30	75.61	121732
Event-2-01-2-2-3-01	8.94	3.27E+29	13.44	121732
Event-2-01-2-2-3-02	9.19	7.76E+29	31.88	121732
Event-2-01-2-2-3-03	9.44	1.84E+30	75.61	121732
Event-2-01-3-1-1-01	8.77	1.80E+29	10.42	86478
Event-2-01-3-1-1-02	9.02	4.28E+29	24.72	86478
Event-2-01-3-1-1-03	9.27	1.01E+30	58.61	86478
Event-2-01-3-1-2-01	8.77	1.80E+29	10.42	86478
Event-2-01-3-1-2-02	9.02	4.28E+29	24.72	86478
Event-2-01-3-1-2-03	9.27	1.01E+30	58.61	86478
Event-2-01-3-1-3-01	8.77	1.80E+29	10.42	86478
Event-2-01-3-1-3-02	9.02	4.28E+29	24.72	86478
Event-2-01-3-1-3-03	9.27	1.01E+30	58.61	86478
Event-2-01-3-2-1-01	8.79	1.96E+29	10.8	90650
Event-2-01-3-2-1-02	9.04	4.64E+29	25.6	90650
Event-2-01-3-2-1-03	9.29	1.10E+30	60.71	90650
Event-2-01-3-2-2-01	8.79	1.96E+29	10.8	90650
Event-2-01-3-2-2-02	9.04	4.64E+29	25.6	90650

ID	M <sub>w</sub>	M <sub>0</sub> (dyne.cm)	D <sub>ave</sub> (m)	Area (km <sup>2</sup> )
Event-2-01-3-2-2-03	9.29	1.10E+30	60.71	90650
Event-2-01-3-2-3-01	8.79	1.96E+29	10.8	90650
Event-2-01-3-2-3-02	9.04	4.64E+29	25.6	90650
Event-2-01-3-2-3-03	9.29	1.10E+30	60.71	90650

## Appendix F. Tsunami code validation

### F.1. Introduction

In 2011, the National Tsunami Hazard Mitigation Program (NTHMP) organized a tsunami model validation workshop where a large number of codes were validated against analytical, experimental and real-life scenarios (NTHMP, 2012). The current GeoClaw-based code was developed after this workshop, but as part of this project we ran most of the Benchmark Problems (BP's), the results of which are presented in this Appendix.

### F.2. Model Description

Our model, which was used for all benchmark problems, is based on the core of the GeoClaw solver. It solves the two-dimensional depth-averaged nonlinear shallow water equations using high-resolution finite volume methods:

$$\begin{aligned}h_t + (hu)_x + (hv)_y &= 0, \\(hu)_t + (hu^2 + \frac{1}{2}gh^2)_x + (huv)_y &= -ghB_x - Du, \\(hv)_t + (huv)_x + (hv^2 + \frac{1}{2}gh^2)_y &= -ghB_y - Dv, \\h_t + (hu)_x + (hv)_y &= 0, \\(hu)_t + (hu^2 + \frac{1}{2}gh^2)_x + (huv)_y &= -ghB_x - Du, \\(hv)_t + (huv)_x + (hv^2 + \frac{1}{2}gh^2)_y &= -ghB_y - Dv,\end{aligned}\tag{10-1}$$

where  $u(x, y, t)$  and  $v(x, y, t)$  are the depth-averaged velocities in the two horizontal directions,  $B(x, y, t)$  is the topography or bathymetry, and  $D(h, u, v)$  is the drag coefficient. In case of the existence of friction, Manning correlation is used for the friction:

$$D = \frac{gn^2\sqrt{u^2 + v^2}}{h^{5/3}} \quad D = \frac{gn^2\sqrt{u^2 + v^2}}{h^{5/3}}\tag{10-2}$$

where  $n$  is the Manning's coefficient, generally taken to be 0.025. The Coriolis terms can be turned on in the model.

### F.3. Benchmark Problem #1: Single wave on a simple beach (Analytic)

#### *Problem description*

This benchmark is to compare numerical and analytical solutions for a solitary wave on a simple beach. The bathymetry consists of a deep region of constant depth  $d$  connected to a sloping beach of angle  $\beta = \text{arccot}(19.85)$ . The initial waveform is given by

$$\eta(x,0) = H \operatorname{sech}^2(\gamma(x - X_1)/d) \quad \eta(x,0) = H \operatorname{sech}^2(\gamma(x - X_1)/d) \quad (10-3)$$

where  $H$  is the wave amplitude,  $L = \operatorname{acosh}(\sqrt{20})/\gamma$ ,  $X_1 = X_0 + L$ ,  $L = \operatorname{acosh}(\sqrt{20})/\gamma$ ,  $X_1 = X_0 + L$ , and  $\gamma = \sqrt{3H/4d}$ .  $\gamma = \sqrt{3H/4d}$ . The initial wave speed is

$$u(x,0) = -\sqrt{g/d}\eta(x,0) \quad u(x,0) = -\sqrt{g/d}\eta(x,0) \quad (10-4)$$

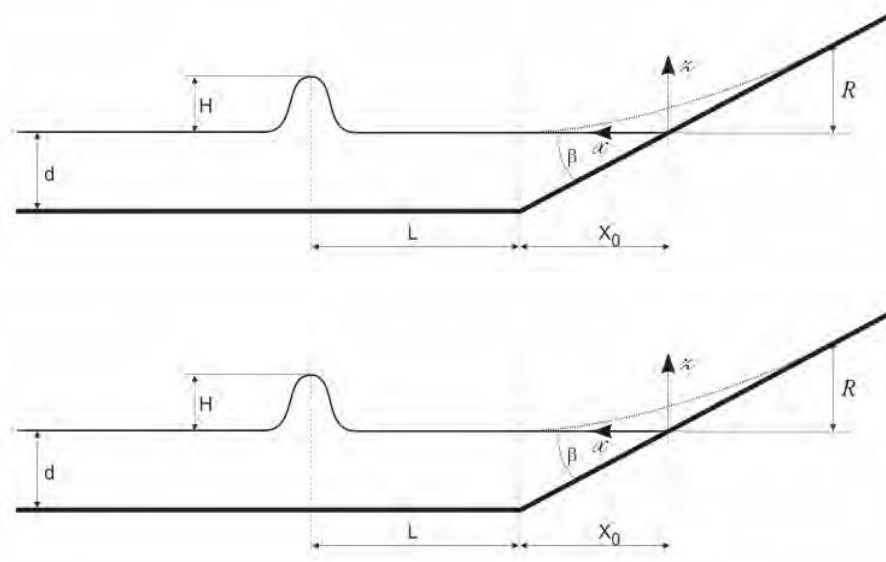


Figure F-1 Sketch of canonical beach and approaching wave.

*Model setup*

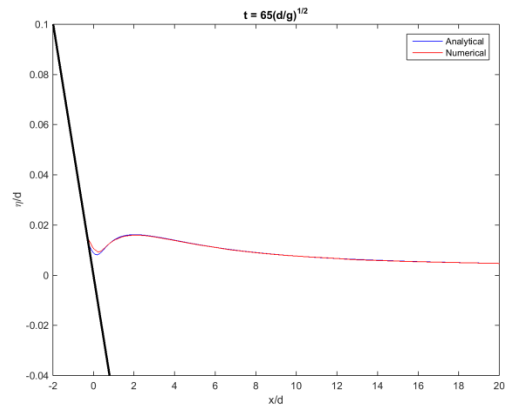
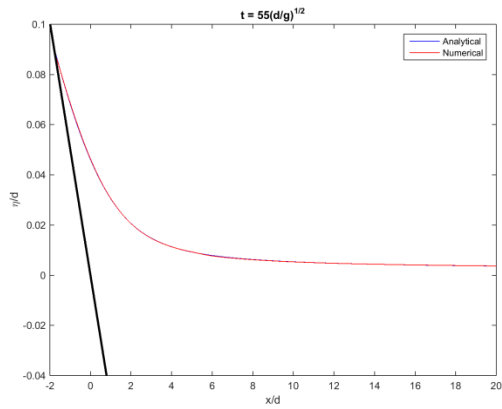
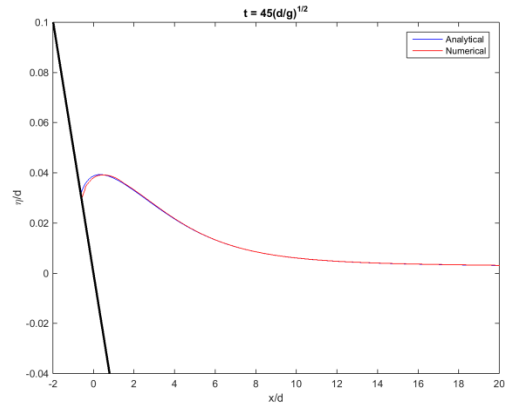
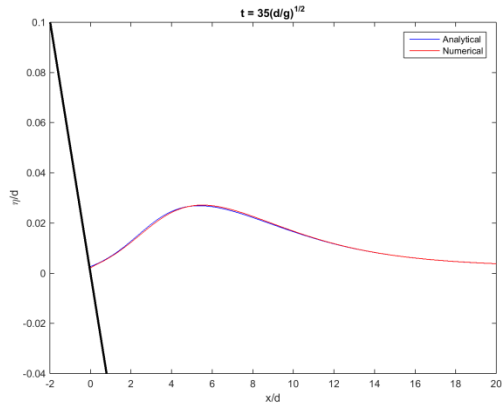
Used  $g = 9.81 \text{ m/s}^2$ ,  $d = 1 \text{ m}$  and no friction.

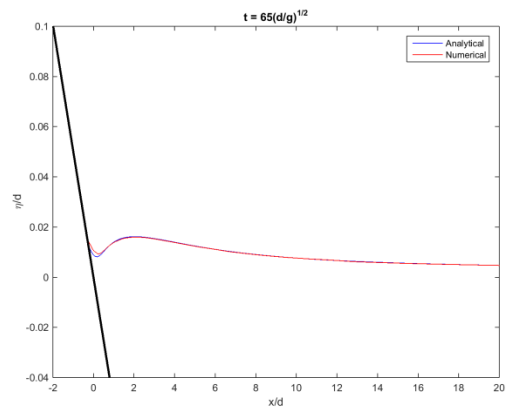
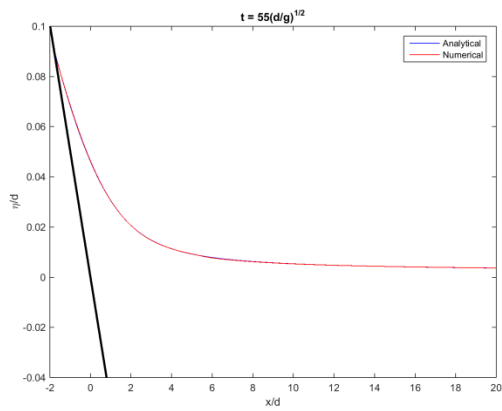
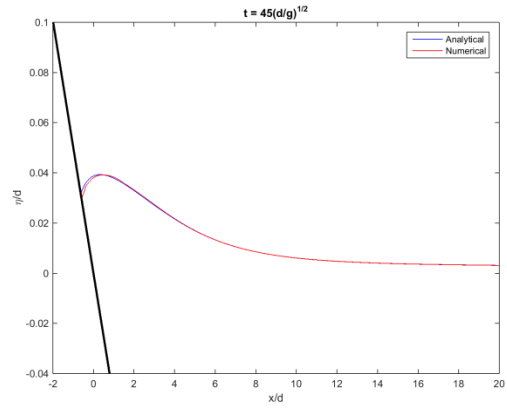
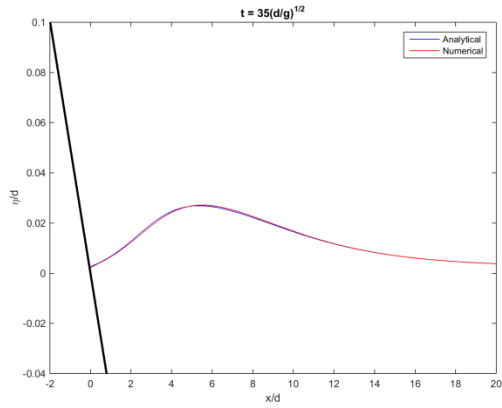
The grid cell size is 1 cm.

The Courant-Friedrichs-Lewy (CFL) number, a measure for the stability of the calculations, is 0.75.

*Results*

Good agreement between computed and analytical water level profiles / time series is presented in Figures F-2 and F-3. The computed maximum runup on the beach is 0.0885, which is close to the analytical value 0.08897.





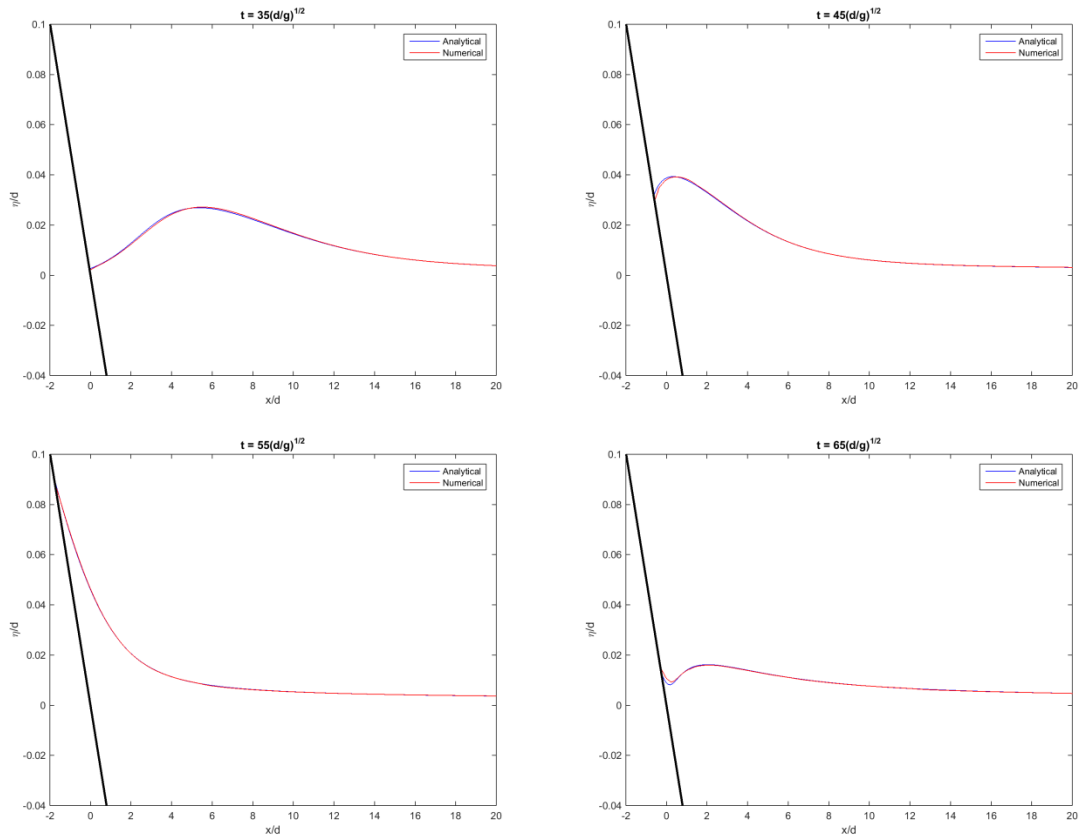


Figure F-2 Water level profiles at the specified times.



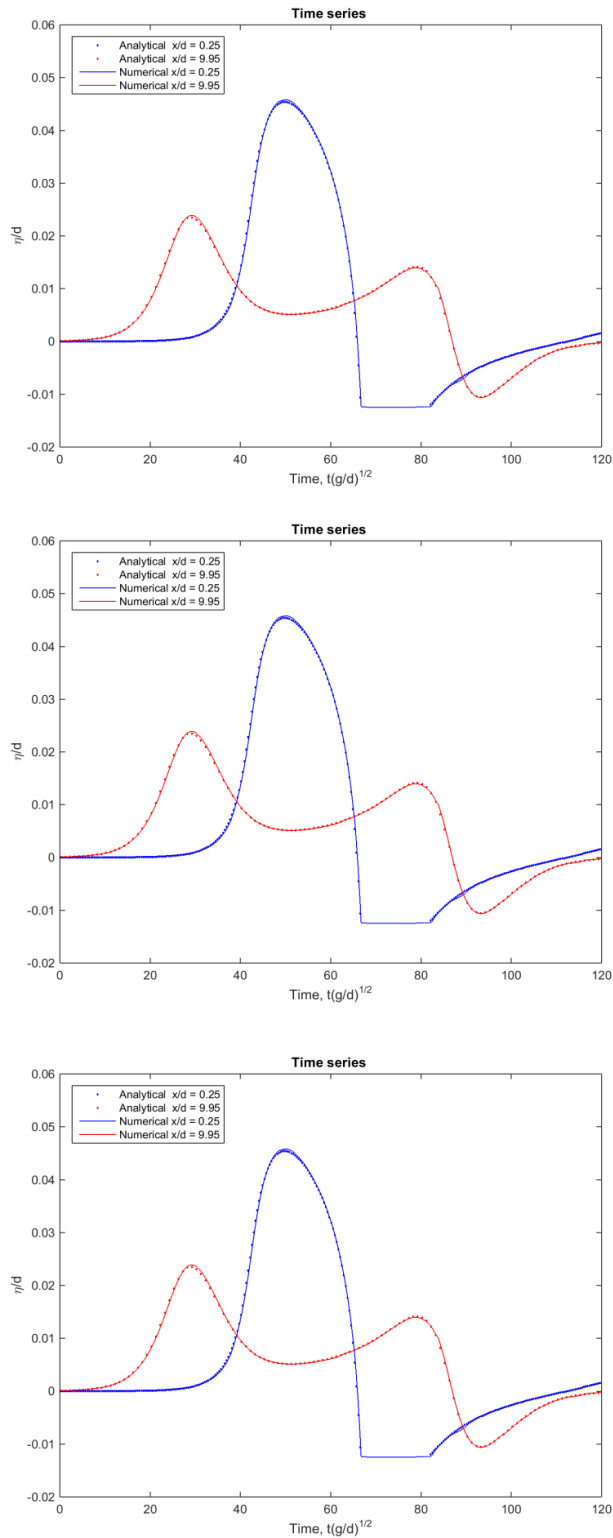


Figure F - 3 Water level time series at  $x/d = 0.25$  and  $9.95$ .

**F.4. Benchmark Problem #2: Solitary wave on composite beach (Analytic)**

*Problem description*

A composite beach simulating geometrical dimensions of the Revere Beach in Revere, Massachusetts, was constructed in a water tank by the U.S. Army Corps of Engineers at the Coastal Engineering Research Center in Vicksburg, Mississippi. The constructed beach consists of three piece-wise linear segments, and a vertical wall, against which the maximum runup was measured. The schematic of the beach is shown in Figure F-4.

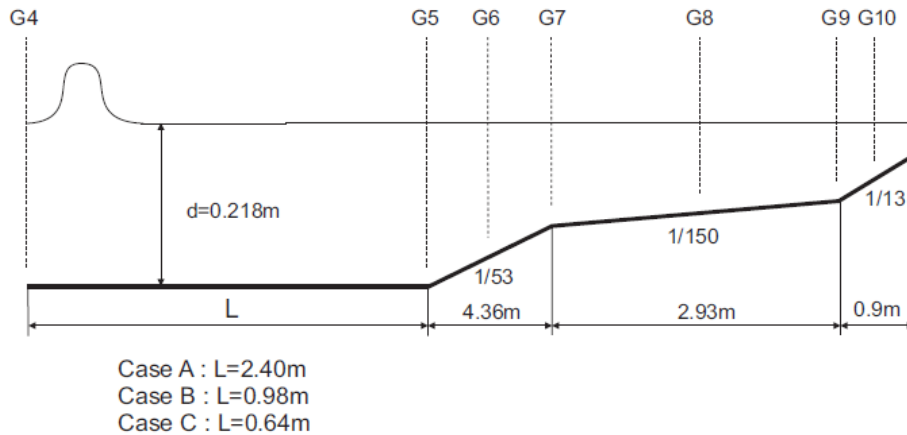


Figure F-4 Schematics of the composite beach and locations of water gauges.

*Model setup*

Used  $g = 9.81 \text{ m/s}^2$  and no friction in Cartesian coordinates.

The tank size is

10.6 m × 0.05 m for Case A

9.17 m × 0.05 m for Case B

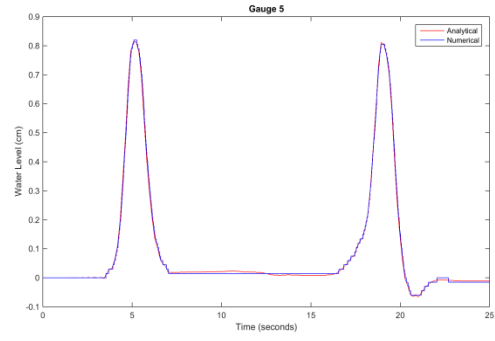
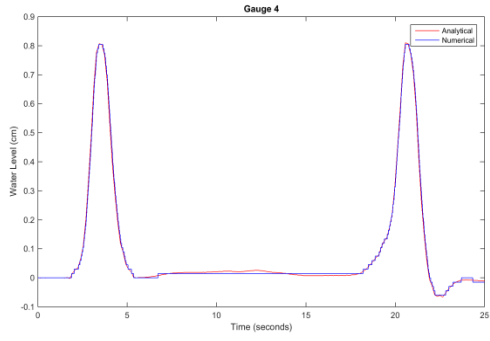
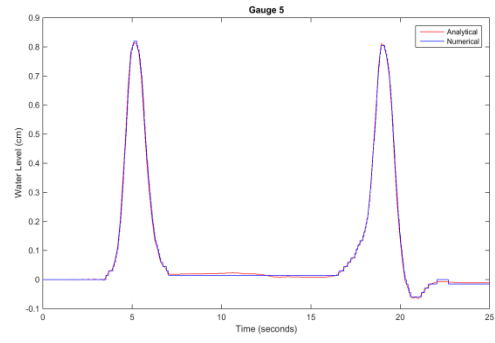
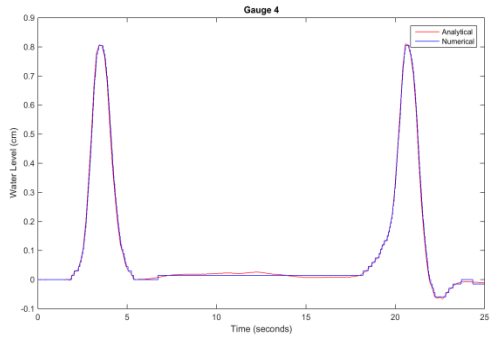
8.83 m × 0.05 m for Case C

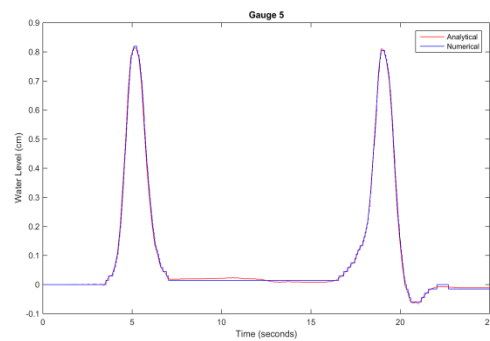
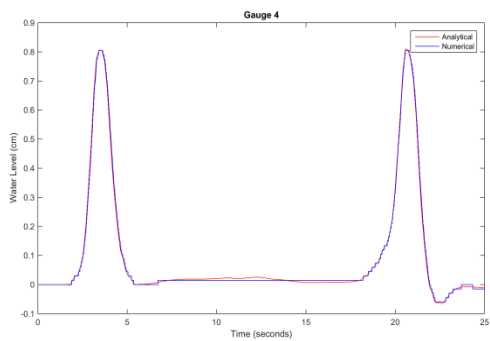
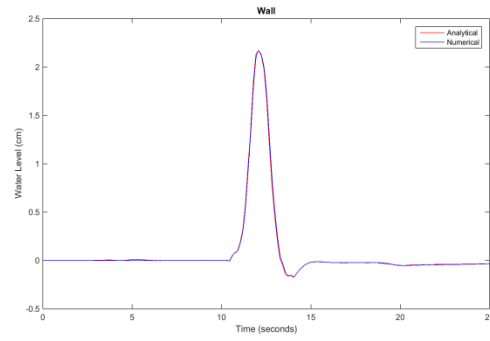
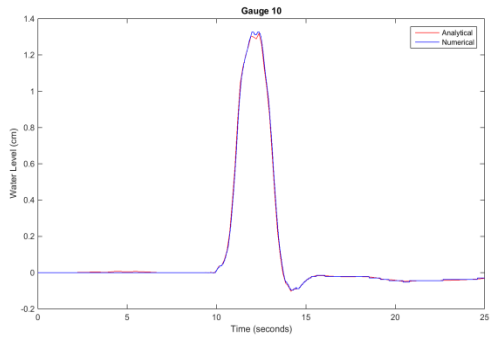
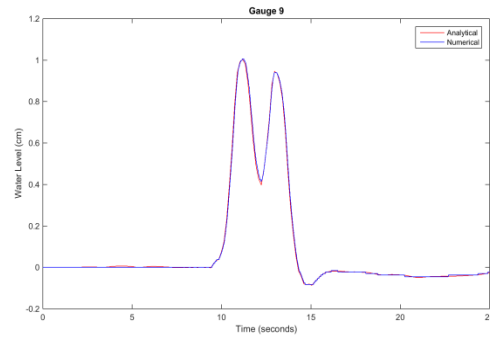
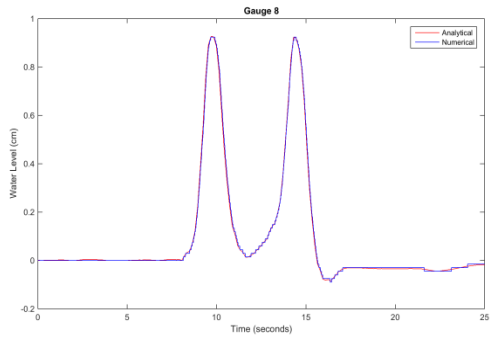
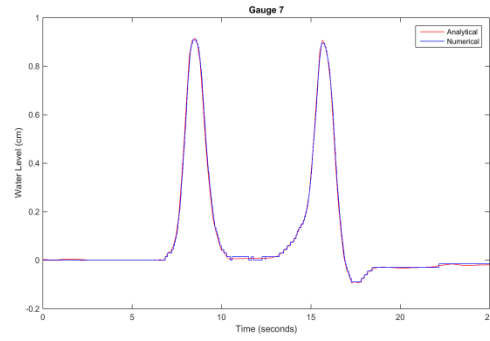
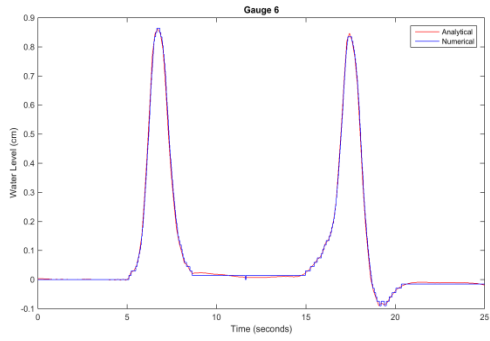
The grid cell size is 1 cm.

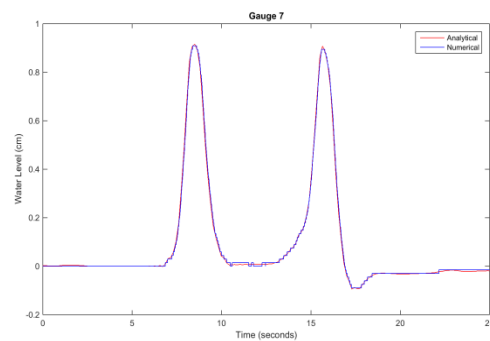
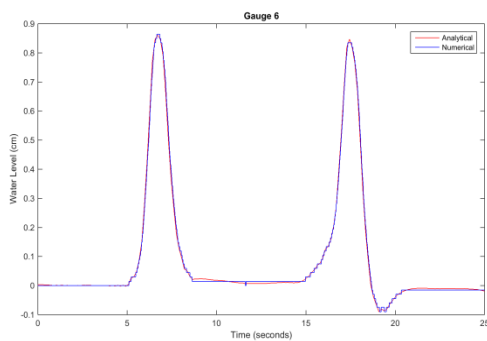
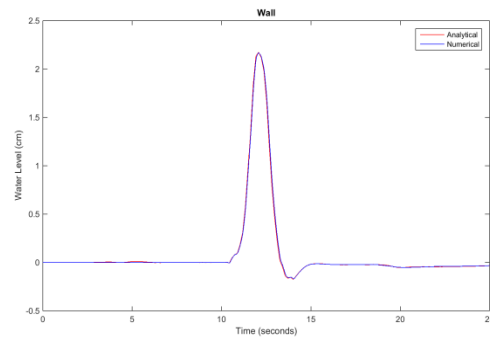
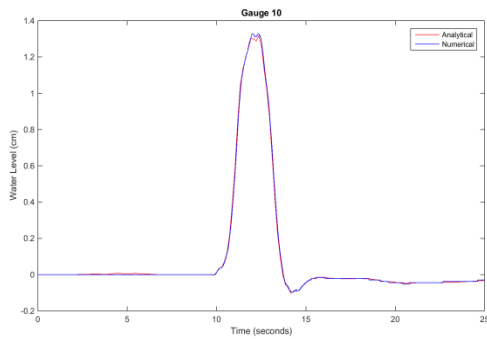
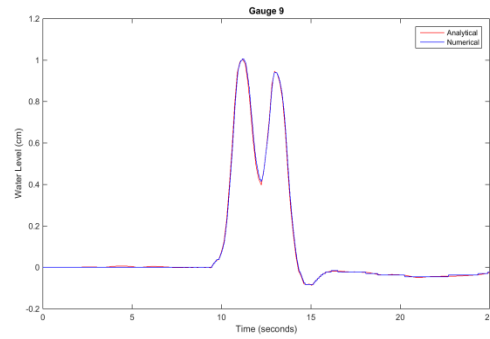
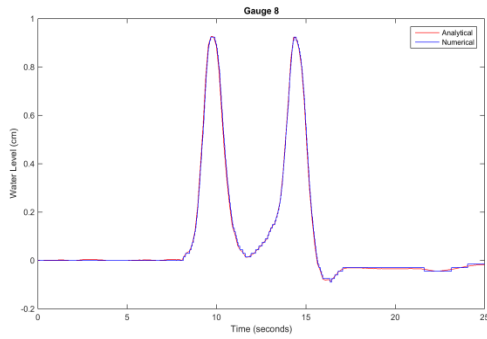
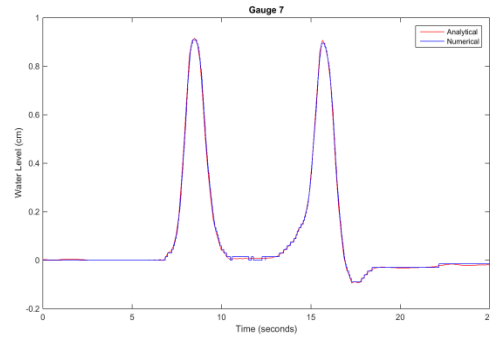
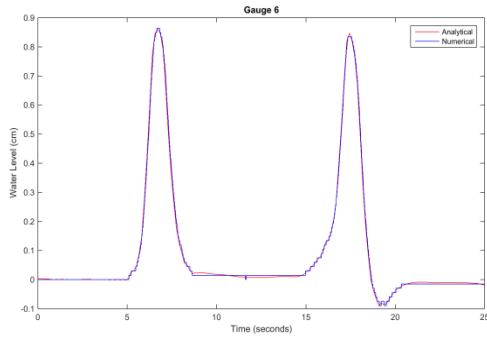
To impose linearization, we scaled the incoming wave by  $10^{-4}$  then scaled up the gage readings by  $10^4$  to compare with the analytical solutions.

*Results*

The time series at the gauges G4-G10 and the wall for Cases A, B and C are shown in Figures F-5 through F-7.







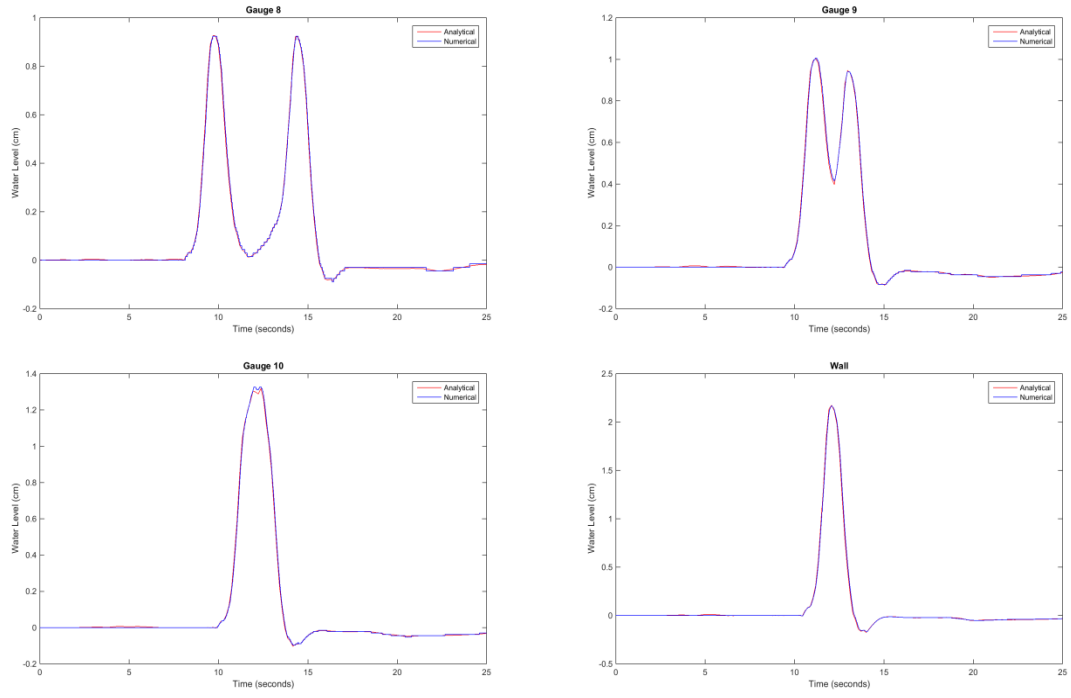
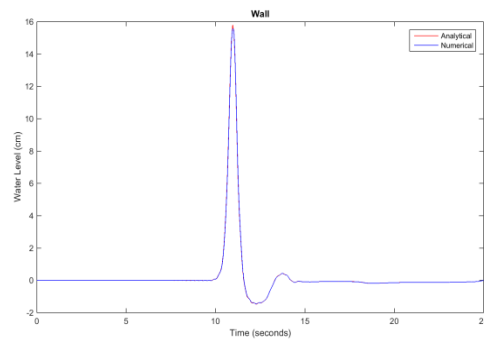
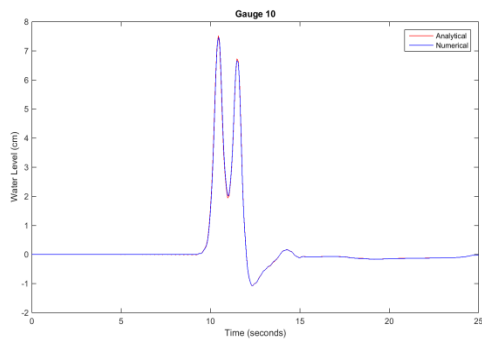
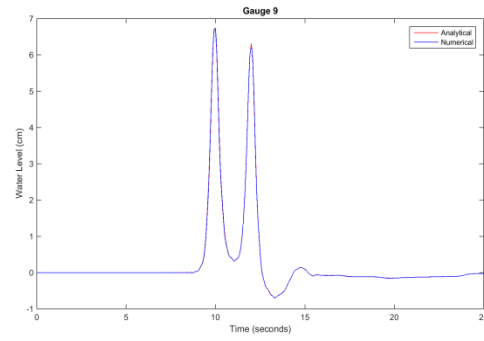
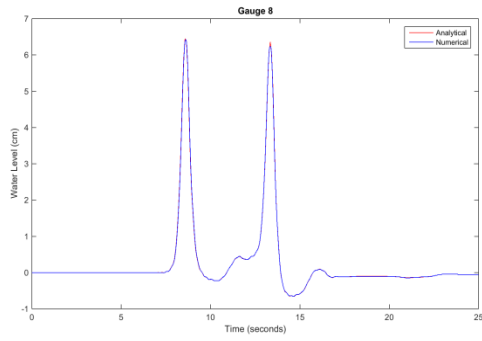
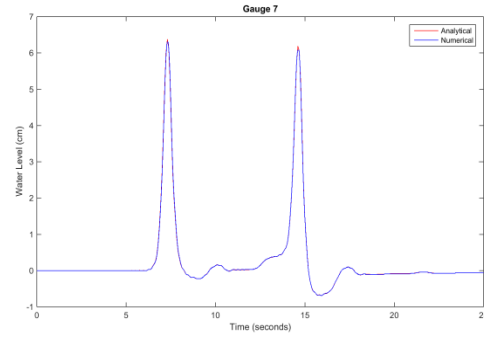
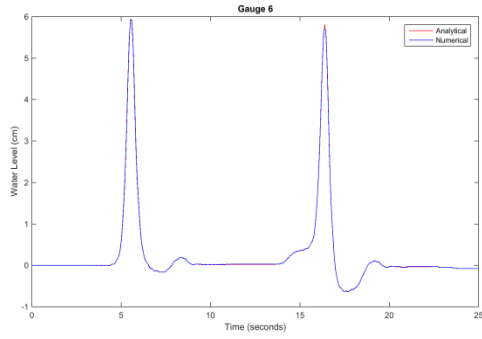
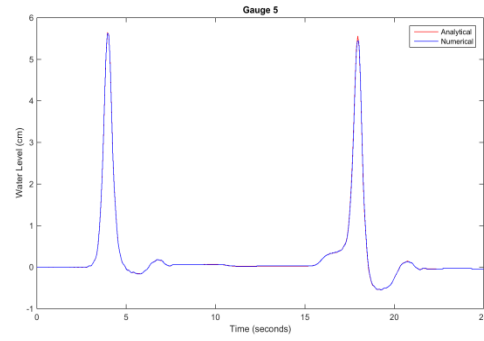
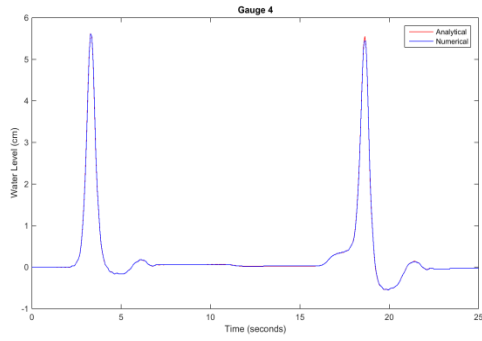
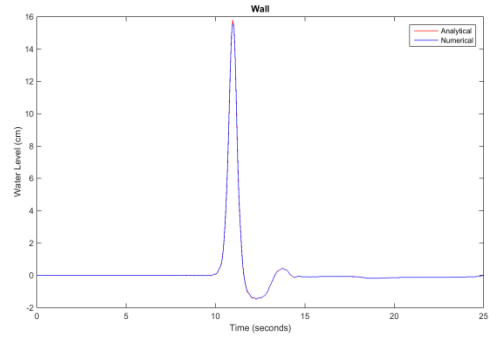
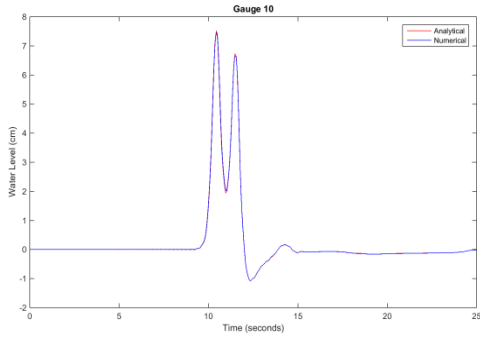
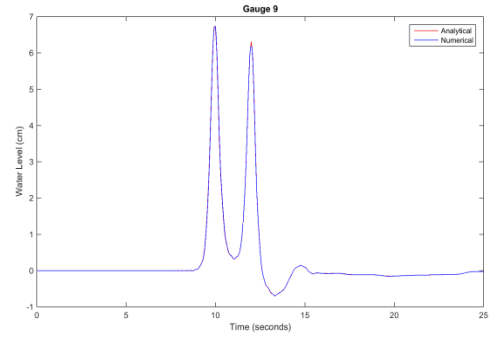
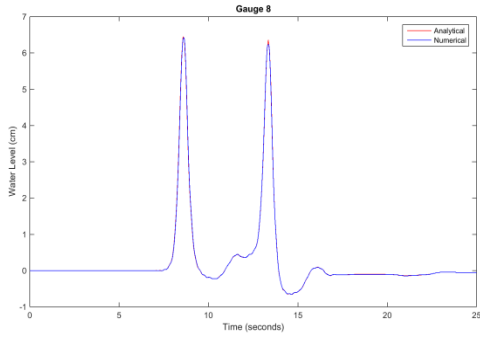
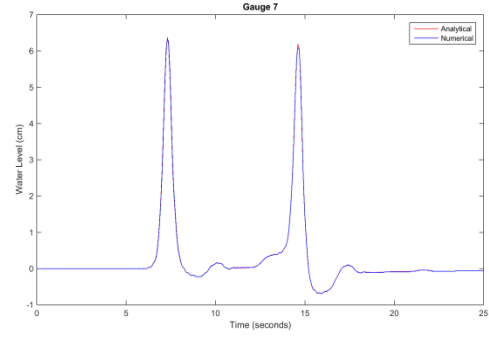
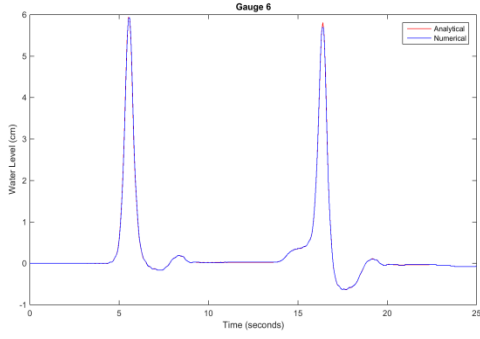
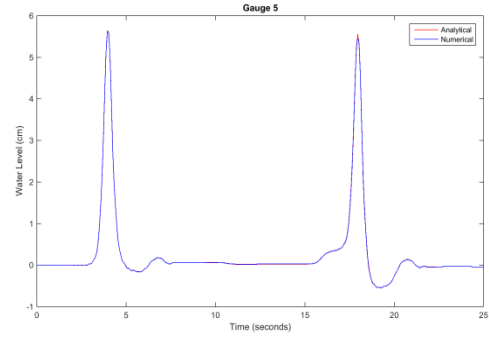
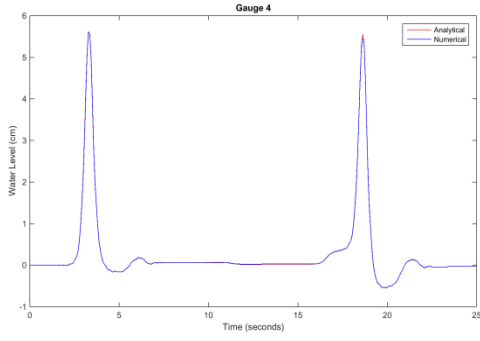


Figure F-5 Time series at gauges G4-G10 for Case A.







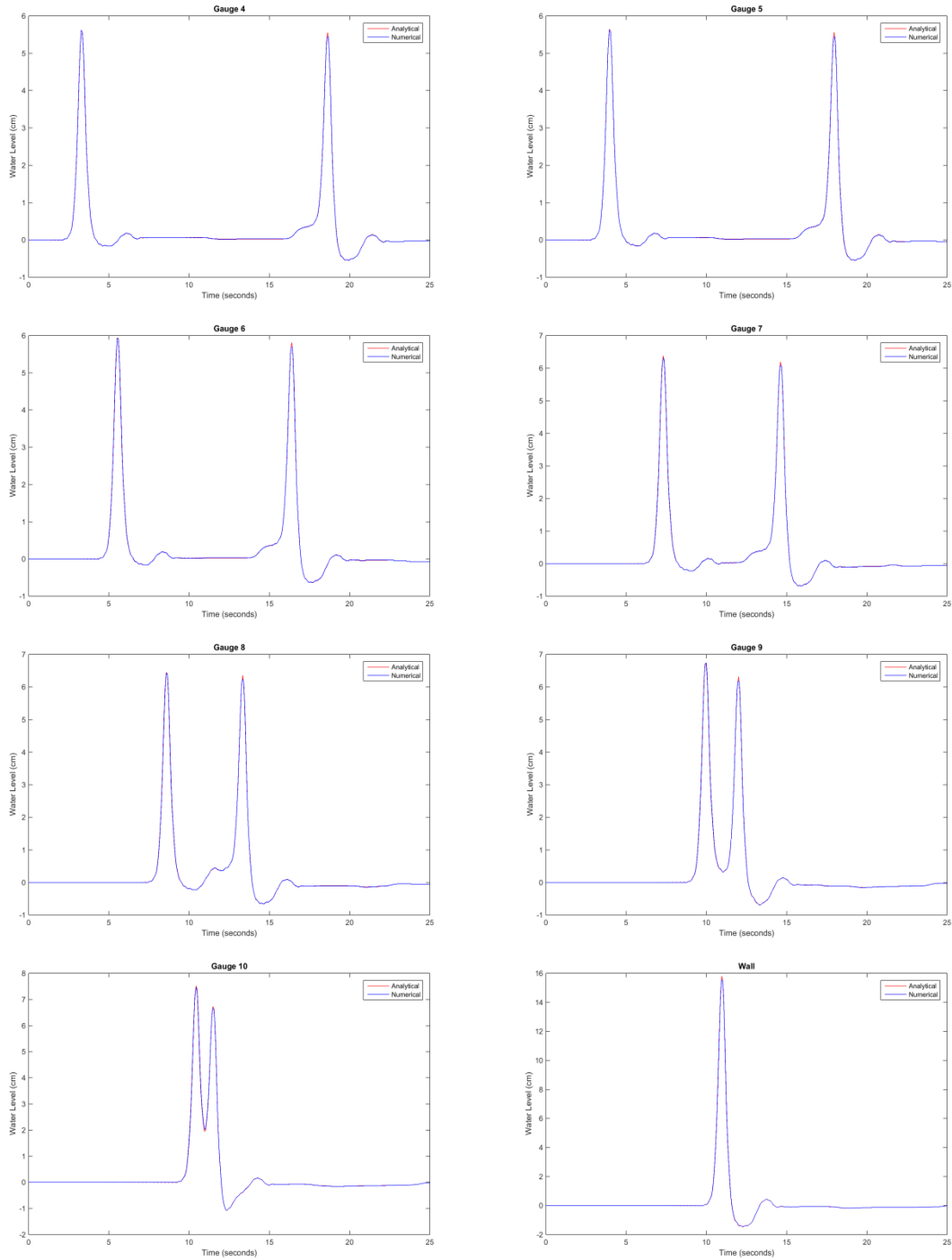
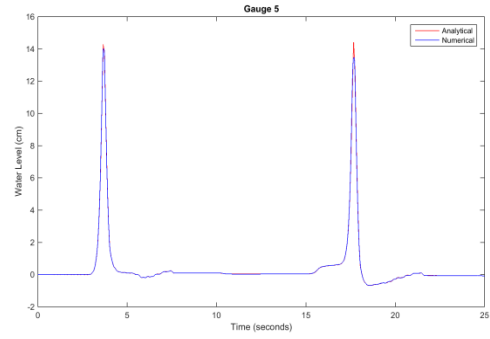
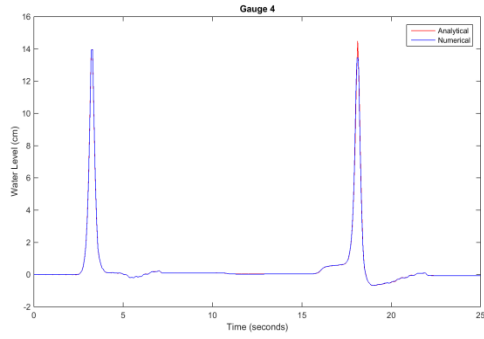
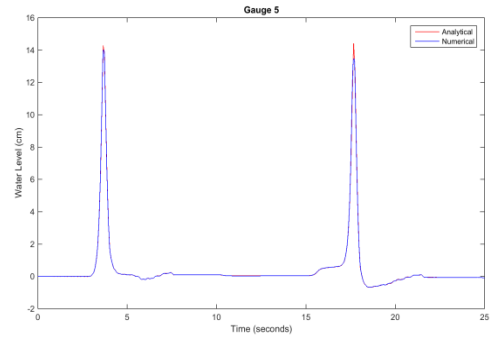
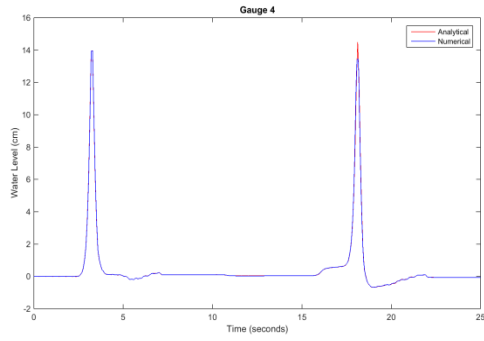
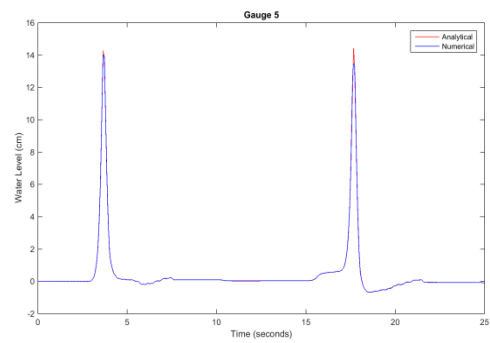
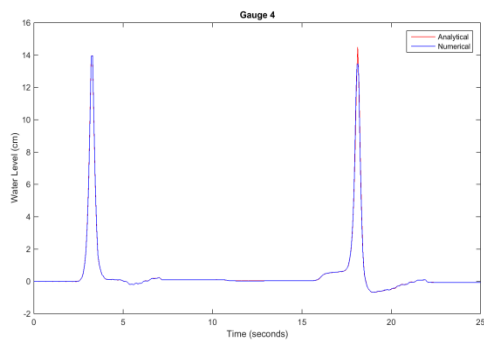
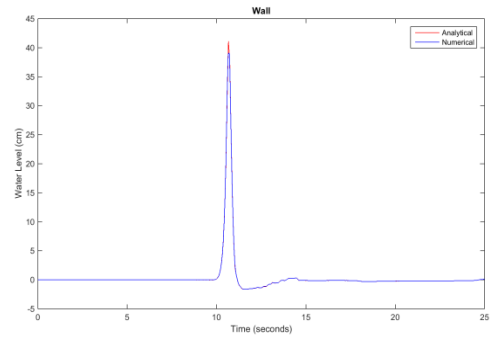
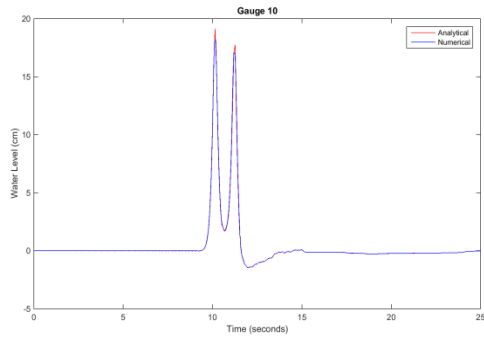
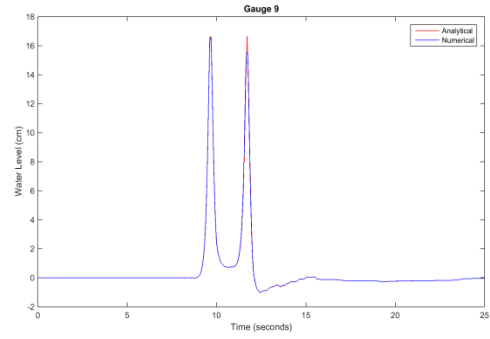
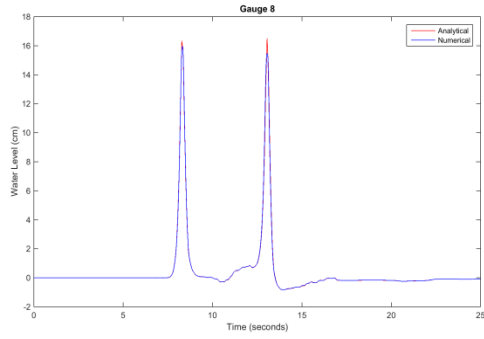
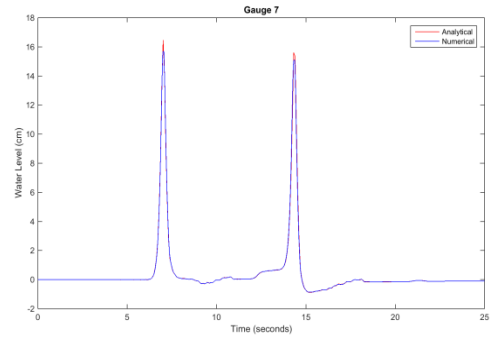
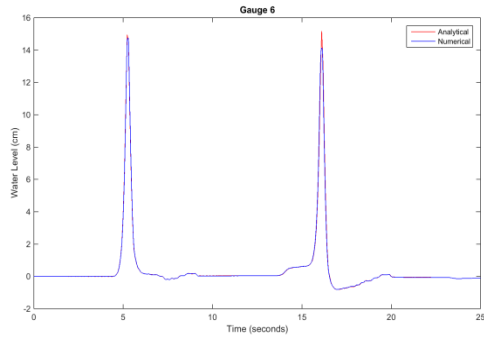
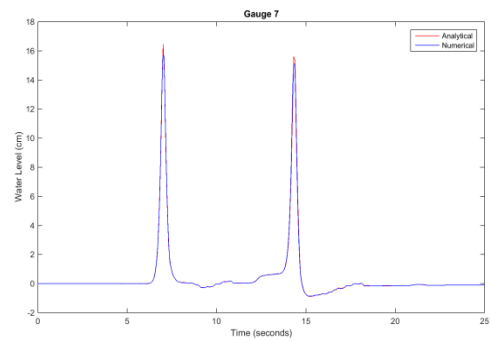
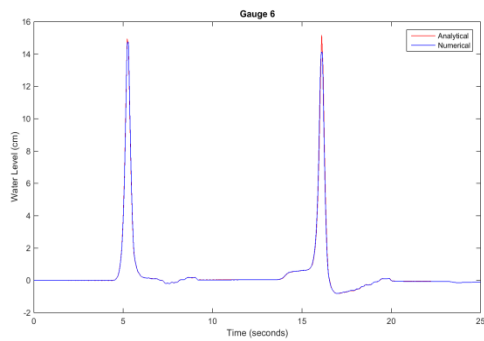
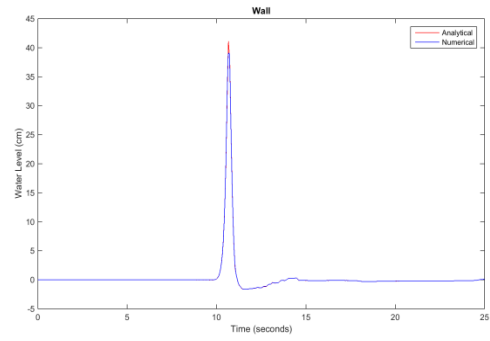
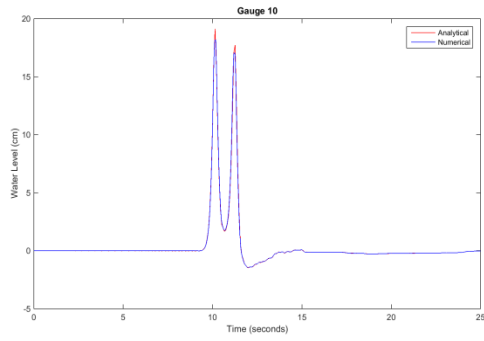
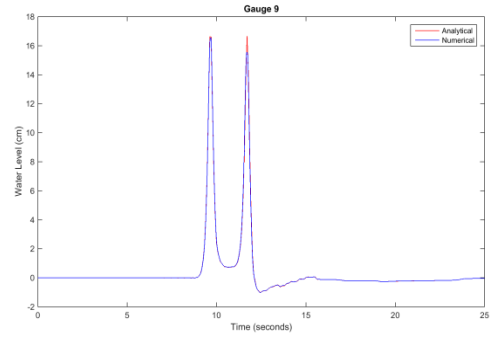
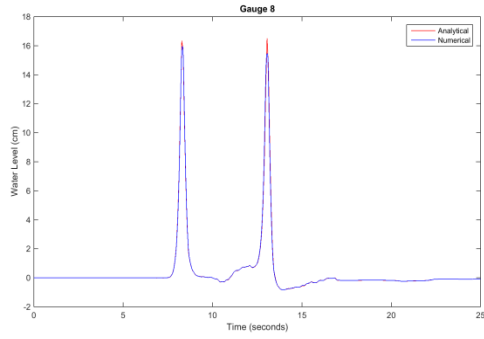
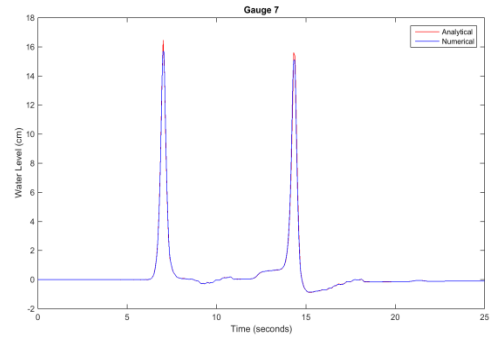
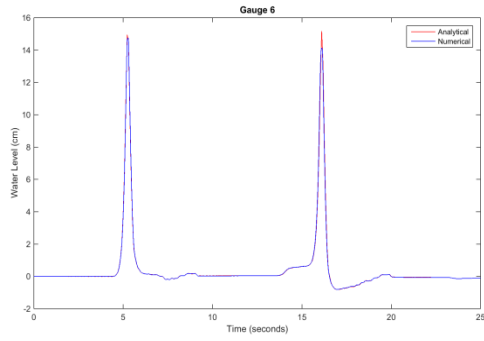


Figure F-6 Time series at gauges G4-G10 for Case B.







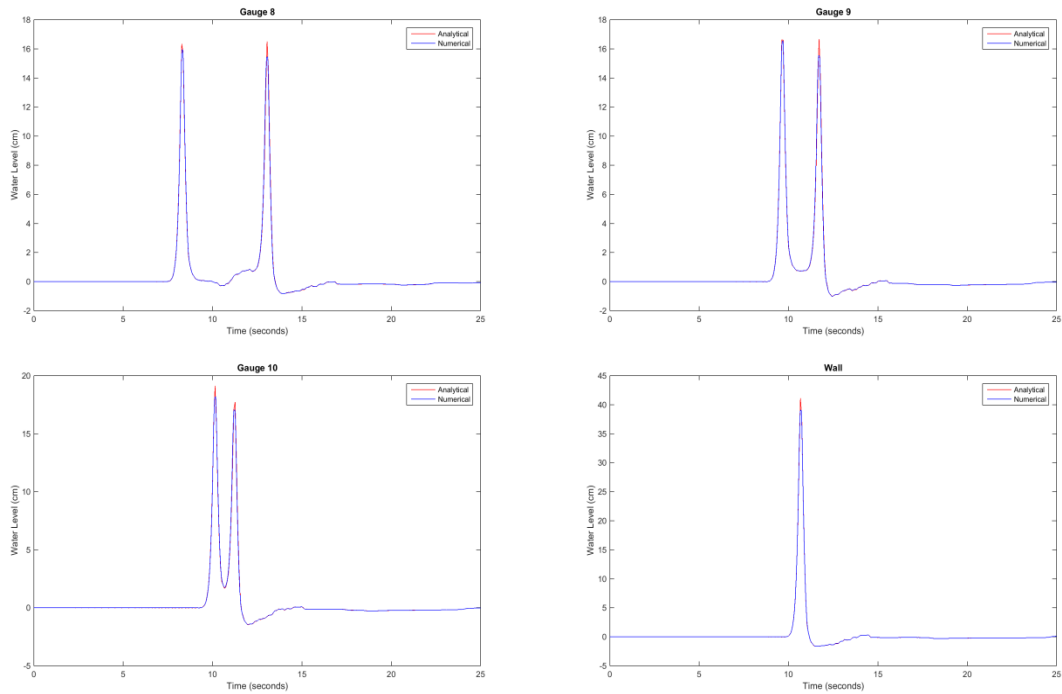


Figure F-7 Time series at gauges G4-G10 for Case C.

## F.5. Benchmark Problem #3: Saucer landslide (Laboratory)

### Problem description

The laboratory experiments were performed in the University of Rhode Island (URI) wave tank, of width 3.6 m, length 30 m and depth 1.8 m. A plane aluminum slope of angle  $\vartheta = 15^\circ$  was built in the middle of the tank and the water depth was set to  $h_0 = 1.5$  m in all experiments (Figure F-8 and F-9).

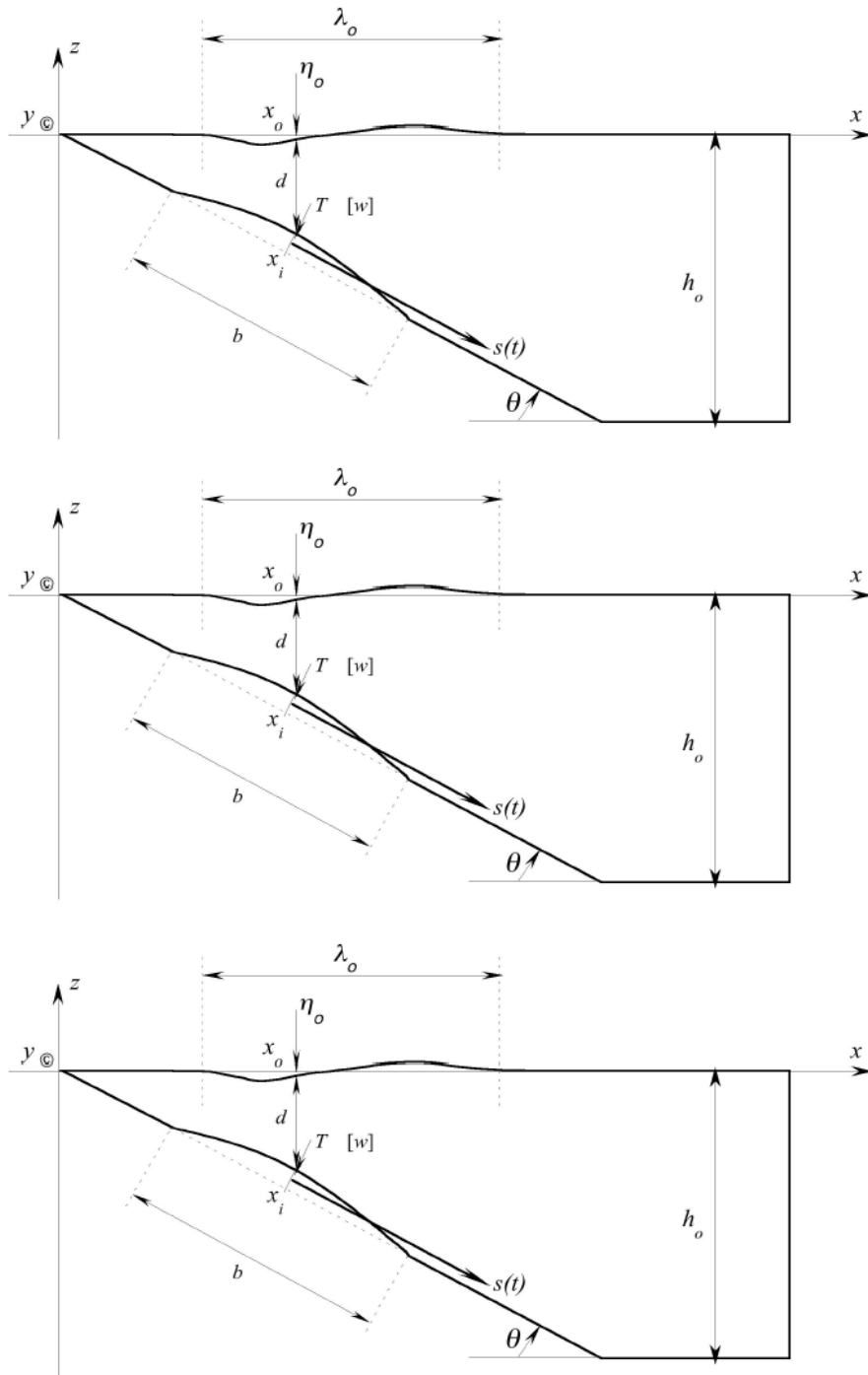
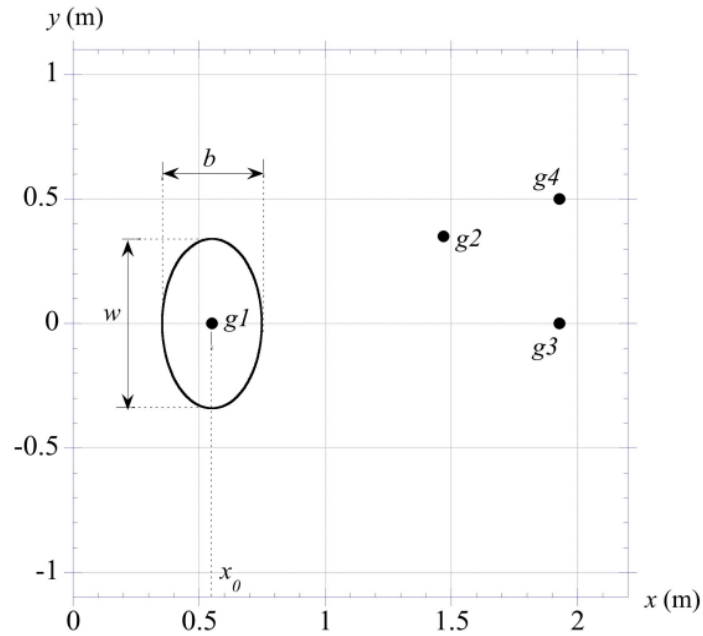
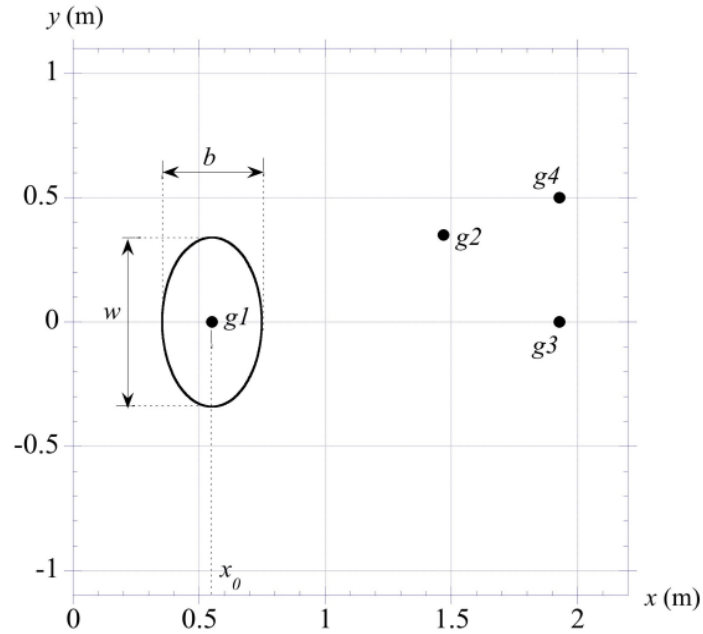


Figure F-8 Vertical cross section for underwater landslide experiments.

The data files were provided to us for each of the seven initial submergence depths ( $d = 61, 80, 100, 120, 140, 149, 189$  mm). All time series of surface elevation measured at up to the four gages ( $g1, g2, g3, g4$ ).



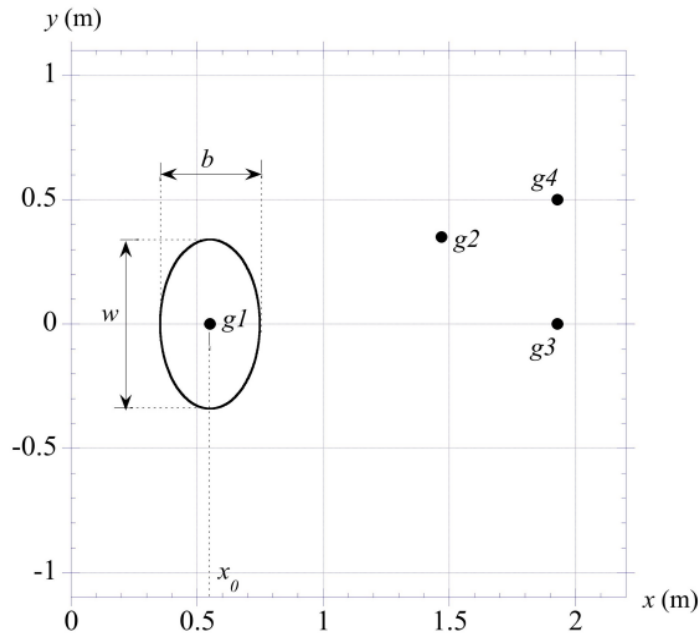


Figure F-9 Landslide and gage locations for case  $d = 61$  mm.

*Model setup*

The problem was solved using a fixed grid cell of 1 cm on the domain  $-1 \text{ m} \leq x \leq 8 \text{ m}$  and  $0 \text{ m} \leq y \leq 1.8 \text{ m}$ .

Solid wall boundary conditions were used at  $y = 0$  and  $y = 1.8 \text{ m}$ . At  $x = -1 \text{ m}$ , the boundary condition doesn't matter since the region is always dry, and at  $x = 8 \text{ m}$ , outflow boundary conditions were used. Zero-order extrapolation generally gives a very good approximation to non-reflecting boundary conditions.

*Results*

Simulated gauges were placed at the four locations that match wave tank measurements. The water surface elevation at each gauge was recorded. These results are presented in Figures F-10 through F-16 for the seven test cases.

The runup is measured at  $y = 0$ . The laboratory and numerical results are presented in Table F-1.

Table F- 1 Comparisons of maximum runup values in mm

d (mm)	61	80	100	120	140	149	189
Runup (exp)	6.2	5.7	4.4	3.4	2.3	2.7	2.0
Runup (num)	6.4	5.0	4.1	3.3	2.7	2.6	2.1



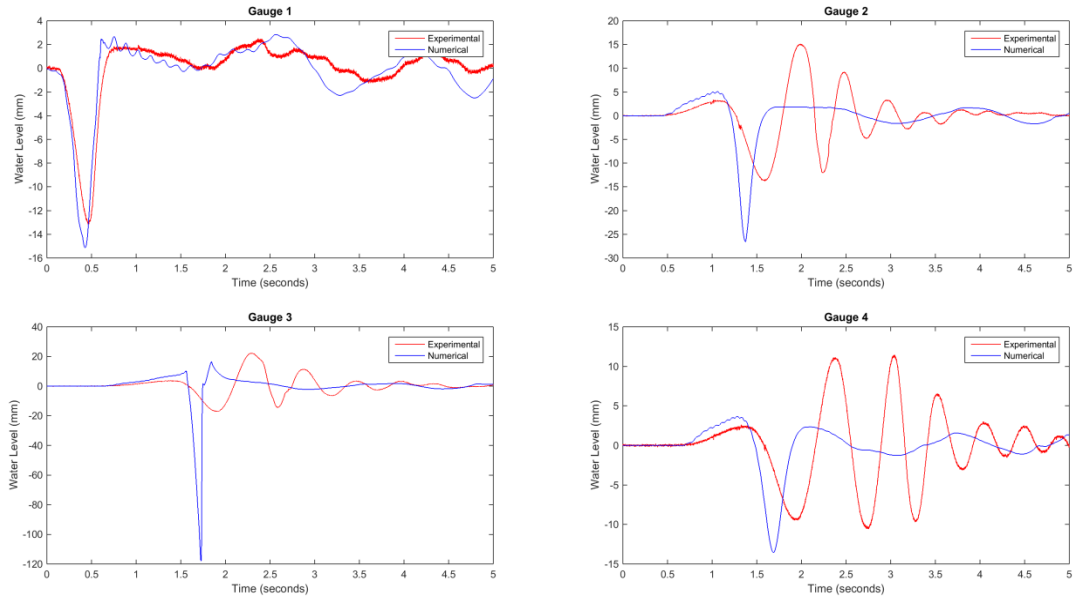


Figure F-10 Water level time series for gauges g1-g4 in for  $d = 61$  mm.

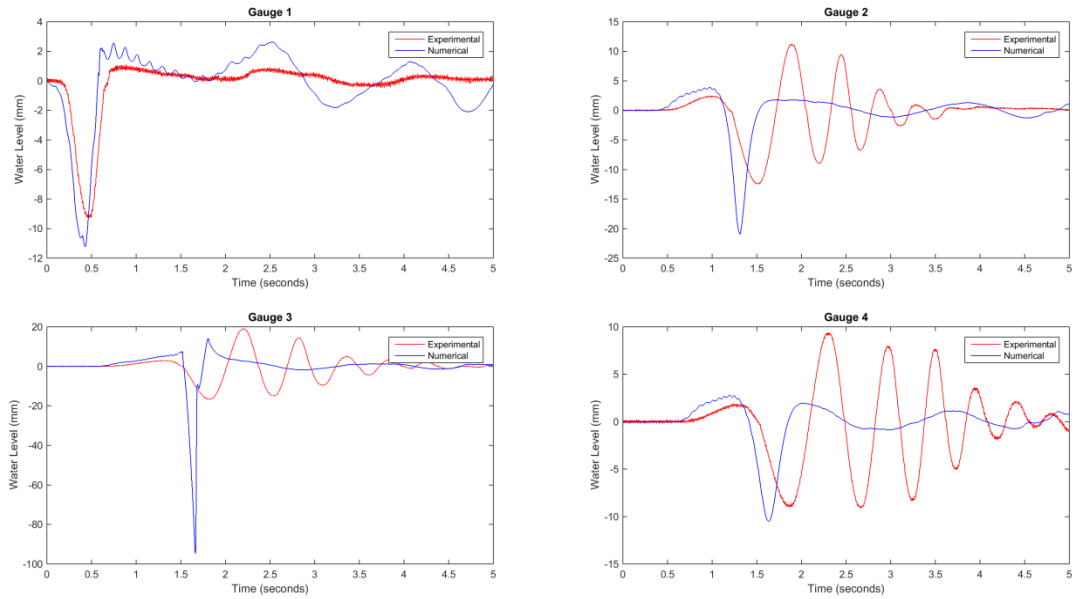


Figure F-11 Water level time series for gauges g1-g4 in for  $d = 80$  mm.

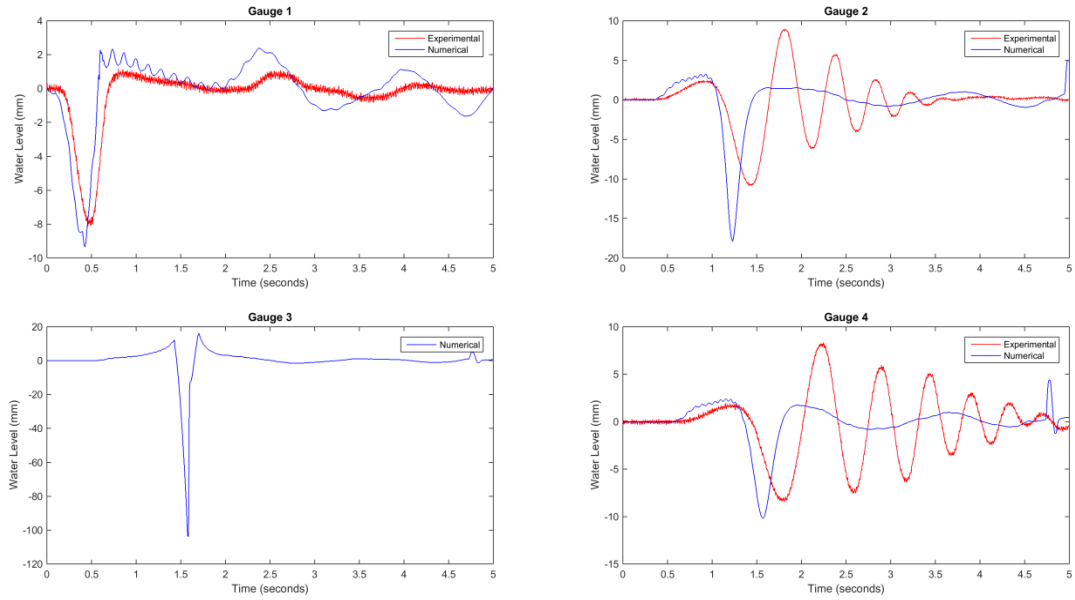


Figure F - 12 Water level time series for gauges g1-g4 in for d = 100 mm.

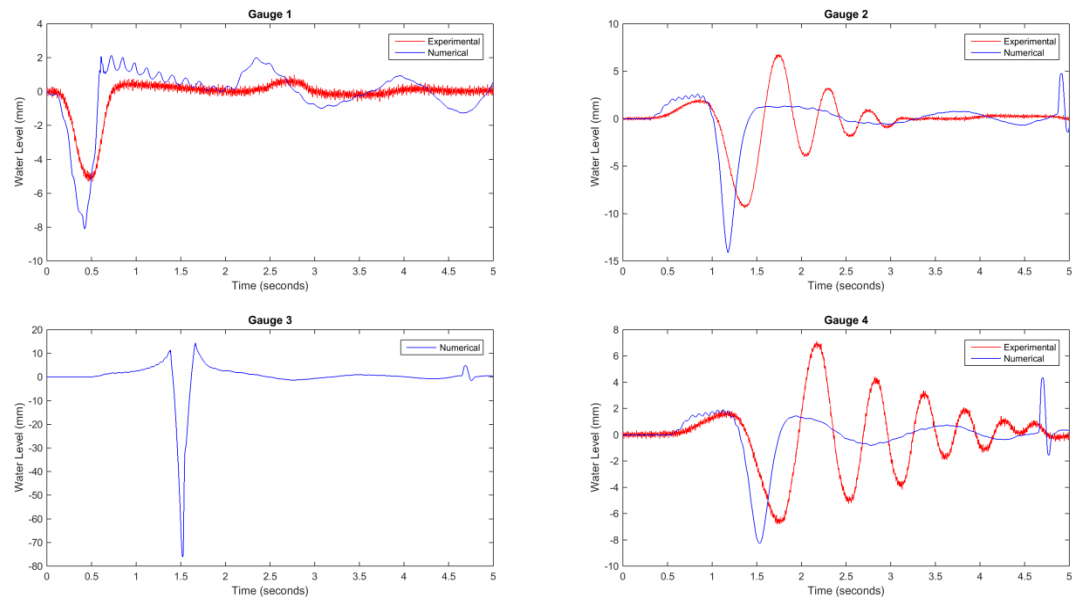


Figure F-13 Water level time series for gauges g1-g4 in for d = 120 mm.

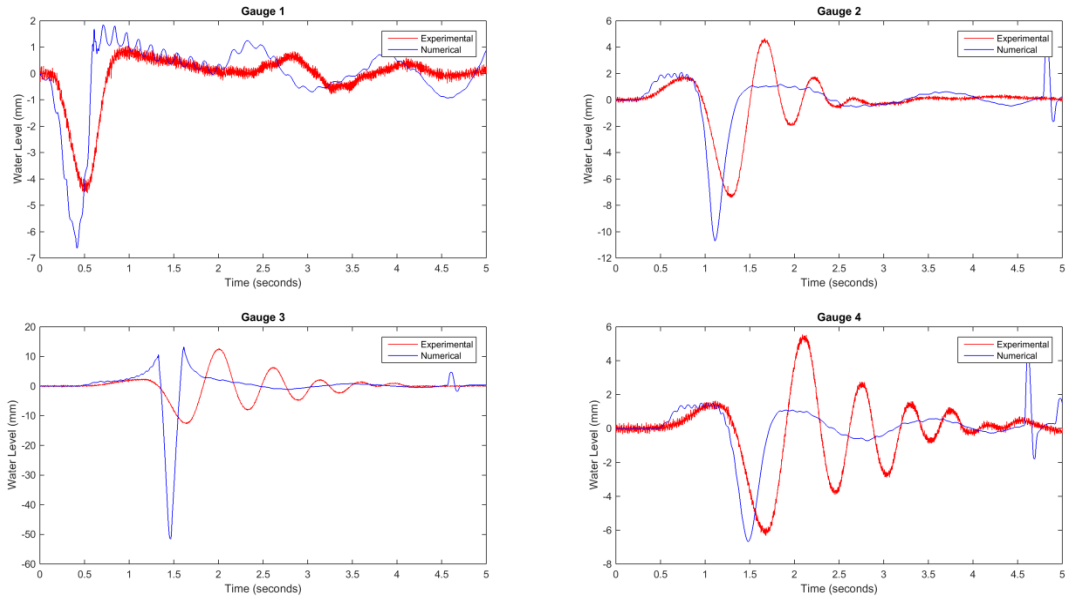


Figure F-14 Water level time series for gauges g1-g4 in for d = 140 mm.

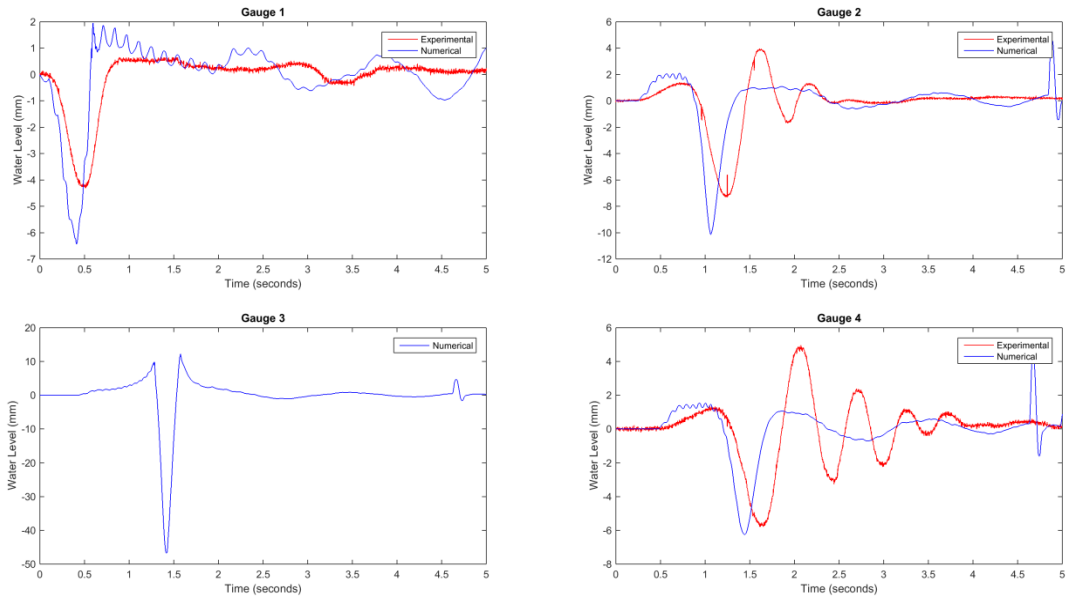


Figure F-15 Water level time series for gauges g1-g4 in for d = 149 mm.

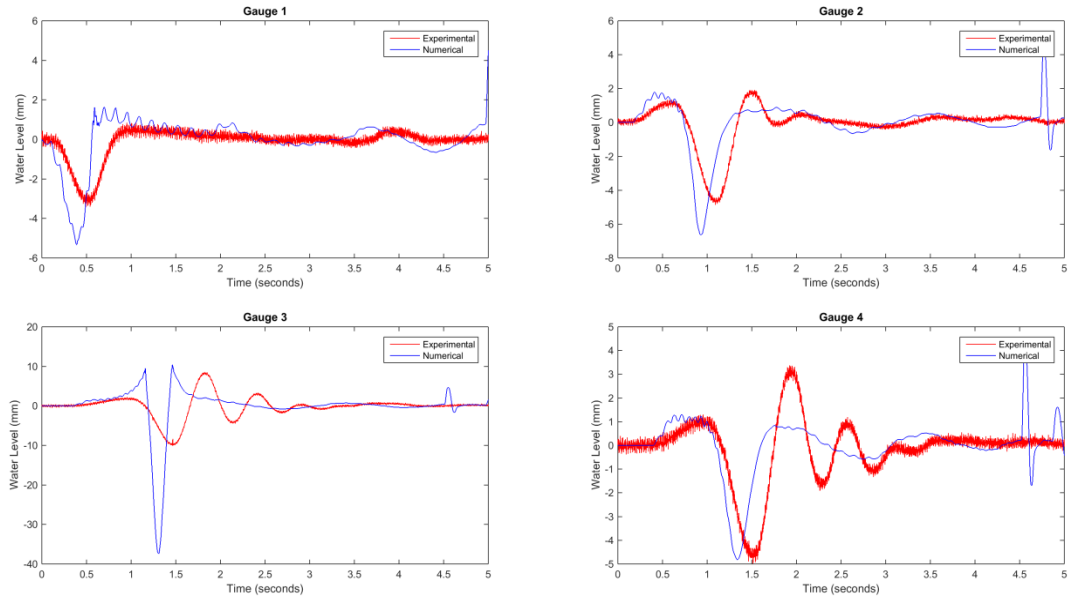


Figure F-16 Water level time series for gauges g1-g4 in for d = 189 mm.

**F.6. Benchmark Problem #4: Single wave on simple beach (Laboratory)**

*Problem description*

This benchmark is the laboratory counterpart to BP 1. In the experiments, a wave tank at the California Institute of Technology, Pasadena, California was used. The tank was 31.73 m long, 60.96 cm deep and 39.97 cm wide. The beach ramp was sealed to the tank side walls. The beach slope corresponded to angle  $\beta = \text{arccot}(19.85)$ . Figure F-17 shows the computational domain sketch.

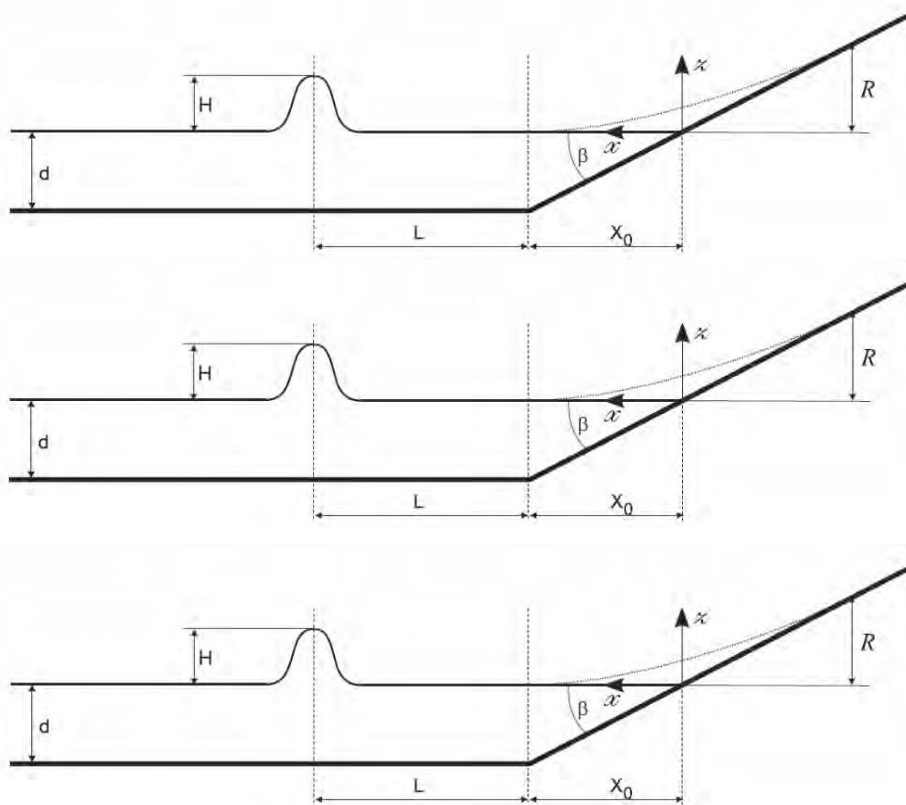


Figure F-17 Schematic of computational domain

*Model setup*

Used  $g = 9.81 \text{ m/s}^2$ ,  $d = 1 \text{ m}$  and no friction.

The grid cell size is 1 cm.

The CFL number used is 0.45.

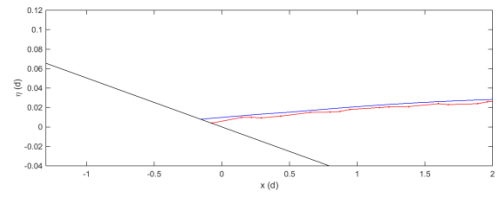
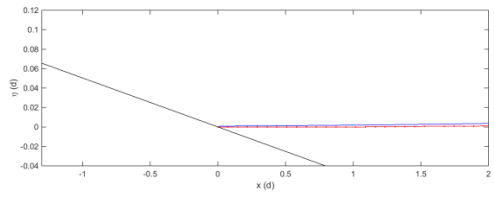
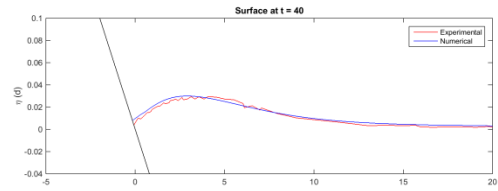
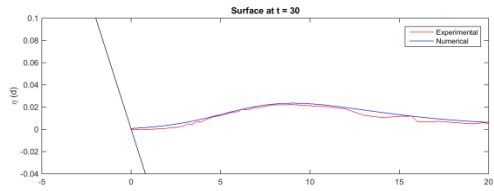
For  $H/d = 0.0185$ , the domain spanned from  $x = -66.08$  to 10 m.

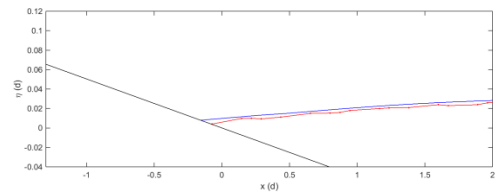
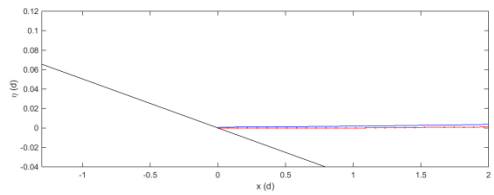
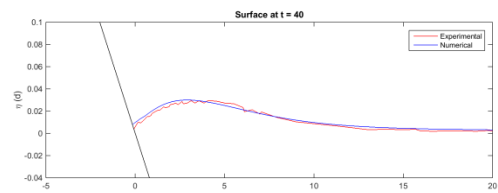
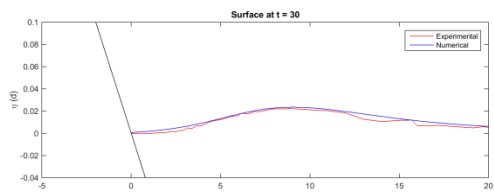
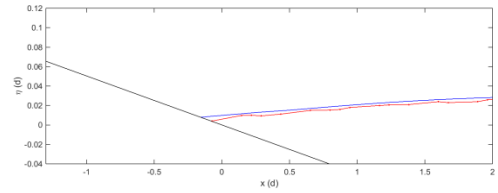
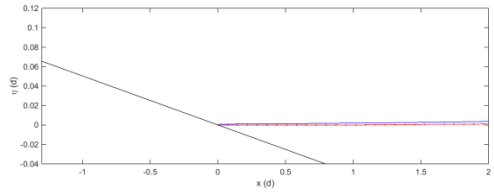
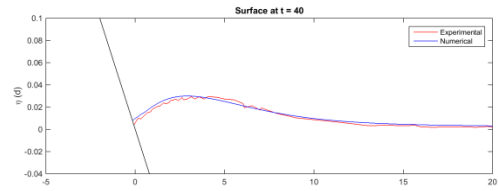
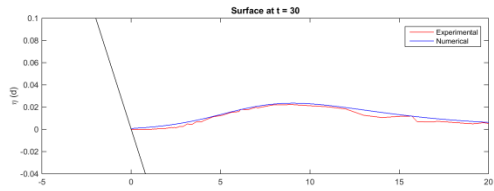
For  $H/d = 0.3$ , the domain spanned from  $x = -65$  to  $20$  m.

### *Results*

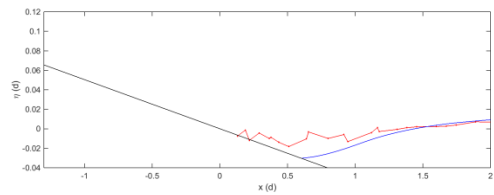
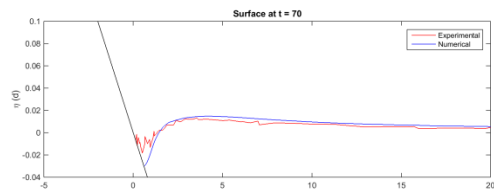
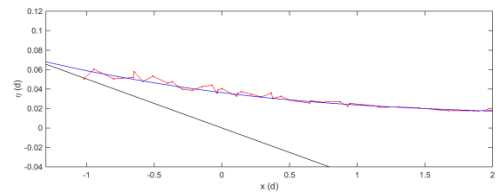
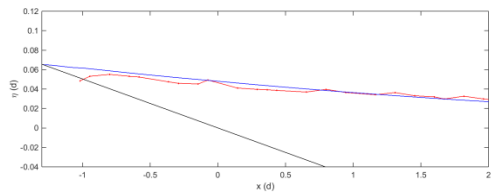
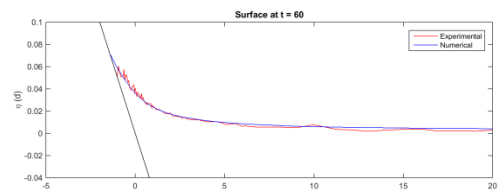
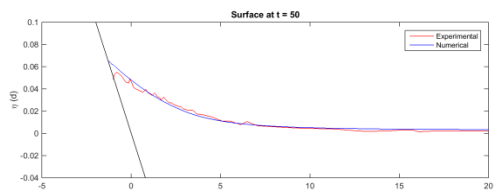
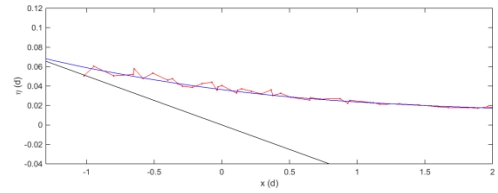
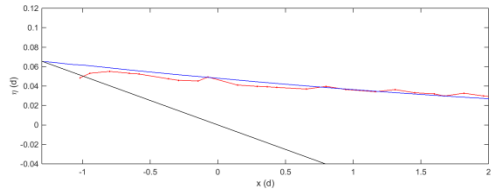
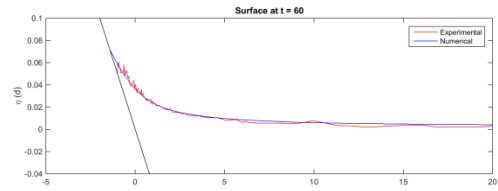
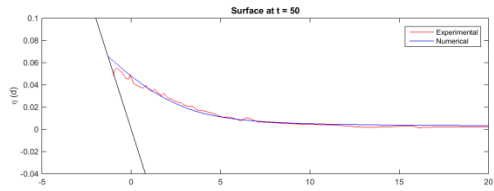
Figures F-18 and F-19 present the computed and measured surface profiles for the cases  $H/d = 0.0185$  and  $H/d = 0.3$ . Good agreement is shown in the low amplitude case. In the high amplitude case, the computed amplitude is smaller and the steepness is greater than that of the measured wave, because the experimental parameters violate the shallow water wave assumptions.

Figure F-20 shows the maximum runup for the low amplitude and high amplitude cases. The low amplitude result matches well with the results of Zhan (2011) while the high amplitude result is higher than the measurements.









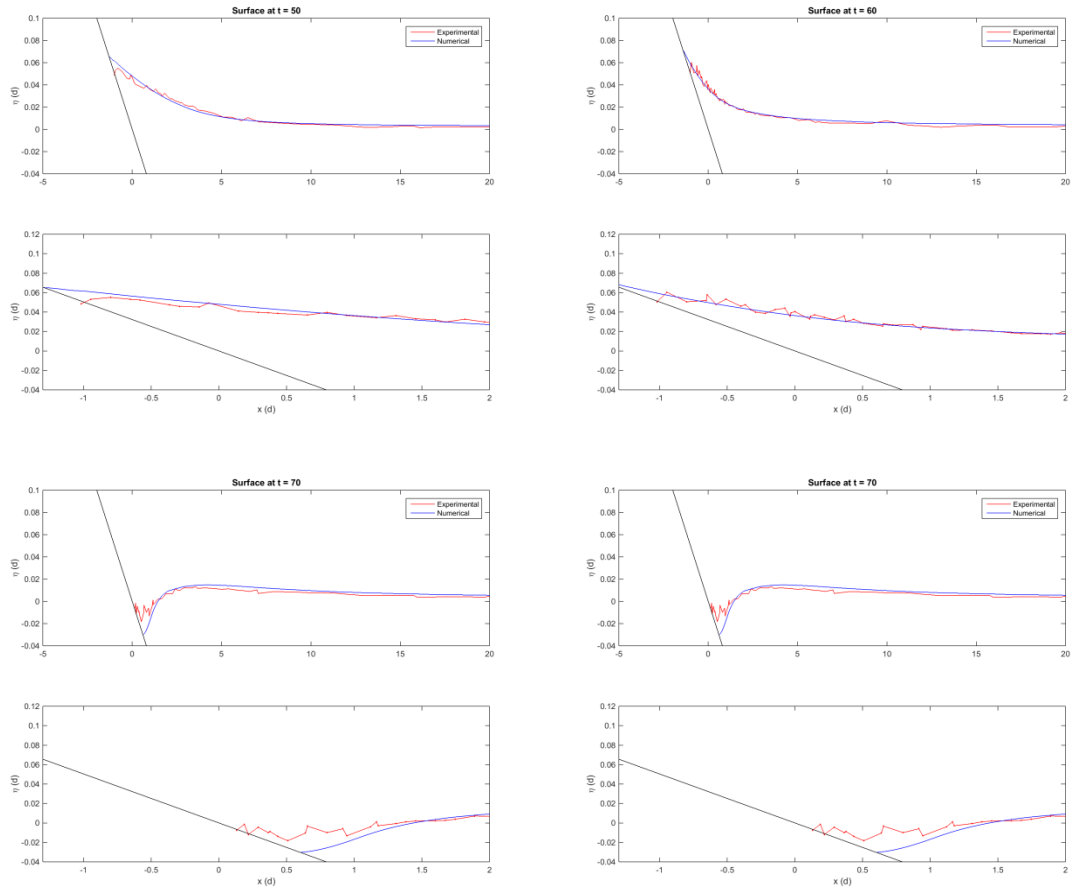


Figure F-18 Computed and measured surface profiles for  $H/d = 0.0185$ . The bottom frame provides a zoomed view of the inundation area.



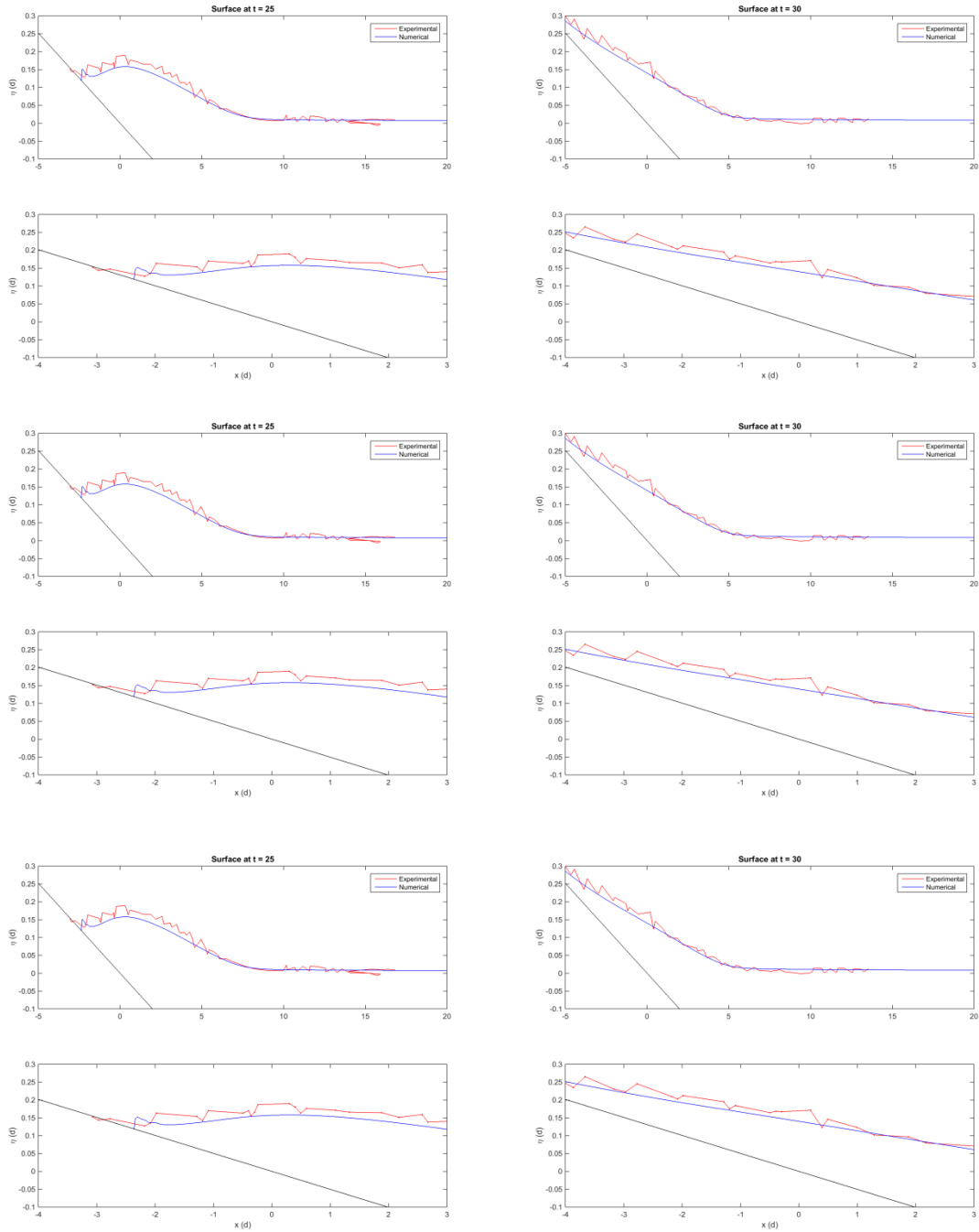


Figure F-19 Computed and measured surface profiles for  $H/d = 0.3$ . The bottom frame provides a zoomed view of the inundation area.

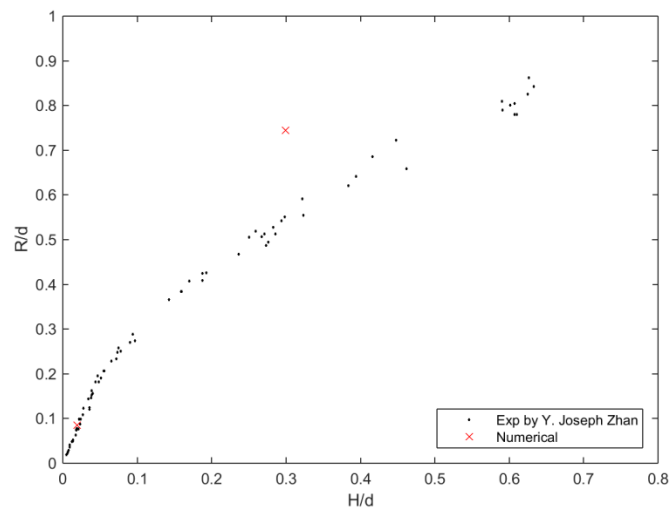
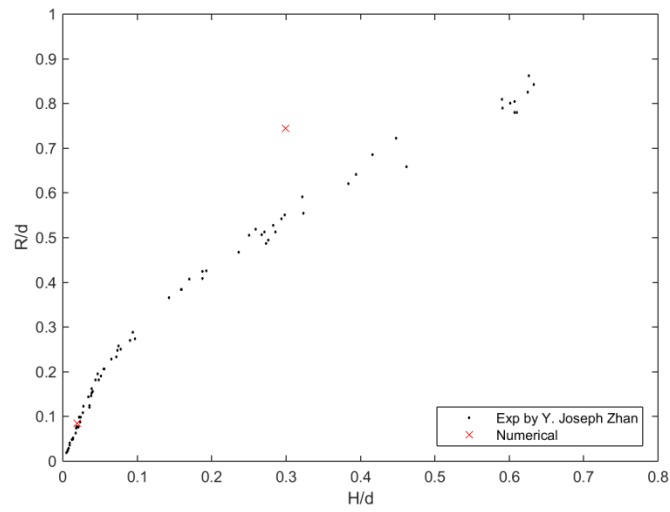
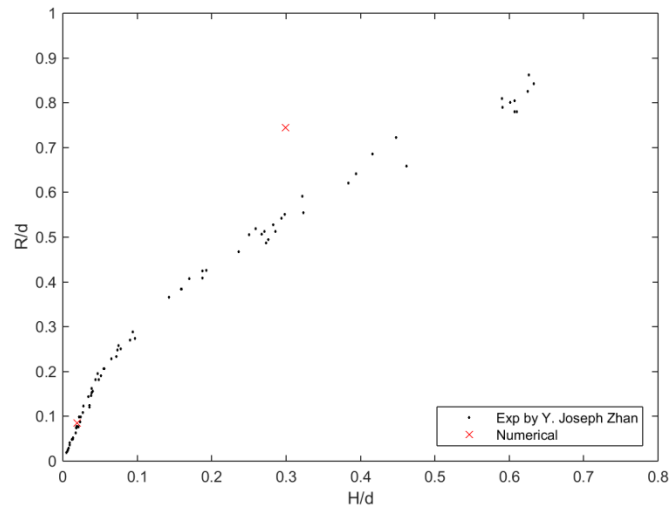


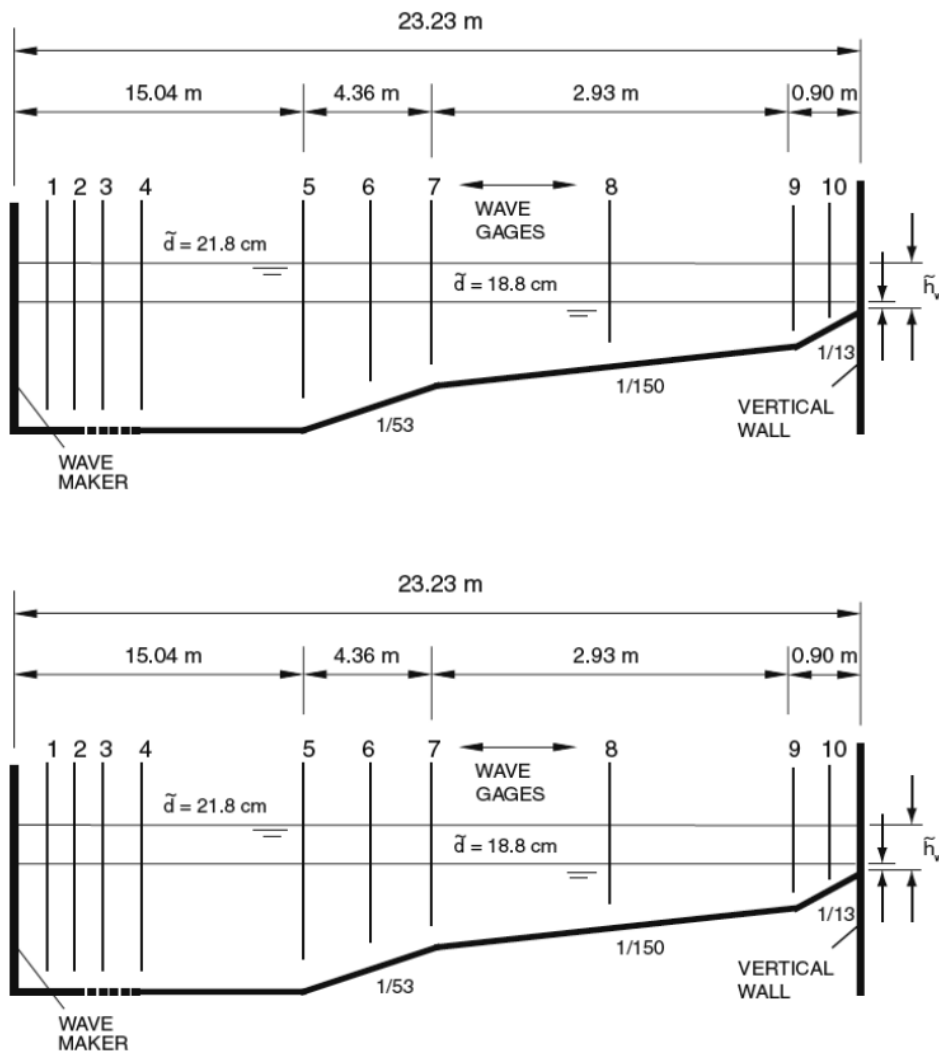
Figure F-20 Non-dimensional maximum runup versus non-dimensional wave height.

**F.7. Benchmark Problem #5: Solitary wave on composite beach (Laboratory)**

*Problem description*

The basin for the experiment was a long narrow flume with reflecting side walls (glass), shown in Figure F-21. The objective of this benchmark is to model the experiment, compute time histories at the gages 4-10 and maximum runup on the wall, and compare the results with the measurements.

This is the similar problem as in BP 2, but using the nonlinear shallow water equations and comparing to laboratory data rather than to the analytic solution of linear equations.



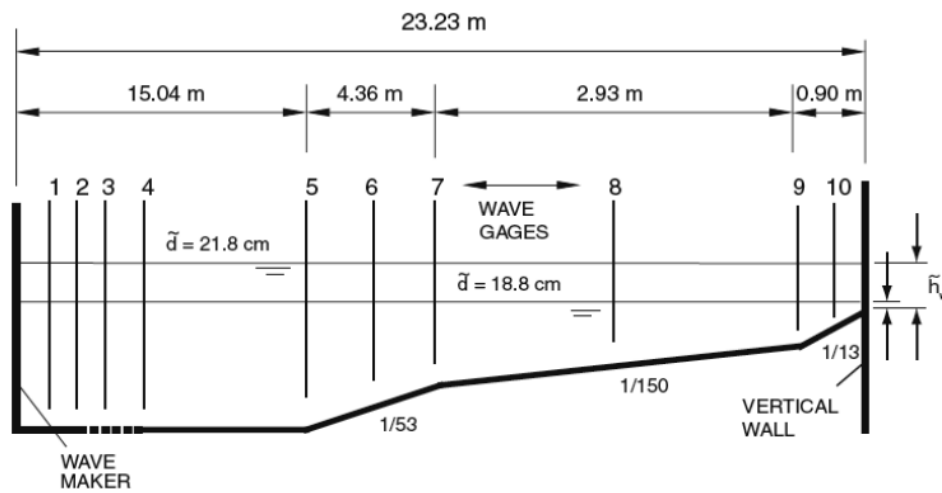


Figure F-21 Sketch of the flume with the gage locations.

*Model setup*

Used  $g = 9.81 \text{ m/s}^2$  and no friction in Cartesian coordinates.

The tank size is

10.6 m  $\times$  0.05 m for Case A

9.17 m  $\times$  0.05 m for Case B

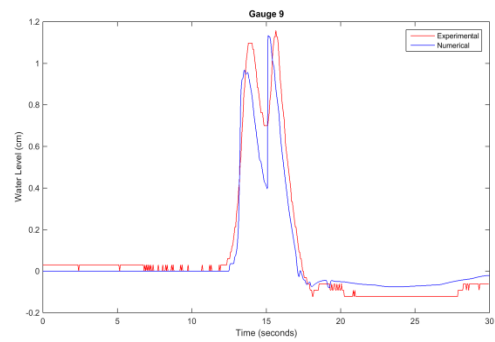
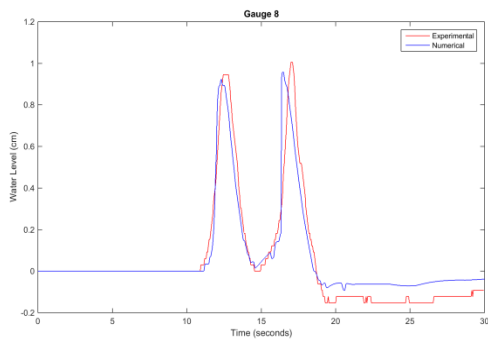
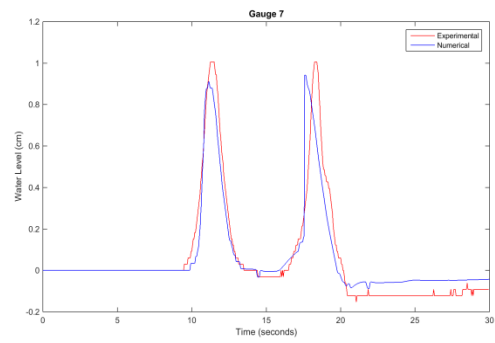
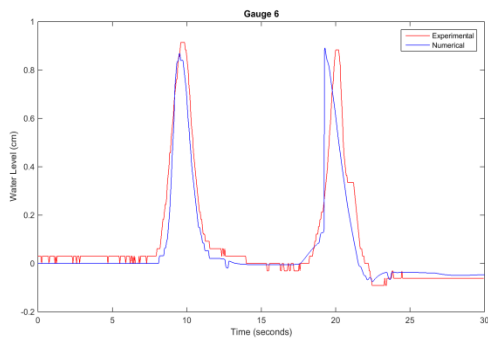
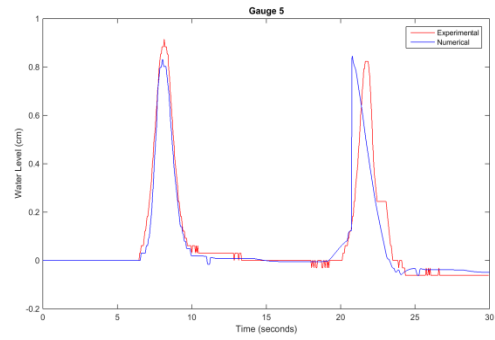
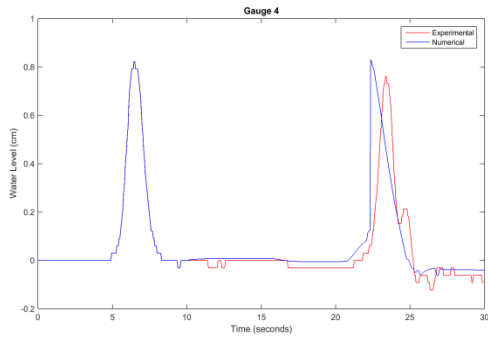
8.83 m  $\times$  0.05 m for Case C

The grid cell size is 1 cm.

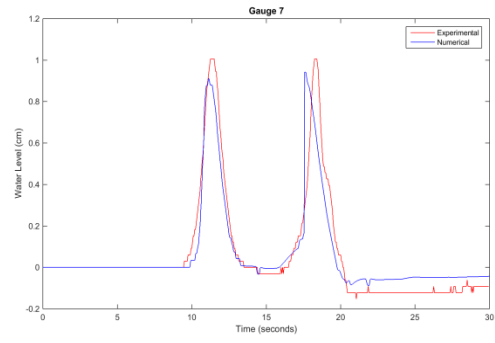
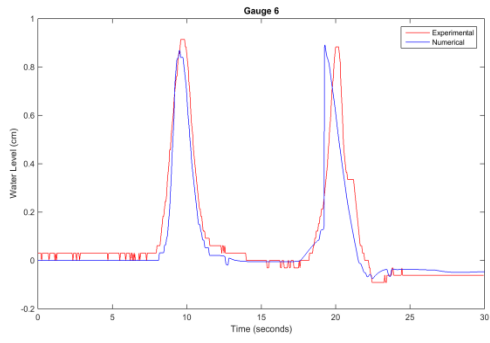
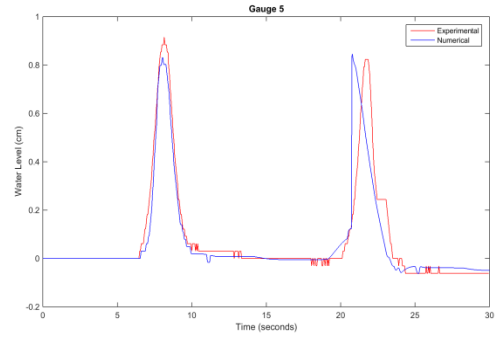
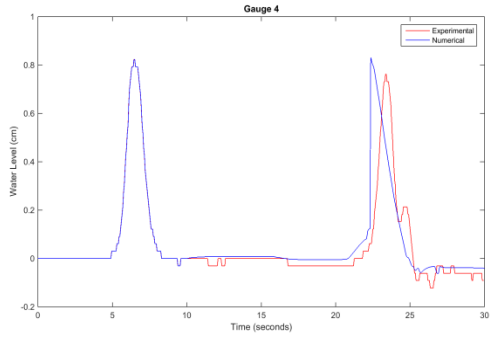
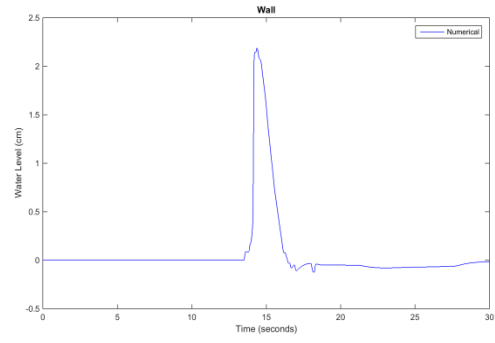
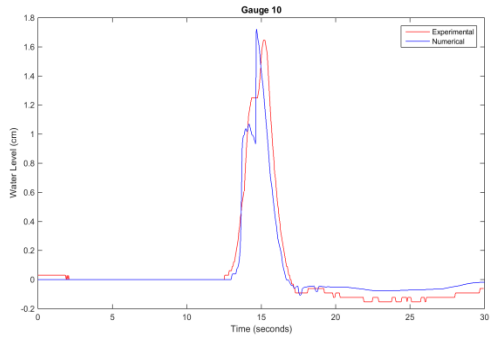
To specify the incoming wave from the left boundary of the computational domain, the first ten seconds of measurements taken at Gage 4 were used. After ten seconds the left boundary switched to be a non-reflecting boundary.

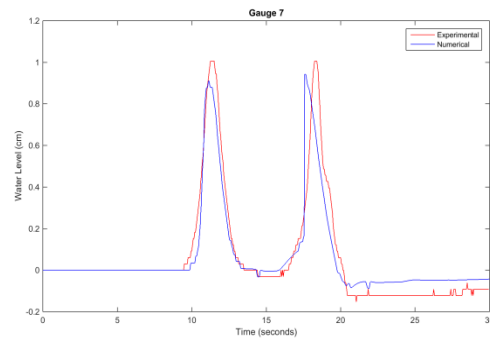
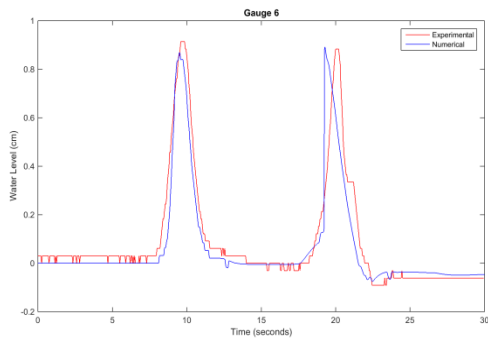
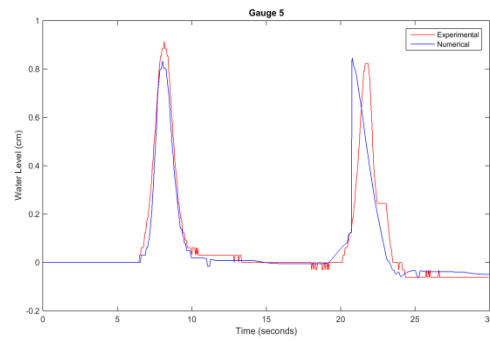
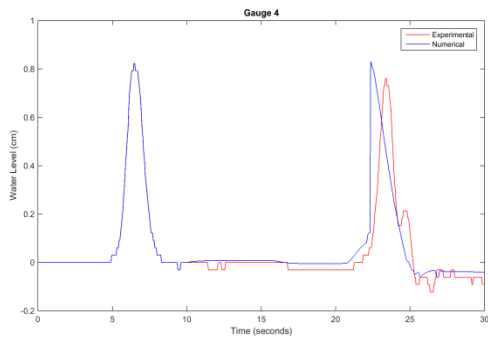
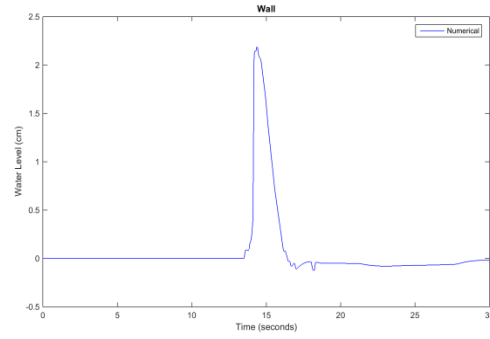
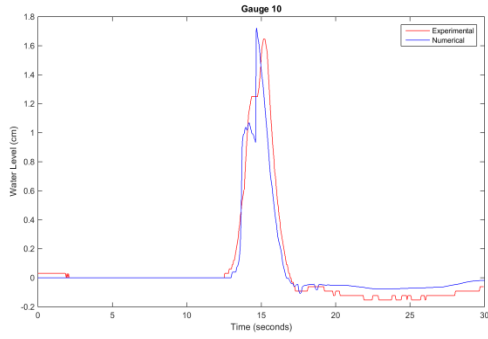
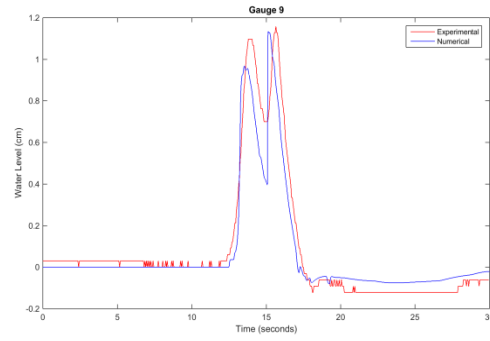
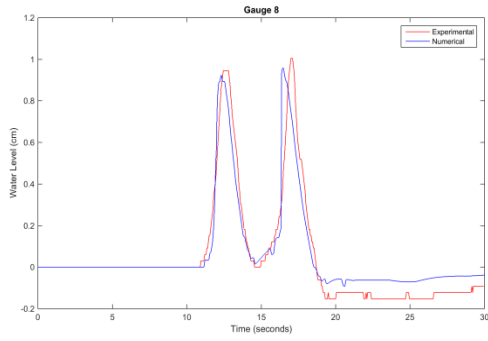
*Results*

Figure F-23 presents the time histories at gages 4-10 and at the wall for Cases A, B and C. Cases B and C exhibit dispersion in the experimental results which is not seen with the nonlinear shallow water equations.









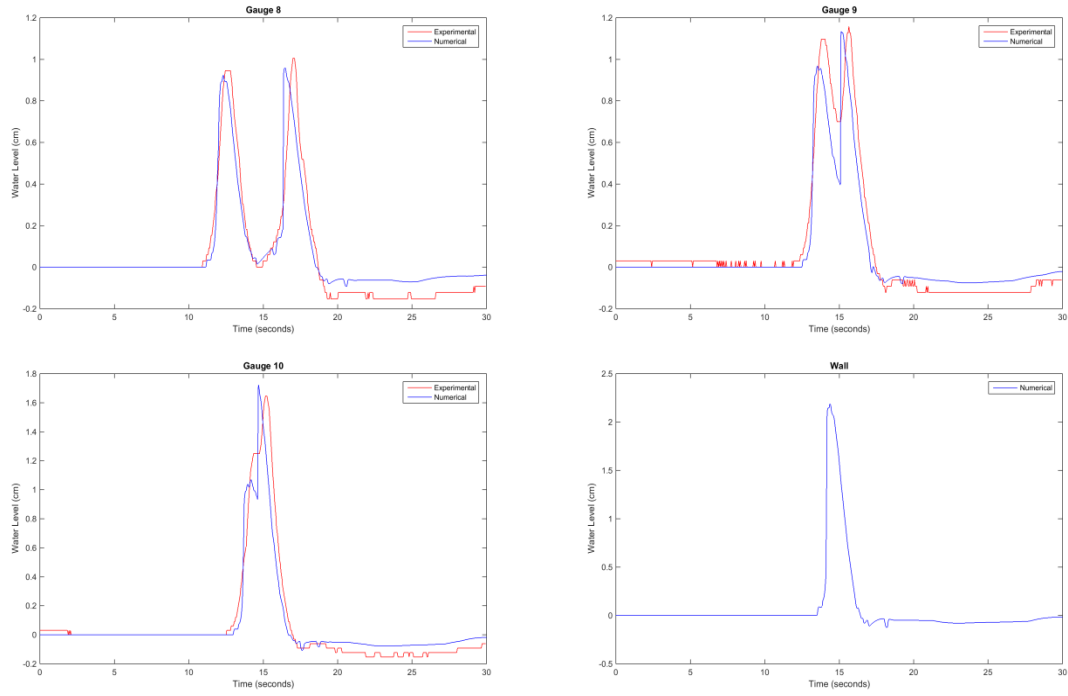
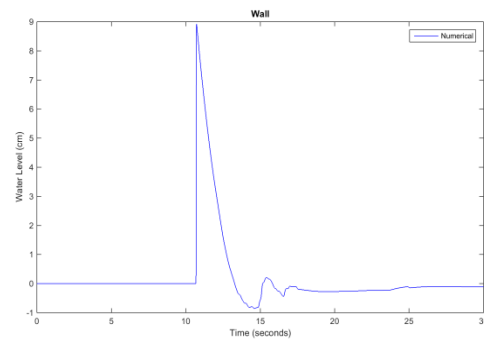
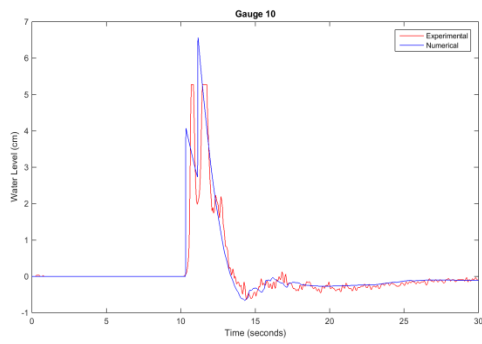
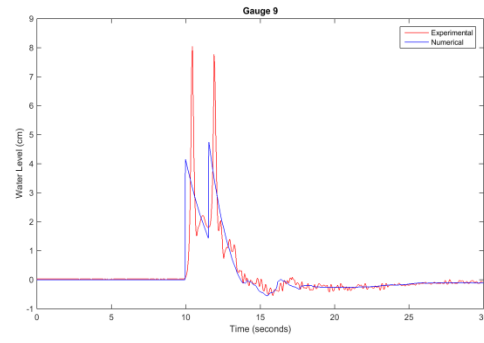
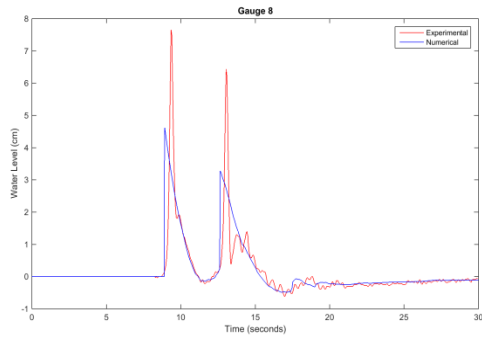
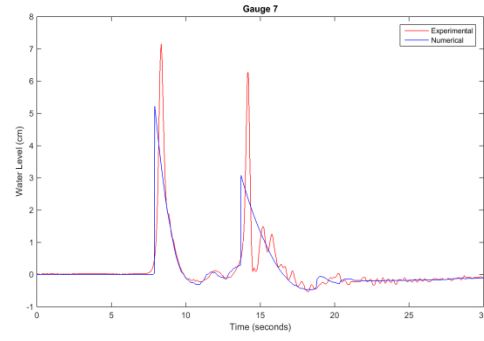
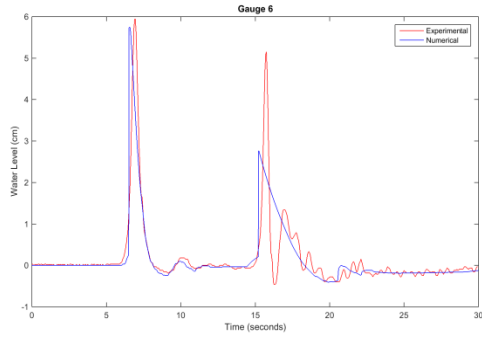
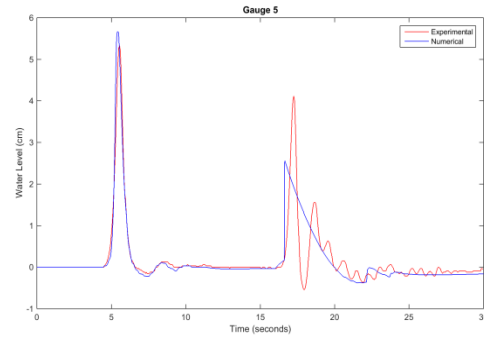
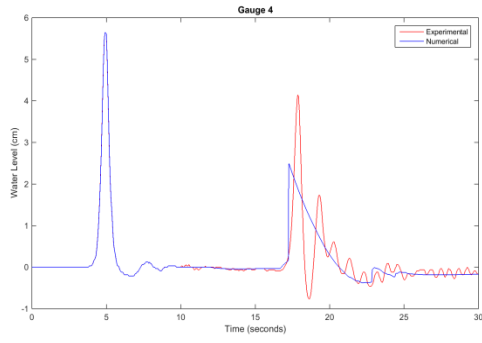
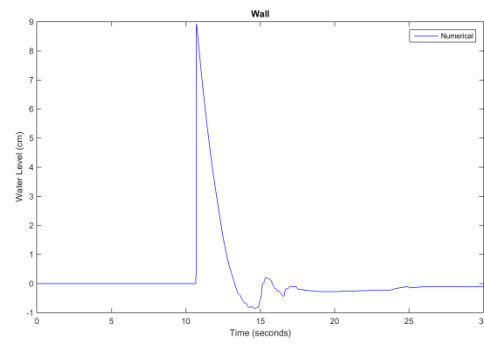
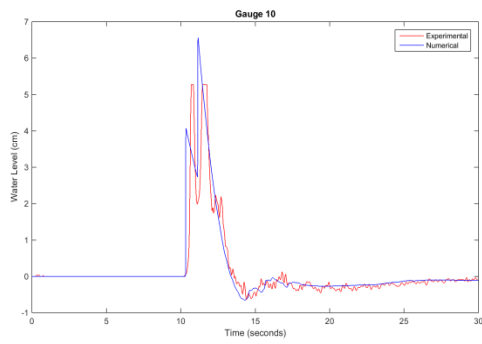
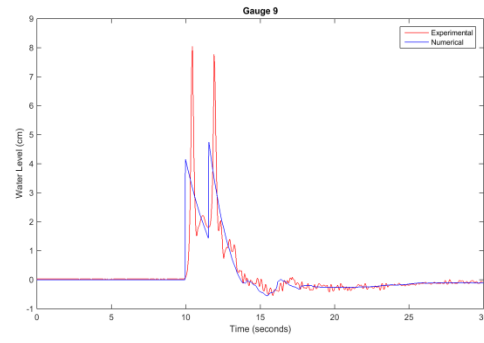
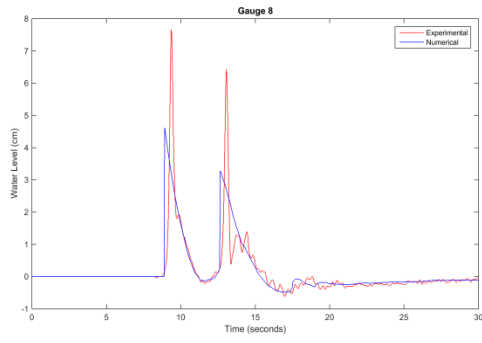
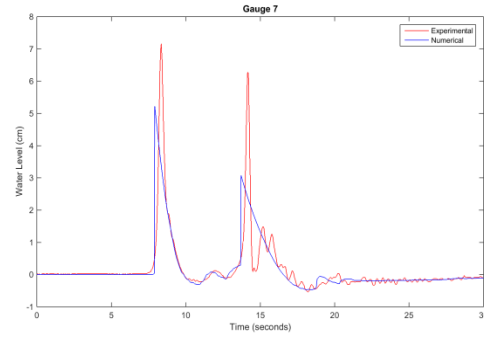
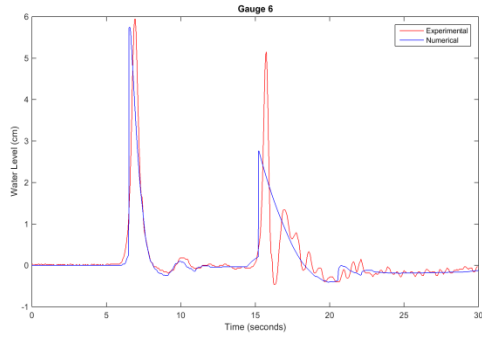
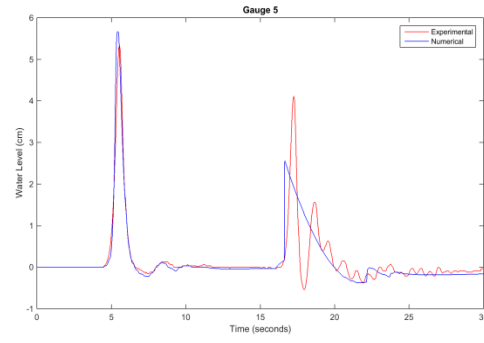
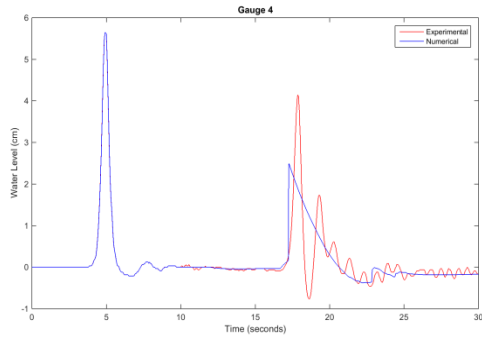


Figure F -22 Time histories for Case A.





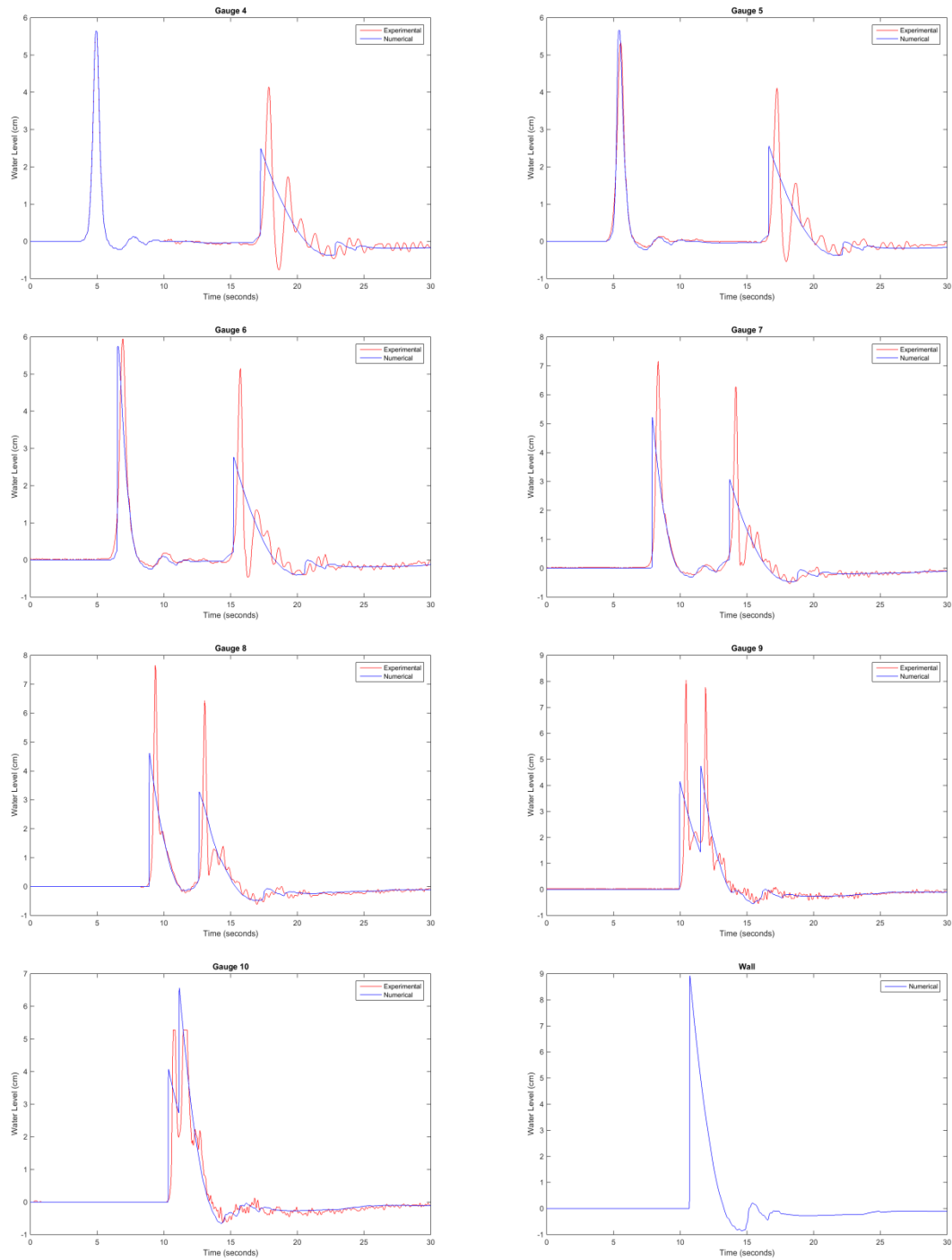
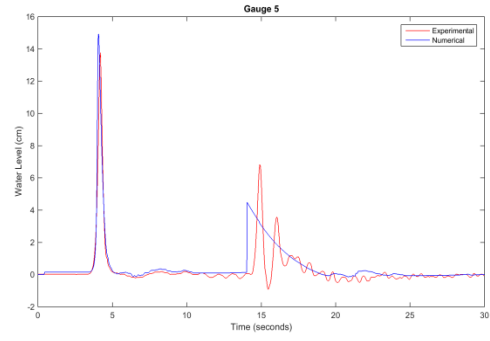
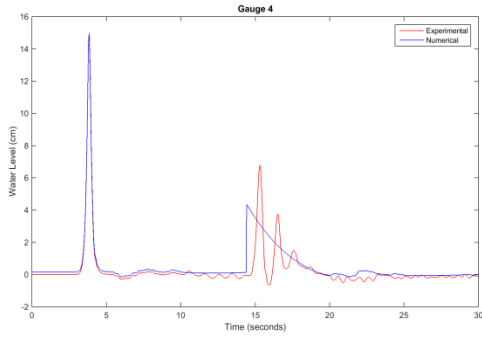
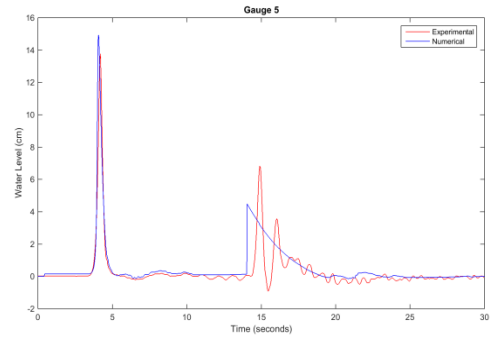
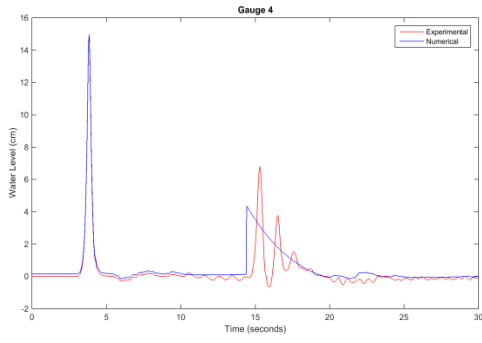
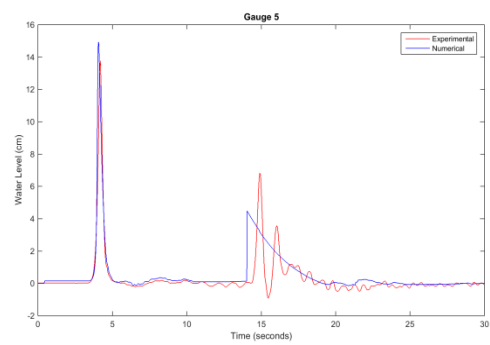
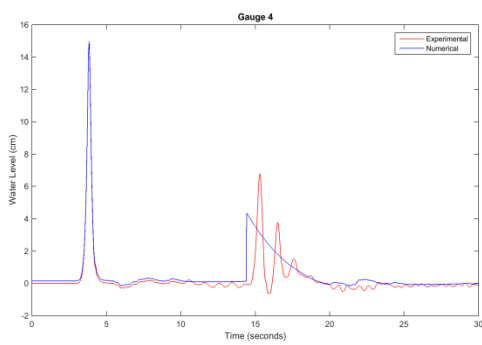
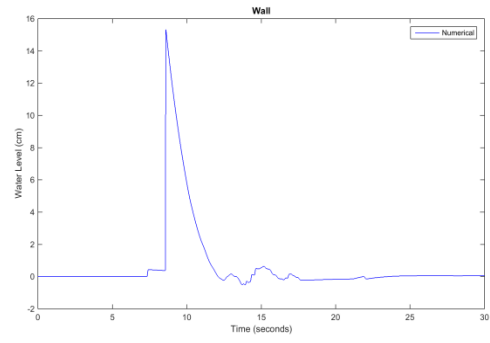
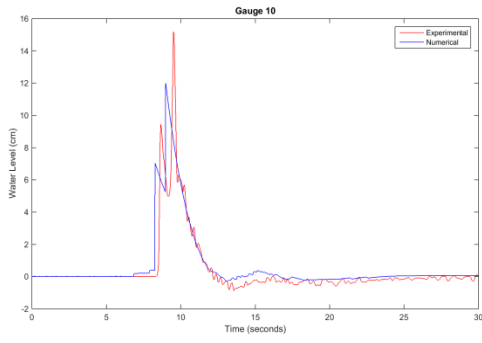
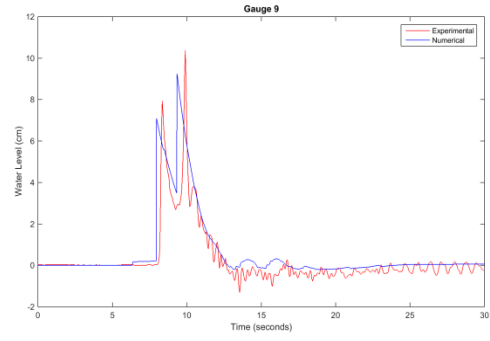
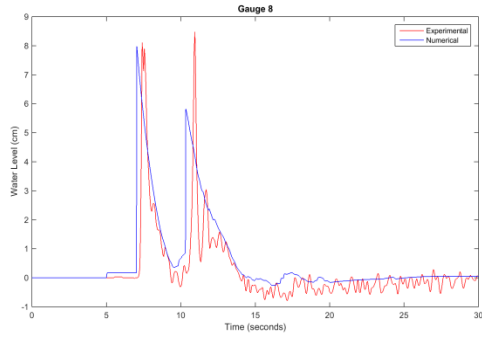
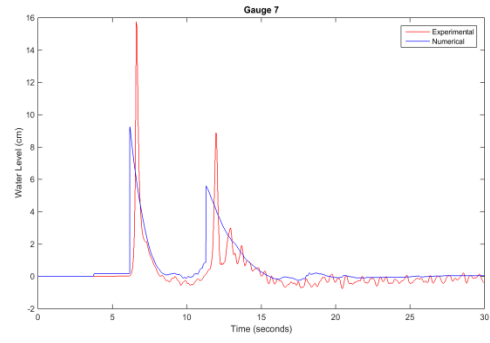
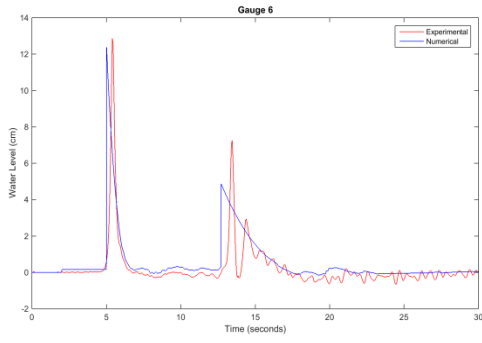
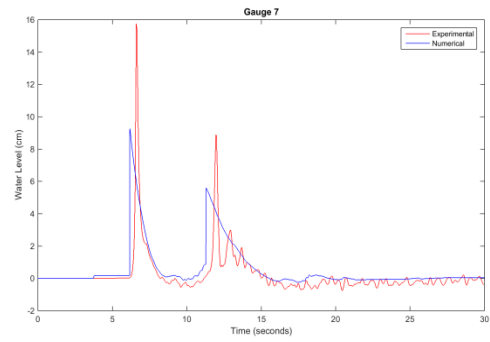
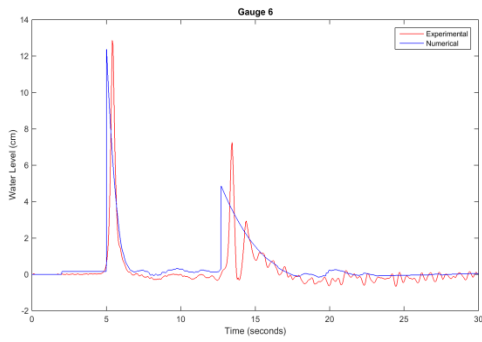
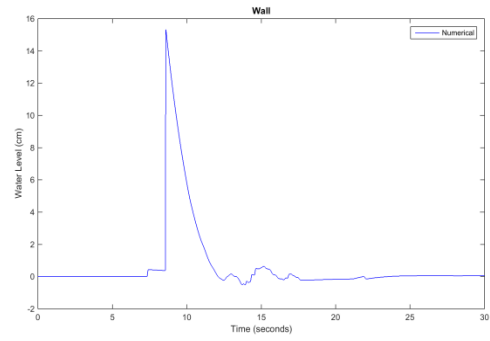
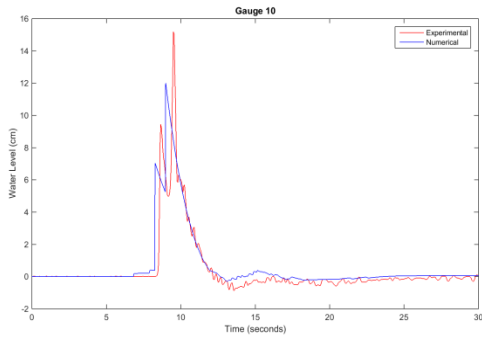
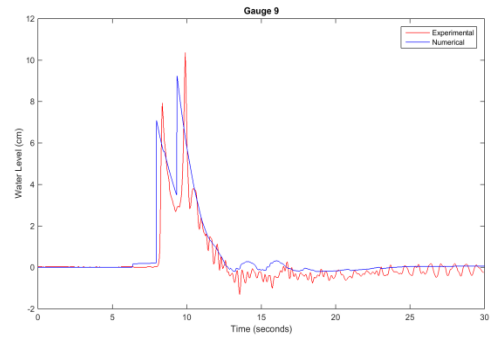
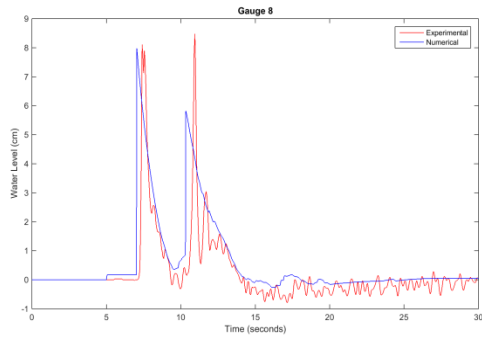
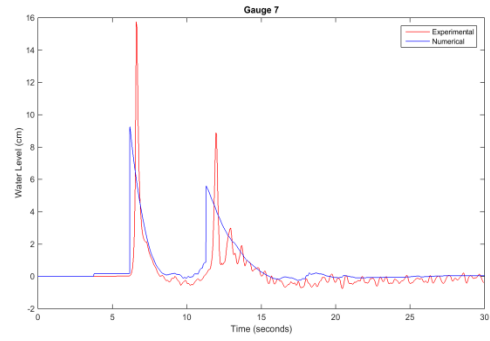
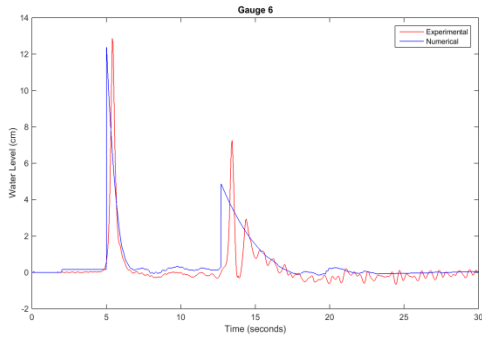


Figure F- 23 Time histories for Case B.









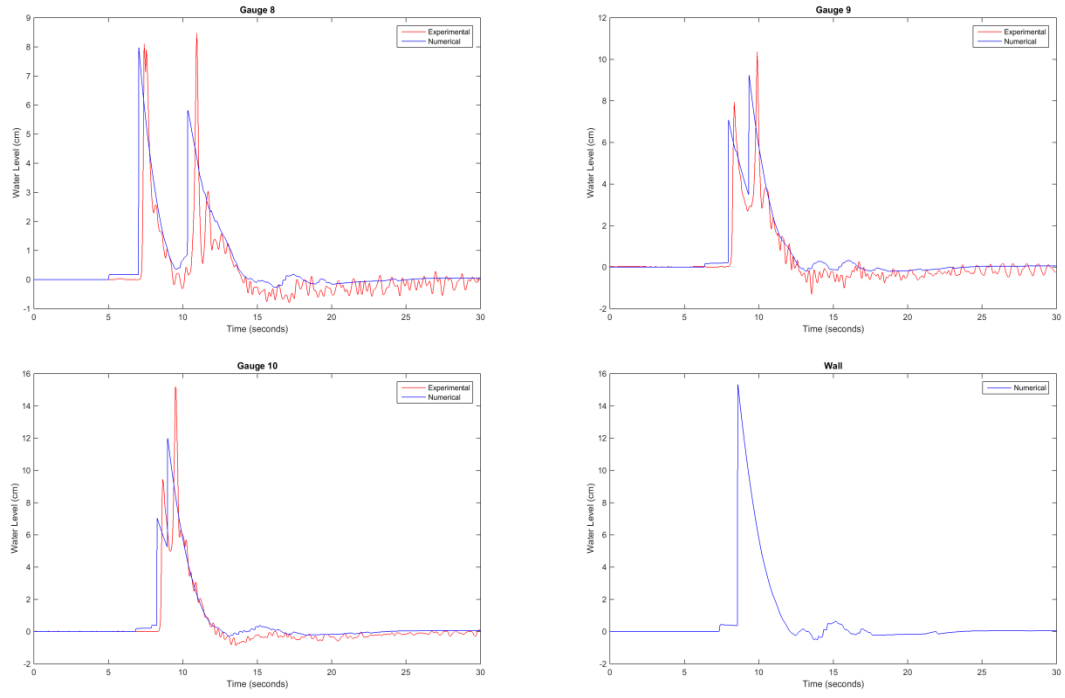
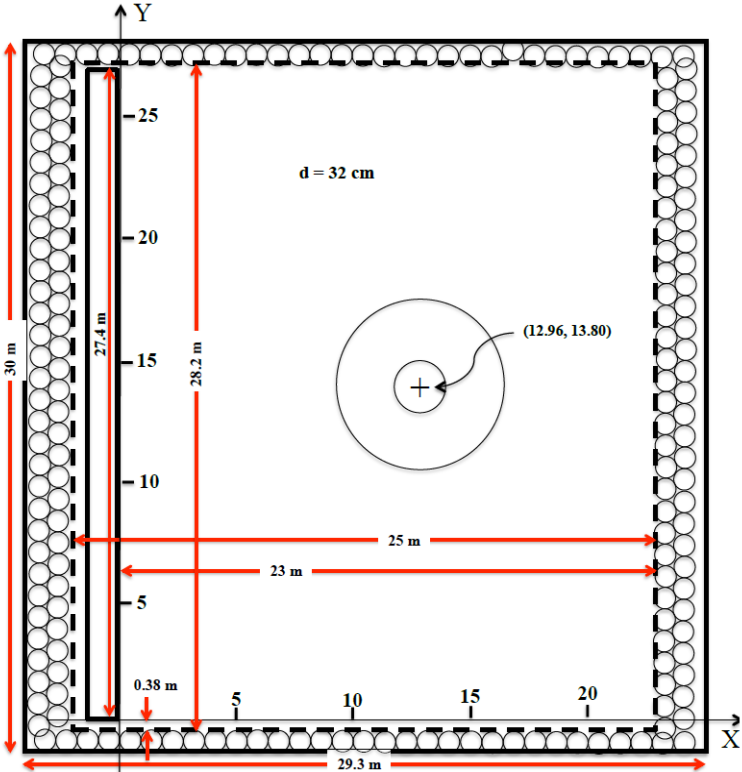
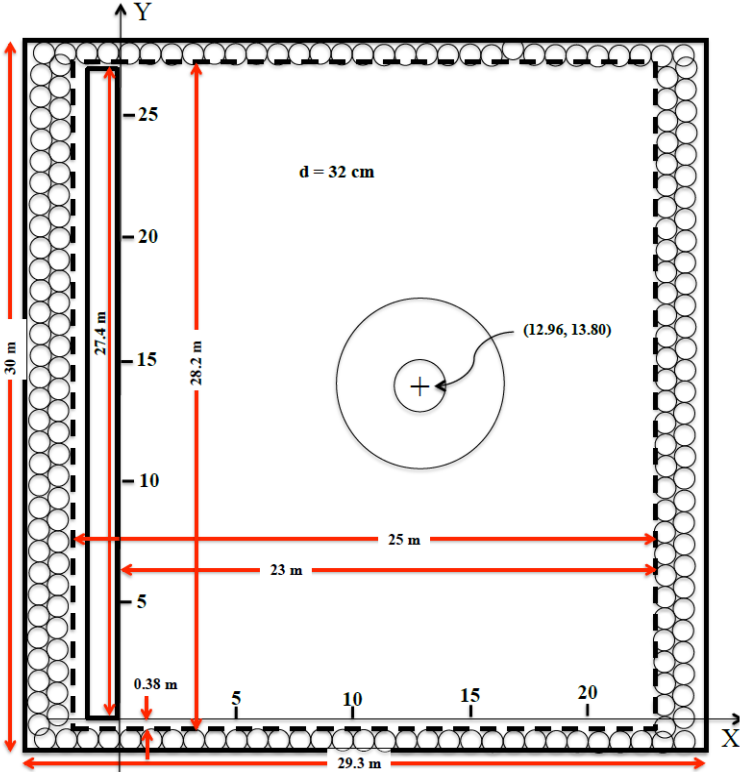


Figure F-24 Time histories for Case C.

**F.8. Benchmark Problem #6: Solitary wave on a conical island (Laboratory)***Problem description*

The goal of this benchmark is to compare computed model results with laboratory measurements obtained during a physical modeling experiment conducted at the Coastal and Hydraulic Laboratory, Engineer Research and Development Center of the U.S. Army Corps of Engineers. The laboratory physical model was constructed as an idealized representation of Babi Island in the Flores Sea, Indonesia, to compare with Babi Island runup measured shortly after the 12 December 1992 Flores Island tsunami (Yeh et al., 1993).



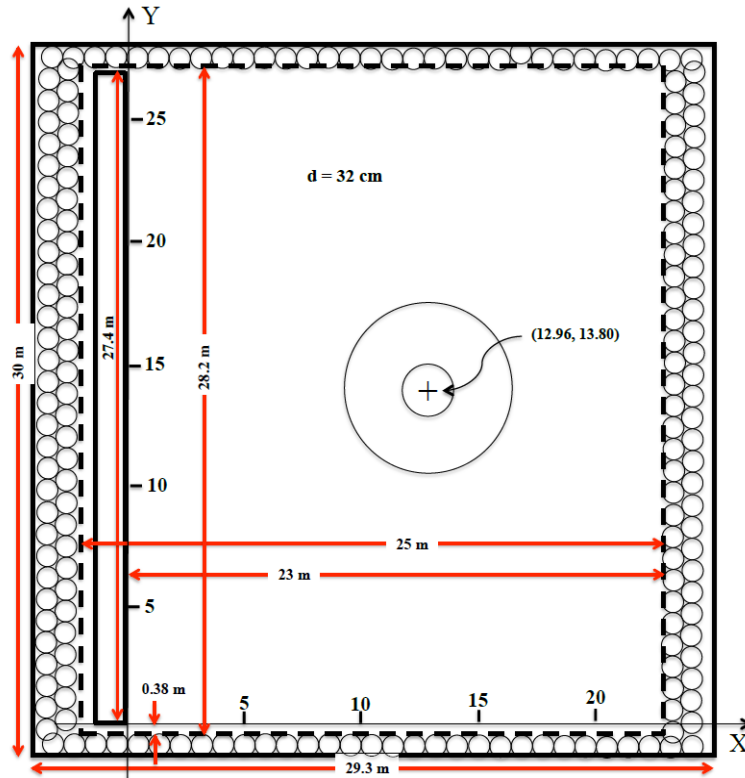


Figure F-25 Basin geometry and coordinate system. Solid lines represent approximate basin and wavemaker surfaces. Circles along walls and dashed lines represent wave absorbing material. Note the gaps of approximately 0.38 m between each end of the wavemaker and the adjacent wall. Gage positions are given in Table F - 2.

**Table F-2 Laboratory Gage positions.**

Gage ID	X, m	Y, m	Z, cm	Comment
1	A: 5.76 B: 6.82 C: 7.56	16.05	32.0	Incident gage
2		14.55	32.0	
3		13.05	32.0	
4		11.55	32.0	
6	9.36	13.80	31.7	270 deg transect
9	10.36	13.80	8.2	
16	12.96	11.22	7.9	0 deg transect
22	15.56	13.80	8.3	90 deg transect

*Model setup*

Used  $g = 9.81 \text{ m/s}^2$ .

Used two varying model parameters – the Manning’s coefficient of friction ( $n = 0.015$  and  $0.025$ ) and the “dry cell depth” ( $d = 1 \text{ mm}$  and  $3 \text{ mm}$ ).

The computational domain is presented in Figure 25 ( $x: 0 - 23$ ;  $y: -0.38 - 27.83$ ).

Open boundary conditions were used for the top, bottom and right wall, and for the gaps between the ends of the wave-maker and the top and bottom walls (Figure F-25). The inflow boundary conditions were used for the face of the wave-maker.

Two levels of refinement were used in the model with the computational grid resolutions of 10 cm and 2.5 cm (around the island).

*Results*

Figure F-26 to Figure F-28 present the comparisons of computed water level with laboratory data for Cases A, B and C at gauges 1, 2, 3, 4, 6, 9, 16, and 22 (Manning’s friction coefficient  $n = 0.015$  and dry cell depth  $d = 3 \text{ mm}$ ). The agreement between computed and measured time series is good overall, in particular, for the first wave. Worse agreement is seen for later wave details as multiple reflections and refractions occur at the boundaries.

The comparisons of island runup for Cases A, B and C are shown in Figure F-29 to F-31. Good agreement is seen between the computed and measured runup on the conical island. We see that the computed runup values can be significantly affected by changes in the value of Manning’s friction coefficient and dry cell depth. The case ( $n = 0.015$ ,  $d = 3 \text{ mm}$ ) provides the best fit for runup values.

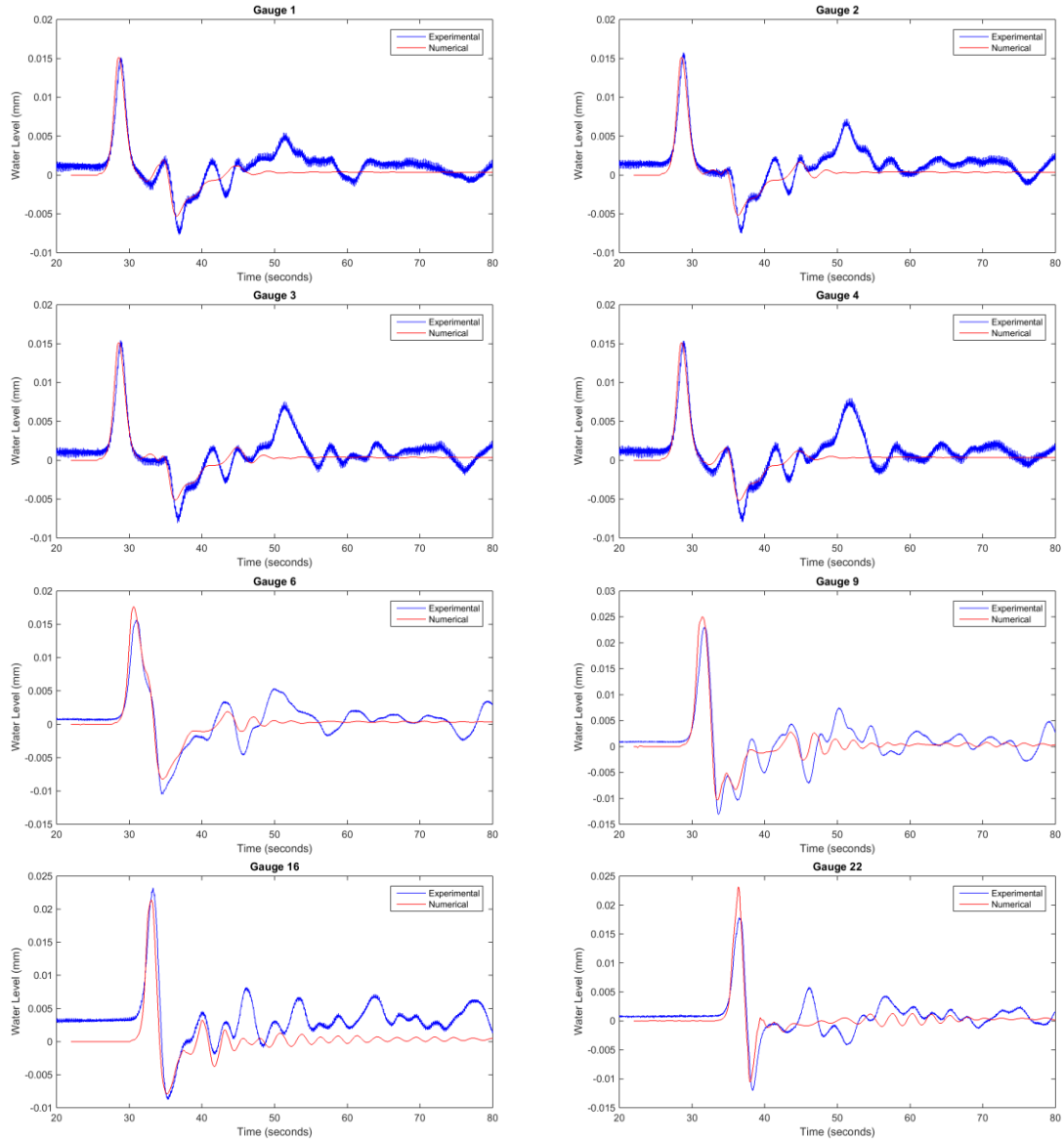


Figure F-26 Comparison of computed and measured time series at 8 gauges for Case A ( $n = 0.015$ ,  $d = 3$  mm).

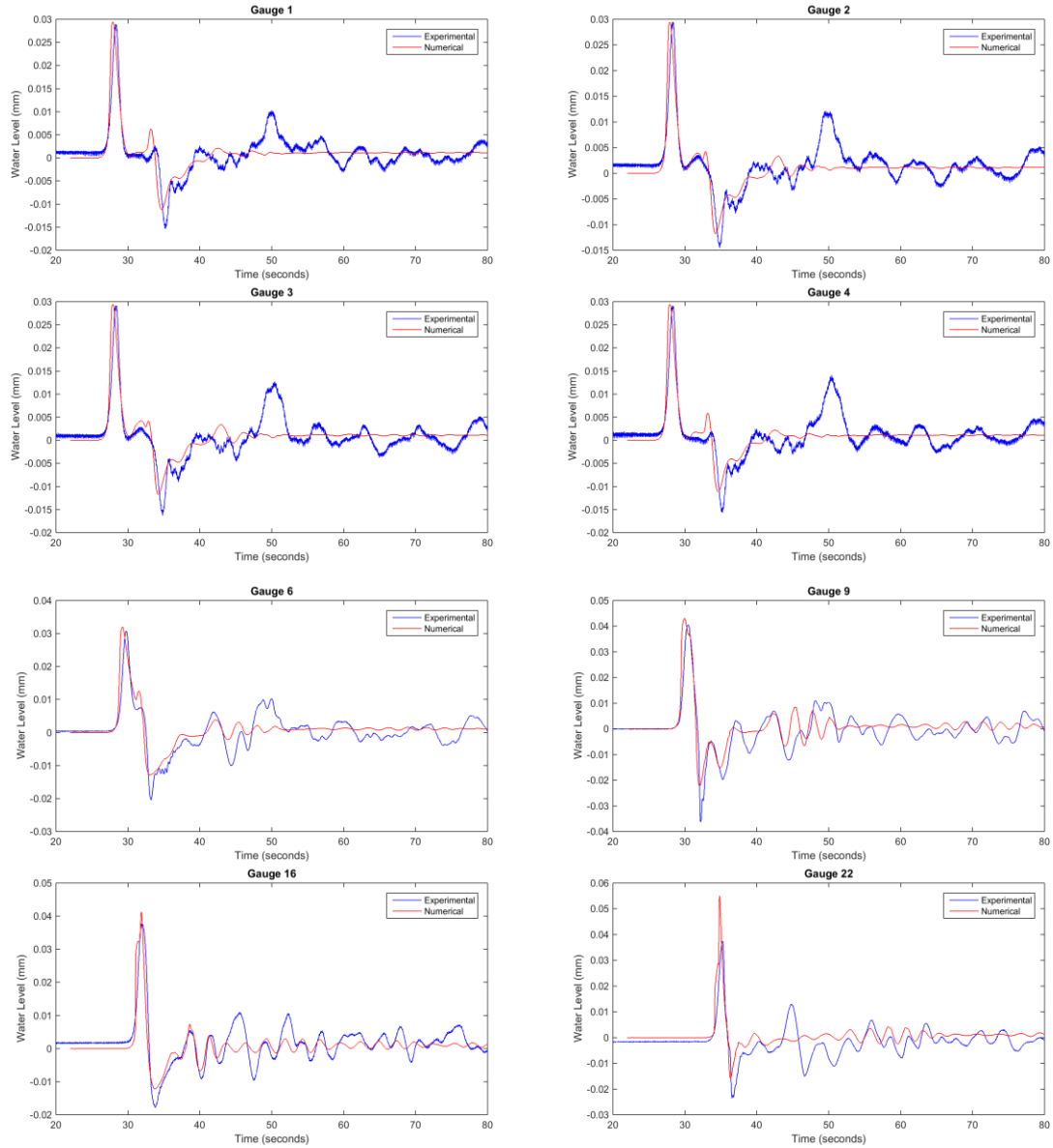


Figure F-27 Comparison of computed and measured time series at 8 gauges for Case B ( $n = 0.015$ ,  $d = 3$  mm).



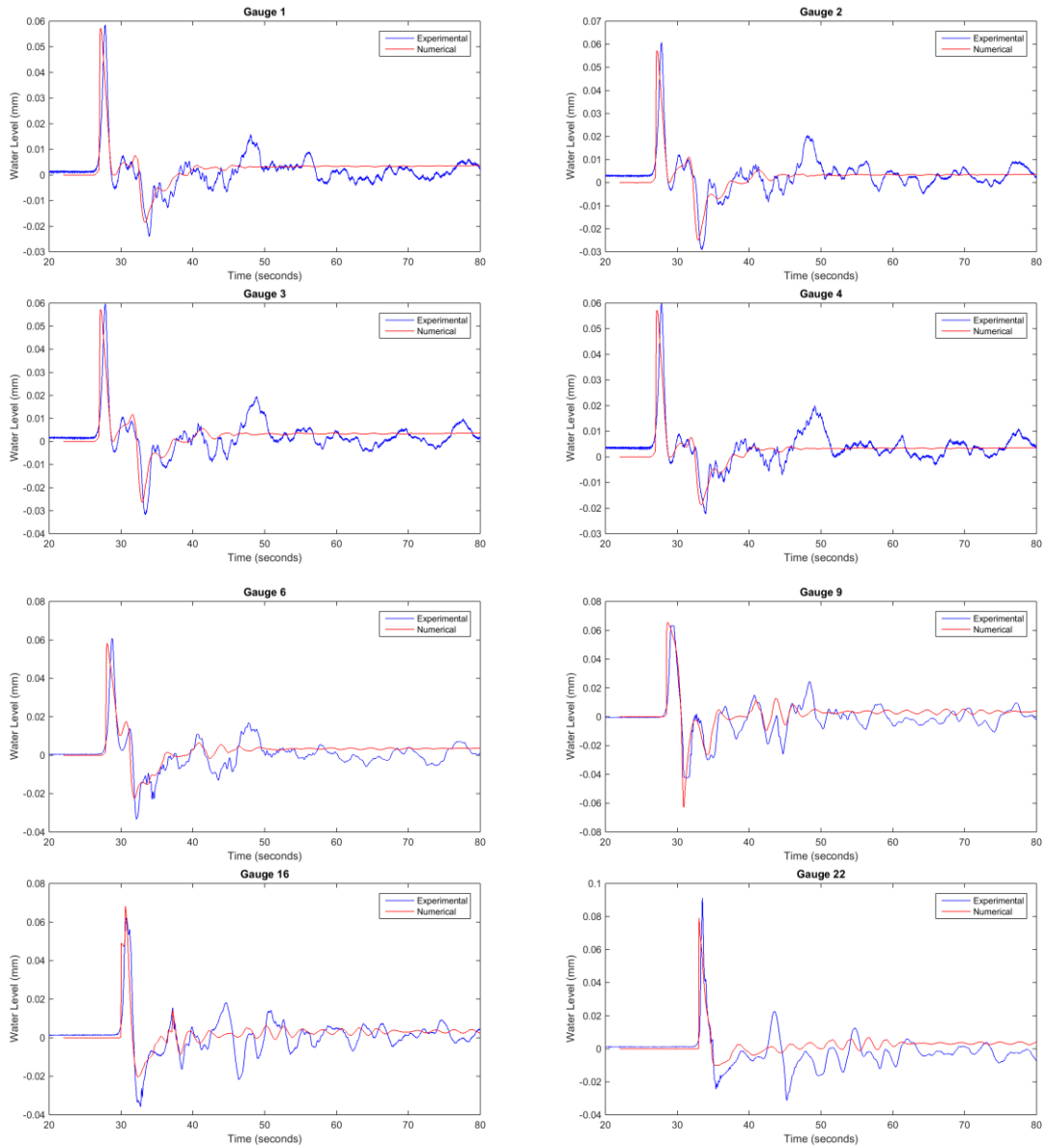


Figure F-28 Comparison of computed and measured time series at 8 gauges for Case C ( $n = 0.015$ ,  $d = 3$  mm).

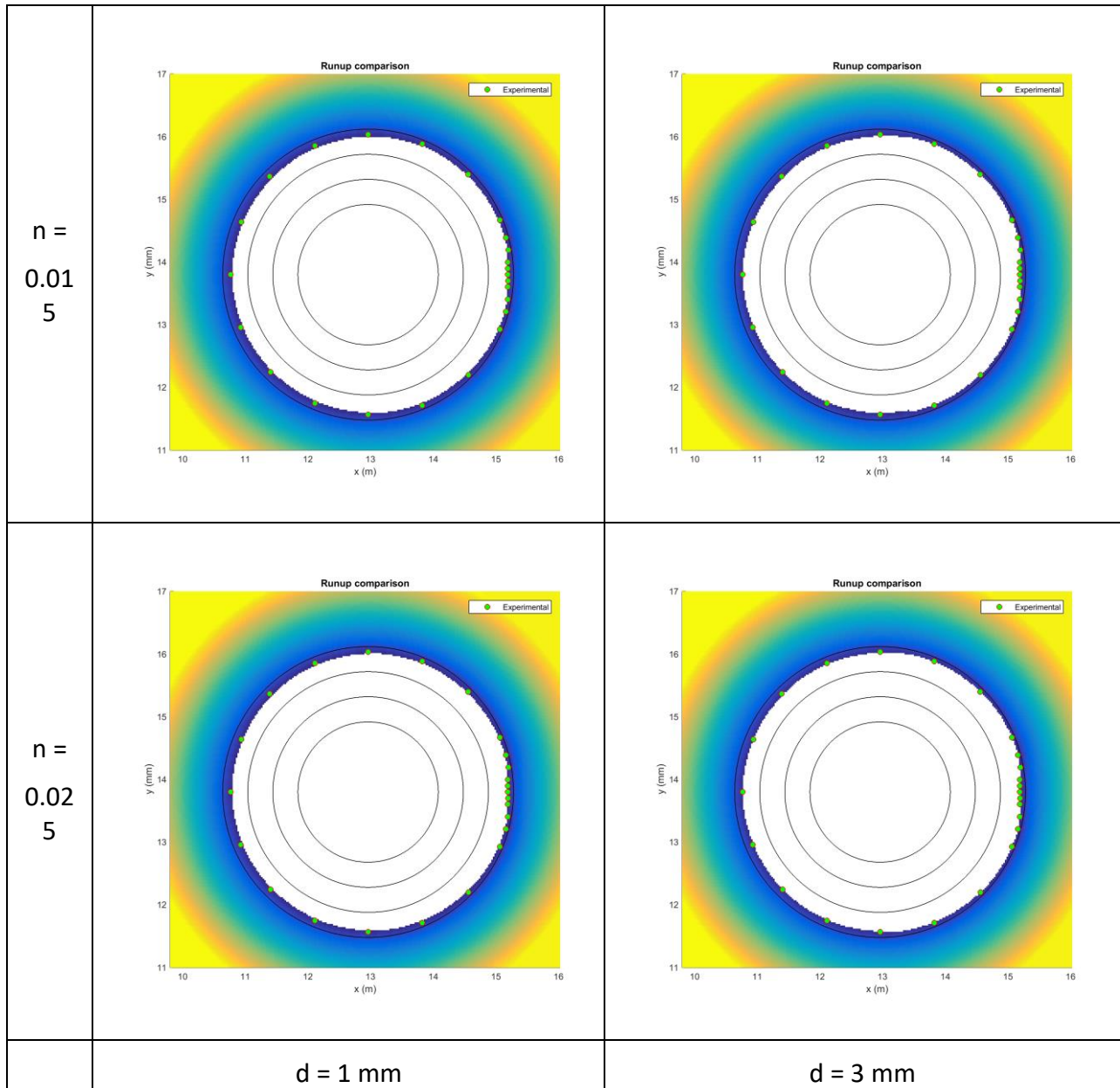


Figure F-29 Island runup for Case A with different values of Manning's coefficient,  $n$  and dry cell depth,  $d$ .

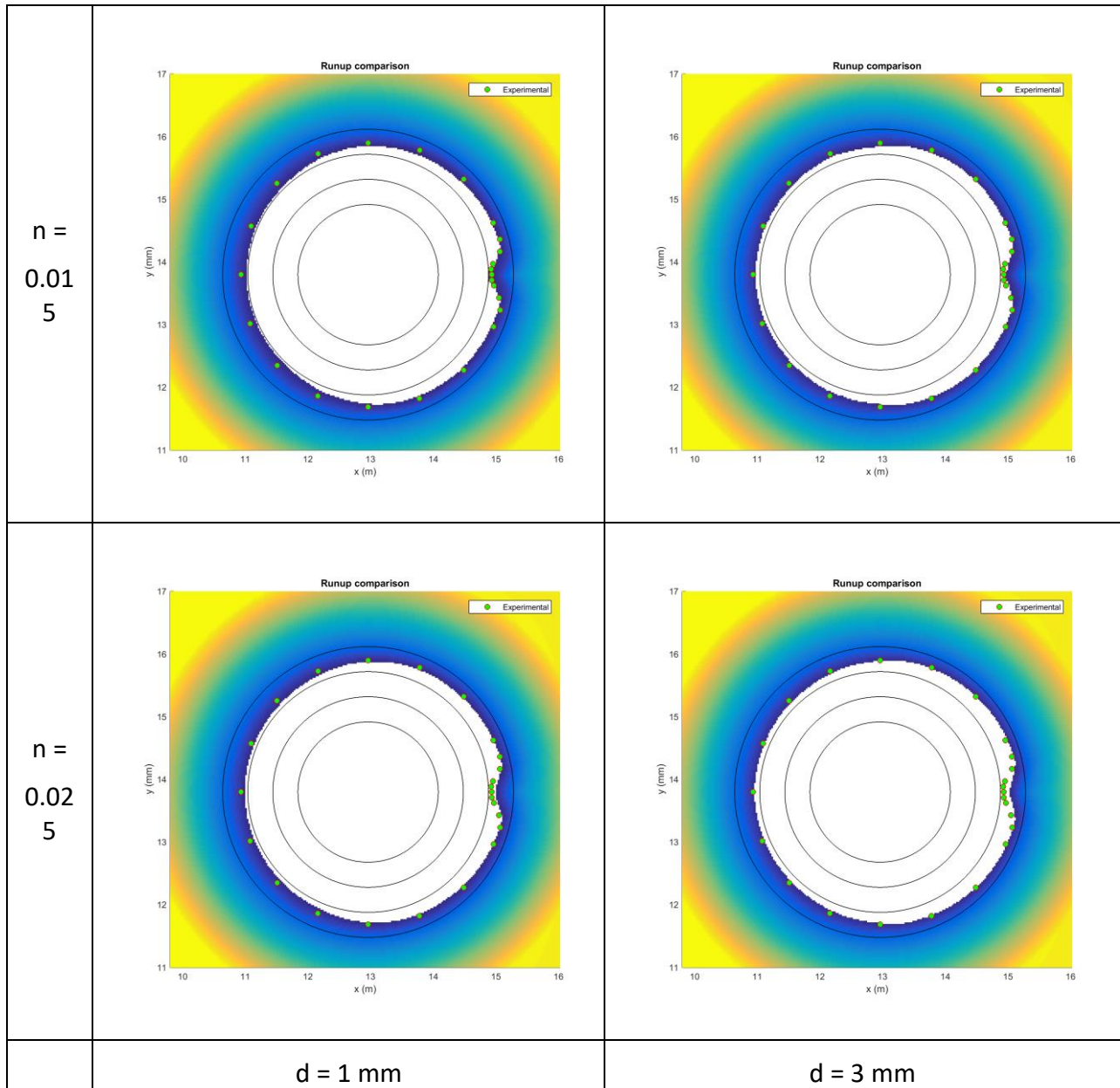


Figure F-30 Island runup for Case B with different values of Manning's coefficient,  $n$  and dry cell depth,  $d$ .

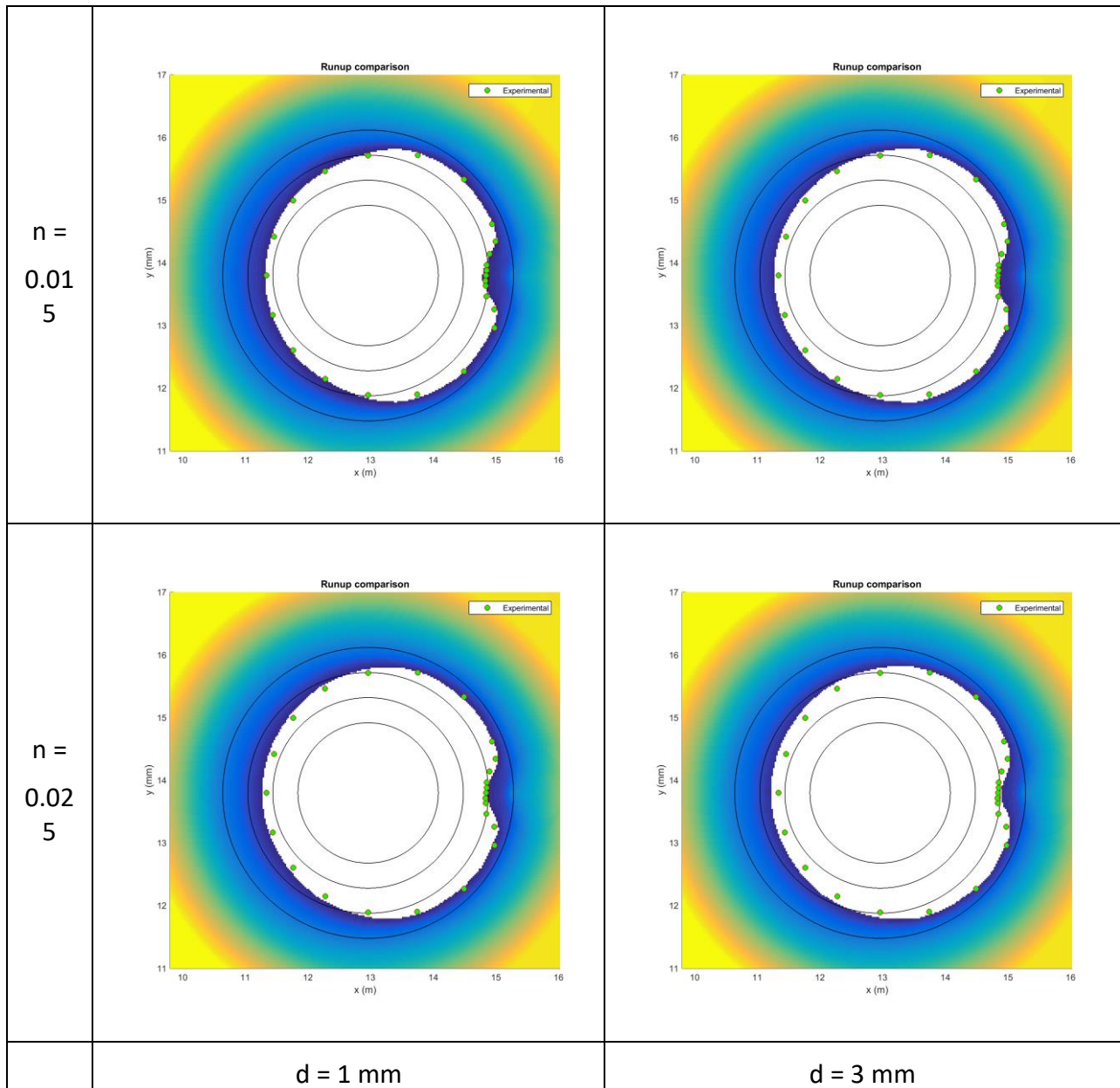


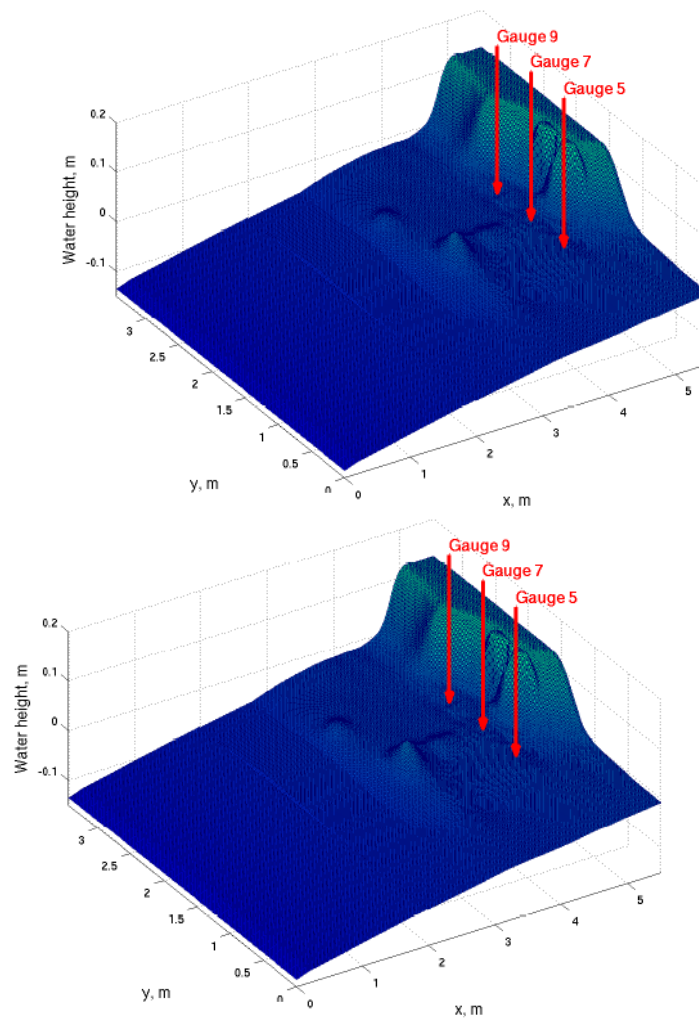
Figure F-31 Island runup for Case C with different values of Manning's coefficient, n and dry cell depth, d.

**F.9. BP #7: Monai valley beach (Laboratory)**

*Problem description*

A laboratory experiment using a large-scale tank at the Central Research Institute for Electric Power Industry in Abiko, Japan, was focused on modeling runup of a long wave on a complex beach near the village of Monai (Liu et al., 2008). The beach in the laboratory wave tank was a 1:400 scale model (Figure F-32) of the bathymetry and topography around a very narrow gully, where extreme runup was measured. The incoming wave in the experiment was created by wave paddles located away from the shoreline, and the induced water level dynamics were recorded at several locations by gauges.

The primary theme of this benchmark problem is the temporal and spatial variations of the shoreline location, as well as the temporal variations of the water-surface elevations at specified nearshore locations.



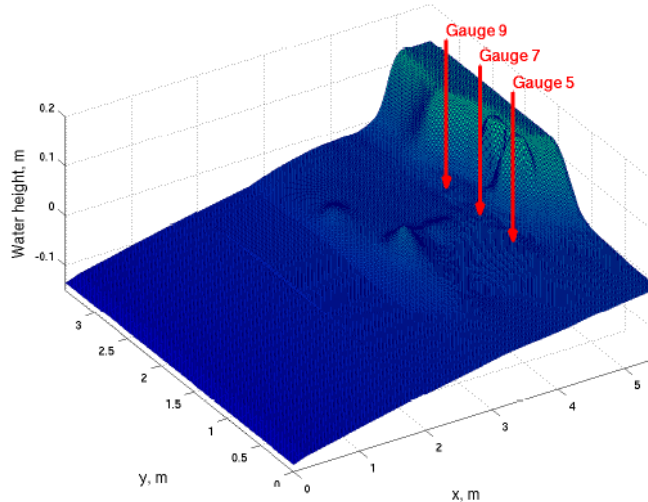


Figure F-32 The 3-D view of the computational domain. The inlet boundary is modeled at  $x = 0$ ; at  $y = 0$  and  $y = 3.4$ , the reflective boundary conditions are set.

### Model setup

The nonlinear shallow water equations were solved in Cartesian coordinates with  $g = 9.81 \text{ m/s}^2$  and no friction. The computational domain represents a 5.488 by 3.402 meter portion of the wave tank near the shore and the computational grid cell size is  $0.014 \times 0.014$  (same as the given bathymetry). The incident wave is prescribed at  $x = 0$  for the first 22.5 seconds, after which a non-reflective boundary condition is set at  $x = 0$ . The boundary conditions along  $y = 0$ ,  $y = 3.4$  and  $x = 5.5$  are set completely reflective.

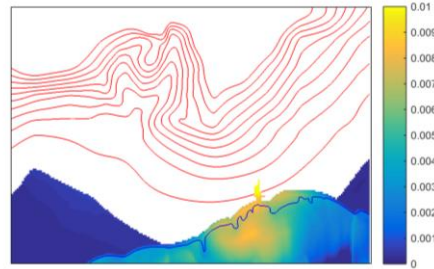
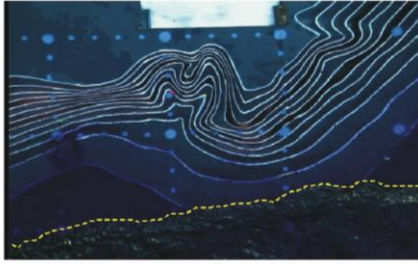
### Results

Figure F-33 presents the comparisons of the frames 10, 25, 40, 55 and 70 extracted from the overhead video taken during the laboratory experiment with the computed results at roughly corresponding times. The movie has the frequency of 30 frames per second, and we selected frames that are 0.5 seconds apart. In the benchmark description, it is stated that “frame 10 approximately occurs at 15.3 seconds” and “it is recommended that each modeler find times of the snapshots that best fit the data”. We found the best fit starting at 15.6 seconds for Frame 10 and then taking 0.5 seconds increments.

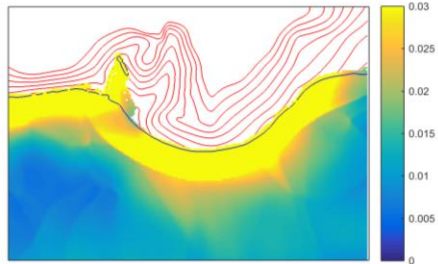
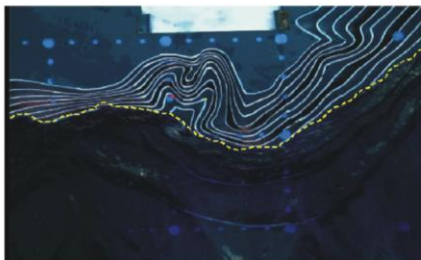
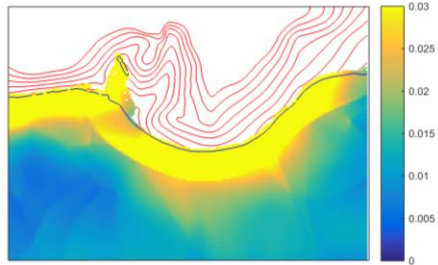
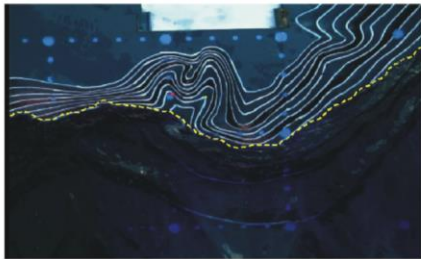
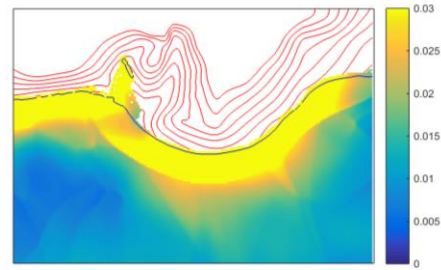
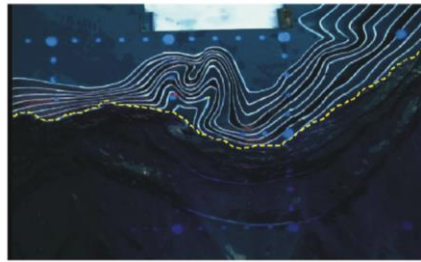
The computed and laboratory temporal variations of the water-surface elevations at the three gauges are shown in Figure F-34. The computed results are in general a good match to the laboratory measurements.

The file “OBS\_RUNUP.txt” from benchmark specification contains the runup at three locations as observed in six runs of the same wave tank experiment. Figure F-35 demonstrates the comparison of the computed and measured maximum runup.

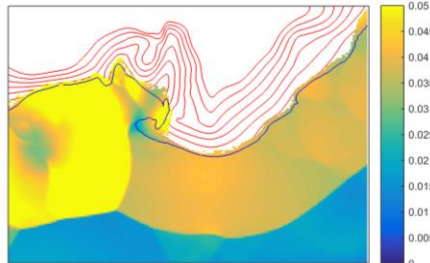
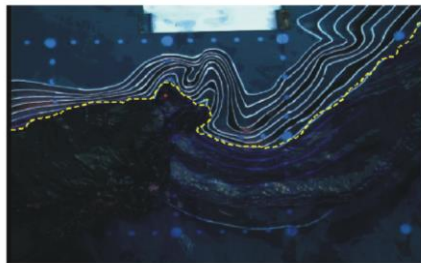
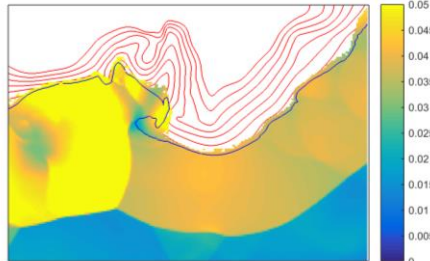
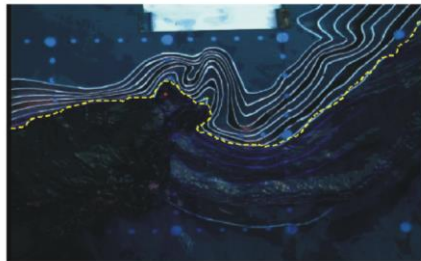
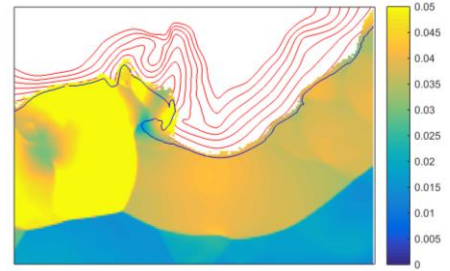
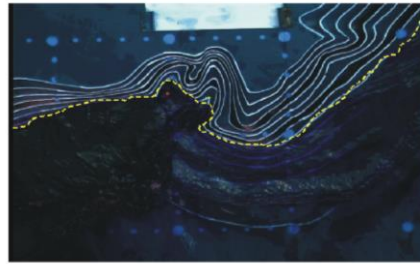
Frame 10



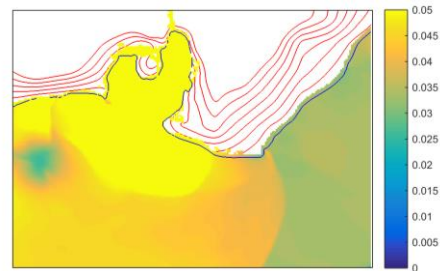
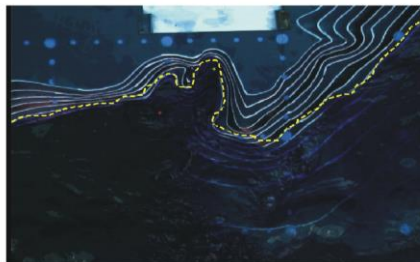
Frame 25



Frame 40



Frame 55



Frame 70

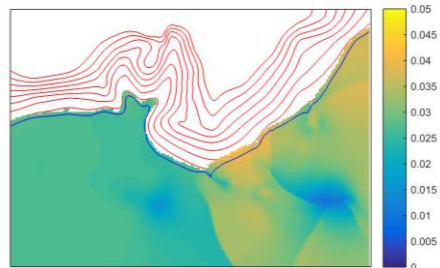
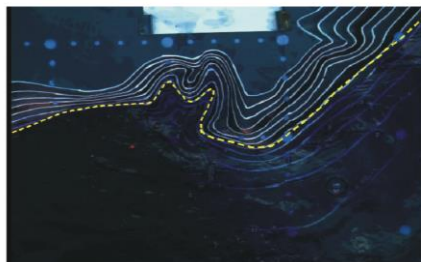
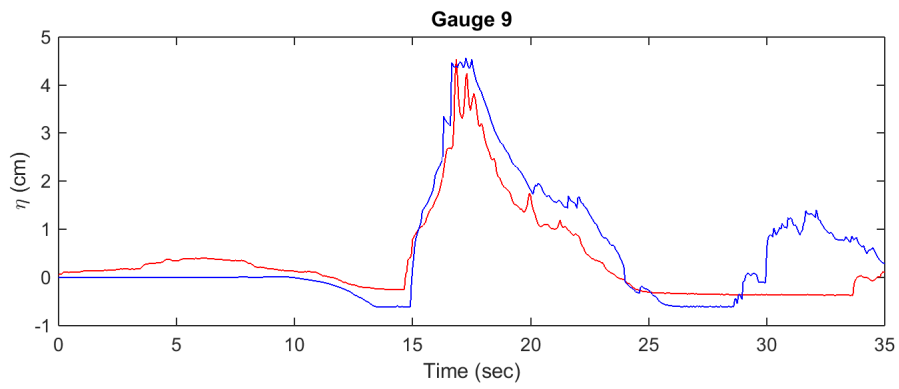
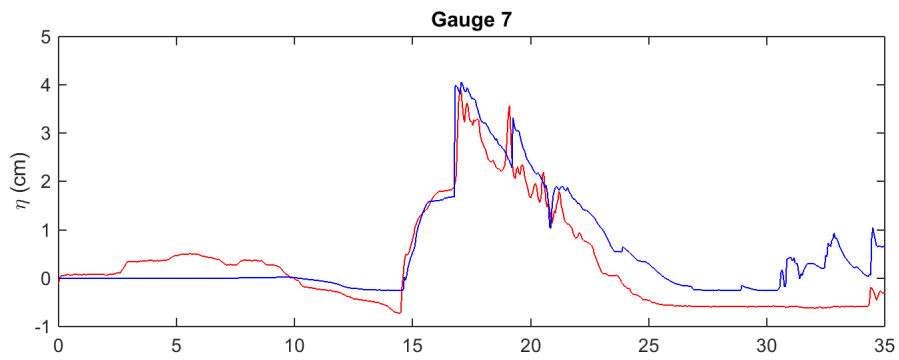
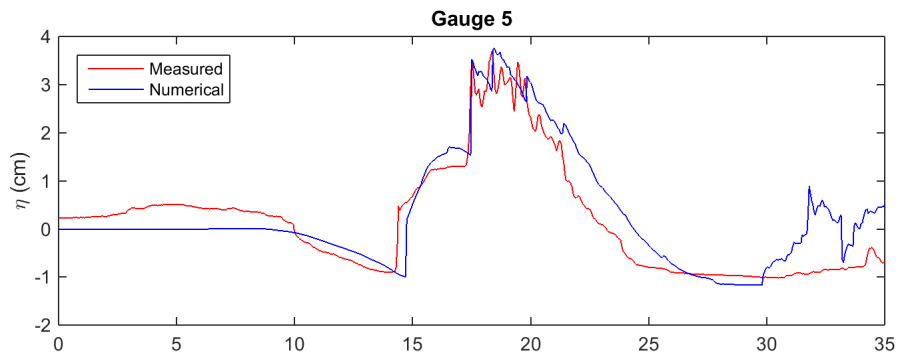
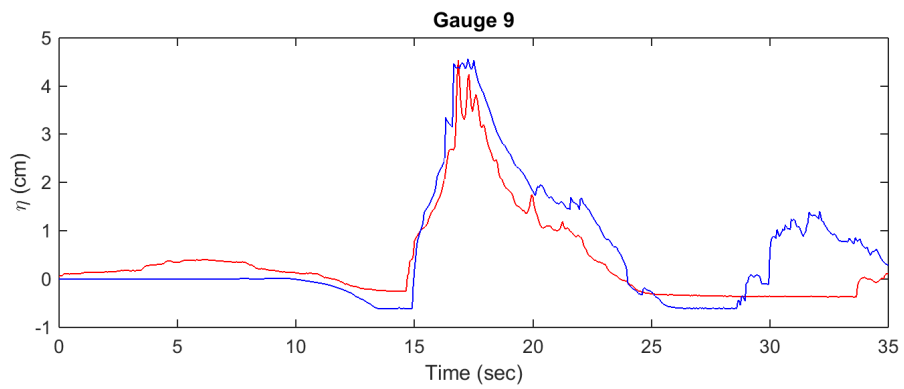
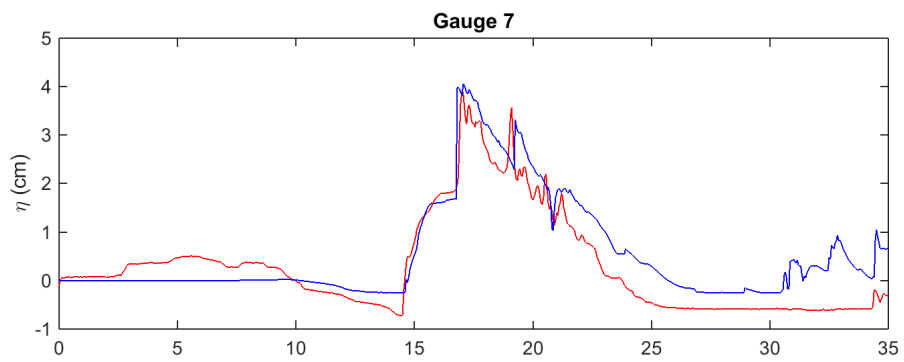
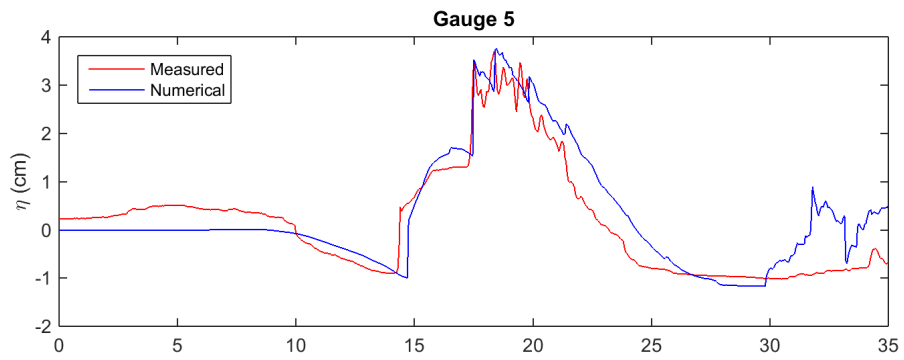


Figure F-33 Comparisons of the extracted frames 10, 25, 40, 55 and 70 from the overhead movie of the laboratory experiment (left column) with computed results (right column). The time interval between frames is 0.5 seconds. The dashed yellow line shows the instantaneous location of the shoreline.









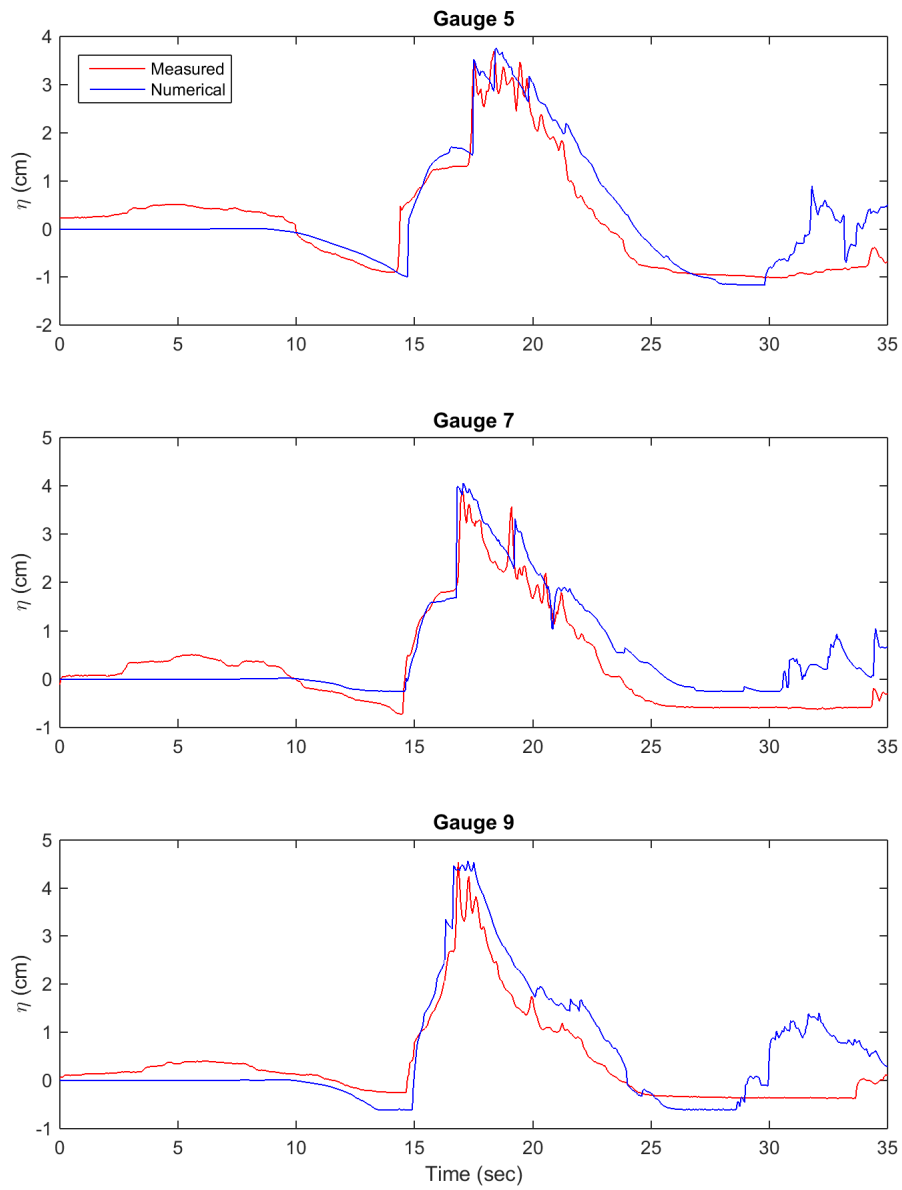
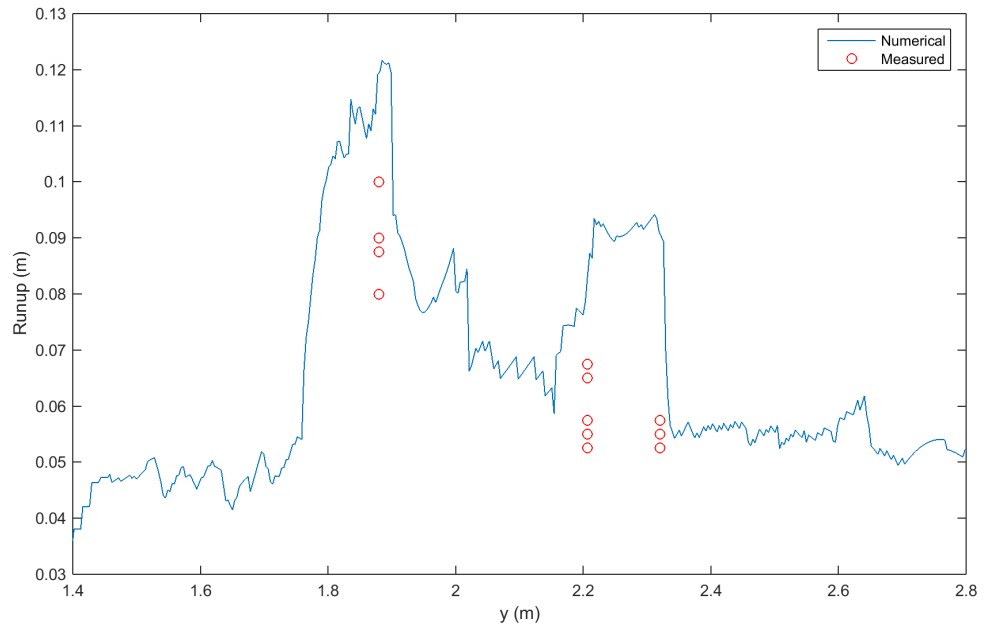
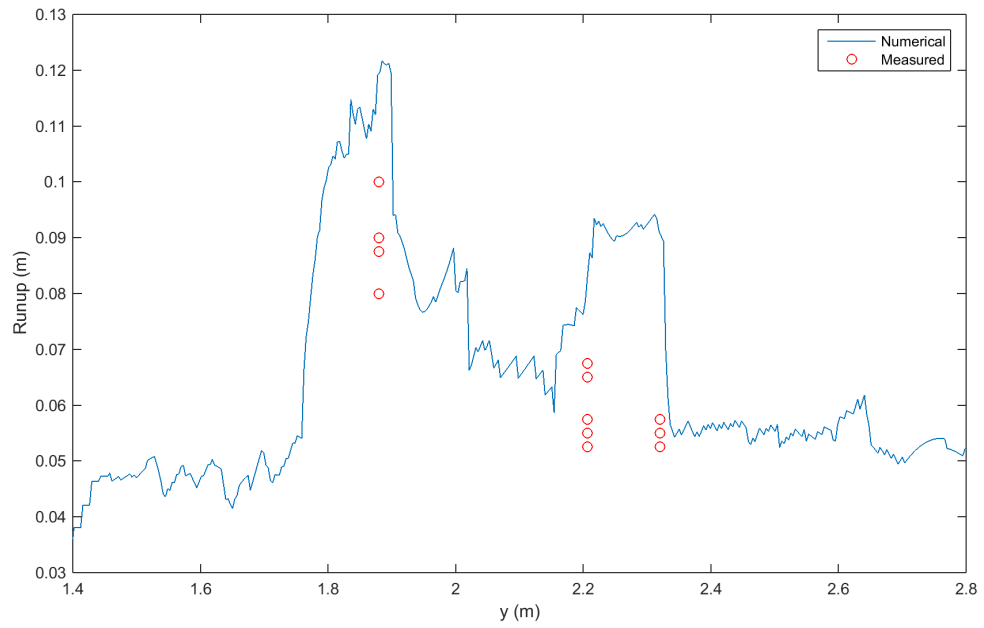


Figure F-34 Comparison of the computed results with the laboratory measurements at the three gauges.



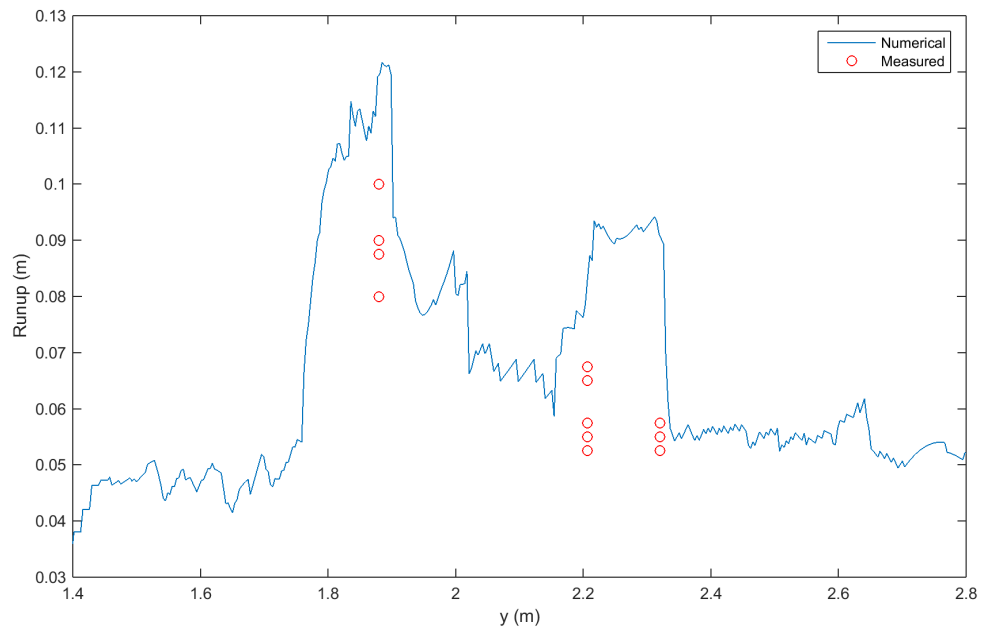


Figure F-35 Maximum runup.

## F.10. Benchmark Problem #9: Okushiri Island (Field)

### *Problem description*

The goal of this benchmark problem is to compare computed model results with field measurements gathered after the 12 July 1993 Hokkaido-Nansei-Oki tsunami (also commonly referred to as the Okushiri tsunami).

Objectives:

1. Compute runup around Aonae
2. Compute arrival of the first wave to Aonae
3. Show two waves at Aonae approximately 10 min apart; the first wave came from the west, the second wave came from the east
4. Compute water level at Iwanai and Esashi tide gauges
5. Maximum modeled runup distribution around Okushiri Island
6. Modeled runup height at Hamatsumae
7. Modeled runup height at a valley north of Monai

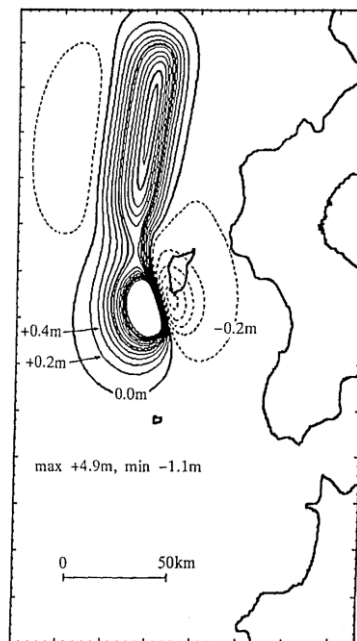
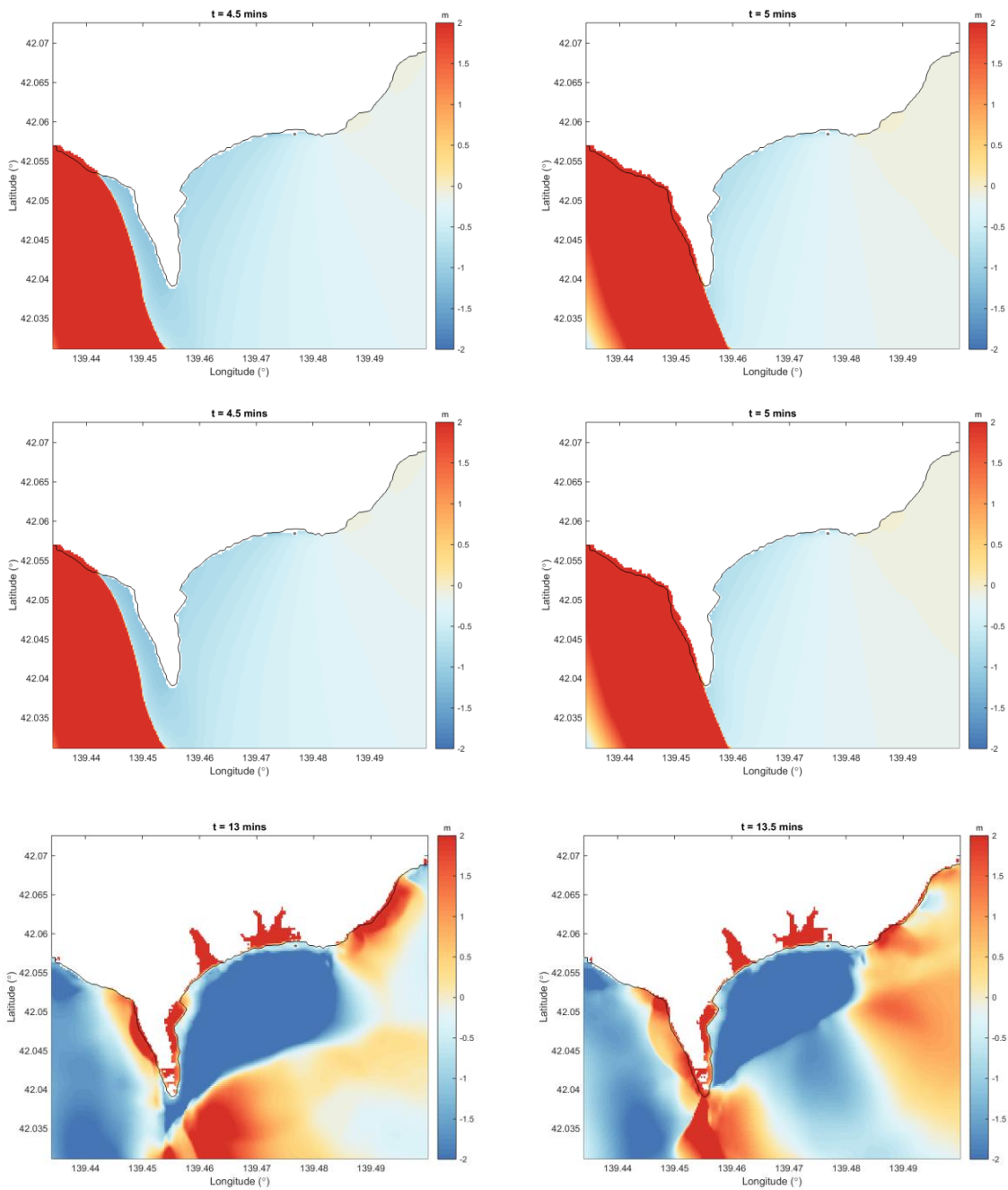


Figure F-36. Source model DCRC17a (Takahashi et al., 1995).

### *Model setup*

Used  $g = 9.81 \text{ m/s}^2$  and Manning's friction coefficient  $n = 0.025$  in Spherical coordinates. Five levels of refinement were used in the model with the computational grid resolutions of 24 arcsec, 8 arcsec, 8/3 arcsec, 8/9 arcsec and 8/45 arcsec. The source model is shown in Figure F-36.

## Results





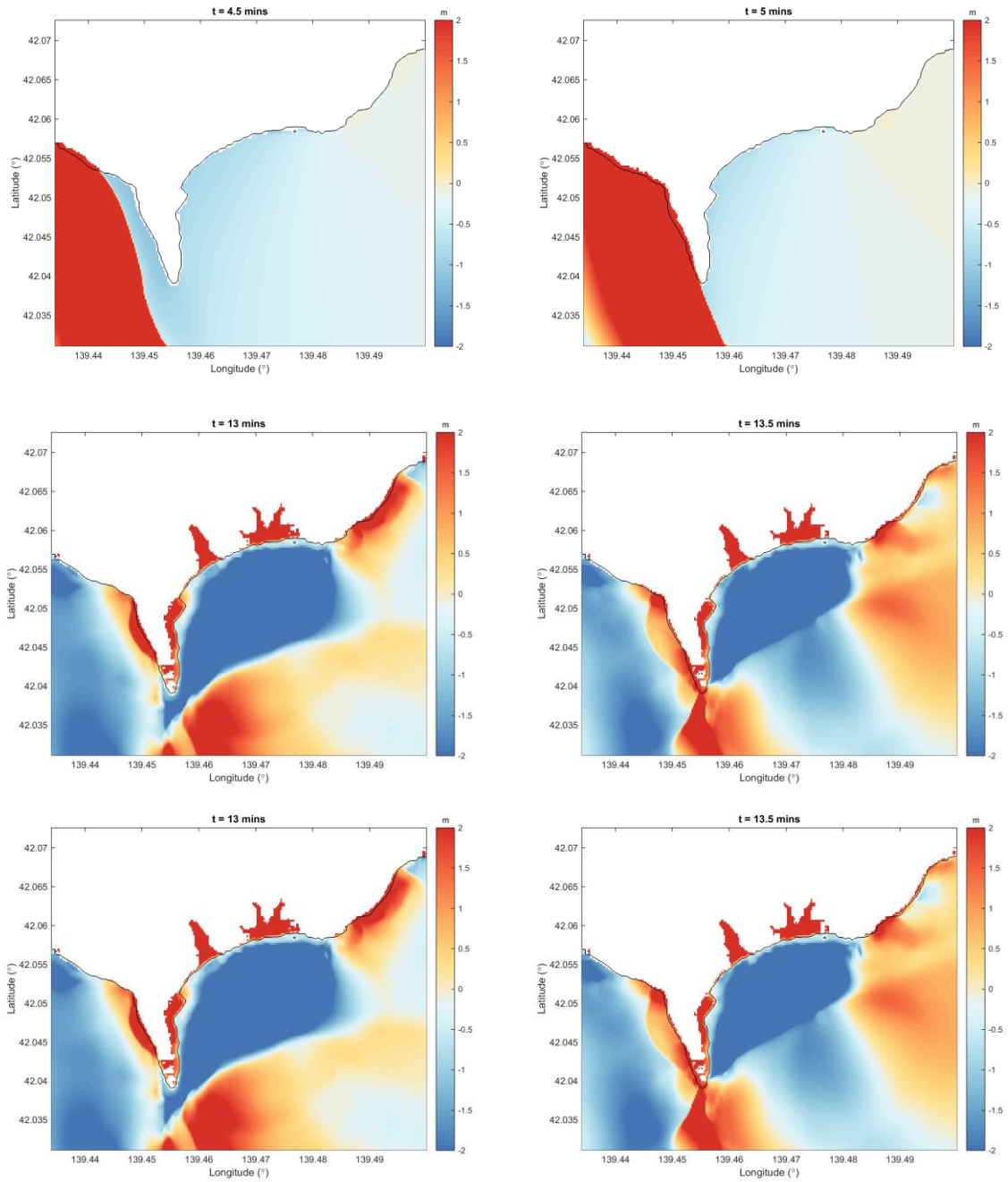


Figure F-37. Runup around Aonae.

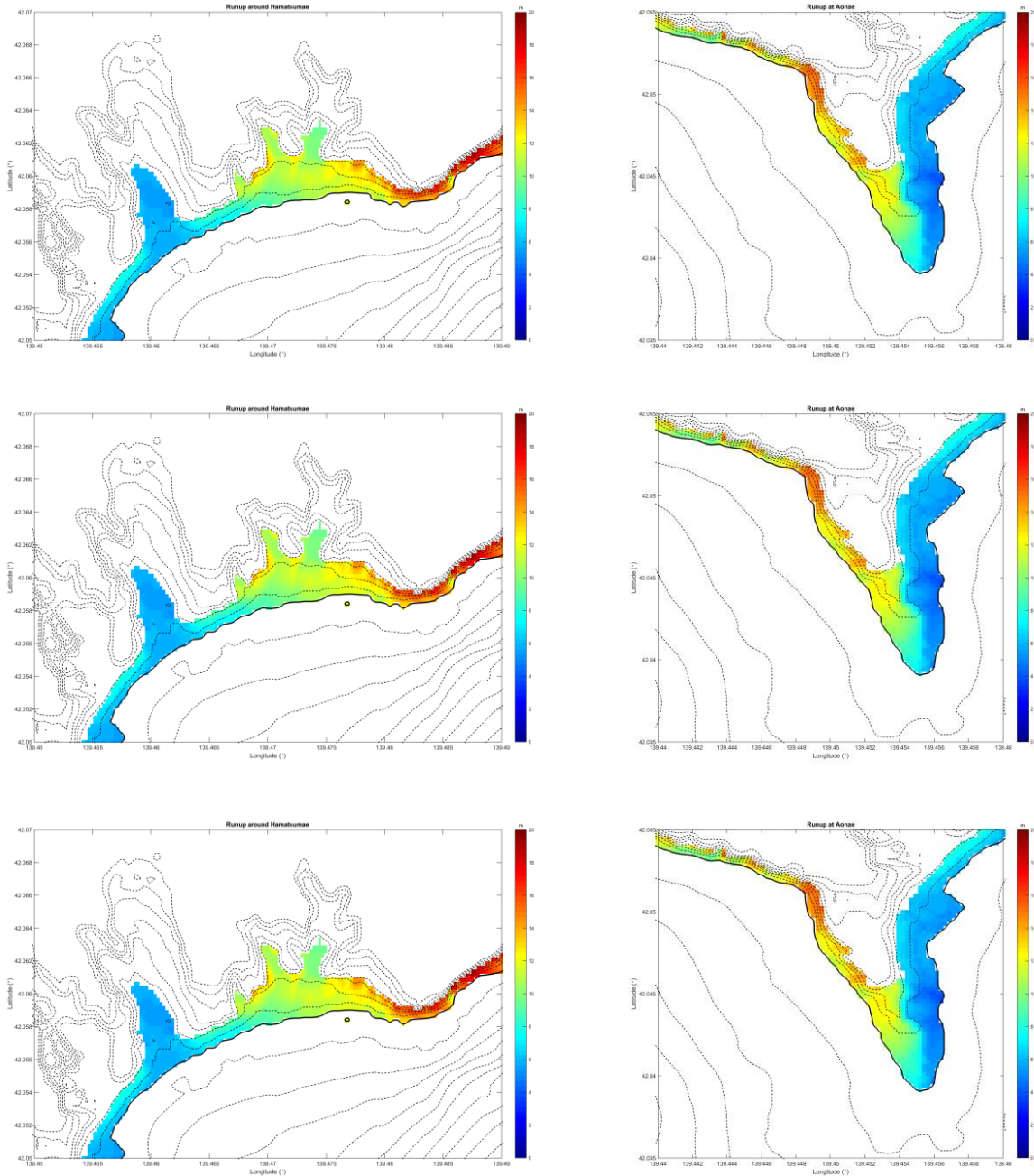


Figure F- 38 The inundation map for the area near Hamatsumae (left) and Aonae Peninsula (right). The color represent the maximum surface elevation achieved. The contour lines are 4m each.

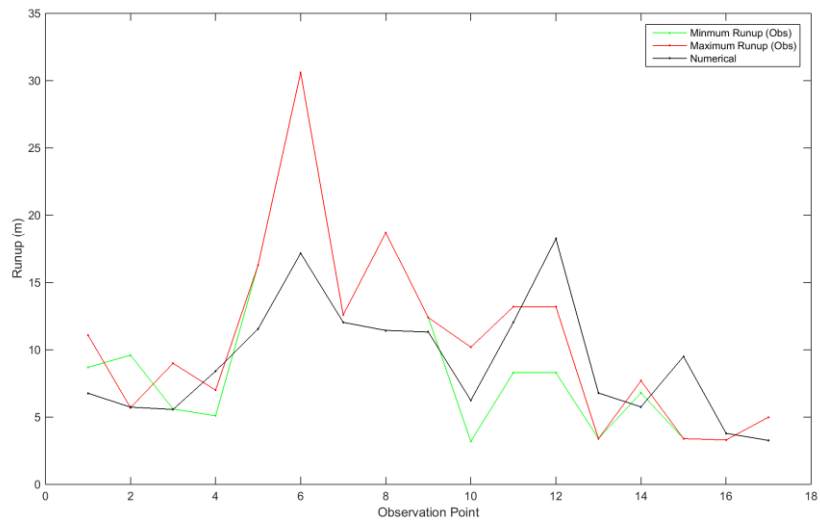
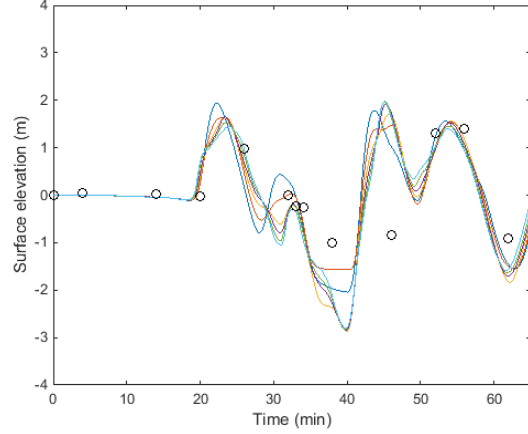
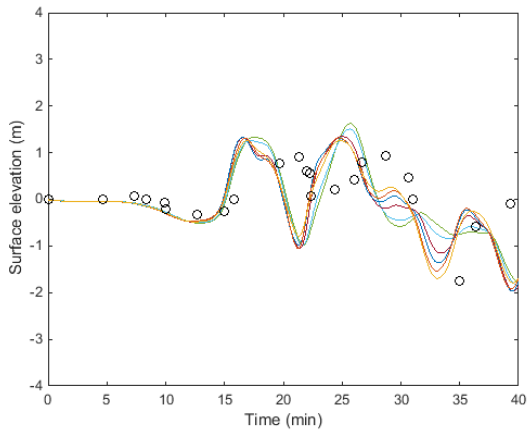
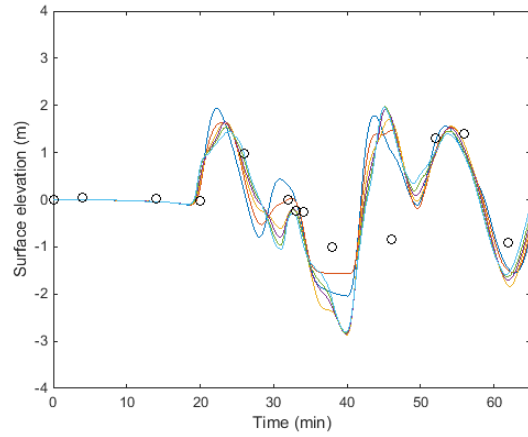
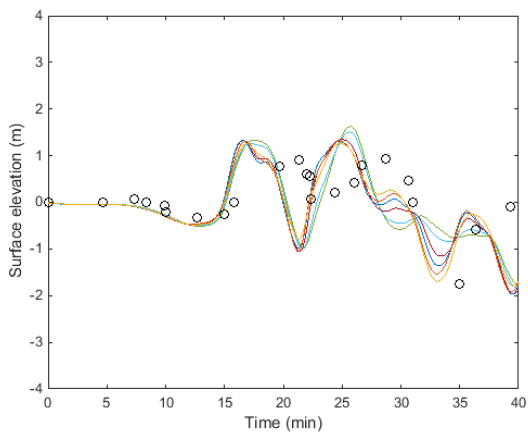


Figure F-39 Comparisons of observed and simulated runup.



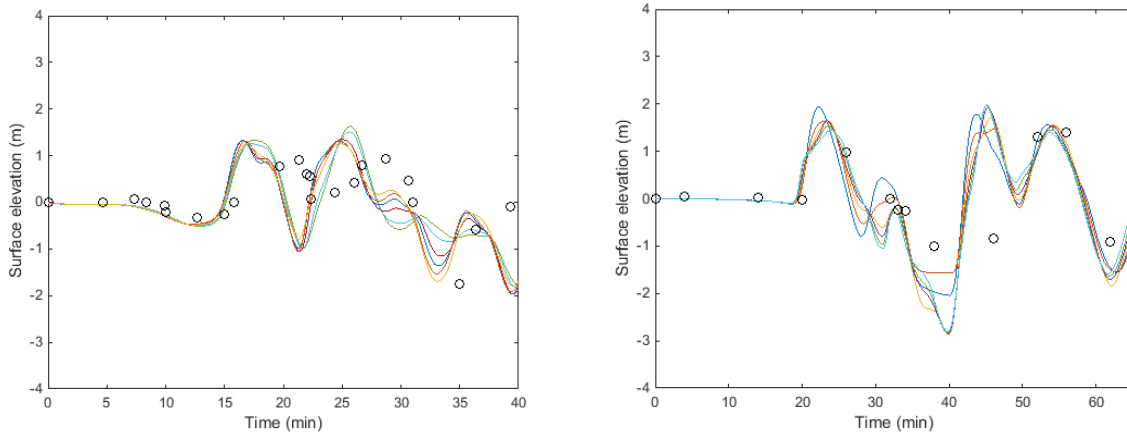
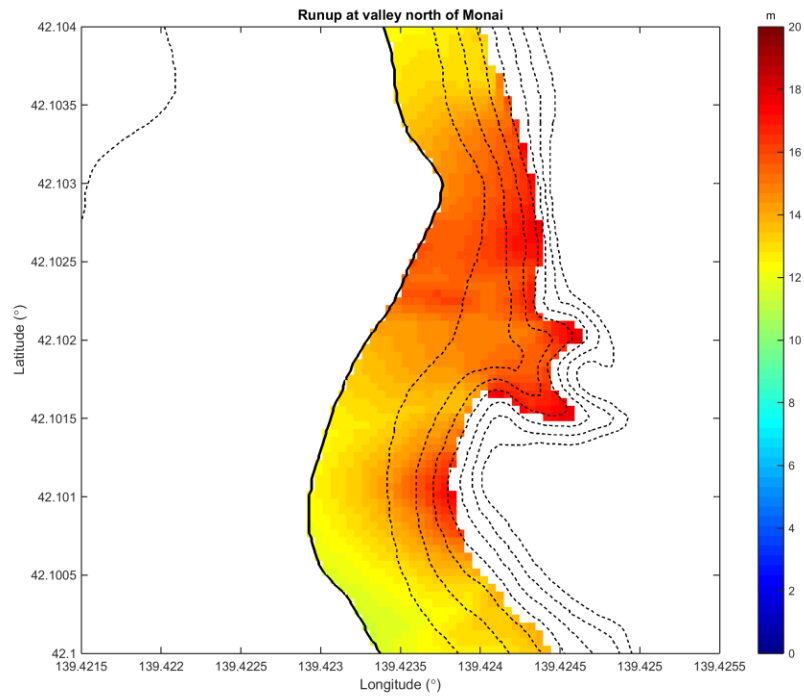


Figure F-40 Water-level time series of at Esashi (left) and Iwanai (right) tide gauges.



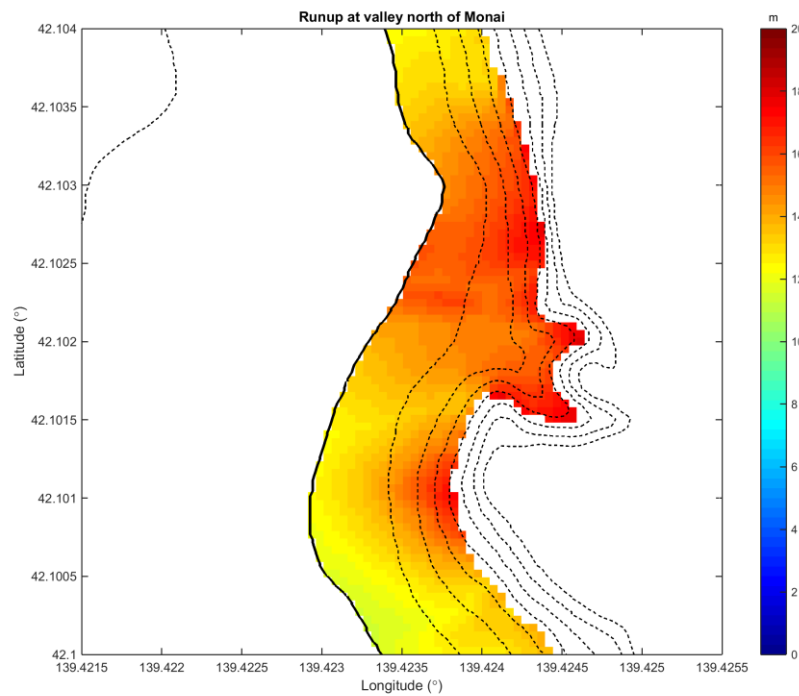


Figure F-41 Inundation map for the valley north of Monai.

**F.11. References**

Liu, P. Yeh, H. and Synolakis, C., 2008. Advanced Numerical Models for Simulating Tsunami Waves and Runup: in *Advances in Coastal and Ocean Engineering 10*, (World Scientific, Singapore 2008).

National Tsunami Hazard Mitigation Program (NTHMP), 2012. Proceedings and Results of the 2011 NTHMP Model Benchmarking Workshop. Boulder: U.S. Department of Commerce/NOAA/NTHMP; (NOAA Special Report). 436 p.

Takahashi, T., Takahashi, T., Shuto, N., Imamura, F. and Ortiz, M., 1995. Source models for the 1993 Hokkaido-Nansei-Oki earthquake tsunami *Pure and Appl. Geophys.* **144** (3/4), 747-768.

Yeh, H., Imamura, F., Synolakis, C., Tsuji, Y., Liu, P., and Shi, S., 1993. The Flores Island tsunamis, *EOS, Transactions, American Geophysical Union*, **74**(33), 371–373.

## Appendix G. Tsunami velocity validation

### G.1. Model Background

AECOM has developed an in-house version of the GeoClaw code to facilitate the use in the current AECOM work environment, which requires the computation of large numbers of scenarios with multiple high-resolution target areas. The most important change is the use of nested grids rather than adaptive meshing. This code is currently being used in the development of probabilistic tsunami inundation maps for the State of California. The results of the following Benchmark exercises are included in Lynett et al. (2017).

### G.2. Model Equations

The model solves the two-dimensional depth-averaged nonlinear shallow water equations:

$$\begin{aligned}h_t + (hu)_x + (hv)_y &= 0, \\(hu)_t + (hu^2 + \frac{1}{2}gh^2)_x + (huv)_y &= -ghB_x - Du, \\(hv)_t + (huv)_x + (hv^2 + \frac{1}{2}gh^2)_y &= -ghB_y - Dv, \\h_t + (hu)_x + (hv)_y &= 0, \\(hu)_t + (hu^2 + \frac{1}{2}gh^2)_x + (huv)_y &= -ghB_x - Du, \\(hv)_t + (huv)_x + (hv^2 + \frac{1}{2}gh^2)_y &= -ghB_y - Dv,\end{aligned}\tag{10-5}$$

where  $u(x, y, t)$  and  $v(x, y, t)$  are the depth-averaged velocities in the two horizontal directions,  $B(x, y, t)$  is the topography or bathymetry, and  $D(h, u, v)$  is the drag coefficient. In case of the existence of friction, Manning correlation is use for the friction:

$$D = \frac{gn^2\sqrt{u^2 + v^2}}{h^{5/3}}\tag{10-6}$$

where  $n$  is the Manning's coefficient, generally taken to be 0.025.

### G.3. Numerical Solution Method

The model is based on the core of the GeoClaw solver which solves the two-dimensional depth-averaged nonlinear shallow water equations using high-resolution finite volume methods. The methods are based on Godunov's method that consists of solving the Riemann problem and using the resulting wave structure to update cell averages in the adjacent finite volume cells. In practice, an approximate Riemann solution is used. Refer to GeoClaw for details of the model numerical scheme (the numerical accuracy and sources of numerical dissipation; the model shoreline boundary scheme).

#### **G.4. Benchmark Problem #1: Steady Flow over Submerged Obstacle**

The computational domain is  $0 \text{ m} \leq x \leq 20 \text{ m}$  and  $0 \text{ m} \leq y \leq 1.52 \text{ m}$ . The grid cell size is 7.6 mm. The Courant/CFL number used is 0.70. The constant velocity  $u = 0.115 \text{ m/s}$  is imposed at the left boundary. The Manning coefficient is set to zero where the tank bottom is flat and is only nonzero on the conical hill. If we apply a non-zero Manning's coefficient throughout the model, the flow would slow down too much due to friction. When friction is set to zero except on the cone, the slow-down is minimal.

The comparison plots with the different Manning's Coefficient  $n = 0.015$  and  $0.01$  applied only on cone are shown in Figure G-1. We found the Manning's coefficient  $n = 0.015$  is the optimum value other than the requested value  $0.01$ . The results with unstable vortex street development are very sensitive to any changes in the model (such as the Courant number). Figure G-2 presents the development of vortex street with the slightly different Courant numbers  $0.70$  and  $0.69$  – changing the Courant number from  $0.70$  to  $0.69$  (resulting in slightly smaller time steps) gives very different vortex shedding patterns. Note that the differences are starting to appear at  $t = 32$  sec and the patterns are very different at  $t = 100$  sec.

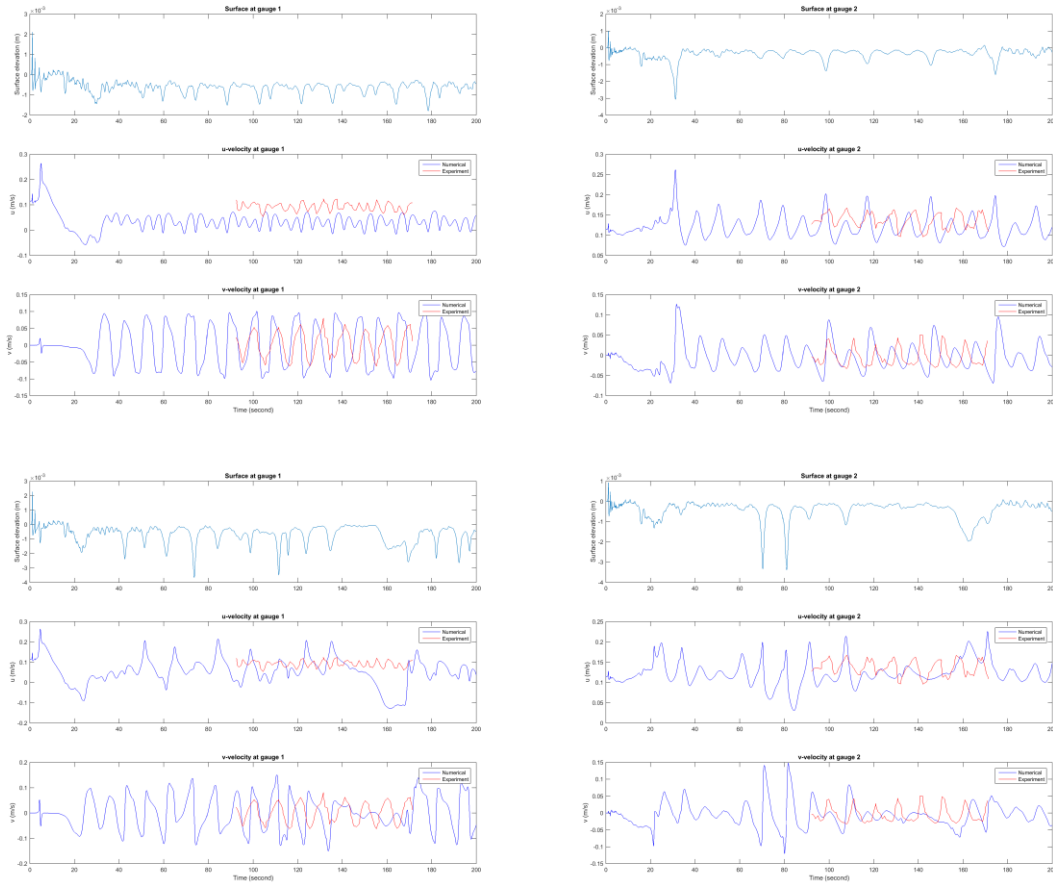
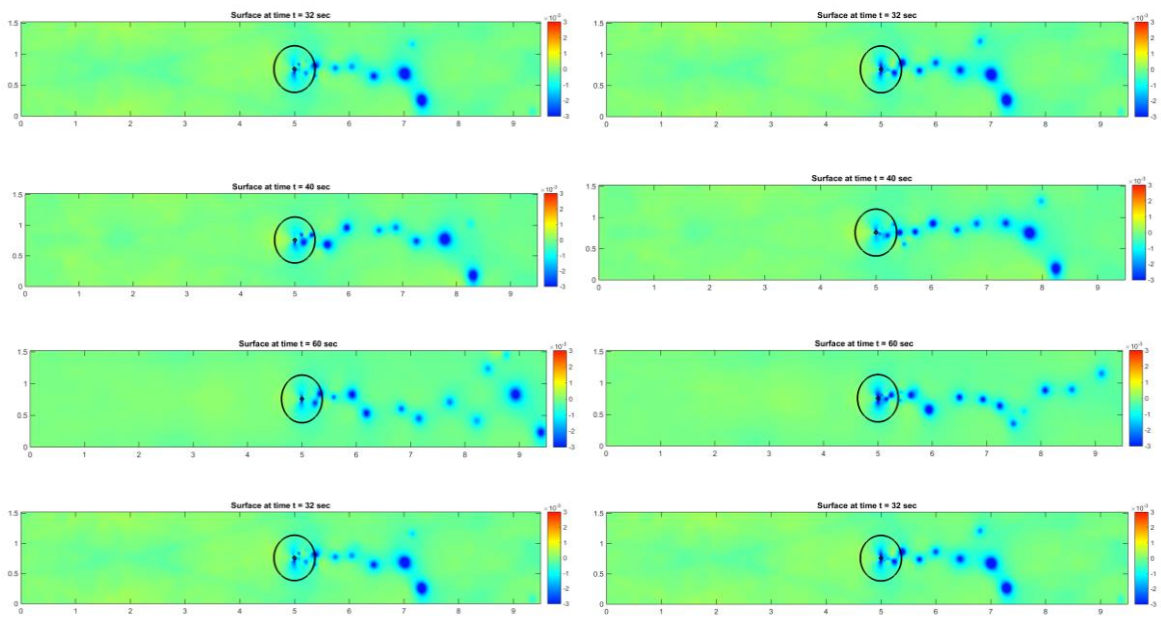


Figure G-1 Comparisons of numerical simulation (blue line) and experimental data (red line) for Gauge 1 (left) and Gauge 2 (right) with the Manning's coefficient  $n = 0.015$  (top) and  $n = 0.01$  (bottom) applied only on cone.





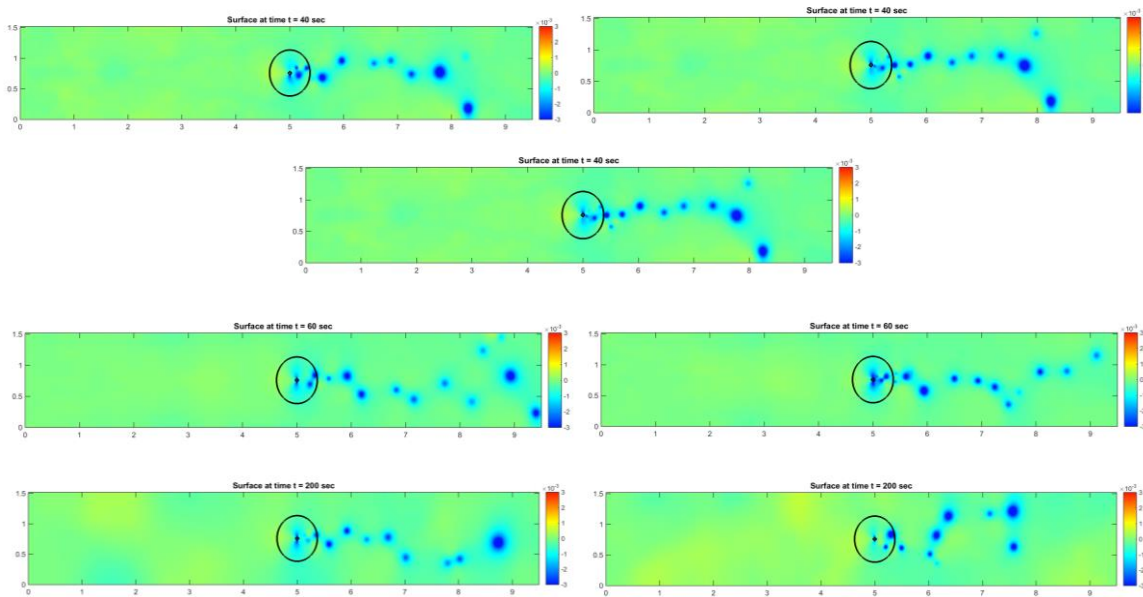
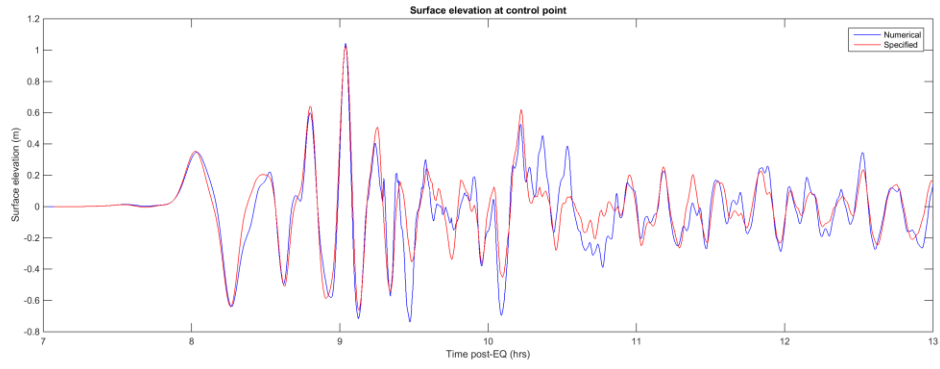


Figure G-2. Development of vortex street: CFL = 0.70 (left) and 0.69 (right); no friction ( $n = 0$ ) everywhere;  $t = 32, 40, 60$  and  $200$  sec.

### G.5. Benchmark Problem #2: Tsunami Currents in Hilo Harbor

The computational domain is longitude  $204.901^\circ \leq x \leq 204.965^\circ$  and latitude  $19.710^\circ \leq y \leq 19.774^\circ$ . The Manning’s coefficient is set to  $n = 0.025$ . The Courant number used is 0.75. The incident wave was specified at the control point (204.93, 19.7576). The boundary condition at  $y = 19.774$  was based on this information. There are three different numerical configurations:  $\sim 20$  m ( $2/3$  arcsec) resolution,  $\sim 10$  m ( $1/3$  arcsec) resolution, and  $\sim 5$  m ( $1/6$  arcsec) resolution.

Figure G-3 shows the simulated and specified wave profiles at the control point. Figure G-4 presents comparisons of the simulated and measured water surface elevation at the Hilo tide station (204.9447, 19.7308) with three different grid resolutions. Figure G-5 and Figure G-6 demonstrate the comparisons at the two ADCP locations (HA1125, harbor entrance: (204.9180, 19.7452); HA1126, inside harbor: (204.9300, 19.7417)) with three different grid resolutions.



*Figure G-3 Wave profiles at the control point (5-m grid).*

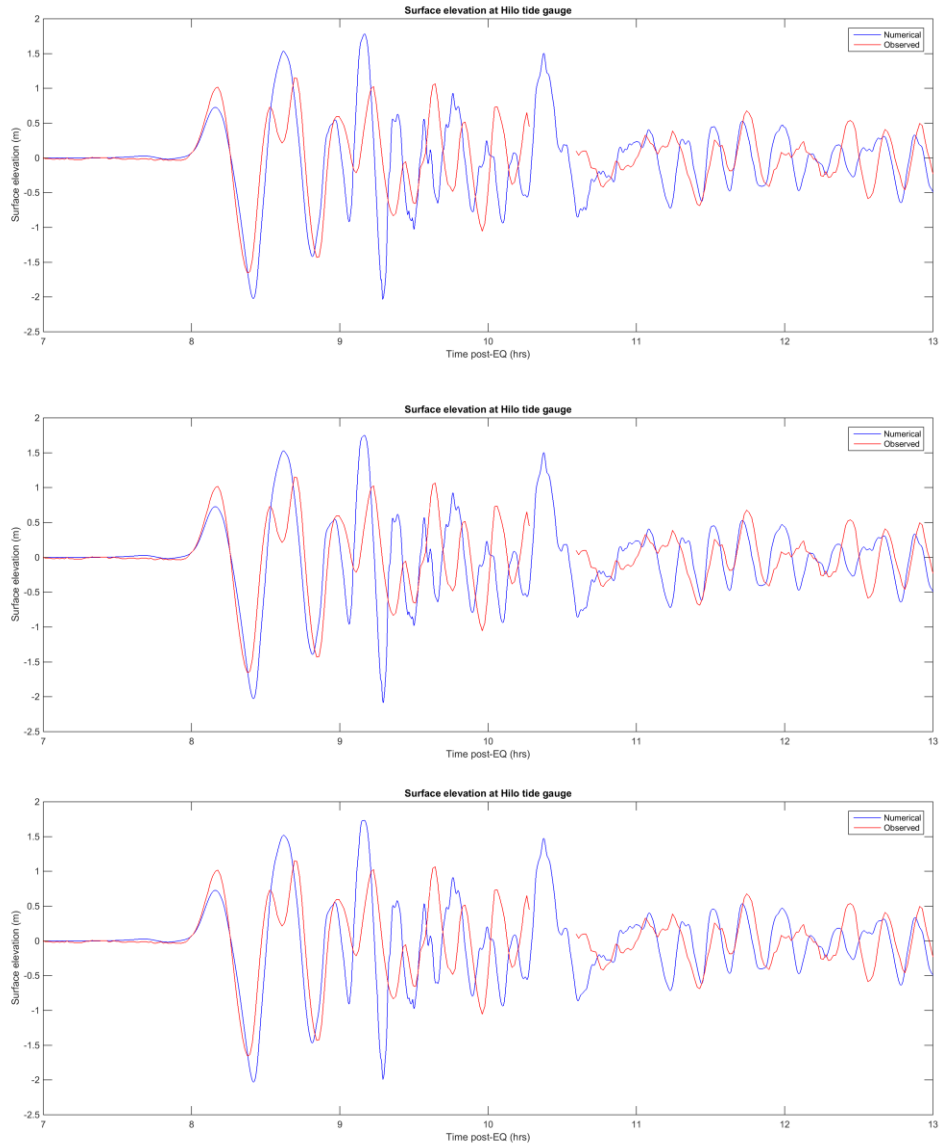
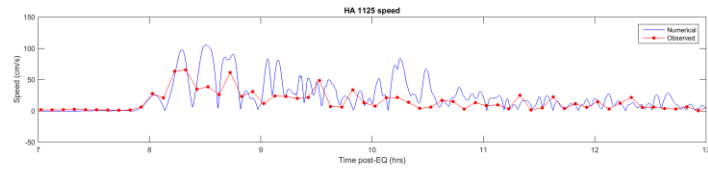
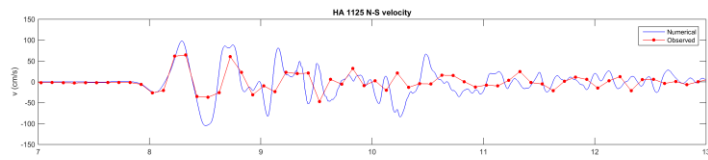
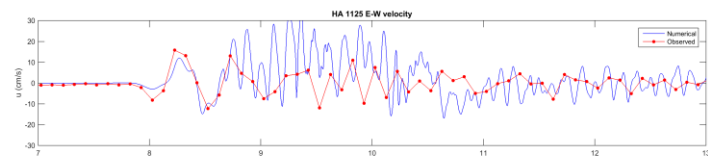
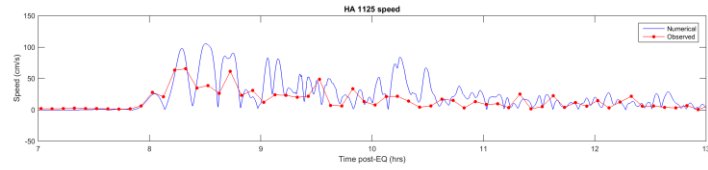
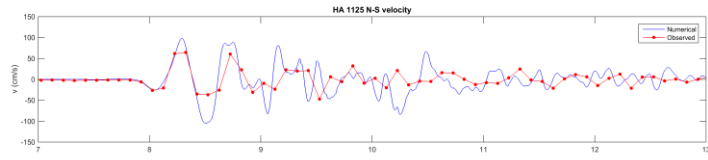
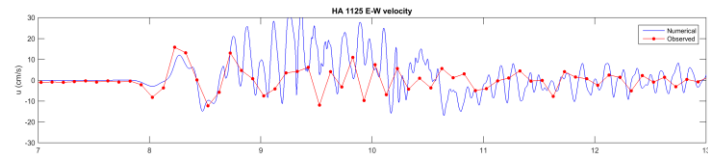


Figure G-4 Comparisons of the surface elevation at the Hilo tide gauge with the grid resolutions of 5 m (top), 10 m (middle) and 20 m (bottom): numerical – blue line; measured – red line.



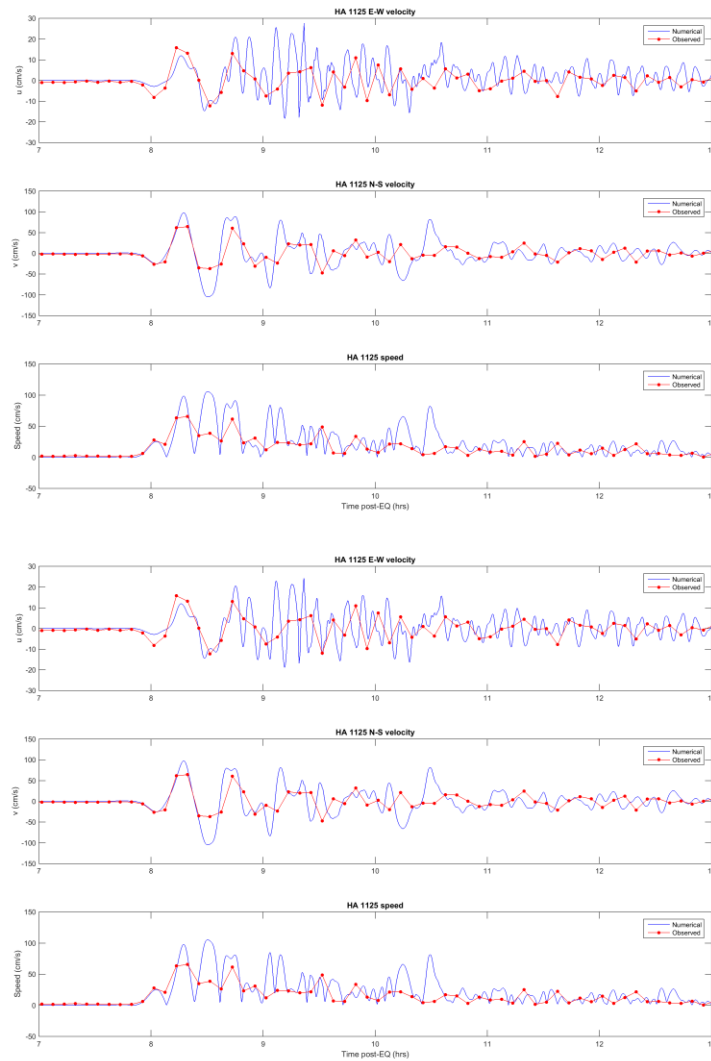


Figure G-5. Comparison plots at the ADCP location HA1125 with the grid resolutions of 5 m (top), 10 m (middle) and 20 m (bottom): numerical – blue line; measured – red line.

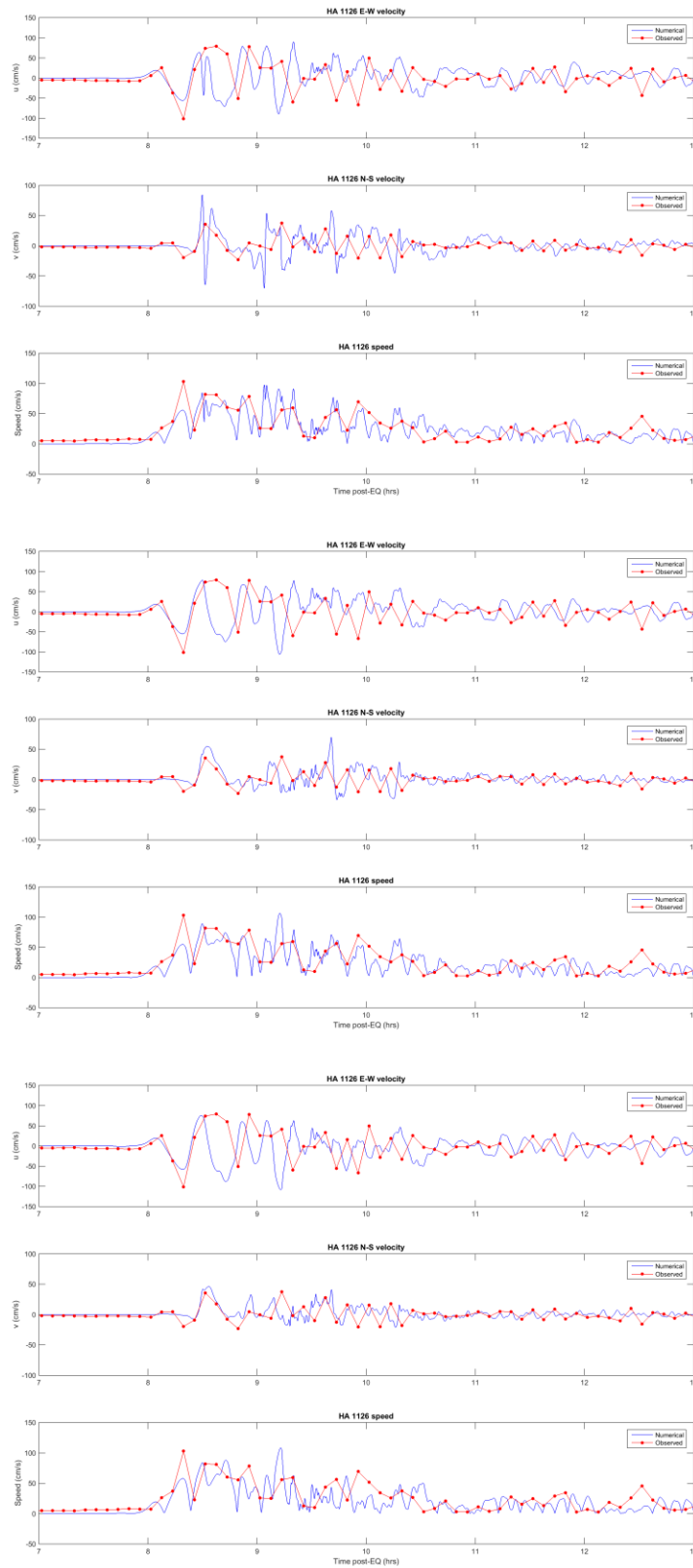


Figure G-6 Comparison plots at the ADCP location HA1126 with the grid resolutions of 5 m (top), 10 m (middle) and 20 m (bottom): numerical – blue line; measured – red line.

**G.6. Benchmark Problem #4: Flow through a City Building Layout**

The computational domain is  $5 \text{ m} \leq x \leq 43.52 \text{ m}$  and  $-13.24 \text{ m} \leq y \leq 13.24 \text{ m}$ . The given time series of incident wave elevation at  $x = 5 \text{ m}$  was used at the left boundary. The CFL number used is 0.75. The different Manning’s coefficient  $n = 0, 0.01$  and  $0.025$  were used in the computations. Three levels of refinement were used in the model with the computational grid resolutions of 12 cm, 3 cm and 1 cm.

Figure G-7 shows comparisons of the simulated and measured free surface elevation data at Gauges 3 and 4. The comparison plots of the computed and measured overland flow depth, cross-shore velocity and cross-shore momentum flux at the four locations B1, B4, B6 and B9 are presented in Figure G - 8, Figure G - 9 and Figure G - 10 respectively with the Manning’s coefficient  $n = 0.01$ .

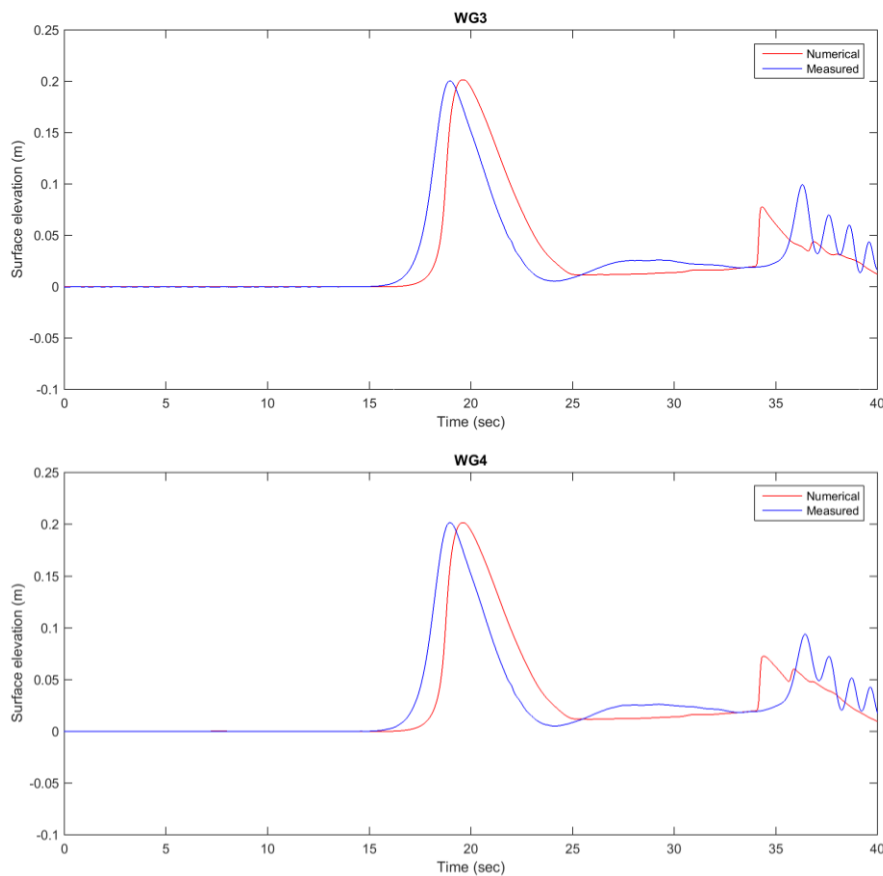


Figure G-7 Comparisons of simulated (red) and measured (blue) wave profiles at WG3 and WG4 with the Manning’s coefficient  $n = 0.01$ .

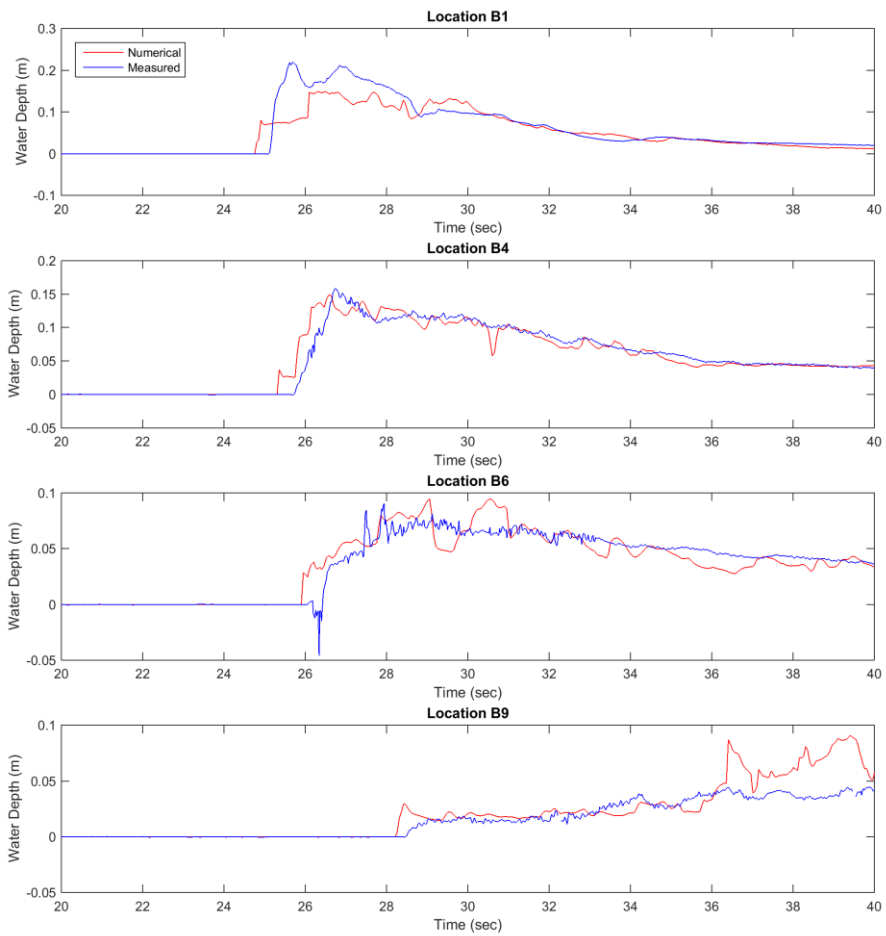


Figure G-8 Comparisons of the computed (red) and measured (blue) overland flow depth at four locations: B1, B4, B6 and B9 (Manning's  $n = 0.01$ ).



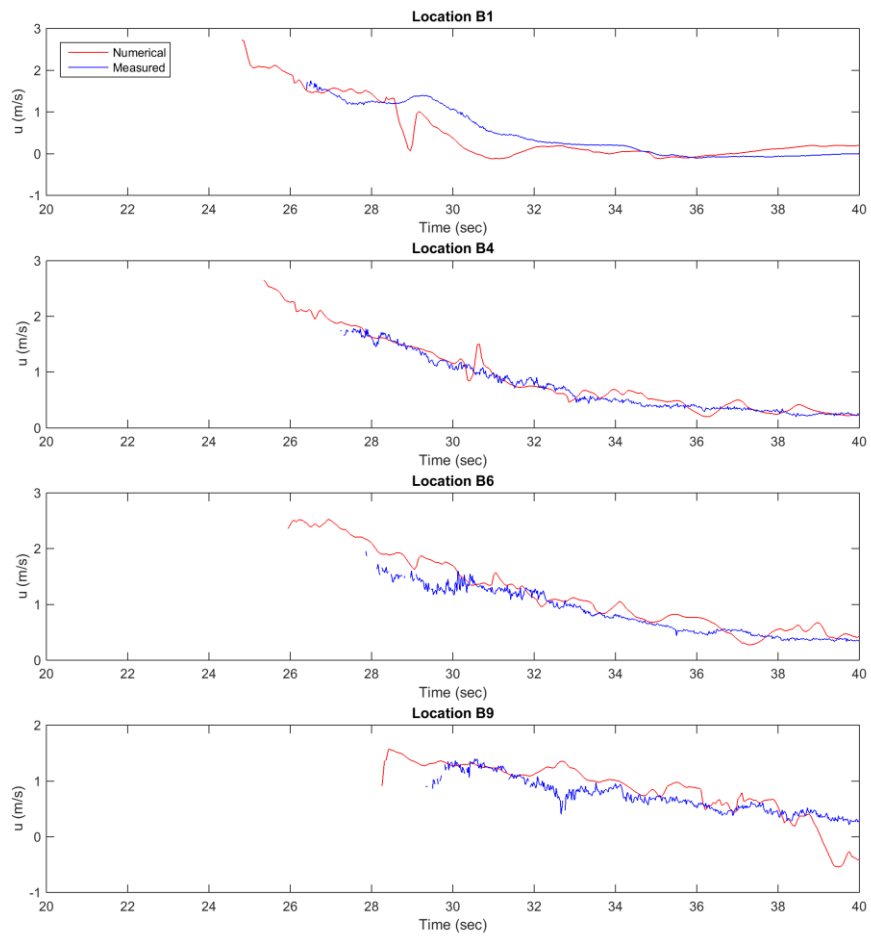
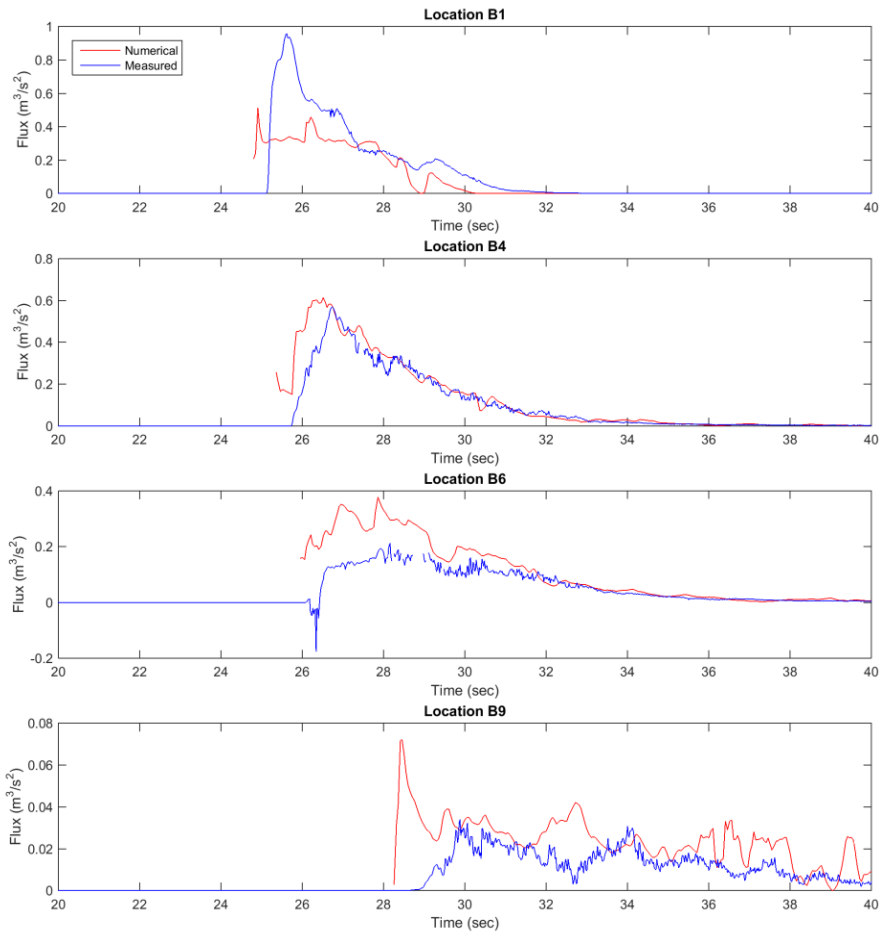


Figure G-9 Comparisons of the computed (red) and measured (blue) cross-shore velocity ( $u$ ) at four locations: B1, B4, B6 and B9 (Manning's  $n = 0.01$ ).



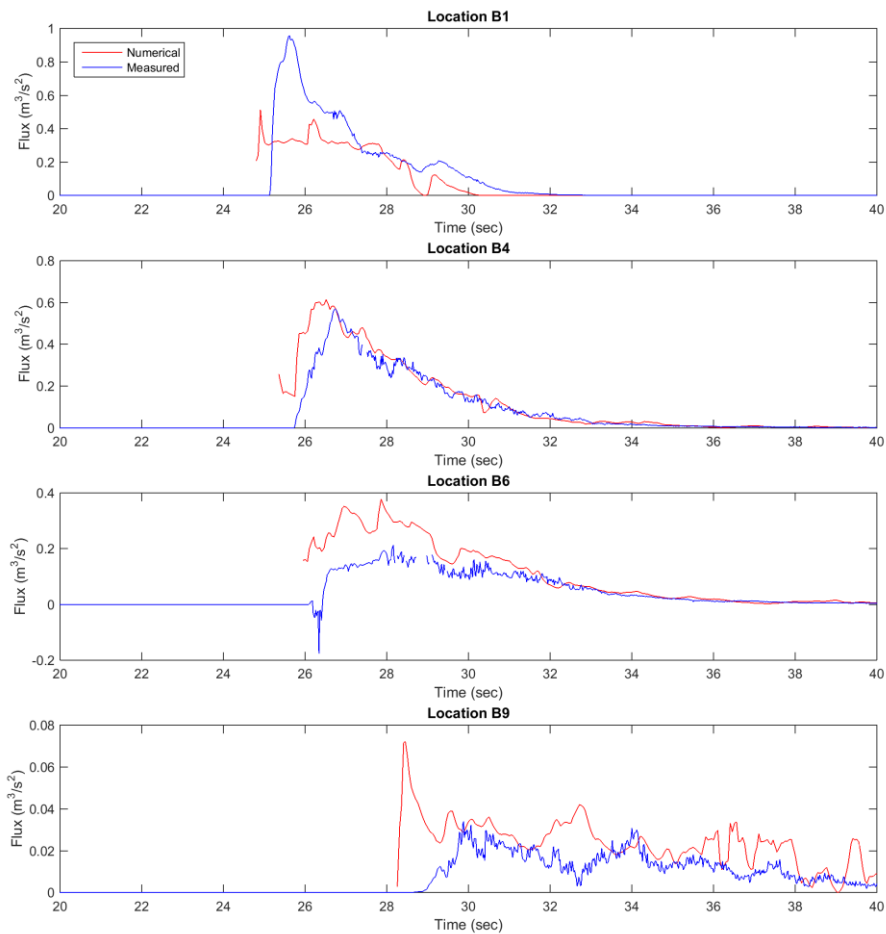


Figure G-10. Comparisons of the computed (red) and measured (blue) cross-shore momentum flux ( $Hu^2$ ) at four locations: B1, B4, B6 and B9 (Manning's  $n = 0.01$ ).

### G.7. Benchmark Problem #5: Solitary Wave Propagation over a Complex Shelf

The computational domain is  $0 \leq x \leq 43.6$  m and  $-13.2$  m  $\leq y \leq 13.2$  m. The grid cell size is 2.5 cm. The CFL number used is 0.75. The different Manning's coefficient  $n = 0, 0.01, 0.015$  and  $0.025$  were used in the computations.

Figure G-11 shows comparisons of measured and computed free surface elevation at 9 wave gauge locations with the Manning's coefficient  $n = 0.01$ . The comparisons of measured velocity components and numerical simulation (the Manning's coefficient  $n = 0.01$ ) at three ADV locations are presented in Figure G-12. The non-dispersive shallow water equations give the steep wave front in the numerical simulations for this benchmark problem.

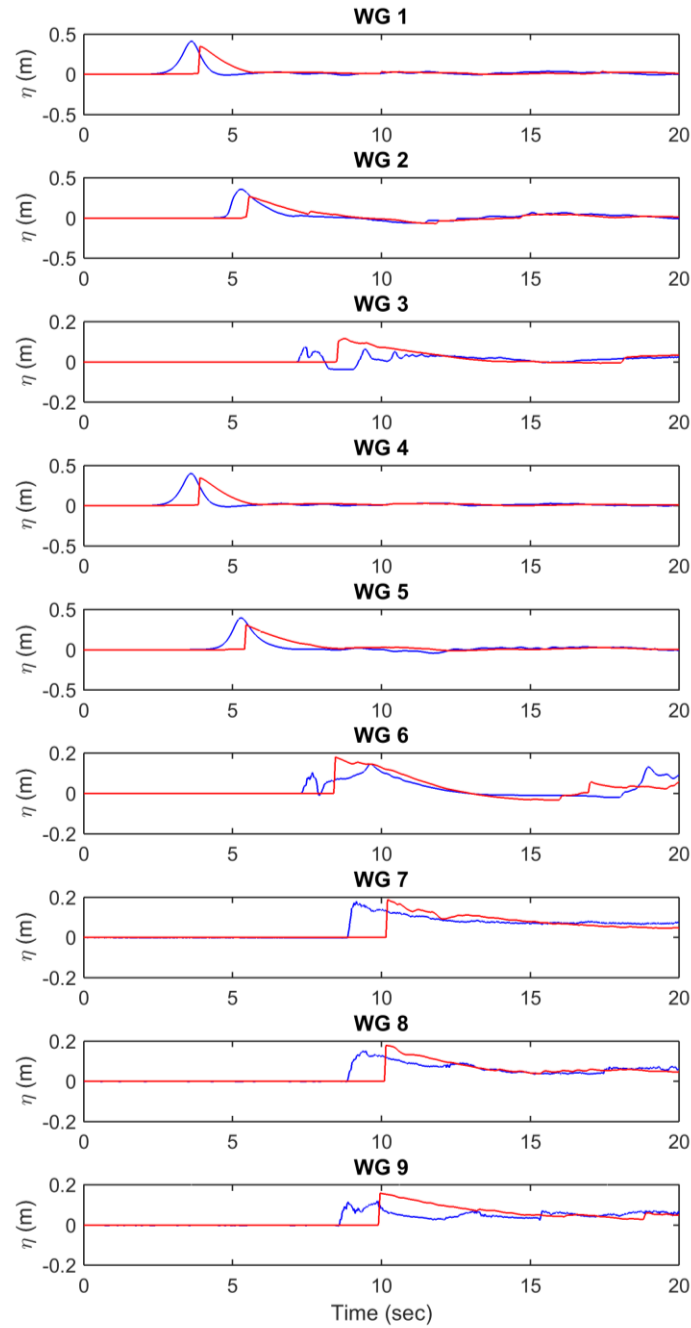


Figure G-11 Comparisons of the measured (blue) and computed (red) free surface elevation at 9 wave gauge locations (Manning's  $n = 0.01$ ).

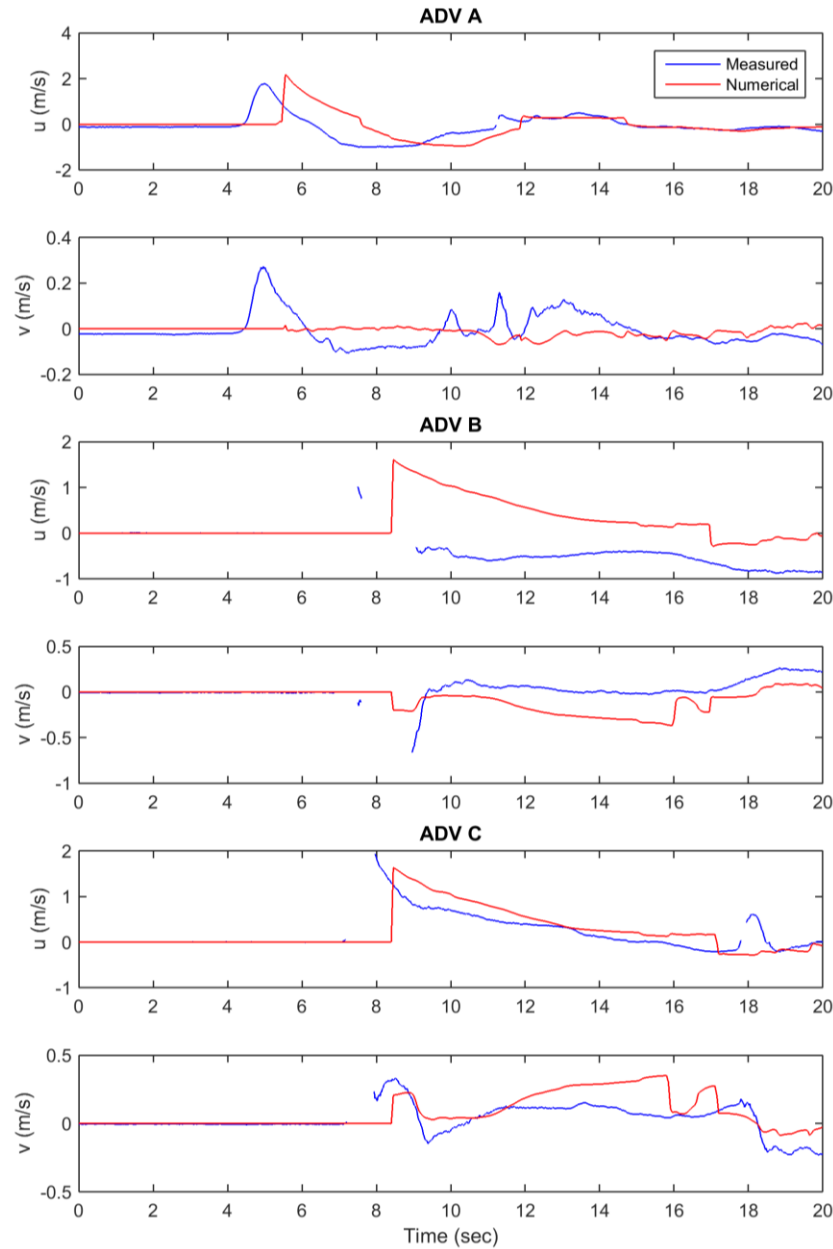


Figure G-12. Comparisons of the measured (blue) and computed (red) velocity components at three ADV locations (Manning's  $n = 0.01$ ).

## G.8. Conclusions

The overall reasonable agreement between measured data and numerical simulation demonstrates the validity of our numerical model (nonlinear and non-dispersive shallow water equations) with the above benchmark problems. The dispersive effects are important for some cases that cannot be captured by the non-dispersive shallow water equations.

The numerically computed runup values can be significantly affected by changes in the value of the Manning's coefficient of friction. Since the friction term is a function of water depth, the effects are more important for shallow water.

## **G.9. References**

Lynett, P.J., Gately, K., Wilson, R., Montoya, L., Arcas, D., Aytore, B., Bai, Y., Bricker, J.D., Castro, M.J., Cheung, K.F., David, C.G., Dogan, G.G., Escalante, C., González-Vida, J.M., Grilli, S.T., Heitmann, T.W., Horrillo, J., Kânoğlu, U., Kian, R., Kirby, J.T., Li, W., Macías, J., Nicolsky, D.J., Ortega, S., Pampell-Manis, A., Park, Y.S., Roeber, V., Sharghivand, N., Shelby, M., Shi, F., Tehranirad, B., Tolkova, E., Thio, H.K., Velioglu, D., Yalçiner, A.C., Yamazaki, Y., Zaytsev, A., and Zhang, Y.J., 2017. Inter-model analysis of tsunami-induced coastal currents. *Ocean Modelling* **114**, 14–32.

**Appendix H. Offshore amplitude match (ASCE 7-16)**